Investigations into the cytoplasmic binding and cell signalling of NrCAM, a cell adhesion molecule found in neurons.

By Maria Hill BA.

School of Biology.

September 2005.

CONTENTS

Declaration:

I, Maria Hill, hereby certify that this thesis, which is approximately 50,000 words in length, has been written by me, that it is the record of work carried out by me and that it has not been submitted in any previous application for a higher degree.

Date: 7/2/06

Maria Hill

I was admitted as a research student in September, 2001 and as a candidate for the degree of PhD in October, 2002; the higher study for which this is a record was carried out in the University of St Andrews between 2001 and 2004.

Date: 7/2/06

Maria Hill

I hereby certify that the candidate has fulfilled the conditions of the Resolution and Regulations appropriate for the degree of PhD in the University of St Andrews and that the candidate is qualified to submit this thesis in application for that degree.

Date: 16/2/06

Copyright declaration.

In submitting this thesis to the University of St Andrews I understand that I am giving permission for it to be made available in accordance with the regulations of the University Library for the time being in force, subject to any copy right vested in the work being affected thereby. I also understand that the title and abstract will be published, and that a copy of the work may be made and supplied to any bona fide library or research worker.

Date: 7/2/06

Maria Hill

Acknowledgements:

I would like to thank Dr. F. Gunn-Moore for his endless help and tireless enthusiasm, his door was always open. If it wasn't for him this thesis would never have been completed.

Many thanks to rest of the lab gang, particularly:

To Dr Fleur Davey who proved that SAP102 could indeed bind and who was "my Post Doc" and did lots of the boring work but most of all for being my email agony aunt.

To Margaret Taylor "Margo" who provided much needed morale support despite hating yeast-two hybrids and never attending my lab meetings. Margaret introduced "real coffee" into the lab and is therefore personally responsible for fuelling the entire floor's research.

To Frances who was her own person, to Michelle for always laughing and to Claire for introducing me to Alan Rickman.

Good luck to Lissa and Yimin who are carrying on the FLAG.

Thanks to Tina the fountain of all practical knowledge and who I have a sneaking suspicion may know Santa Claus personally.

Thanks to the project students Anna, Graham, James and Kaelan who worked on NrCAM for their sins and were a great help once they got over the shock.

Thanks to the people who provided the cDNA, antibodies and other stuff that made the project possible: Prof P. Brophy, Dr. C. Faivre-Sarrailh, Prof. Vann Bennett and Dr. S. Salton.

Thanks to the people who provided the support to make the project possible: Dr T. Vaughan for helping me with the Delta Vision (in between coffee and and cigs.) Alex and Ian in stores who sometimes delivered my orders to me before I had made them.

Most importantly thanks to my Mother for her unfailing support throughout the years.

Abbreviations used in this thesis.

3AT	3-amino-1,2,4-triazole
A	alanine
ACP	acyl carrier protein
AD	activation domain
ADAM	a disintegrin and a metalloprotease
AP	alkaline phosphatase
APC	adenomatous polyposis coli
BD	binding domain
Bp	base pair
BSA	bovine serum albumin
C	cysteine
CAM	cell adhesion molecule
CASPR	contactin-associated protein
CBB	calmodulin binding buffer
cDNA	complementary DNA
CEB	calmodulin elution buffer
CGCs	cerebellar granule cells
CHL1	close homologue of L1
CHO	chinese hamster ovary
CIAP	calf intestinal alkaline phosphatase
CNS	central nervous system
COS-7	african green monkey cells
CRASH	corpus callosum agenesis, mental Retardation, Adducted thumbs, Spastic paraplegia and Hydrocephalus syndrome
C-terminus	carboxy terminus
DCC	deleted in colon cancer
Dlg	discs large
DMEM	Dublecco's modified eagle's medium
DMF	N,N-dimethylformamide
DNA	deoxyribonucleic acid
dNTP	deoxynucleoside triphosphate
DPBS	Dublecco's phosphate buffered saline.
DRG	dorsal root ganglion
DTT	dithiothreitol
E	glutamic acid or glutamate
E with a number (e.g. E7)	embryonic day (e.g. embryonic day 7)
E.coli	escherichia coli
EBP50	ERM-binding phosphoprotein 50
EC	endothelial cells
ECM	extracellular matrix
ED	extracellular domain
EGF	epidermal growth factor
EGTA	ethyleneglycol-bis-(β-aminoethyl)-N,N'-tetraacetic acid
ERK	extracellular signal-regulated kinase
ERM	ezrin-radixin-moesin
EST	expressed sequence tag
EtBr	ethidium bromide

F	phenylalaline
FCS	foetal calf serum
FERM	four-point-one/ezrin/radixin/moesin
FHL2	four and a half LIM domains 2
FN	fibronectin
FNIII-like	fibronectin type III-like
G	glycine
GAP	GTPase activating protein,
GFP	Green Fluorescence Protein.
GGA	Golgi-localized, gamma-ear-containing, Arf binding
GIPC	GAIP Interacting Protein C terminus
GLUT1CBP	GLUT1 C-terminal binding protein.
GPI	glycosylphospatidyl inositol
GSH	reduced glutathione
GSK-3β	glycogen synthase kinase-3β
GST	glutathione s-transferase`
GTP	guanosine triphosphate
GUK domain	guanylate kinase-like domain
H	histidine
HEK	human embryonic kidney cells
HIV	human immunodeficiency virus
HRP	horse radish peroxidase
I	isoleucine
IgCAM	immunoglobulin-like domain containing cell adhesion molecule.
IgG- like	immunoglobulin-like
IPTG	isopropyl-β-D-thiogalactopyranoside
K	lysine
L	leucine
LB	Luria broth
LEF	lymphocyte enhancer factor
LM	laminin
M	methionine
MAGUK	membrane-associated guanylate kinase
MAPK	mitogen-activated protein kinase
MEM	minimum essential medium Eagle
MQH_2O	milli-Q water
N	asparagines
NCAM	neural cell adhesion molecule
NgCAM	neuron-glia cell adhesion molecule
NGF	nerve growth factor
NHERF	Na^+/H^+ exchange-regulatory factor
NIP-1	neuropilin -1 Interacting Protein
NP-40	nonident P40
NrCAM	NgCAM related cell adhesion molecule
N-terminus	amino terminus
P	Praline
PCR	polymerase chain reaction
PDZ	PSD-95, discs-large, and zonula occulens-1
PEG	polyethylene glycol 3350

pen.	penicillin
PMSF	phenylmethylsulfonyl fluoride
PNGASE-F	peptide: N-glycosidase F
PNS	peripheral nervous system
PSB	protein sample buffer
PSD	postsynaptic density
PTK	protein tyrosine kinase
Q	glutamine
R	arginine
r.p.m.	revolutions per minute
RGS	regulator of G-protein signalling
RIPA	radio-immunoprecipitation assay
RPTP	receptor protein tyrosine phosphatase
S	serine
SDS	sodium dodecyl sulfate
SDS-PAGE	sodium dodecyl sulphate polyacrylamide gel electrophoresis
SEMCAP-1/2	m-SemF cytoplasmic domain associated protein – 1/2. a.k.a GIPC1/2
SH2	src-homology 2
SKI	the human homologue of v-ski the transforming gene of the Sloan-Kettering virus
strep.	streptomycin
T	threonine
TBE	tris borate EDTA buffer
TBS	tris buffered saline
TBS-T(0.x%)	tris buffered saline with tween 20 (percentage v/v of tween 20)
TGN	trans Golgi network
TIP-2	tax interacting protein – 2. a.k.a GIPC1.
t-PA	tissue-type plasminogen activator
Tris	tris(hydroxymethyl)methylamine
Tris-HCL	tris(hydroxymethyl) aminomethane hydrochloride
Tween 20	polyoxyethylenesorbitan monolaurate
UV	ultra violet
V	valine
VHS	Vps27, Hrs, STAM
W	tryptophan
X-gal	5-bromo-4-chloro-3-indolyl-D-galactopyranoside
Y	tyrosine

Abstract:

NgCAM related cell adhesion molecule (NrCAM) is a cell adhesion receptor found in the plasma membrane of the initial segment, nodes of Ranvier and growth cone of neurons. It is a member of the L1-CAM family of cell adhesion molecules and together with other family members has an important role in the development of the mammalian nervous system. The L1-CAM family is defined by its ability to bind to ankyrin proteins that in turn link the family members to the underlying cytoskeleton. Until recently, ankyrin was the only known cytoplasmic binding partner of NrCAM and subsequently little was known of the cytoplasmic signalling pathways of the receptor. The aim of this thesis was both to establish if any other proteins could bind to the cytoplasmic terminus of NrCAM and to further examine the ankyrin-NrCAM interaction.

Three novel binding partners of the cytoplasmic terminus were discovered, GIPC, SAP102 and GGA1. GIPC and SAP102 contained PDZ domains and appeared to be binding to the very last C-terminal amino acids of the NrCAM cytoplasmic terminus. Both GIPC and SAP102 were developmentally regulated in a similar manner to NrCAM in the mammalian brain and co-localised at the plasma membrane of cells. A third potential binding partner was GGA1, which appears to be binding via a VHS domain to the ankyrin binding motif of NrCAM. Other L1-CAM family members, L1 and neurofascin, showed different binding abilities for GIPC, SAP102 and GGA1, highlighting for the first time the different cytoplasmic signalling pathways employed by the

different family members. This was also true for the potential binding of the L1-CAM family to the members of the 4.1 superfamily. Members of the 4.1 family appeared to be binding to two different motifs in the cytoplasmic tails of L1 and neurofascin and did not bind to NrCAM.

Table of contents

Table of Figures.
Chapter 1.

List of Tables.

Chapter 1: Introduction.

1.0 Introduction.

NrCAM is a cell adhesion molecule that belongs to the L1-CAM family of cell adhesion molecules (CAMs) that in turn belong to the superfamily of immunoglobulin-like domain containing cell adhesion molecules (IgCAMs). Members of the L1-CAM family have immunoglobulin G-like (IgG-like) domains and fibronectin type III-like (FNIII-like) repeats in their extracellular cellular domain and a short highly conserved cytoplasmic terminus of approximately 120 amino acids. The other vertebrate L1-CAM family members include L1, Close Homologue of L1 (CHL1) and neurofascin.

1.1 Cell Adhesion molecules.

Cells adhere to other cells and the extracellular matrix (ECM) via CAMs. The three major CAMs of the nervous system are integrins, cadherins and the IgCAMs.

1.1.1 Integrins.

Integrins are composed of heterodimers of non-covalently associated α and β subunits, both of which mediate cell adhesion to the ECM and/or with other CAMs. They are one of the oldest families of CAMs, for example the genes that code for integrin β subunits are found in the primitive animal phyla Cnidaria and Porifera (Brower *et al.*, 1997). Both α subunits and β subunits are type 1 transmembrane glycoproteins and specific $\alpha\beta$ combinations bind specific ligands. There are at least 18 different α subunits and eight different β subunits (Hynes, 2002). Most ECM proteins are recognised by multiple integrins, e.g. at least 12 bind to fibronectin, and most integrins recognise more than one ECM protein, e.g $\alpha_3\beta_1$ recognises

fibronectin, laminin, collagen, thrombosondin and fibrillin (Dzamba *et al.*, 2001). The cytoplasmic terminus of β subunits link integrins to the cytoskeleton via proteins such as talin, α-actinin and filamin, and this linkage can lead to the formation of focal adhesions between the cell and the ECM (Calderwood *et al.*, 2000). Integrins are important for cell migration, extracellular matrix assembly, regulation of tissue specific gene expression, differentiation, cell survival and cell proliferation (Dzamba *et al.*, 2001). They are known to interact with members of the same family as NrCAM for example L1 (Mechtersheimer *et al.*, 2001; Skaper *et al.*, 2002; Thelen *et al.*, 2002) and CHL1 (Buhusi *et al.*, 2003).

1.1.2 The cadherin superfamily.

This family is made up of four categories: 1).classical cadherins; 2). desmosomal cadherins; 3). protocadherins and 4). cadherin related proteins (Radice and Takeichi, 2001). Most cadherins are single pass transmembrane glycoproteins, containing four to 30 cadherin repeats (a conserved motif of 110 amino acids related to immunoglobulin repeats) in the extracellular portion (Radice and Takeichi, 2001). Cadherins are Ca^{2+} dependent, with Ca^{2+} ions binding between the cadherin repeats making the molecules more rigid and protecting them from proteolytic cleavage (Nagar *et al.*, 1996). Classical cadherins have a protease processing sequence K/RRXKR in their N-terminal signal sequence (Radice and Takeichi, 2001). This sequence allows proteolytic processing of the precursor protein and is essential for the activation of the cadherin. It is similar to a furin cleavage sequence found in NrCAM and other members of the L1-CAM family (Posthaus *et al.*, 1998; Posthaus *et al.*, 2003). In the nervous system cadherins are concentrated at synapses and have a role in synaptogenesis and synapse stabilisation (Huntley *et al.*, 2002).

1.1.3 The immunoglobulin superfamily (IgCAMs).

IgCAMs can be associated with many different signalling molecules including, non-receptor and receptor like protein tyrosine phosphatases (RPTP) and serine/threonine kinases (Walsh and Doherty, 1997; Volkmer, 2001). They are important in the development of the nervous system and have roles in cell migration, axon guidance, myelination, learning and memory, and are implicated in certain neurodegenerative disorders (Walsh and Doherty, 1997; Kamiguchi *et al.*, 1998a; Kamiguchi and Lemmon, 2000a; Bartsch, 2003). Subfamilies of IgCAMs are categorised according to the number of IgG-like domains they possess, the presence and number of FNIII-like repeats, their mode of attachment to the membrane and the presence of a catalytic cytoplasmic domain (Figure 1-1) (Brummendorf and Rathjen, 1996; Volkmer, 2001). IgG-like domains are 70 to 110 amino acids long and consist of highly conserved amino acid residues. They also contain two well-characterised cysteine residues that form a disulphide bridge between two opposed β-sheets (Atkins *et al.*, 2001; Volkmer, 2001). FNIII-like repeats are approximately 90 amino acids in length and contain conserved tyrosine and tryptophan residues. They too are also composed of two opposing β-sheets but are not normally linked by a disulfide bridge (Volkmer, 2001). The domain structure of the subfamilies of L1-CAMS are described in Figure 1-1 and include the NCAM family, the L1-CAM family, the F11 family, the IgLON family, the RPTP family and the DCC family. NrCAM is a member of the L1-CAM family of IgCAMs and interacts with members of the F11 family (Crossin and Krushel, 2000; Volkmer, 2001).

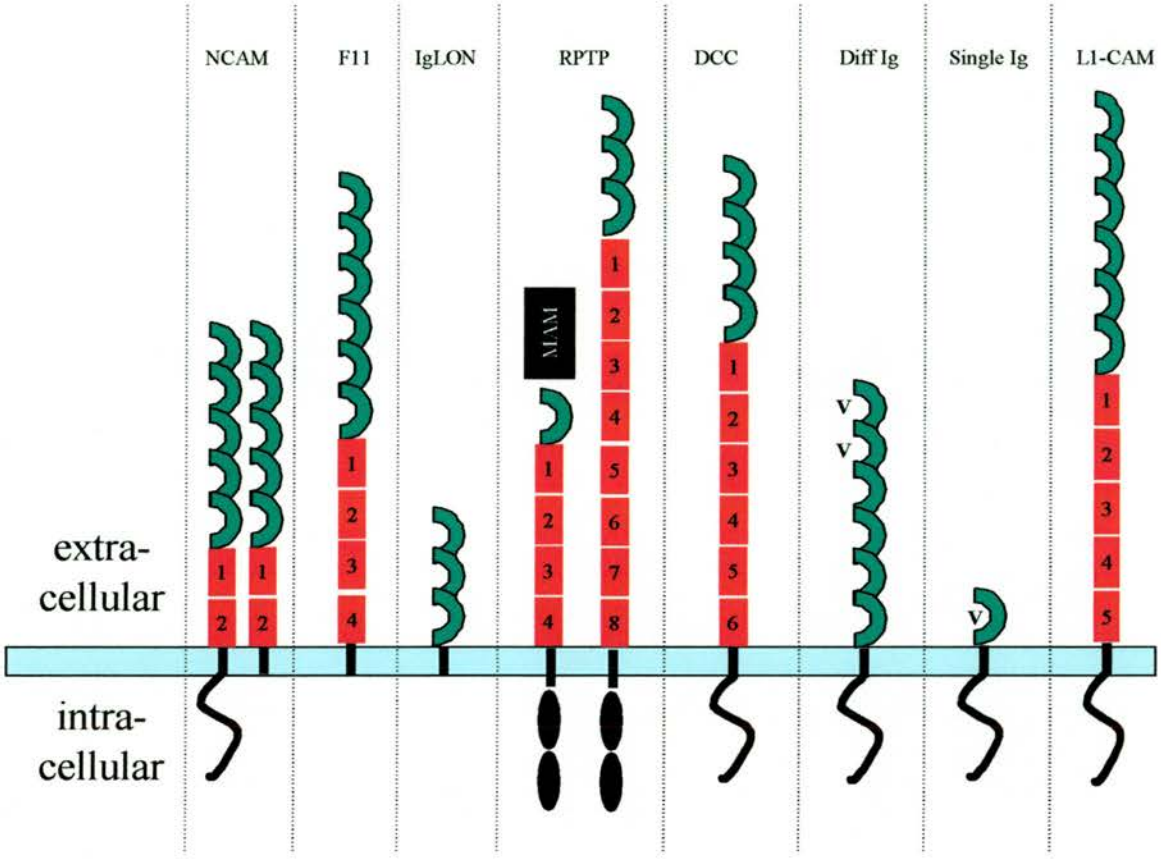

Figure 1-1. A schematic diagram of the domain structure of the immunoglobulin superfamily members. The pale blue bar represents the plasma membrane. Extracellular IgG-like domains are shown as green hemispheres, FNIII-like repeats as red boxes and mephrin A5 RPTPμ (MAM) domains as black boxes. Intracellular phosphatase like domains are shown as black as ellipses. This Figure is adapted from (Volkmer, 2001).

1.2 The L1-CAM family.

This family possesses six IgG domains, three to five FNIII-like repeats, a single transmembrane region and a cytoplasmic terminus (Brummendorf *et al.*, 1998). Members of the family have an important role in nervous system development from invertebrates to mammals.

1.2.1 The L1-CAM family gene.

Invertebrates have only one L1 gene (Zhao and Hortsch, 1998). Invertebrate L1 homologs include tractin in leech, neuroglian in the fly and LAD-1 in nematode worm (Brummendorf *et al.*, 1998). There are four homologous L1 type genes found in vertebrates, L1 (also known as Neuron glial associated Cell Adhesion Molecule (NgCAM) in chick), CHL1, neurofascin and NgCAM related Cell Adhesion Molecule (NrCAM, also known as Bravo) (Brummendorf *et al.*, 1998). It is postulated that these four proteins are the result of two gene duplication events after the appearance of the first vertebrate L1 gene (Hortsch, 2000). Both the NrCAM and neurofascin genes (but not L1 or CHL1) are subject to extensive exon splicing (Hassel *et al.*, 1997; Hortsch, 2000) and in the case of neurofascin this results in alternative isoforms that are not only cell and tissue specific but also developmentally regulated (Figure 1-2). The vertebrate members of the L1-CAM family are described in sections 1.2.1.1 to 1.2.1.4.

1.2.1.1 L1.

L1 is the prototypical L1-CAM family member, and after neural cell adhesion molecule (NCAM), the most studied IgCAM molecule. This is unsurprising as mutations in the L1 gene in humans cause congenital developmental defects such as Corpus callosum agenesis, mental Retardation, Adducted thumbs, Spastic paraplegia and Hydrocephalus syndrome (CRASH) (Fransen *et al.*, 1997; Kamiguchi *et al.*, 1998a; Kenwrick *et al.*, 2000). In the adult L1 contributes to learning and memory and long term potentiation (Luthl *et al.*, 1994; Welzl and Stork, 2003). L1 knockout

mice show a number of developmental abnormalities such as decreased axonal association with non-myelinating Schwann cells, abnormal morphogenesis of cortical dendrites, altered distribution of dopaminergic neurons and a reduced size of the corpus callosum (Fransen *et al.*, 1998; Demyanenko *et al.*, 1999; Demyanenko *et al.*, 2001).

1.2.1.2 Neurofascin.

NrCAM is most closely related to neurofascin (Volkmer *et al.*, 1992; Davis *et al.*, 1996). Neurofascin and NrCAM together account for 1% of the total membrane protein in brain tissue (Davis *et al.*, 1993; Davis and Bennett, 1994). The neurofascin gene is subject to extensive alternative splicing (Hassel *et al.*, 1997). In adult brain some of the more commonly found isoforms are the 186 kDa, 155 kDa and 140 kDa isoforms respectively (Davis and Bennett, 1993) (Figure 1-2). Neurofascin 186 was cloned in 1992 (Volkmer *et al.*, 1992). This splice variant lacks the third FNIII-like repeat and has a mucin like sequence after the fourth FNIII-like repeat (Davis *et al.*, 1996). Neurofascin 155 has the third FNIII-like repeat but lacks the mucin like sequence and neurofascin 140 lacks both the third FNIII-like repeat and mucin sequence (Davis *et al.*, 1996). Neurofascin 186 and neurofascin 155 are important molecules in the formation of myelin and the node of Ranvier (Davis *et al.*, 1996; Collinson *et al.*, 1998; Lustig *et al.*, 2001; Scherer and Arroyo, 2002). The central importance of neurofascin is probably best demonstrated by a global neurofascin knockout mouse, which dies within a few days of birth (personal communication Prof. P. Brophy, University of Edinburgh).

1.2.1.3 CHL1.

This protein was first discovered as a cDNA clone similar in amino acid sequence to L1 (Tacke *et al.*, 1987). CHL1 is able to promote neurite elongation, neurite survival and is upregulated in axonal regeneration (Chen *et al.*, 1999; Hillenbrand *et al.*, 1999; Chaisuksunt *et al.*, 2000a; Chaisuksunt *et al.*, 2000b; Zhang *et al.*, 2000). In the CHL1 knockout, murine axons are mis-guided and NCAM 180 expression is upregulated (Montag-Sallaz *et al.*, 2002). Mutations in the CHL1 gene are associated with schizophrenia (Sakurai *et al.*, 2002).

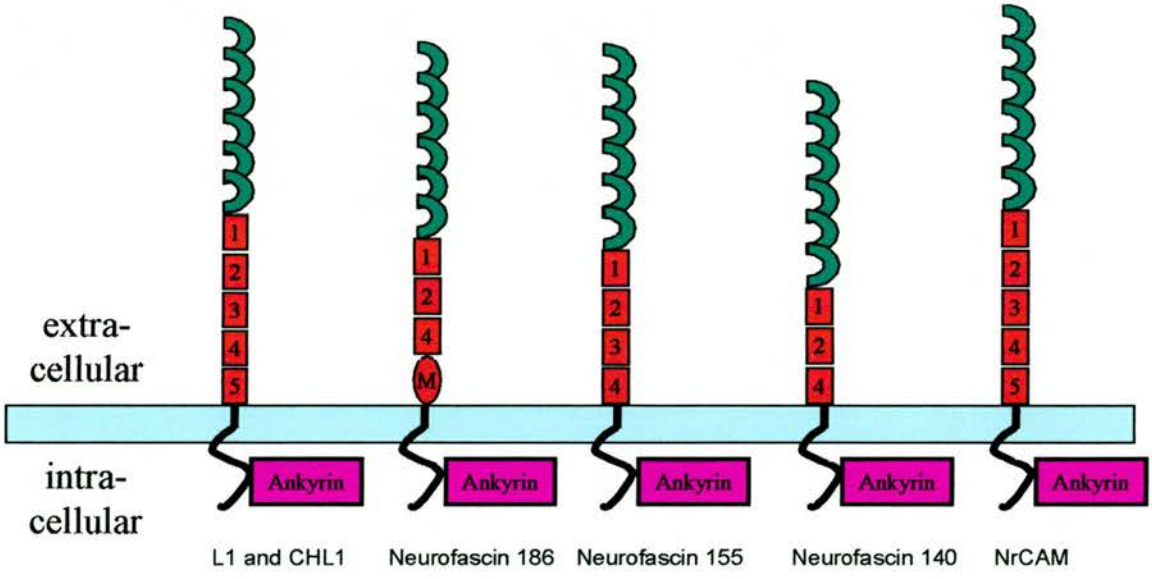

Figure 1-2. The domain structure of the L1-CAM family in mammals. L1 and CHL1 have a similar structure. The three most common isoforms of neurofascin have been shown. NrCAM's fifth fibronectin domain is not in all splice variants of the protein. The pale blue bar represents the plasma membrane. Extracellular IgG-like domains are shown as green hemispheres, FNIII-like repeats as red boxes and mucin domains as red ellipses with an M. Cytoplasmic tails are homologous, primarily around an ankyrin binding region.

1.2.1.4 NrCAM.

Two independent groups identified NrCAM as an important Cell Adhesion Molecule of the Nervous system. The first group identified NrCAM as the antigen of a monoclonal antibody against biotinylated cell surface molecules of the chick optic tectum (Rosa *et al.*, 1990). The anti-NrCAM antibody was the second monoclonal antibody raised using this investigation and was named Bravo (after the second letter of the international phonetic alphabet) (Rosa *et al.*, 1990). The second group independently cloned the cDNA clone of chick NrCAM while characterising polyclonal antibodies against denatured NgCAM and thus called it NgCAM related Cell Adhesion Molecule or NrCAM (Grumet *et al.*, 1991).

1.2.2 The L1-CAM family cytoplasmic terminus.

The most highly conserved part of the L1-CAM family proteins is their 85-148 amino acid residue cytoplasmic termini (Volkmer *et al.*, 1992; Hortsch, 2000). The sequence of NrCAM's cytoplasmic terminus has been 100 % conserved for more than 200 million years of evolution, from chicken to mammals (Davis and Bennett, 1994; Lane *et al.*, 1996). The strong conservation of the cytoplasmic terminus of the L1 family suggests that the family probably share important cytoplasmic signalling events.

The most conserved region of the cytoplasmic terminus of L1-CAM family members is a 36 amino acid residue ankyrin-binding domain that appears in both invertebrates and vertebrates (Zhang *et al.*, 1998a; Hortsch, 2000). Ankyrins are a family of proteins that link the L1-CAMs to the spectrin-ankyrin cytoskeleton (Zhang *et al.*, 1998a).

All of the vertebrate L1 family member genes (except CHL1) contain an alternatively spliced 12-nucleotide exon that codes for an RSLE amino acid sequence that so far has only been seen in neuronal transcripts (Wang *et al.*, 1998; Hortsch, 2000). This amino acid sequence is downstream of a tyrosine residue (i.e. YRSLE) and gives rise to an YXXL motif. YXXL motifs are common in proteins that traffic to the plasma membrane and the motif is essential for rapid internalisation of these proteins from the plasma membrane (Bonifacino and Traub, 2003). The RSLE motif in L1 is necessary for the sorting of L1 to the growth cone and receptor mediated endocytosis of L1 (Kamiguchi *et al.*, 1998b).

1.3 The NrCAM gene, transcription, translation and expression.

1.3.1 The NrCAM gene.

The human NrCAM gene has 34 exons and has been localised to chromosome 7q31.1-q31.2. (Lane *et al.*, 1996; Dry *et al.*, 2001). It codes for a protein with six IgG domains and five FNIII-like repeats, a transmembrane sequence and a short cytoplasmic terminus (Lane *et al.*, 1996; Dry *et al.*, 2001). It is extensively spliced around the fifth FNIII-like domain and isoforms of NrCAM missing the entire fifth FNIII-like domain have been identified in chick, rat and human (Lane *et al.*, 1996; Wang *et al.*, 1998). The NrCAM gene has an exon that codes for a premature stop codon that would give rise to an isoform of NrCAM without an ankyrin binding motif (Dry *et al.*, 2001).

1.3.2 Transcriptional regulation of NrCAM expression.

The transcriptional regulation of NrCAM expression has been poorly defined to date. Recent studies have shown that it may be downstream of the upregulation of Hox transcription factors (Valerius *et al.*, 2002) or downstream of a classical wnt signaling pathway (Conacci-Sorrell *et al.*, 2002).

Hox transcription factors are known to enhance L1 expression (Crossin and Krushel, 2000). Similarly the NrCAM gene is upregulated 2 fold in Human Embryonic Kidney (HEK293) cells when Hoxa11 is expressed (Valerius *et al.*, 2002).

The expression of NrCAM is induced by both β-catenin and a homologous protein plakoglobin (Conacci-Sorrell *et al.*, 2002). NrCAM has lymphocyte enhancer factor/ T cell factor (LEF/TCF) binding sites in its promoter region and dominant LEF-1 expression increases NrCAM expression (Conacci-Sorrell *et al.*, 2002). Two proteins, the human homologue of v-ski (SKI) and four and a half LIM domains 2 (FHL2) enhance β-catenin dependent activation of the NrCAM promoter in melanoma cells (Chen *et al.*, 2003). Therefore it is theorised that NrCAM transcription may be downstream of a classical Wnt signalling pathway (Gottardi *et al.*, 2001). In this pathway wnt signalling via Frizzled and Dishevelled prevents the degradation of β-catenin by the glycogen synthase kinase-3β (GSK-3), adenomatous polyposis coli (APC) and axin degradation complex (Gottardi *et al.*, 2001). This results in a build up of β-catenin in the cytoplasm and nucleus of the cell. β-catenin in the nucleus is able to bind to LEF-1/TCF transcription factors, act as a co-activator, and induce the transcription of NrCAM. FHL2 and SKI potentiate the

function of β-catenin and induce NrCAM expression (Figure 1-3) (Gottardi *et al.*, 2001; Conacci-Sorrell *et al.*, 2002; Chen *et al.*, 2003).

1.3.3 NrCAM expression in the nervous system.

NrCAM is expressed in the axons and glia of the central nervous system (CNS) and peripheral nervous system (PNS). Its temporal expression varies during embryonic and postnatal development of the CNS and PNS and correlates to important events such as cell proliferation, cell migration, axonal outgrowth and myelination (Krushel *et al.*, 1993). Northern blots show mRNA expression in various human brain tissues including the amygdala, caudate nucleus, corpus callosum, hippocampus, hypothalamus, substantia nigra, subthalamic nucleus and the thalamus (Lane *et al.*, 1996).

In the cerebellum NrCAM can be found in migratory and post-migratory granule cells as well as post-migratory Purkinje neurons (Krushel et al., 1993; Sakurai et al., 2001). NrCAM knockout mice are viable but exhibit subtle size difference in lobes in vermis of the cerebellum (Sakurai et al., 2001). Anti-L1 antibody treatment disrupts survival and maintenance of primary cultures of the cerebellar granule cells (CGCs) from NrCAM knockout mice (Sakurai et al., 2001). Furthermore double knockout mice without NrCAM or L1 show severe cerebellar defects, which are more extensive than if only one of the molecules were knocked out (Sakurai et al., 2001). This suggests that both NrCAM and L1 have an important role in granule cell development of the cerebellum and that their role may be compensatory.

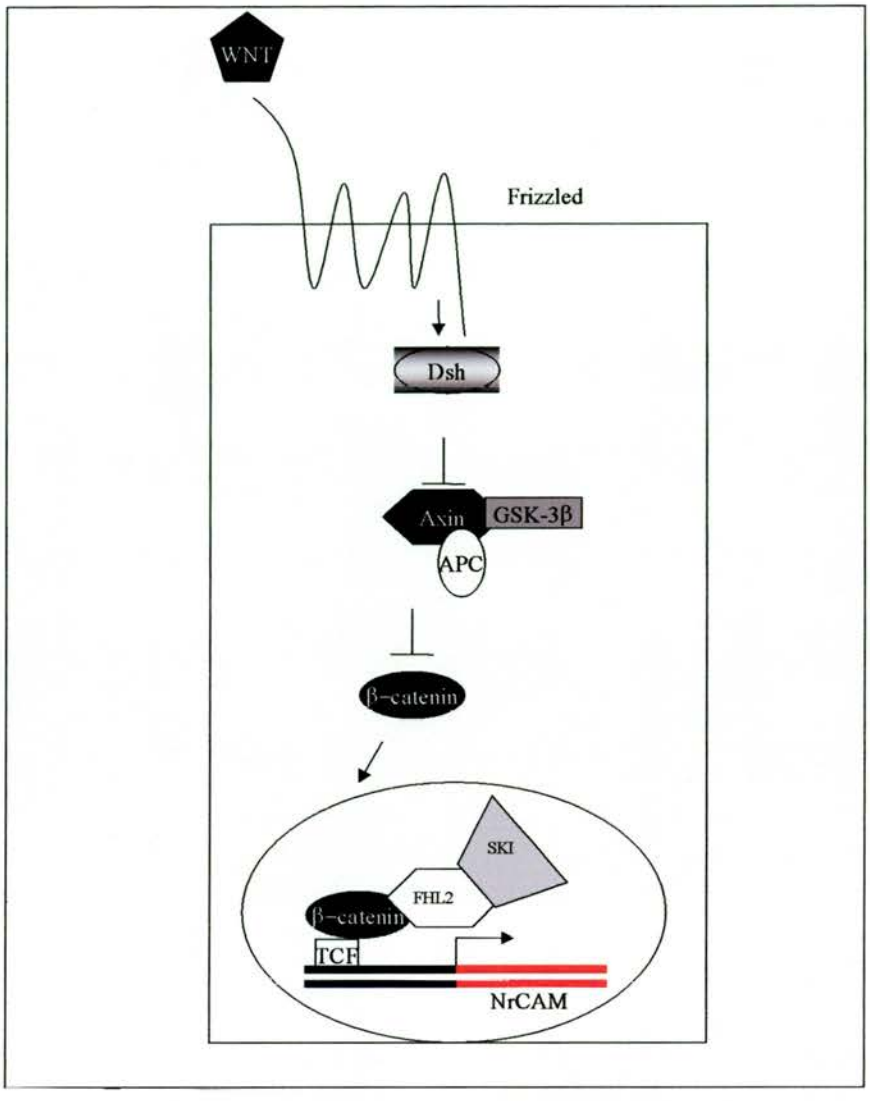

Figure 1-3. Proposed signalling mechanism for the expression of NrCAM. The pathway is based upon the findings of (Chen *et al.*, 2003) and (Conacci-Sorrell *et al.*, 2002). The diagram has been adapted from (Gottardi *et al.*, 2001).

1.3.4 NrCAM expression outside of the nervous system.

It was originally believed that NrCAM was only expressed in the cells of the nervous system (Krushel *et al.*, 1993; Grumet, 1997). However in 1998 its mRNA was shown to be highly expressed by the pancreas, adrenal glands and placenta (Wang *et al.*, 1998). Its roles outside of the nervous system are extensive, for

example NrCAM protein is highly expressed in the cell membrane and at sites of cell-to-cell contact of the acinar cells of the pancreas where it may play a role both in cell adhesion and in preventing autodigestion of the pancreas by pancreatic enzymes (Dhodapkar *et al.*, 2001).

NrCAM is also expressed in endothelial cells (EC) that are important in angiogenesis (Aitkenhead *et al.*, 2002). During angiogenesis EC degrade the local basement membrane, migrate into the stroma, proliferate, extend long pseudopodia that go on to form capillary sprouts that in turn form hollow tubes and new blood vessels. NrCAM has been found to show increased expression *in vitro* in tube forming EC when compared to migrating and proliferating cells (Glienke *et al.*, 2000; Aitkenhead *et al.*, 2002).

NrCAM is expressed in the lens of the eye, where it is essential for lens transparency and the ordered arrangement of the lens fibre cells (More *et al.*, 2001). No other member of the L1-CAM family is believed present in the lens and so in NrCAM deficient mice the lens becomes disorganised and develops into a cataract in the adult animal (More *et al.*, 2001).

1.3.5 NrCAM over-expression in cancer.

NrCAM has also been hypothesised to have an important role in certain cancers. Conacci–Sorrell *et al.* (2002) have shown that NrCAM is a target gene of the β-catenin/LEF1 pathway (Figure 1-3 and section 1.3.2) and as such confers motility, growth and tumourigenesis in NIH3T3 cells. They also showed that NrCAM expression is increased in malignant melanoma lines, that NrCAM is highly tumourgenic in nude mice and that increased NrCAM expression is observed in human colon cancer tissue (Conacci-Sorrell *et al.*, 2002). Other studies showed

differential NrCAM expression during the progression of pancreatic cancers that may correlate to their invasive/metastatic properties (Dhodapkar *et al.*, 2001). NrCAM is also over-expressed in malignant human brain tumours when compared to normal brain tissue (Sehgal *et al.*, 1998).

1.4 The structure and post-translational modification of the NrCAM protein.

NrCAM is predicted to be a type 1 transmembrane protein with six IgG domains and four to five FNIII-like repeats (Grumet, 1997). Its crystal structure has not been solved and its three dimensional structure is undetermined.

1.4.1 The horse-shoe conformation of NrCAM.

The Ig domains of IgCAMs are believed to adopt two conformations. The first is an open chain rod like structure (Figure 1-4(A)) and the second a horse-shoe shape, where the Ig-domains fold back in a sharp bend (Figure 1-4(B)). L1 has been shown to primarily exist in the horse-shoe conformation in solution (Schurmann *et al.*, 2001). This folding allows contact between the first and fourth IgG domains and the second and third IgG domains (Figure 1-4(B)). It is not known whether NrCAM adopts this confirmation. However axonin-1, one of NrCAM's binding partners discussed below, is believed to interact with NrCAM when it adopts a horse-shoe conformation and it has been suggested that NrCAM may be adopting a similar conformation (Rutishauser, 2000).

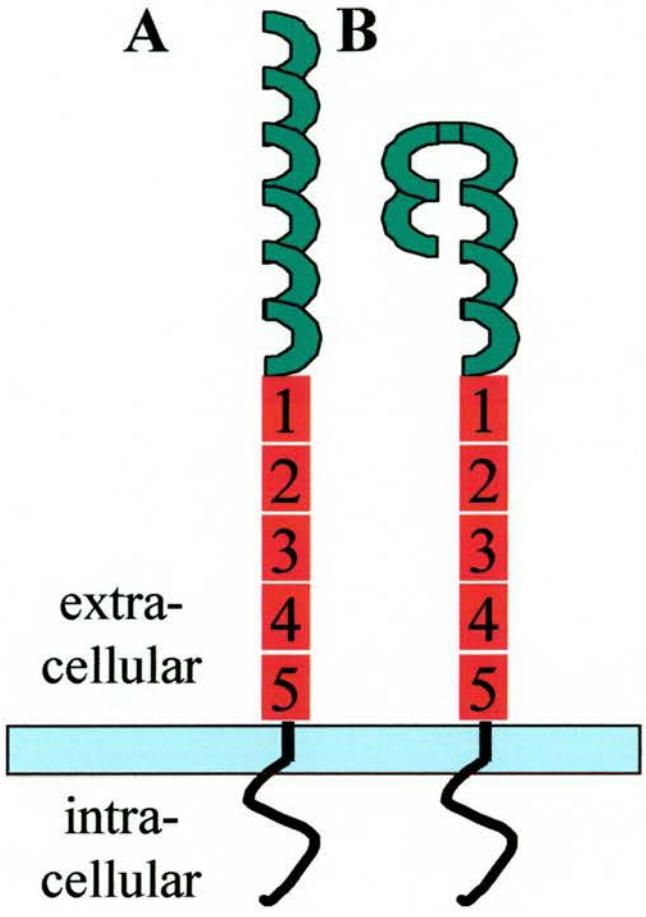

Figure 1-4. Proposed structures of the extracellular domain of NrCAM. **A)** shows a rod like structure. **B)** shows the first two IgG-like domains folded back to generate a horseshoe like structure. The pale blue bar represents the plasma membrane. Extracellular IgG-like domains are shown as green hemispheres, FNIII-like repeats as red boxes. This picture was adapted from Volkmer, 2001.

1.4.2 Glycosylation and NrCAM.

Glycosylation is a post-translational modification of a protein as it passes through the endoplasmic reticulum and the Golgi apparatus. Sugar residues or glycans are added to a protein backbone. The presence of these glycan chains can confer certain properties onto the protein such as adhesion/repulsion of other proteins (Breen *et al.*, 1998). Glycosylation and glycoproteins play an important role in the correct development and functioning of the CNS (Breen *et al.*, 1998). It has not been

reported whether NrCAM is subject to glycosylation; however neurofascin is subject to N-linked and O-linked glycosylation (Volkmer *et al.*, 1992; Volkmer *et al.*, 1996) and differential glycosylation of leech tractin has been shown to regulate neurite extension (Huang *et al.*, 1997; Jie *et al.*, 1999; Jie *et al.*, 2000).

1.4.3 Post-translational cleavage of NrCAM.

Figure 1-5 describes three of the possible conformations of NrCAM. It is still unclear which of the three is the correct. Most work has been perfomed on chick NrCAM. Full-length glycosylated chick NrCAM/Bravo is believed to be a 200 kDa protein that exists as a heterodimer of 130/140 kDa and 60/80 kDa fragments (Kayyem *et al.*, 1992). The entirely extracellular 130/140 kDa sequence is believed to non covalently associate with the 60/80 kDa membrane spanning fragment (Figure 1-5(B)) (Kayyem *et al.*, 1992).

Full-length glycosylated mammalian NrCAM is expected to be a protein of approximately 180 kDa to 200 kDa (Davis *et al.*, 1996). However most antibodies made to the extracellular domain pick up bands of approximately 140 kDa (Davis and Bennett, 1994; Davis *et al.*, 1996; Volkmer *et al.*, 1996; Lambert *et al.*, 1997). An antibody to common amino acid residues in the cytoplasmic terminus of all L1-CAMs is unable to detect this 140 kDa and so the 140 kDa band is unlikely to contain the cytoplasmic terminus of NrCAM (Davis and Bennett, 1994; Davis *et al.*, 1996). Therefore mammalian NrCAM is cleaved in a similar method to chick NrCAM and may adopt the conformations described in Figure 1-5(B) or Figure 1-5(C).

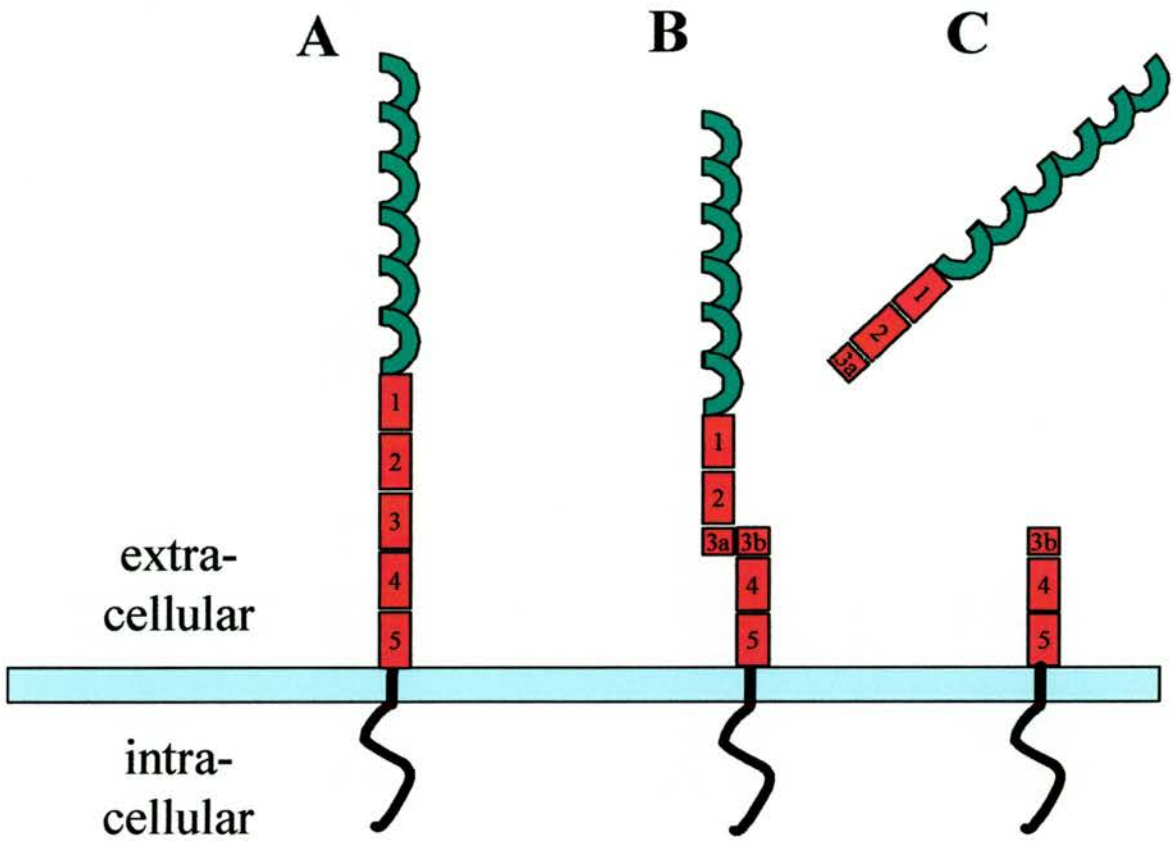

Figure 1-5. NrCAM may exist as one or more isoforms at the plasma membrane. **A)** shows a single transmembrane molecule, **B)** a dimer of two molecules that are cleaved and then associated at the third FNIII-like domain and **C)** a molecule that when cleaved at the third FNIII-like domain secretes most of its extracellular domain in to the ECM. The pale blue bar represents the plasma membrane. Extracellular IgG-like domains are shown as green hemispheres, FNIII-like repeats as red boxes.

1.4.3.1 The third FNIII-like domain.

The cleavage of NrCAM is believed to occur in the third FNIII-like domain (Grumet, 1997). The third FNIII-like domain of all the L1-CAMs with the exception of neurofascin is highly susceptible to cleavage, particularly by members of the serine protease superfamily (Hortsch, 1996). The third FNIII-like domain of

NrCAM, L1, neurofascin, CHL1, and NgCAM has been aligned using the CLUSTALW software (Figure 1-6). Regions that have been shown to be subject to serine protease cleavage have been highlighted. Highlighted in yellow are trypsin cleavage sites, in red font is the plasmin cleavage site of L1 and boxed areas are furin cleavage sites.

1.4.3.2 Trypsin cleavage.

Trypsin is a serine protease and cleaves after the terminal arginine of an R/K-R motif in a well-studied catalytic mechanism. Figure 1-6 (yellow highlight) indicates a S-R/K-R motif that is common to L1, NrCAM and NgCAM. This site was identified as potentially important for cleavage of chick NrCAM into 130/140 kDa and 60/80 kDa fragments (Kayyem *et al.*, 1992).

1.4.3.3 Plasmin/Plasminogen cleavage.

Plasmin is a serine protease that has an important role in the development of the nervous system (Seeds *et al.*, 1997). L1 in cerebellar granule cell growth cones is subject to the actions of exogenous plasmin which cleaves L1 in its third FNIII-like domain and releases a 140 kDa fragment in to the extracellular matrix (Nayeem *et al.*, 1999; Mechtersheimer *et al.*, 2001). This cleavage is at two sites, the first site is after the lysine of QRK (Figure 1-6, red font) and the second site is after the lysine of SKR (Figure 1-6 red font) (Nayeem *et al.*, 1999; Stilletti *et al.*, 2000). NrCAM has a SKR motif (Figure 1-6, red font) and NrCAM is present in cerebellar granule cell growth cones. Thus it is possible that NrCAM is also subject to plasmin cleavage. If

NrCAM is indeed subject to plasmin cleavage the extracellular portion may be lost into the ECM and it could adopt a conformation as described by Figure 1-5(C).

Sequence alignment of the third fibronectin domain of NrCAM to other members of the L1CAM family.

NrCAM (rat)	A	P	G	N	V	R	V	S	V	V	N	S	T	L	A	E	A	H	W	D	P	-	V	P	P	K	S	V
L1 (rat)	S	P	E	L	E	D	I	T	I	F	N	S	S	T	V	L	V	R	W	R	P	-	V	D	L	A	Q	V
Neurofascin 155 (rat)	A	P	T	E	V	K	I	R	V	L	N	S	T	A	I	S	L	Q	W	N	R	-	V	Y	P	D	T	V
CHL1 (rat)	A	P	V	I	Q	R	V	D	V	M	N	S	T	L	V	K	V	T	W	S	S	-	I	P	K	E	T	V
NgCAM (L1 in chick)	Y	P	E	N	V	G	V	E	L	L	N	S	S	T	V	R	V	R	W	T	L	G	G	G	G	P	K	E
Conserved residues		**P**					**Φ**		**Φ**		**N**	**S**							**W**									

NrCAM (rat)	R	G	H	L	Q	G	Y	R	I	Y	Y	W	K	A	Q	S	S	S	K	R	N	R	R	H	I	E	K	K
L1 (rat)	K	G	H	L	R	G	Y	N	V	T	Y	W	W	K	G	S	Q	R	K	H	S	K	R	H	V	H	K	S
Neurofascin 155 (rat)	Q	G	Q	L	R	E	Y	R	A	Y	Y	W	R	E	S	S	L	L	K	N	L	W	V	S	Q	K	R	Q
CHL1 (rat)	H	G	L	L	R	G	Y	Q	I	N	W	W	K	T	K	S	L	L	D	G	R	T	H	P	K	E	V	N
NgCAM (L1 in chick)	L	R	R	L	R	G	F	R	V	L	Y	W	R	L	G	W	V	G	E	R	S	R	R	Q	A	P	P	D
Conserved residues				**L**	**+**							**W**																	

NrCAM (rat)	-	-	-	-	-	-	-	-	-	-	-	-	-	-	-	-	-	-	I	L	T	F	Q	G	S	K	T	H
L1 (rat)	-	-	-	-	-	-	-	-	-	-	-	-	-	-	-	-	-	-	H	M	V	V	P	A	N	T	T	S
Neurofascin 155 (rat)	-	-	-	-	-	-	-	-	-	-	-	-	-	-	-	-	-	-	Q	A	S	T	P	G	D	R	P	R
CHL1 (rat)	-	-	-	-	-	-	-	-	-	-	-	-	-	-	-	-	-	-	I	L	R	F	S	G	Q	R	N	S
NgCAM (L1 in chick)	P	P	Q	I	P	Q	S	P	A	E	D	P	P	P	F	P	P	V	A	L	T	V	G	G	D	A	R	G
Conserved residues																													

NrCAM (rat)	G	M	L	P	G	L	Q	P	Y	S	H	Y	V	L	N	V	R	V	V	N	G	K	G	E	G				
L1 (rat)	A	I	L	S	G	L	R	P	Y	S	S	Y	H	V	E	V	Q	A	F	N	G	R	G	L	G				
Neurofascin 155 (rat)	G	V	V	G	R	L	F	P	Y	S	N	Y	K	L	E	M	V	V	V	N	G	R	G	D	G				
CHL1 (rat)	G	M	V	P	S	L	D	P	F	S	E	F	H	L	T	V	L	A	Y	N	S	K	G	A	G				
NgCAM (L1 in chick)	A	L	L	G	G	L	R	P	W	S	R	Y	Q	L	R	V	L	V	F	N	G	R	G	D	G				
Conserved residues						**L**		**P**		**S**										**N**			**G**		**G**				

Figure 1-6. Sequence alignment of the third FNIII-like domain of all four rat L1-CAM family members and NgCAM of chick. Highlighted in yellow are common trypsin cleavage sites, in red font is the plasmin(ogen) cleavage site of mammalian L1 and boxed areas are furin cleavage sites of NgCAM and NrCAM. Accession numbers are NrCAM P97686, L1 S36126, neurofascin AAL27854, CHL1 CAA63972 and NgCAM A37967.

1.4.3.4 Furin cleavage.

Furin is a ubiquitously expressed 794 amino acid type 1 membrane protein that has been found in all vertebrate cell lines and tissues examined (Nakayama, 1997). It is a member of the proprotein convertase family and is involved in the cleavage of proproteins to their active form. Proproteins cleaved by furin include human integrin

α_3 and α_6 chains and the L1-CAM member in leech Tractin (Lehmann *et al.*, 1996) (Xu *et al.*, 2003). At steady state, furin is localised principally in the trans-Golgi network (TGN) were it cycles between the sorting compartment, the cell surface and the early endosomes (Nakayama, 1997; Molloy *et al.*, 1999; Thomas, 2002). Furin cleavage can occur at the cell surface, in the endocytic pathway and in the TGN/biosynthetic pathway (Nakayama, 1997; Thomas, 2002). Furin normally cleaves after the carboxy terminus of the last arginine of the consensus sequence -R-X-K/R-R and this motif can be found in the third FNIII-like domain of chick and mammalian NrCAM (Nakayama, 1997; Thomas, 2002) (Figure 1-6, boxed). Furin cleavage has not been studied in NrCAM however tractin also has the furin cleavage motif RKRRSR in its third FNIII-like domain (Xu *et al.*, 2003). Tractin is constitutively cleaved in a furin dependent process so that the full length molecule never reaches the plasma membrane (Xu *et al.*, 2003). This gives rise to a heterodimer consisting of the N-terminus and the C-terminus of the molecule that bind to each other through non covalent interactions (Xu *et al.*, 2003). It is currently believed that furin is the principal protease responsible for NrCAM's cleavage (Grumet, 1997) and that NrCAM adopts a conformation described by Figure 1–5 (B).

1.5 NrCAM in myelinated neurons.

In mature neurons NrCAM is normally found at sites of Na^+ channel clustering, namely the nodes of Ranvier and the initial segment (Davis *et al.*, 1996; Jenkins and Bennett, 2001) (Figure 1-7 and Figure 1-8).

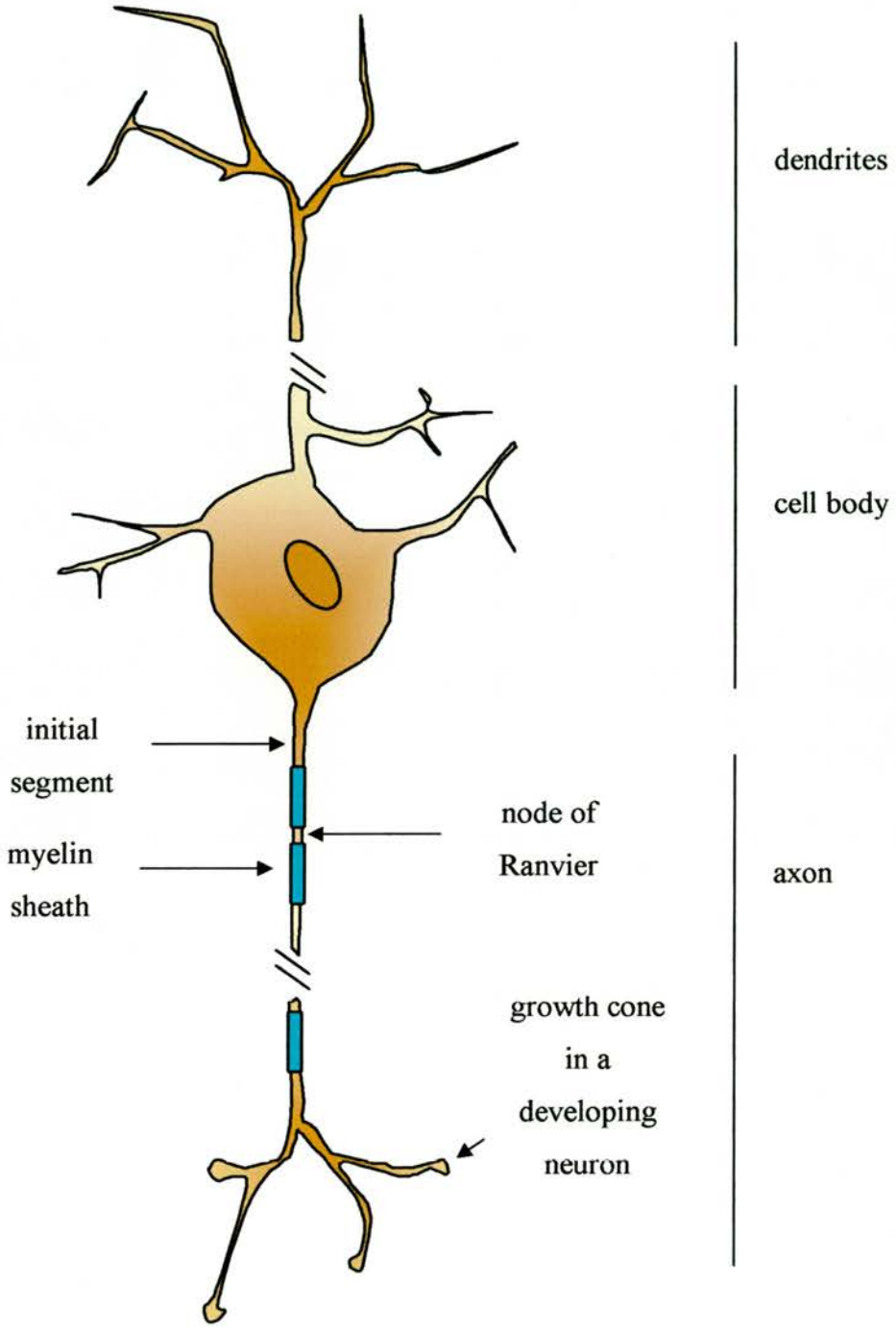

Figure 1-7. An illustration of NrCAM expression in a neuron. NrCAM is found at the initial segment, the nodes of Ranvier and in growth cones. More detailed pictures of the node of Ranvier and Growth cone are in Figure 1-8 and Figure 1-10 respectivley.

1.5.1 Nodes of Ranvier.

Gaps in the myelin sheath surrounding neurons were first discovered by light microscopy by Ranvier in 1874 and have become known as nodes of Ranvier (Rosenbluth, 1999). The node is essential for saltatory conduction and is rich in cell adhesion molecules, ion channels and scaffolding proteins. NrCAM is one of the pioneer molecules that play a role in the development of the node in the immature animal.

1.5.1.1 Myelination and saltatory conduction.

Myelination has evolved as a means of increasing the conduction velocity of nerves. Myelin consists of a stack of specialised plasma membrane sheets that is produced by a glial cell that wraps itself around an axon. In the PNS the glial cells are Schwann cells and in the CNS they are oligodendrocytes. The high phospholipid content of the myelin sheath insulates the axon and reduces the ability of current to leak out of the axon. At regular intervals along the axon shaft there are gaps in the myelin sheath called nodes of Ranvier, where Na^+ channels are clustered at high densities. These nodes are in direct contact with the extracellular fluid thus allowing the flow of ions out of the axon. The result is a restriction of current flow to the nodes. When an action potential is generated at one node of Ranvier it elicits a current that flows passively along a myelinated segment until the next node of Ranvier. The local current flow then generates an action potential in the neighbouring segment, and the cycle is repeated along the length of the axon. The excitation jumps from node to node and thus increases the conduction velocity of the

axon (Salzer, 1997; Arroyo and Scherer, 2000; Salzer, 2003). This process is called saltatory (from the Latin verb saltare to jump) conduction and was first described by Tasaki (1939) and Huxley and Staempfli (1949) (Rosenbluth, 1999).

1.5.1.2 Regions within myelinated nerves.

After myelination the axon can be divided into four domains:

(1) The internode. This is the part of the axon covered in compact myelin.

(2) The paranode. Here the tightly wrapped glial myelin of the internode expands at its extremities to form cytoplasm filled paranodal loops. The axon is connected to the ends of these paranodal loops by septate like junctions (Figure 1-8).

(3) The juxtaparanode. This is the region between the internode and paranode (Figure 1-8).

(4) The node itself. Here Na^+ channel clustering occurs. It is opposed by Schwann cell microvilli in the PNS or an astrocytic process in the CNS (Salzer, 1997) (Figure 1-8). NrCAM is found within the plasma membrane (axolemma) of the node.

Multiple cell adhesion molecules have been identified within the membranes of the axon and glial cells at the node, paranode and juxtaparanode (Scherer and Arroyo, 2002). Currently it is believed that various adaptor proteins such as ankyrins, members of the 4.1 superfamily or PDZ domain containing proteins link all of these cell adhesion molecules to the cytoskeleton of their respective glial or neuronal cell (Girault and Peles, 2002; Girault *et al.*, 2003). The known cell adhesion complexes of the node, paranode and juxtaparanode are shown in Figure 1-8.

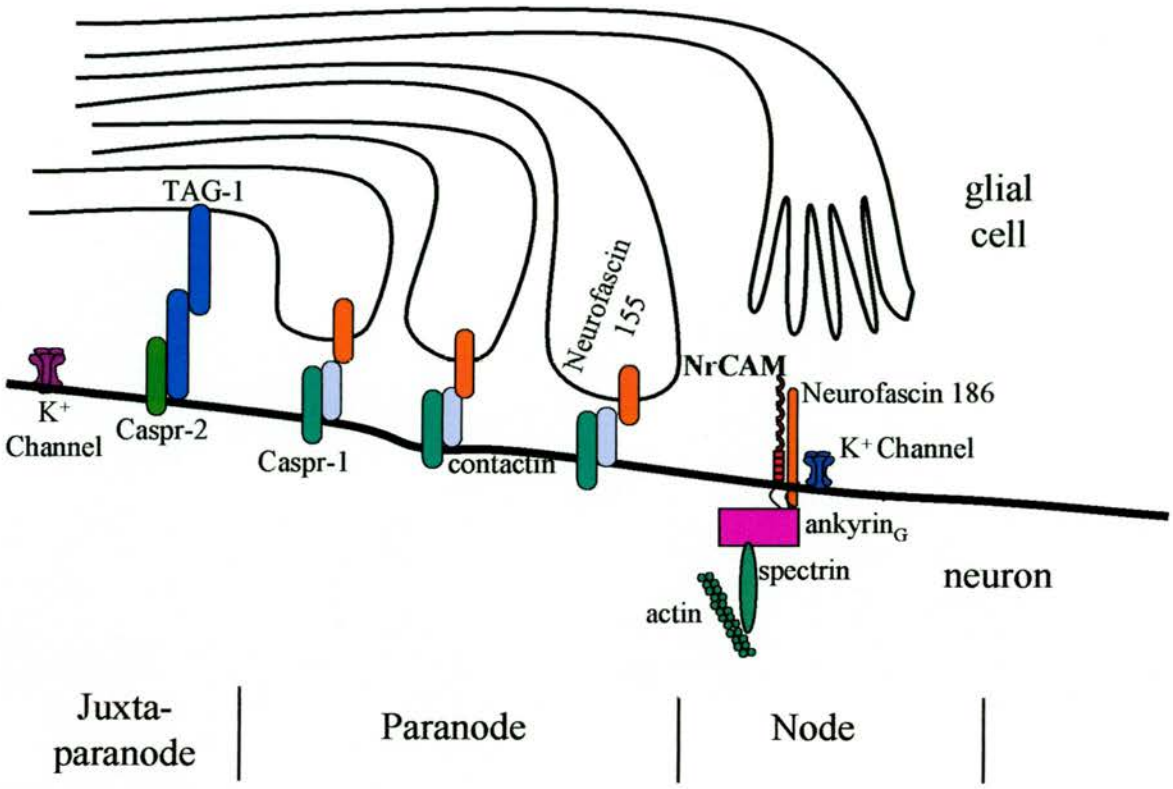

Figure 1-8. A schematic diagram of the molecular composition of the node of Ranvier in the PNS. Adapted from Trapp and Kidd (2000).

1.5.1.3 NrCAM is at the node.

The major component of the plasma membrane of the node are voltage gated Na^+ channels, namely Nav1.2 channels during axon development and Nav1.6 channels in the adult axon (Kaplan *et al.*, 2001; Girault *et al.*, 2003). The Na^+ channels are composed of a pore forming α subunit and two β subunits. The β subunit can associate with itself, tenascin R, contactin, neurofascin 186 and NrCAM (Ratcliffe *et al.*, 2001; Bhat, 2003; Salzer, 2003). In addition to Na^+ channels the nodal axolemma contains the Na^+/K^+ ATPase, Na^+/Ca^{2+} exchanger, neurofascin 186 and NrCAM (Davis *et al.*, 1996; Berghs *et al.*, 2000; Girault and Peles, 2002).

Clustered in the cytoplasm of the adult node are ankyrin$_G$ 480/270 kD and the membrane skeletal protein βIV spectrin (Kordeli *et al.*, 1995; Lambert *et al.*, 1997; Bennett and Lambert, 1999; Berghs *et al.*, 2000). Ankyrin is the only known cytoplasmic partner of NrCAM and the regulation of its binding to NrCAM is discussed in section 1.8. In the node ankyrin$_G$ binds to the β subunits of the Na^+ channels; the cytoplasmic terminus of neurofascin 186 and NrCAM, and links all of the molecules in a complex (Girault and Peles, 2002; Lemaillet *et al.*, 2003). This complex binds via ankyrin$_G$ to spectrin βIV which in turn binds to the actin cytoskeleton (Girault and Peles, 2002; Lemaillet *et al.*, 2003) (Figure 1-8). Notably NrCAM and neurofascin 186 can associate with themselves, with each other or with the β1 subunit of the Na^+ channel and so the NrCAM/neurofascin association with ankyrin$_G$ at the node could be both indirect as well as direct (Lustig *et al.*, 2001; Ratcliffe *et al.*, 2001).

1.5.1.4 NrCAM and neurofascin are important molecules in the early development of the node of Ranvier.

Independent studies show that NrCAM and neurofascin are pioneer molecules that potentially organise the subsequent clustering of Na^+ channels and ankyrins at the sites of early node formation (Lambert *et al.*, 1997; Lustig *et al.*, 2001; Custer *et al.*, 2003). During the embryonic and postnatal development of a myelinating rat neuron, both NrCAM and neurofascin cluster at early nodes of Ranvier before Na^+ channel and ankyrin$_G$ begin to cluster (Lambert *et al.*, 1997; Custer *et al.*, 2003). NrCAM null mice show a delay in Na^+ channel and ankyrin$_G$ clustering (Custer *et al.*, 2003), and neurofascin null mice are incapable of clustering Na^+ channels (personal communication, Prof. P. Brophy, University of Edinburgh). Furthermore a

NrCAM–Fc fusion protein inhibits Na^+ channel and ankyrin clustering at nodes of Ranvier by binding to and clustering neurofascin (Lustig *et al.*, 2001). Thus neurofascin is necessary for, and NrCAM enhances, the Na^+ channel clustering at the node of Ranvier.

1.5.2 NrCAM at initial segments.

The initial segment is the site at which synaptic inputs are integrated and the action potential is initiated. Therefore voltage-dependent Na^+ channels are also localised at high density at the initial segment of the axon. Molecules that are co-localised with Na^+ channels at initial segments are similar to those found at the node, and include βIV spectrin, $ankyrin_G$, neurofascin and NrCAM (Salzer, 2003). However unlike the node, the initial segment of some CNS neurons have Kv1.1 and Kv 1.2 channels (Salzer, 2003).

NrCAM's role in the initial segment is as yet unknown. It appears at postnatal day 9 in Purkinje neuron initial segments. This is 7 days after the first appearance of $ankyrin_G$ and βIV spectrin in the initial segment of the Purkinje neuron (Jenkins and Bennett, 2001). Furthermore it is not clustered at initial segments in mice deficient in $ankyrin_G$ (Jenkins and Bennett, 2001). Thus NrCAM is an unlikely candidate to initiate protein assembly at initial segments. However it may be necessary for stabilising the Na^+ channel/$ankyrin_G$/spectrin βIV complex after clustering.

1.6 Growth cones.

"...a concentration of protoplasm of conical form, endowed with amoeboid movements" Cajal.

1.6.1 Defining the growth cone.

Axons emerge from neuroblasts, elongate and grow towards their postsynaptic targets. The tips of these growing axons expand to form growth cones and were first identified by Ramón y Cajal, in the 19th century, as the region of the axon responsible for navigation towards a target (Sotelo, 2002).

1.6.2 Growth cone guidance.

Growth cones of axons are guided by a variety of cues that are attractive or repulsive to the growth cone. Long-range guidance cues consist of factors secreted by a target cell and short-range clues operate by contact mediated mechanisms between receptors on the growth cone and ligands on either the ECM or other cells (Tessier-Lavigne and Goodman, 1996). NrCAM can act as both a short-range guidance clue and as a receptor in the growth cone (Grumet, 1997).

The structures and regions of the growth cone are described by Figure 1-9. Filopodia are narrow finger like extensions of the growth cone that are capable of extending tens of microns from the leading edge of the growth cone (Dent and Gertler, 2003). They are highly dynamic structures that expand and contract at rapid rates as well as having side-to-side movement (Wood and Martin, 2002). Lamellipodia (membrane ruffles) are flattened fan like membranous extensions at the leading edge of the growth cone that expand and contract as the growth cone advances (Bamburg, 2003). There are three regions in the growth cone, the

peripheral (P) domain, which contains the filopodia and lamellae, the central domain (C), which contains the vesicles and organelles of the growth cone and the transitional (T) domain, which acts as interface between the P and C domains (Bamburg, 2003; Dent and Gertler, 2003).

The shape and movement of the growth cone, its lamellipodia and filopodia depend on the underlying cytoskeleton (Bamburg, 2003; Dent and Gertler, 2003). F-actin forms two types of actin structures in the growth cone: bundles of polarised F-actin that extend from the filopodia as far as the T region; and a meshwork like array that fills the bulk of the P region (Bamburg, 2003; Dent and Gertler, 2003). Recruitment and activation of myosin lead to the retrograde flow of F-actin from the leading edge of the growth cone to wards the C domain (Lin *et al.*, 1996; Cramer, 1997; Suter and Forscher, 1998). Polymerisation of actin occurs near the leading edge of the growth cone and depolymerisation at the back of the network, and this results in a treadmilling of actin (Suter and Forscher, 1998). In one model of growth cone advance cell adhesion molecules, for example NrCAM, bind to this retrogradly moving actin network, while simultaneously binding to extracellular molecules (Faivre-Sarrailh *et al.*, 1999; Falk *et al.*, 2004). This has the effect of slowing the rate of retrograde movement of the actin cytoskeleton and as polymerisation continues at the leading edge the growth cone advances (Mitchison and Kirscher, 1988; Lin and Forscher, 1995; Welch *et al.*, 1997).

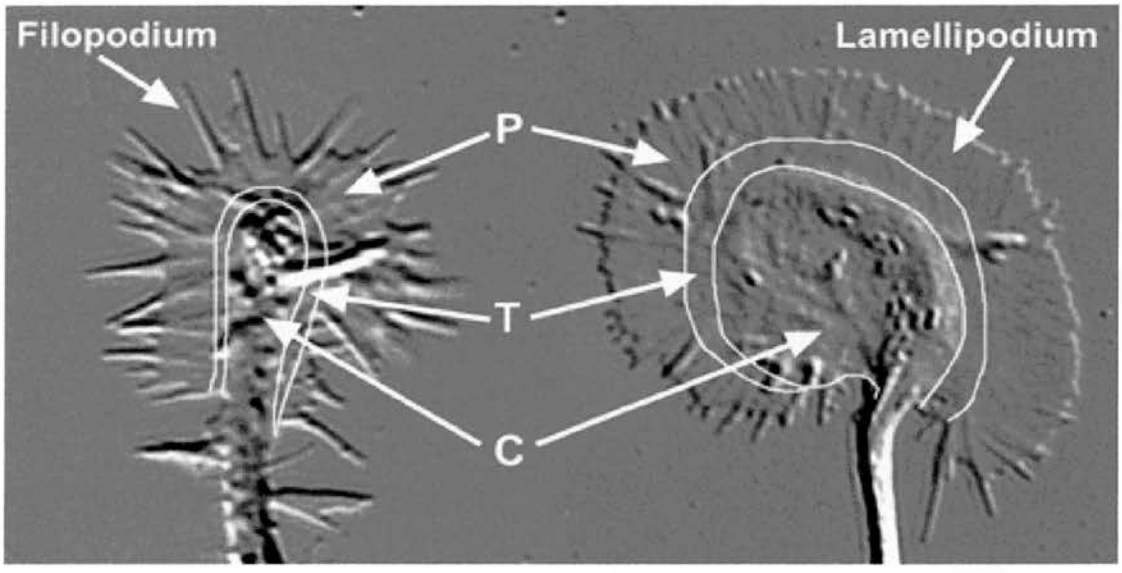

Figure 1-9. The structure of growth cones. P is the peripheral domain, C is the central domain and T is the transitional domain. Picture from Dent and Gertler, 2003.

The binding of the cell adhesion molecule to its extracellular ligand as well as acting as a stabilising force for the growth cone also triggers localised intracellular signalling cascades that can effect the movement and turning of the growth cone (Jay, 1996). These signalling cascades include: localised calcium concentration increases (Doherty *et al.*, 2000; Dunican and Doherty, 2000), the activation of mitogen-activated protein kinase (MAPK) cascades (Doherty *et al.*, 2000), tyrosine phosphorylation of the cell adhesion receptor for example by src kinases (Jay, 2001; Suter and Forscher, 2001), activation of the small GTPases of the RHO family (Dickson, 2001) and localised protein synthesis within the growth cone (Dickson and Senti, 2002).

Attachment of the retrogradly moving cytoskeleton translocates the cell adhesion molecule from the P domain to the C domain. Studies on L1 have shown that L1 in the C-domain is endocytosed and transported along microtubules to the P-domain where it is reinserted into the plasma membrane (Kamiguchi *et al.*, 1998b;

Kamiguchi and Lemmon, 2000b). Notably the endocytosis of L1 is essential for MAPK activation and is mediated by $pp60^{src}$ (Schmid *et al.*, 2000).

1.7 The ectodomain interactions of NrCAM.

Most of NrCAM's known binding partners are to its ectodomain. These interactions can be both homophilic and heterophilic, *in cis* and *in trans* (Mauro *et al.*, 1992; Suter *et al.*, 1995; Sakurai *et al.*, 1997). As with most members of the IgCAM family homophilic interactions are Ca^{2+} and Mg^{2+} independent (Mauro *et al.*, 1992). NrCAM can act as both a ligand for receptors in growth cones and as a receptor in growth cones (Grumet, 1997). NrCAMs extracellular binding partners include axonin-1/TAG-1/TAX-1, F11/contactin/F3, Receptor protein tyrosine phosphatase β (RPTPβ) and neurofascin (Figure 1-10).

1.7.1 NrCAM and axonin-1/TAG-1 interactions guide neurons.

NrCAM and L1 are both binding partners of axonin-1 a member of the F11 family of IgCAMs (Figure 1-1) (Suter *et al.*, 1995; Sonderegger, 1997; Lustig *et al.*, 1999; Pavlou *et al.*, 2002). The NrCAM to axonin-1 interactions are complex and depend on the molecules tertiary structures and cellular contexts. These interactions promote cell-to-cell adherence and direct neurite outgrowth (Suter *et al.*, 1995; Fitzli *et al.*, 2000; Pavlou *et al.*, 2002). The effects of the NrCAM to axonin-1 interaction have been studied in the spinal cord of chicks. In the developing chick spinal cord NrCAM is expressed in the floor plate, which is a group of specialised glial cells at the ventral midline. Axonin-1 is expressed on commissural fibres that have cell bodies in the dorsal part of the spinal cord and extend their axons to the floor plate,

where they cross and extend longitudinally. Antibodies against either NrCAM or axonin-1 prevent approximately 50% of commissural axons from crossing the floor plate midline both *in vitro* and *in vivo* (Stoeckli, 1998; Stoeckli and Landmesser, 1998; Raper and Tessier-Lavigne, 1999). Similarly, injection of a recombinant fusion protein of NrCAMs ectodomain resulted in guidance errors for the commissural axons at the floor plate *in ovo* (Lustig *et al.*, 1999). In mice axonin-1 is known as TAG-1 and the TAG-1/NrCAM interaction plays a similar role in directing commissural axon crossing of the floor plate as it does in chicks. Murine models show that contact with the floor plate itself may be responsible for the correct localisation of NrCAM and TAG-1 in commissural neurons (Matise *et al.*, 1999). Interestingly, an NrCAM knockout mouse does not show errors in commissural fibres crossing the floor plate of the spinal cord (More *et al.*, 2001). This suggests that other molecules can compensate for NrCAM's function of directing commissural axon crossing of the spinal cord.

1.7.2 The NrCAM and F11/contactin/F3 interaction affects neurite outgrowth.

NrCAM can interact with F11 and so direct, guide, enhance and inhibit neurite outgrowth depending on the cellular context studied (Falk *et al.*, 2002). F11 is the receptor for NrCAM in tectal neurons and antibodies against NrCAM or F11 inhibit growth of chick tectal neurons on NrCAM coated substrates (Volkmer *et al.*, 1996). Conversely NrCAM serves as the axonal receptor in chick tectal neurons for immobilised F11 (Morales *et al.*, 1993; Zacharias *et al.*, 1999). In both cases the NrCAM-F11 interaction promotes both cell adherence and neurite outgrowth in the chick tectal cells (Morales *et al.*, 1993; Volkmer *et al.*, 1996; Zacharias *et al.*, 1999).

Importantly, the NrCAM–F11 interaction is dependent on the cellular and extracellular context. For instance in the presence of Tenascin-R (an ECM glycoprotein) NrCAM no longer serves as a receptor for F11 in tectal cells (Zacharias *et al.*, 1999).

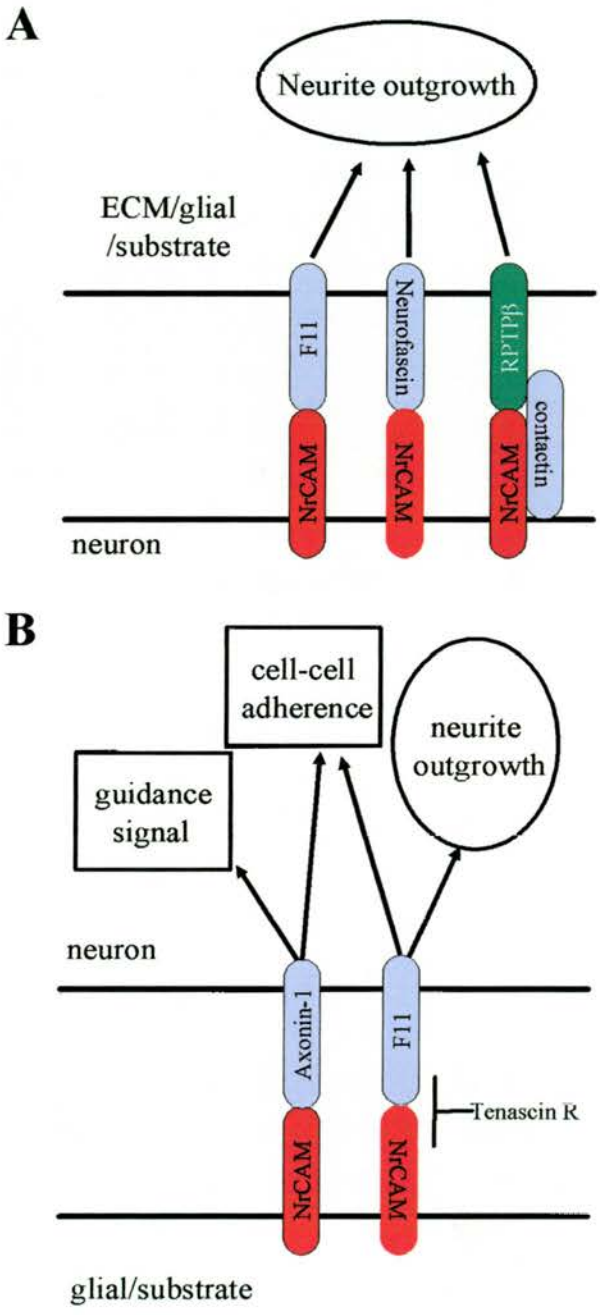

Figure 1-10. Summary of the known extracellular interactions of NrCAM and their effects, when **A)** NrCAM acts as a receptor in neurons and **B)** NrCAM is the ligand for receptors in neurons. NrCAM is shown in red. Binding partners are shown in blue or green. See text for full details.

Chick retinal neurons also express NrCAM but these neurons do not extend neurites when grown on a homogenous F11 substrate (Treubert and Brummendorf, 1998). They do however show an increased outgrowth rate on a mixed fibronectin and F11 substrate when compared to outgrowth on fibronectin alone (growth on fibronectin is generally believed to be due to integrins) (Treubert and Brummendorf, 1998). This increased rate of growth is dependent upon NrCAM binding to F11 and could be explained by NrCAM enhancing the β_1 integrin mediated outgrowth on the fibronectin substrate (Treubert and Brummendorf, 1998). So in this system the NrCAM/F11 interaction enhances but is not necessary for neurite outgrowth, and importantly suggests that NrCAM does not work alone.

NrCAM in murine cerebellar granule cells is a receptor for F3/contactin (Faivre-Sarrailh *et al.*, 1999). Granular cells from NrCAM deficient mice cannot extend neurites on a F3 substratum *in vitro* (Sakurai *et al.*, 2001). However NrCAM deficient mice do not show significant misguidance or defasciculation of parallel fibres of the cerebellum. Therefore NrCAM to F3 interaction must be compensated for by some other mechanism *in vivo* (Sakurai et al., 2001).

1.7.3 RPTPβ binds to NrCAM and contactin and forms a trimeric complex.

RPTPβ is found in radial glial cells and astrocytes that are implicated in axon guidance. Three isoforms exist and consist of two membrane receptor isoforms and a soluble form commonly known as phosphacan (Sakurai *et al.*, 1996). RPTPβ/phosphacan interacts with contactin via the carbonic anhydrase domain and acts as a ligand to stimulate neurite outgrowth (Volkmer, 2001). Associated NrCAM and contactin in tectal neurons act as a receptor for RPTPβ/phosphacan (Sakurai *et*

al., 1997). Thus a trimeric complex is formed between NrCAM, contactin and RPTPβ that stimulates the outgrowth of the neuron (Figure 1-10(A)). Interestingly neurofascin can take NrCAM's binding site in the RPTPβ/contactin complex when NrCAM is absent (Sakurai *et al.*, 1997). The C-domain of RPTPβ co-immunoprecipitates with contactin and NrCAM in wild type mice but in NrCAM deficient mice RPTPβ co-immunoprecipitates with contactin and a 150 kDa neurofascin band (Sakurai *et al.*, 1997).

1.7.4 Interaction of NrCAM and neurofascin.

NrCAM binds to neurofascin and co-precipitates with immunoprecipitated neurofascin from embryonic chick retinae (Volkmer *et al.*, 1996). NrCAM acts as receptor for neurofascin in tectal neurons and induces neurite outgrowth (Volkmer *et al.*, 1996).

1.8 NrCAM has only one known cytoplasmic interaction.

While various binding partners for the ectodomain of NrCAM have been found only one binding partner of the cytoplasmic terminus has been discovered to date. Davis and Bennett reported that NrCAM as well as L1 and neurofascin could associate with ankyrins, a family of spectrin binding proteins (Davis and Bennett, 1994).

1.8.1 L1-CAMs bind to ankyrin proteins at a highly conserved amino acid sequence.

The conserved cytoplasmic termini of L1-CAM family members includes a binding site for ankyrins that is considered so important it is now one of the defining criteria of what makes a L1-CAM family member (Hortsch, 2003). Ankyrins are a family of cytoplasmic proteins that couple membrane proteins, such as voltage gated Na^+ channels and the Na^+/K^+ anion exchanger to the spectrin-actin cytoskeleton (Davis and Bennett, 1994; Bennett and Chen, 2001; Hrniewicz-Janowska *et al.*, 2002). The family includes three genes coding for ankyrin$_G$, ankyrin$_B$ and ankyrin$_R$, all of which have multiple splice variants (Bennett and Chen, 2001; Mohler *et al.*, 2002). 480/270-kD ankyrin$_G$ and 440/220-kD ankyrin$_B$ are the major isoforms expressed in the developing nervous system. The membrane-binding domain of ankyrins contains multiple domains called ank repeats and it is here that there are two high affinity binding sites for L1-CAMs (Michaely and Bennett, 1995; Bennett and Chen, 2001). Therefore ankyrins can link two L1-CAMs to ion channel proteins and couple these to the spectrin cytoskeleton. This is especially important in the formation of initial segments and nodes of Ranvier (Jenkins and Bennett, 2001; Lustig *et al.*, 2001).

Evidence from knockout mice demonstrates the importance of the L1-CAM and ankyrin interactions *in vivo*. In L1 knockout mice, ankyrin-B expression is reduced, suggesting that L1 may be involved in the regulation of the ankyrin-B gene, or the maintenance of the protein's stability (Wiencken-Barger *et al.*, 2004). Analysis of NrCAM deficient mice and ankyrin$_B$ deficient mice show disorganised lens fibres at P1 that are virtually indistinguishable from each other, suggesting that they are both essential for the correct development of the lens in mice (More *et al.*, 2001).

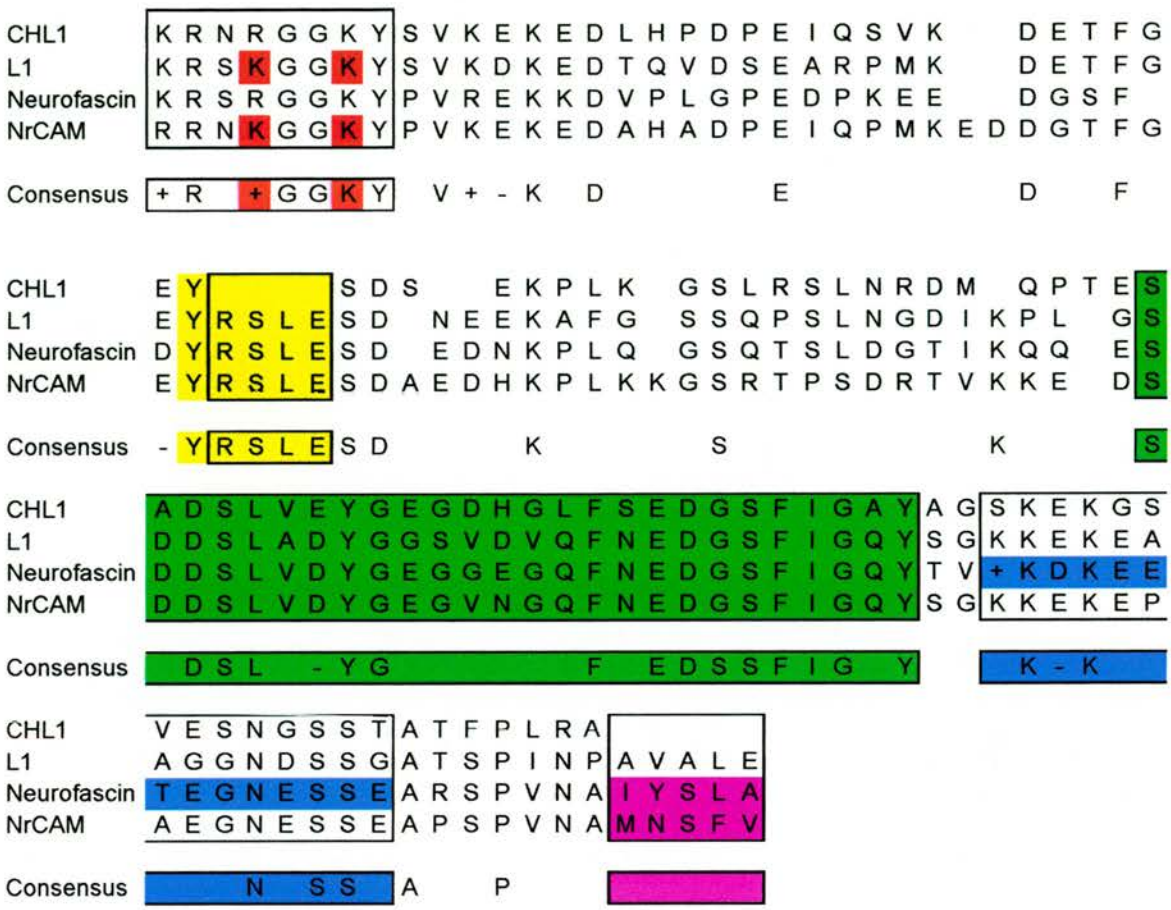

Figure 1-11. Alignment of the cytoplasmic terminus of the L1-CAM family. Shown in green is the ankyrin binding domain common to all family members, in blue is the FERM binding domain of neurofascin, in yellow are important residues for AP-2 binding in L1, in pink are the amino acids of the class 1 PDZ domains and in red are the important lysines in for cytoskeletal binding in L1.

Ankyrin binds to a 25-30 amino acid sequence in the L1-CAM family cytoplasmic termini that contains the motif SFIGQY (Garver *et al.*, 1997; Zhang *et al.*, 1998a) (Figure 1-11). This sequence has been highly conserved from invertebrates to vertebrates. The amino acids that have been shown to be necessary for ankyrin binding have been marked in red in Figure 1-12, two are aromatic phenylalanines and one is a negatively charged glutamic acid residue. The other two marked residues are the serine and tyrosine of the SFIGQY motif. Both of these residues are

commonly found mutated in patients with CRASH syndrome (Saugier-Veber *et al.*, 1998). The serine is mutated to a leucine and the tyrosine to a histidine in CRASH syndrome and both these mutations reduce the ability of L1 to recruit green fluorescent protein tagged ankyrin$_G$ (ankyrin$_G$-GFP) to the membrane of human embryonic kidney cells (Needham *et al.*, 2001). Similarly in neurofascin, mutation of the SFIGQY tyrosine to alanine, glutamic acid or histidine, reduced or eliminated the receptors ability to recruit ankyrin$_G$-GFP, however mutation of the tyrosine to a phenylalanine had no effect on ankyrin$_G$-GFP recruitment (Zhang *et al.*, 1998b).

Protein	Species																														
CHL1	Human	S	A	D	S	L	V		E	Y	G	E	G			D	H	G		L		F	S	E	D	G	S	F	I	G	A	Y
CHL1	Mouse	S	A	D	S	L	V		E	Y	G	E	G			D				Q	S	I	F	N	E	D	G	S	F	I	G	A	Y
L1	Human, primate,rat & mouse	S	D	D	S	L	A		D	Y	G		G	S	V	D		V		Q			F	N	E	D	G	S	F	I	G	Q	Y
NgCAM	Chicken (L1 homolog)	S	E	D	S	L	A		G	Y	G		G	S	G	D		V		Q			F	N	E	D	G	S	F	I	G	Q	Y
Neurofascin	Human, rat, mouse & chick	S	D	D	S	L	V		D	Y	G	E	G		G	E		G		Q			F	N	E	D	G	S	F	I	G	Q	Y
NrCAM	Human, rat, mouse & chick	S	D	D	S	L	V		D	Y	G	E	G		V	N		G		Q			F	N	E	D	G	S	F	I	G	Q	Y
	Conserved	S	-	D	S	L	V/A	-	Y	G	E	G	S	V/G		-/+		V/G	G	Q			F	N	E	D	G	S	F	I	G	A/Q	Y

Figure 1-12. The amino acids for the ankyrin binding site of the L1-CAM vertebrate family.

1.8.2 Tyrosine phosphorylation inhibits ankyrin binding to L1-CAMs.

Importantly phosphorylation of the SFIGQY tyrosine residue abolishes ankyrin binding to both neurofascin (Garver *et al.*, 1997; Tuvia *et al.*, 1997) and L1 (Gil *et al.*, 2003). Tyrosine phosphorylation of L1-CAMs is necessary for the development and growth of the embryonic brain. General NrCAM tyrosine phosphorylation in developing rat brain is at a maximum during the embryonic stages of the developing rat brain reducing to approximately one third of embryonic levels when the rat reaches maturity (Garver *et al.*, 1997). During development of the neonatal cerebellum granule cells migrate from their site of proliferation via the external germinal layer (EGL) and the molecular layer (ML) to the internal granule cell layer

(IGL). FIGQY phosphorylated L1-CAMs are found in the EGL and ML (pre migratory and migratory cells) and to a much lesser degree in the IGL (post migratory cells) (Jenkins *et al.*, 2001).

1.8.3 The role of ankyrin$_B$ in the growth cone.

Currently, ankyrin$_G$ is thought to be important in stabilising structures such as the node of Ranvier but ankyrin$_B$ plays a more dynamic role in structures such as growth cones (Melendez-Vasquez *et al.*, 2001). As discussed in section 1.6.2, NrCAM and L1 are bound to the retrogradely moving cytoskeleton of the growth cone. Studies of neurite initiation in DRG neurons show that ankyrin$_B$ can bind to the retrogradely moving cytoskeleton and initiate neuritogenesis via its interaction with unphosphorylated L1 (Nishimura *et al.*, 2003). However whether this binding between L1, ankyrin and retrogradely moving cytoskeleton continues as the growth cone develops is unclear. Studies in neuroblastoma cell lines show that ankyrin$_B$ does not bind to the retrogradely moving cytoskeleton, instead it restricts unphosphorylated L1 to a non-dynamic cytochalasin D insensitive pool of actin (Figure 1-13) (Gil *et al.*, 2003). Phosphorylated L1 is bound to the retrogradly moving cytoskeleton via an unknown mechanism. Therefore it is hypothesised that there is at least one other molecule that can link L1 (and presumably NrCAM) to the retrogradly moving cytoskeleton in growth cones. The most popular candidates in the literature for this protein are: α-actinin, proteins of the 4.1 superfamily and proteins with class 1 PDZ domains.

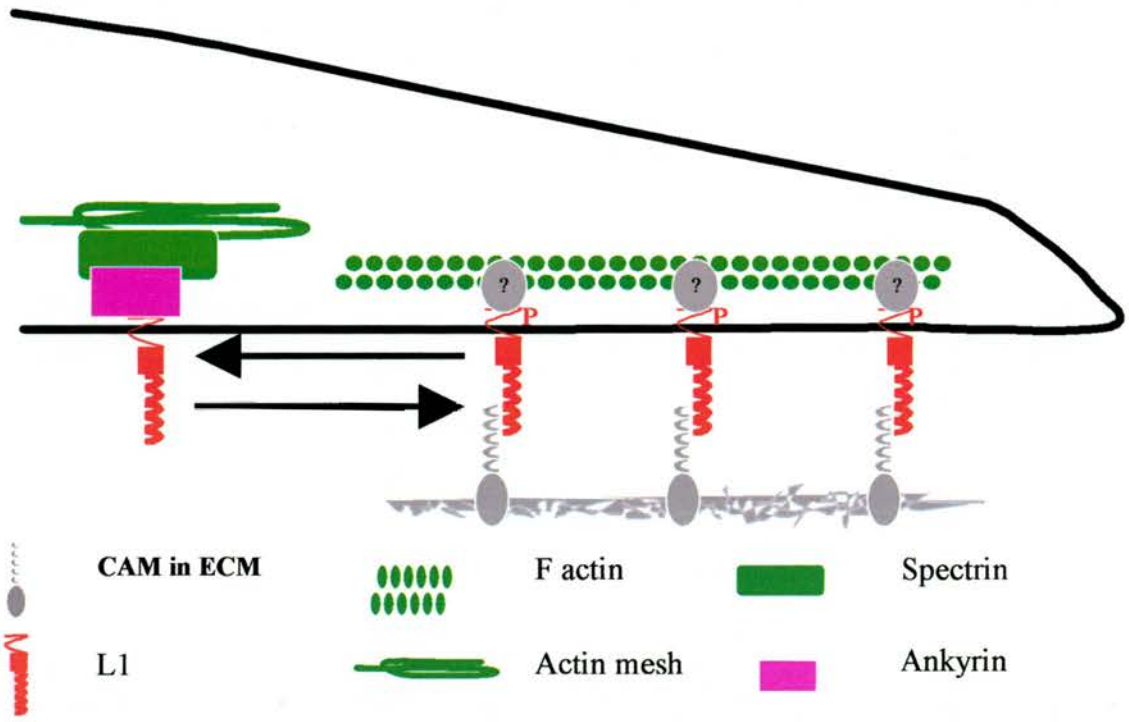

Figure 1-13. A proposed model of L1 and ankyrin$_B$ binding in growth cones (Gil *et al.*, 2003). Ankyrin$_B$ binding to unphosphorylated L1 in the growth cone is a stabilising adherent interaction that links L1 to the actin meshwork via spectrin. Tyrosine phosphorylation of L1 at the SFIGQY motif inhibits ankyrin binding and allows L1 molecules to bind to the retrogradly moving actin cytoskeleton via an unknown mechanism.

1.9 The first seven amino acids of the cytoplasmic terminus of L1 are sufficient to tether it to the actin/myosin cytoskeleton.

In B28 glioma cells the L1 cytoskeletal anchorage, its cell surface expression and organisation, all depend on its cytoplasmic terminus rather than its ectodomain (Dahlin-Huppe *et al.*, 1997). This anchorage to the cytoskeleton is mediated through the first seven amino acids of the cytoplasmic terminus, namely KRSKGGK, of which the seventh, and to a lesser extent, fourth lysine are the most important for cytoskeletal anchorage (Dahlin-Huppe *et al.*, 1997). NrCAM's first seven amino acids are RRNKGGK and it shares the important lysine residues (Figure 1-11, red highlight). It has been suggested that this domain may be responsible for the

recruitment of α-actinin to NrCAM in the lamellipodia of B104 cells in regions where it binds to TAG-1 covered beads (Falk *et al.*, 2004).

1.10 L1-CAMs bind to the cytoskeleton via 4.1 superfamily members.

The 4.1 superfamily of include 4.1, ezrin, radixin, moesin, merlin, MIR and willin (Bretscher *et al.*, 2000, Gunne-Moore, unpublished results). The C-terminal domain of 4.1 superfamily proteins binds directly to actin filaments, whilst the N-terminal either 1). binds directly to transmembrane glycoproteins or 2). binds indirectly to membrane proteins via adaptor molecules such as ERM-binding phosphoprotein 50 (EBP50)/Na^+/H^+ exchange-regulatory factor (NHERF) (Chishti *et al.*, 1998; Bretscher *et al.*, 2000). This N-terminal binding is via a protein domain called the 4.1/ezrin/radixin/moesin (FERM) domain (Chishti *et al.*, 1998; Bretscher *et al.*, 2000). 4.1 superfamily proteins concentrate in and are involved in the formation and functioning of microvilli, filopodia, membrane ruffles and cell adhesion sites (Bretscher *et al.*, 2000).

1.10.1 The 4.1 superfamily has an important role in growth cones and development of the nervous system.

Radixin and moesin have important roles in neuronal growth cones. In chicks removing radixin interferes with growth cone form and function. Radixin staining is localised to the leading edge in chick neuron growth cones and its expression is reduced during growth cone collapse (GonzalezAgosti and Solomon, 1996). Microscale chromophore assisted laser inactivation of radixin in chick DRG growth cones causes a 30 % reduction in lamellipodia size (Castelo and Jay, 1999). In rat

double suppression of both moesin and radixin, protein synthesis is necessary to interfere with the structure and dynamics of rat cultured neurons (Paglini *et al.*, 1998) suggesting redundancy between both proteins functions.

1.10.2 Ezrin binds to L1 and neurofascin, and co-localises with NrCAM.

The cytoplasmic terminus of L1 contains a neuronal-specific amino acid sequence, RSLE and this sequence is essential for the sorting of L1 to the axonal growth cone (Kamiguchi *et al.*, 1998b) (Figure 1-11, yellow highlight). A yeast two-hybrid screen has shown that the first 406 amino acids of ezrin (encoding the FERM domain) binds to a region of the cytoplasmic terminus of the neuronal L1 isoform. This is after the membrane spanning region and up to, but not including, the ankyrin domain (Dickson *et al.*, 2002).

Both ezrin and willin have been pulled out of a sciatic nerve cDNA library using the C-terminus of neurofascin as bait. Retesting of the ezrin and willin clones showed that the interaction was between the FERM domain of ezrin/willin and a RKDKEETEGNESSE sequence just C-terminal of the ankyrin binding sequence of of neurofascin (unpublished results Gunn-Moore *et al)* (Figure 1-11, blue highlight). Though the binding of NrCAM to ezrin has not yet been proven, NrCAM co-localises in membrane protrusions with both actin and ezrin in KTCTL60 cells (Conacci-Sorrell *et al.*, 2002).

1.11 NrCAM has a class 1 PDZ binding motif.

NrCAM has a class 1 PDZ domain and so proteins such as PSD-95 have been suggested as possible binding partners (Davis *et al.*, 1996). PDZ domains are named after the first three proteins in which a PDZ domain was identified: PSD-95, DLG and ZO-1. They are sometimes called GLGF proteins after four critical residues in their ligand-binding site. They are rare in non-metazoans and may have evolved with multi-cellularity (Harris and Wendell, 2001).

PDZ Domain	Consensus binding sequence
Class 1	S/T - X - Φ
Class 2	Φ - X - Φ
Class 3	X - X - Φ
Class 4 (Other)	X - X - X

Figure 1-14. The system used to classify PDZ binding motifs per Harris and Wendell (2001).

PDZ domain containing proteins are nearly always located near the plasma membrane and are usually restricted to specific membrane regions such as synapses or regions of cell-cell contact. They function mainly in the organisation and clustering of signalling complexes at the plasma membrane and the maintenance of cell polarity; but occasionally have their own signalling capabilities (Fanning and Anderson, 1999; Rongo, 2001). However, some PDZ domain containing proteins have a more dynamic distribution and are believed to traffic their interacting proteins within the cell (Sheng and Sala, 2001).

The globular PDZ domain consists of approximately 80-90 amino acids, folded into six β-strands and two α-helices (Fanning and Anderson, 1999; Harris and Wendell, 2001; Sheng and Sala, 2001). PDZ domains recognise four to eight C-terminal amino acid motifs of transmembrane molecules, such as cell adhesion

molecules and ion channels (Fanning and Anderson, 1999; Harris and Wendell, 2001; Sheng and Sala, 2001). Very occasionally they can recognise non C-terminal amino acid residues that have folded into a sharp β-turn that mimics a carboxyl terminus (Hillier *et al.*, 1999).

The residues of a PDZ binding motif are numbered from the C- terminal residue (P_0) in the direction of the N-terminus (P_{-1}, P_{-2}, P_{-3} P_{-4} etc.) (Fanning and Anderson, 1999; Harris and Wendell, 2001). In general the P_0 and P_{-2} residues are considered most critical for PDZ domain recognition of the membrane receptor and this is the basis of the current classification system of PDZ binding motifs (Figure 1-15) (Fanning and Anderson, 1999).

Under this system NrCAM has a class 1 PDZ binding motif. In a class 1 PDZ domain the P_0 residue of the ligand points directly into the base of a large hydrophobic pocket, and the size of this pocket determines what residue it prefers in this position. For example EBP50's P_0 pocket of its first PDZ domain is larger than normal and this may explain its preference for a leucine residue at P_0. (Harris and Wendell, 2001; Sheng and Sala, 2001). The P_{-2} residue fits into a pocket containing a histidine, the N-3 nitrogen of which can hydrogen bond to the hydroxyl group of either a serine or threonine of the ligand (Harris and Wendell, 2001; Sheng and Sala, 2001).

Protein	**P_{-4} - P_{-3} - P_{-2} - P_{-1} - P_0 - COOH**	**PDZ Class**
NrCAM	M - N - S - F - V - COOH	Class 1
Neurofascin	I - Y - S - L - A - COOH	Class 1
L1	A - V - A - L - E - COOH	No PDZ binding
CHL1	F - P - L - R - A - COOH	Class 2

Figure 1-15. Classification of the PDZ binding domains of the vertebrate L1-CAM family members per Harris and Wendell (2001).

Chapter 2: Methods and procedures.

All products were obtained from Sigma unless otherwise stated. See appendix 1 for a list of suppliers.

2.1 Molecular biology and cloning procedures.

2.1.1 Polymerase chain reaction (PCR).

PCR was performed using pfuTURBO® DNA polymerase (Stratagene) in accordance with the manufacturer's instructions in the buffer supplied together with 200 μM dNTPs (Promega), 0.5 μM forward and reverse primers (Invitrogen) and a 10 ng template.

2.1.2 Agarose gel electrophoresis and gel purification.

Linearised plasmid DNA, PCR products, and DNA fragments produced by restriction digests were separated based on molecular weight using agarose gel electrophoresis. Agarose was melted in tris-borate ethylenediamine-tetraacetic acid buffer (TBE) buffer (0.45 M Tris-borate, 10 mM EDTA, pH 8.3) and ethidium bromide was added to a final concentration of 0.5 μg/ml and poured into and set in a AGTI submarine gel casting apparatus unit (VWR). 20 % 6X agarose gel loading buffer (50 % glycerol, 49.75 % TBE and 0.25 % bromophenol blue) was added to the sample. Samples with DNA fragments of ≥ 1 kB were loaded onto 1 % (w/v) agarose gels and samples < 1 kB onto 2 % (w/v) agarose gels. If the gel was being used for analytical purposes (i.e. sizing and quantification of the DNA), 1 kB or 100 bp DNA ladders were loaded into the lanes beside the samples, in 1 % and 2 % gels respectively. Gel electrophoresis was carried out in TBE at 60 V for 45 minutes

to 1 hour. Analytical gels were visualised using UV light and were photographed by a digital camera (Mitsubishi 85 mm lens, from Thistle Scientific). If the DNA in the gel was to be subjected to further cloning procedures the DNA was visualised under low intensity UV (230V-50Hz, Ultratec Ltd) and excised from the gel using a clean scalpel (preparation gels). DNA excised from preparation gels was then recovered from the agarose using the Promega Wizard® SV Gel and PCR Clean-UP System kit as per the manufacturer's instructions.

2.1.3 Restriction Enzyme Digest.

Restriction digest enzymes (Promega) were used according to the manufacturer's instruction using the buffers supplied. In general, 10 units of the restriction enzyme were used to digest 1 μg of plasmid DNA or PCR product for 1 hour at the recommended temperature. Restriction enzyme reactions were subsequently terminated by heat inactivation (65 °C incubation for 15 minutes). Cut plasmids were then alkaline phosphatase treated (see 2.1.4). Restriction digested DNA that was to be used in further restriction digests or ligation reactions was extracted into nuclease free water using the Promega Wizard® SV Gel and PCR Clean-UP System kit as per the manufacturer's instructions.

2.1.4 Alkaline phosphatase treatment of restriction enzyme digested plasmids.

Phosphate groups were removed from cut plasmid vectors with 5' overhangs by the addition of 1 unit of calf intestinal alkaline phosphatase (CIAP) (Promega) for 30 minutes at 37 °C followed by the addition of a further unit of CIAP and a second 30-minute incubation at 37 °C. 3' and blunt end cut plasmid vectors were treated by

the addition of 1 unit of CIAP for 15 minutes at 37 °C and then 15 minutes at 56 °C. This procedure was repeated with a further unit of CIAP.

2.1.5 Bacteria culture.

All culturing of bacteria was done under aseptic conditions unless otherwise stated. Bacteria were cultured overnight at 37 °C in Luria Broth (LB) (Sigma L3522) supplemented with the appropriate antibiotics (ampicillin 100 μg/ml, chloramphenicol 34 μg/ml, kanamycin 50 μg/ml and tetracycline 10 μg/ml) (all Melford laboratories).

2.1.6 Preparation of calcium chloride competent cells.

5 ml of *E. coli* was cultured overnight at 37 °C as described in 2.1.5. 50 ml of LB were inoculated with 500 μl of overnight culture and the culture were grown in a 1.5 litre flask (37 °C, 210 r.p.m) for approximately 2 hours. When the absorbance of the bacterial culture reached 0.3 to 0.4 units at a wavelength of 600 nm the culture was transferred to a pre-chilled 50 ml plastic centrifuge tube. The tube was centrifuged at 3500 g for 10 minutes at 4 °C. The supernatant was discarded and the pellet was resuspended in 20 ml of ice-cold filter sterile 100 mM $CaCl_2$ and incubated on ice for 30 minutes. Bacteria were spun down at 1500 g for 5 minutes and the pellet was resuspended in 1 ml of 100 mM $CaCl_2$. Bacteria were left on ice for a further 30 minutes and either used immediately or DMSO was added to a final concentration of 10 % by gentle swirling and the cells stored at –70 °C for up to 4 weeks.

2.1.7 Preparation of magnesium super competent cells.

Frozen glycerol stocks of DH5α were thawed and streaked onto a LB agar plate and cultured overnight at 37 °C. About ten to twelve large colonies were isolated using a metal hoop or sterile pipette tip and inoculated into 250 ml of SOB (2 % (w/v) tryptone, 0.55 % (w/v) yeast extract 10 mM NaCl, 10 mM KCl, 5 mM $MgSO_4$ and 5 mM $MgCl_2$) in a 1.5 litre flask and grown for two days at 18 °C, at 210 r.p.m, until the cell titre reached A_{600} of 0.6. The flask was removed from the incubator and placed on ice for 10 minutes. The culture was transferred to six pre-chilled sterile 50 ml centrifuge tubes and spun at 2500 g for 10 minutes at 4 °C. The pellets were resuspended in a total of 80 ml of ice-cold filter sterile TB buffer (10 mM PIPES, 55 mM $MnCl_2$, 15 mM $CaCl_2$, 250 mM KCl; pH 6.7) and incubated on ice for 10 minutes and spun down together at 2500 g for 10 minutes. The pellet was resuspended in 20 ml of TB buffer and DMSO was added to a final concentration of 7 % by gentle swirling. After incubating on ice for 10 minutes the competent cells were aliquoted into 2 ml cryotubes, snap frozen in liquid nitrogen and stored in liquid nitrogen until required.

2.1.8 Ligation reactions.

Ligation reactions were performed using T4 ligase (Promega) in accordance with the manufacturer's instructions.

2.1.9 Transformation of competent *E.coli* strains.

Bacteria were transformed by adding either 0.5 µl of plasmid DNA or 10 µl of ligation reaction mixture to either, 200 µl of standard calcium chloride competent

cells or, 50 µl of magnesium ion super competent cells, and incubated on ice for 20 minutes. Bacteria were heat shocked at 42°C for 45 seconds and incubated on ice for a further 3 to 4 minutes. The bacterial culture was made up to 1 ml, with either LB or SOC medium (2 % (w/v) tryptone, 0.55 % (w/v) yeast extract 10 mM NaCl, 10 mM KCl, 5 mM $MgSO_4$, 5 mM $MgCl_2$ and 20 mM glucose), and incubated at 37 °C with vigorous shaking (210 r.p.m) for 1 hour. 100 µl of the culture medium were spread on to an agar plate containing the appropriate selection antibiotic(s) for the plasmid and *E.coli* strain. The remaining bacteria were pelleted (13000 g; 10 seconds) resuspended in approximately 100 µl of culture medium and plated on a second agar plate. Agar plates were placed agar side up into a 37 °C incubator overnight. The next day single colonies were isolated for inoculation into LB for further screening.

2.1.10 Preparation of plasmid DNA.

Small-scale preparation of DNA for analysis, cloning and yeast two-hybrid purposes was prepared using the Qiagen QIAprep® spin miniprep kit in accordance with the manufacturer's instruction. Large-scale preparation of DNA for analysis, cloning, yeast two-hybrid procedures and transfection into mammalian cell lines was prepared using the Qiagen® plasmid midi kit in accordance with the manufacturer's instructions. DNA for transfection of primary cells was prepared using the EndoFree® Plasmid Maxi Kit in accordance with the manufacturer's instructions.

2.1.11 Preparation of glycerol stocks of transformed *E. coli.*

Glycerol stocks were prepared from overnight bacterial cultures. 600 µl of cultures were mixed with 400 µl of sterile 50 % glycerol in sterile milli-Q H_2O (MQH_2O) (18 Ω) and stored at -70°C.

2.2 Cell culture.

All plastic-ware used was from Nunc at VWR unless otherwise stated.

2.2.1 General cell culture.

All cell lines were maintained at 37 °C in the presence of 5 % CO_2. COS-7 (laboratory stocks), SK-N-SH (ECACC), B104 -NrCAM (a kind gift from Dr. C. Faivre-Sarrailh, University of Marseille, France) and CHO.E17 (laboratory stocks) cells were routinely cultured in Dulbecco's modified Eagle medium (DMEM) supplemented with 10% (v/v) foetal calf serum (FCS) (Globepharm), 2 mM L-glutamine, 100 units/ml of penicillin (pen.) and 0.1 mg/ml streptomycin (strep.). Human Embryonic Kidney (HEK293) cells (ECACC and laboratory stocks) were routinely cultured in minimum essential medium (MEM) supplemented with 10 % FCS, 5 % (v/v) non-essential amino acids, 2% L-glutamine, 100 units/ml of pen. and 0.1 mg/ml strep. LoVo cells (ECACC) were routinely cultured in nutrient mixture F-12 Ham supplemented with 10 % FCS, 2 mM L-glutamine, 100 units/ml of pen. and 0.1 mg/ml strep. All stable cell lines were maintained in their normal medium above supplemented with 1 mg/ml G-418 sulfate (geneticin) (Melford laboratories). T-75 flasks (80 cm^3, VWR) were used for routine culture of all cell types.

2.2.2 Passage or splitting cell lines.

Cells were passaged prior to reaching confluence by first washing the flask with pre-warmed trypsin-EDTA (0.25 % (w/v) trypsin, 0.5 mM EDTA in phosphate buffered saline (PBS)), and then incubating with trypsin-EDTA for 1 to 5 minutes, depending on cell type. Detached cells were separated by pipetting and seeded into flasks or onto Petri dishes/coverslips (VWR) at appropriate seeding densities.

2.2.3 Freezing down of cell lines.

Liquid nitrogen stored stocks were prepared by trypsin-EDTA treating near confluent flasks and pelleting detached, separated cells (2000 g, 5 minutes, room temperature). Pelleted cells were resuspended in 50 % FCS, 40 % normal growth medium for that cell line (see above) and 10 % DMSO and 1 ml aliquots were pipetted into cryotubes. The cryotubes were brought to –80 °C slowly by placing in a cryo 1 °C freezing container (Naglene) in a - 80°C freezer from 5 hours to overnight. Cryotubes were then placed in liquid nitrogen for long term storage.

2.2.4 Breaking out of cell lines.

Cell stocks were recovered by thawing for 1 minute in a 37 °C water bath and placing in a T75 flask together with 15 ml of the appropriate cell culture medium. Media was changed 24 hours later to remove DMSO.

2.2.5 Transfection of cell lines.

Cell lines were routinely transfected using lipofectamine^{TM} reagent. The appropriate amount of DNA (usually 0.05-1.0 μg per 35 mm dish, 1.0-2.0 μg per 60 mM dish, 2.0-5.0 μg per 90 mM dish and 2.5-6.0 μg per 80 mM flask) was incubated with four times the volume in micro litres of lipofectamine^{TM} reagent to 1.0 μg of DNA in reduced serum Optimem^{TM} medium for 30 minutes. Dishes/flasks of cells to be transfected were washed twice in an appropriate volume of Optimem^{TM} (pre-warmed to 37 °C) and the lipofectamine/DNA transfection mix was added and made up to the appropriate volume using pre-warmed Optimem. Optimem^{TM} was removed from the dishes/flasks after 5 hours to 6 hours incubation at 37°C incubation and replaced with the normal medium for the cell line as described 2.2.1.

2.2.6 Transfection of primary cerebellar granule cells.

4 x 10^6 P7 mouse cerebellar granule cells (CGC) were co-nucleofected with 2 μg HA-NrCAM and 2 μg FLAG-ezrin, using the Amaxa mouse neuron nucleofector™ kit (Amaxa biosystems) according to the manufacturer's instructions. Transfected neurons were seeded onto 60 mm dishes containing glass coverslips pre-coated with poly-D-lysine and fibronectin as described 2.2.7.

2.2.7 Coating coverslips.

Poly-D-lysine coverslips were prepared by covering the coverslip surface with 50 μg/ml poly-D-lysine in sterile PBS for 2 hours. The coverslips were washed twice with sterile DMEM before use. Laminin coated coverslips were prepared by

covering coverslips with 20 μg/ml laminin, in sterilised PBS. Fibronectin coated coverslips were prepared by covering coverslips with 10 μg/ml fibronectin in sterilised PBS, for 2 hours. The coverslips were washed twice with sterile DMEM before use.

2.2.8 Making stable cell lines.

The HEK293 stable cell lines were made by transfecting three to four T75 flasks, at 30-40 % confluencey, with 7 μg of the relevant DNA per flask using Lipofectamine™ protocol described above and in accordance with the manufacturer's instructions. Cells were grown for 48 hours after transfection in their normal growth medium. Medium was then supplemented with 1 mg/ml G418-sulfate and the cells were maintained in this medium thereafter.

2.2.9 Cloning out stable cell lines.

Stable cell lines were cloned out by plating HEK293 cells at low seeding densities (typically 10 to 50 cells) on to 90 mM plates. Plates with seeding densities low enough to select for individual colonies were chosen, selected colonies were enclosed and separated from the rest of the plate by placing a sterile stainless steel ring around the colony. Individual colonies were trypsinised (as described above) and grown in an individual well of a 16 well plate to 80-90 % confluency.

2.2.10 Fixing and staining cells for immunofluorescence microscopy.

All cell lines with the exception of transient NrCAM transfected HEK293s, were seeded onto 35 mm dishes containing an uncoated glass cover slip and transfected

with the appropriate DNA as described in 2.2.5. Transient NrCAM transfected HEK293s, were seeded onto 35 mm dishes containing a glass coverslip pre-coated with either fibronectin or laminin as described in 2.2.7 and transfected as described in 2.2.5. Transfected CGC neurons were seeded onto 60 mm dishes containing two glass coverslips pre-coated with both poly-D-lysine and fibronectin as described in 2.2.7. Cell lines and CGCs were treated the same way unless specified. Post-transfection, cells were washed three times in ice cold PBS pH 7.4 and fixed in ice-cold paraformaldehyde (4 % (w/v) in PBS) for 10 minutes at room temperature. Cells were washed 4 times in PBS and cell lines and CGCs were permeabilised with (0.2 % and 0.1 % (w/v) respectively) Triton X-100 for 5 minutes. If phalloidin staining of actin was used, undiluted Alexa568-phalloidin (Invitrogen) was diluted one in a hundred and 100 µl was added to each slide in a humidified chamber and allowed to incubate at room temperature for 15 minutes. Cells were washed three times in PBS and incubated for 1 hour at room temperature with the appropriate primary antibodies at the appropriate concentrations (1/200 anti-GIPC (Santa Cruz), 1/500 anti-HA (Roche), 1/300 anti-FLAG M2-FITC, 1/500 anti-NrCAM (a kind gift from Dr. C. Faivre-Sarrailh, University of Marseille, France), 1/2000 anti-neurofascin (a kind gift from Prof. Peter Brophy, University of Edinburgh) in 3 % bovine serum albumin in PBS. If GIPC immunostaining was being performed, cells were washed 3 times with PBS and incubated for 1 hour at room temperature with a 1/200 dilution of anti-goat antibody before incubations with anti-rabbit or anti-mouse Alexa Fluor® 568 (this prevented cross-reaction of antibodies). Cells were washed 3 times in PBS and incubated for 1 hour at room temperature with Alexa Flour® 568 anti-mouse IgG 1/1000 for HA-NrCAM and HA-neurofascin staining or Alexa Flour® 568 anti-rabbit IgG 1/1000 for anti-NrCAM and anti-

Neurofascin staining. Following three washes in PBS coverslips were mounted on glass slides using the aqueous mountant moviol, plus 1 % DAPI. Images were recorded on a Zeiss Axiovert S100 2TV Delta-Vision Restoration microscope (Applied Precision) using a 60X Zeiss Planachromat objective and a CCD-1300-Y/HS camera (Roper Sci and processed by constrained iterative deconvulation using SoftWorx (Applied Precision).

2.3 Protein assays and Western blot.

2.3.1 Protein concentration assay.

Protein concentration was assayed using Bradford's reagent (Sigma B6916). Samples to be assayed were diluted with a mixture of deionised water and cell extraction buffer to a final volume of 500 µl, to which 500 µl of Bradford reagent was added. Absorbance was measured at 595 nm, and protein concentrations calculated using a standard curve created using known concentrations of BSA (Promega).

2.3.2 Protein expression of GST-NrCAM.

5.0 ml of pGEX-NrCAM transfected BL21 C+ *E. coli* were cultured overnight in LB, 100 µg/ml ampicillin and 25 µg/ml chloraphemicol. This 5 ml culture was added to 500 ml of fresh LB, 100 µg/ml ampicillin and 25 µg/ml chloraphemicol and grown to A_{600} 0.3. A 1 ml sample of the culture was spun at 13000 g for 2 minutes and the pellet resuspended in 50 µl protein sample buffer (PSB); this was an uninduced control. Isopropyl-β-D-thiogalactopyranoside (IPTG) was then added to

the *E.* coli to a final concentration of 5 mM and the cells grown for a further 3 hours. A further 500 µl culture sample was spun at 13000 g for 2 minutes and the pellet resuspended in 100 µl PSB; this was an induced control. Both uninduced and induced controls were run on a sodium dodecyl sulphate polyacrylamide gel electrophoresis (SDS PAGE) gel. The gel was stained with Coomassie brilliant blue stain (see section 2.3.8), and protein expression was seen as a protein band between 40 kDa and 50 kDa in the induced sample and not the uninduced sample. The remaining *E. coli* were spun for 10 minutes at 5000 g, the cell pellet was washed in ice cold PBS, the sample was re-spun, the supernatant was removed and the pellet snap frozen by immersion in liquid nitrogen. Pellets were stored at –70 °C for a few days or used immediately. 15 ml of ice-cold lysis buffer (100 mM Tris pH 8.0, 50 mM NaCl, 5 mM EDTA, 1X Roche protease inhibitors (Cat. No. 1 697 498) and 1 mM phenylmethylsulfonyl fluoride (PMSF) was added to the sample which was then lysed by vigorous pipetting and then left on ice for 20 minutes. Further lysis was carried out using sonication (6 x 10 second bursts with 45 second rests on ice) and then by adding 1 % (v/v) Triton X-100. Lysed cells were tumbled at 4 °C for 20 minutes and cell debris were removed by centrifugation (12000 g, 10 minutes at 4 °C). GST-NrCAM was purified by coupling to reduced glutathione (GSH) beads. Beads had previously been washed by tumbling in PBS 5 mM EDTA at 4 °C for 5 minutes and by removing the supernatant by centrifugation (2000 g, 5 minutes at 4 °C). The supernatant from the lysed cells was added to the washed beads and tumbled for 45 minutes at 4 °C. The GST-NrCAM coupled beads were washed three times in PBS 5 mM EDTA as already described and then place in a 10 ml column and the PBS 5 mM EDTA added to a total volume of 10 ml. GST-NrCAM was eluted from the column using 10 ml of 50 mM Tris pH 8.0, 10 mM reduced

glutathione and fractions were taken in 1.0 ml aliquots. A 100 µl sample from each fraction was taken and the remainder snap frozen in liquid nitrogen and stored at -70 °C. Fractions containing GST-NrCAM were verified using a mixture of UV spectroscopy and SDS PAGE. 80 µl of each fraction were diluted in 920 µl of MQH_20 (18Ω) and their absorbance read at 280 nm. PSB was added to the remainder and equal volumes of sample were run on an SDS PAGE gel and stained using Coomassie blue as described below. The concentration of fractions that contained significant amounts of GST-NrCAM was measured using the Bradford assay as described in 2.3.1.

2.3.3 Sodium orthovanadate activation.

A solution of sodium orthovanadate was prepared by bringing a 200 mM solution to pH 10.0 using either NaOH or HCl as appropriate. The sample was boiled until colourless and then cooled to room temperature. The solution was brought back to pH 10.0 and the boiling, cooling pHing procedure repeated until the solution remained colourless and stabilised at pH 10.0.

2.3.4 Treatment of positive controls for phophotyrosine assays.

Equal volumes of a freshly prepared 0.341 % H_2O_2 and activated sodium orthovanadate were mixed together and 50 µl of the solution added to each 90 mM dish to be treated. After a five-minute incubation at 37 °C each dish was extracted in ice-cold radio-immunoprecipitation assay (RIPA) buffer (Tris-HCl 50 mM, pH 7.4, 1 % NP-40, 0.25 % Na-deoxycholate) with PMSF (1 mM), aprotinin (1 µg/ml),

leupeptin (1 μg/ml), pepstatin (1 μg/ml), Na_3VO_4 (1 mM) and NaF (1 mM) as described below.

2.3.5 General preparation of tissue culture samples for SDS-PAGE, immunoprecipitation and GST pull-down assays.

All procedures were carried out at 4 °C. Cultured cells were washed twice in calcium free Dulbecco's phosphate buffered saline (DPBS) and the appropriate volume of cold lysis buffer added (see appendix 2 for lysis buffers, normal buffer used was RIPA, pH 7.4, with the Roche cocktail of protease inhibitors). Cells were scraped from cell culture dishes, and lysed by vigorous pipetting and then left on ice for 20 minutes. Cell debris was removed by centrifugation (12000 g, 10 minutes at 4 °C). If the cell extract was to be used for immunoprecipitation or pull-down assays, a second centrifugation step was routinely done.

2.3.6 Whole brain, cerebellum and CGC sample preparation.

Postnatal day 7 (P7) whole mouse brain, isolated cerebellum and CGC cultures maintained for up to 7 days *in vitro* (DIV), were prepared for Western blotting with anti-NrCAM, anti-GIPC or anti-SAP102. Whole brain was prepared by adding 2 % SDS, 1 M Tris, 0.5 mM PMSF and the Roche cocktail of protease inhibitors (Cat. No. 1 697 498), followed by brief sonication to solubilise the tissue. Cerebellum was homogenised using a 1 ml Wheaton glass homogenisor (Fisher) in the presence of PBS and protease inhibitors (Roche Cat. No. 1 697 498). 300 μg samples of cerebellum were stored at –70 °C for further use. An aliquot was solubilised by tumbling in GHB1 (see appendix 2) at 4°C for 30 minutes and the cellular debris removed by centrifugation (14000 g for 10 minutes). CGC samples were solubilised

by adding 1 % Triton-X100, 0.5 mM PMSF, and a mixture of protease inhibitors (Roche Cat No 1 697 498) in PBS. Samples were incubated at 4 °C for 10 minutes and centrifuged at 14000 g for 10 minutes to separate the pellet and supernatant fractions.

2.3.7 SDS-PAGE.

Unless otherwise stated SDS-PAGE was performed using Invitrogen's NuPAGE® polyacrylamide gel system as per the manufacturer's instructions. When necessary SDS PAGE gels were also prepared in house. The resolving gel was made first. The gel solution was prepared (8-10 % (v/v) acrylamide, 0.37 M Tris-HCl pH 8.8, 0.1 % w/v SDS) and polymerisation agents (10 % (w/v) ammonium persulfate (APS), 20µl NNN'N'-Tetramethylethylenediamine (TEMED)) were added to it. The resulting mixture was poured gently into a gel-casting rig and covered with water-saturated butanol. When the gel was set the butanol was removed, the stacking gel was prepared (acrylamide 4.7 % (v/v), 0.121 M Tris-HCl pH 6.8, 0.46 % (v/v) SDS), the gel was polymerised (10 %(w/v) APS, 20 µl TEMED), and the polymerised mixture poured gently upon the stacking gel, a comb was placed on top, and the polymerised mixture was allowed to set at room temperature. Gels were stored in a moist atmosphere for up to 3 days at 4 °C.

Samples were prepared as described above and reduced in NuPAGE® LDS Sample Buffer (4X) at 70 °C for 10 minutes (for Invitrogen gels) or reduced in standard sample buffer 0.001 % (w/v) bromophenol blue, 4.3 % (w/v) dithiothreitol, 1 % (w/v) glycerol, 0.06 M Tris-HCl pH 6.8, 2.2 % (w/v) SDS) at 100°C for 5 minutes if "in house" gels were being used.

When analysing proteins of less than 100 kDa, samples were loaded onto Invitrogen NuPAGE® Novex® 4-12 Bis-Tris gel together with 5 µl of SeeBlue® Plus2 protein standards. When analysing proteins greater than 100 kDa, samples were loaded onto Invitrogen NuPAGE® Novex 3-8% Tris-Acetate gel together with 5.0 to 7.5 µl of HiMark® high MW protein standards. If in house gels were being used 6.0 µl of Prestained Protein Marker, Broad Range (New England BioLabs INC.) was run with the protein samples.

2.3.8 Coomassie staining of SDS-PAGE gels.

Gels were stained using Coomassie stain solution (0.1 % (w/v) Coomassie brilliant blue R-250, 45 (v/v) % methanol, 10 % (v/v) glacial acetic acid for 5 to 10 minutes at room temperature. Superfluous Coomassie brilliant blue was removed using multiple changes of destain solution (10 % (v/v) glacial acetic acid, 40 % (v/v) methanol) for several hours at room temperature. Gels were subsequently dried using Promega's gel drying kit in accordance with the manufacturer's instructions.

2.3.9 Transfer of proteins separated by SDS-PAGE to nitrocellulose.

Proteins separated by SDS-PAGE were transferred to a nitrocellulose membrane using NuPAGE® transfer buffer by Invitrogen supplemented with appropriate amounts of methanol and antioxidant in accordance with the manufacturer's instructions. Transfer was completed at 30 V for 1 hour (for proteins <100 kDa) or 25 V for 1 hour (proteins > 100 kDa). Transfer was verified by staining membranes with Ponceau S solution (0.1 % Ponceau S (w/v), 5 % acetic acid) for 3 minutes to

5 minutes at room temperature. Excess Ponceau S was removed by washing with distilled water.

2.3.10 Western blotting.

The Western blotting protocol was adapted for the requirements of different primary antibodies. All Western blot procedures used are detailed in appendix 3. In general the following protocol was used. Protein binding sites on Western blot membrane were blocked in 5 % (w/v) fat free powdered milk in TBS-T (0.5 %) (TBS (0.05 M Tris, 0.138 M NaCl, 0.0027 M KCl, pH 8.0) + 0.5 % (v/v) polyoxyethylenesorbitan monolaurate (Tween-20)) either at 4 °C overnight or 2 hours at room temperature. Blots were washed with TBS-T (0.1 %) and incubated with the primary antibody for 1 hour in 3 % (w/v) fat-free powdered milk in TBS-T (0.1 %) for 1 hour. Primary antibody was removed by washing the blot three times, for 10 minutes with TBS-T (0.1 %). Blots were incubated with HRP conjugated antibody diluted with 3 % (w/v) fat free powdered milk in TBS-T (0.1 %) for 1 hour at room temperature and was removed by washing the blot three times, for 10 minutes with TBS-T (0.1 %). Immunoreactive bands were visualised with chemiluminescence (Pierce) as per the manufacturers instructions.

2.3.11 GST pull-down assay.

Cell extracts were prepared as described in section 2.3.5. 2 X 37.5µl of unwashed GSH-sepaharose were aliquoted in to two clean microfuge tubes and washed twice in the appropriate extraction buffer (see appendix 2 and 2.3.5) by centrifugation (2000 g for 1 minute at 4 °C). 10 µg of GST or GST-NrCAM were added to each tube and

the volume made up to 500 µl with extraction buffer and the fusion protein allowed to couple to the beads by tumbling at 4 °C for 2 hours. Cell extracts were prepared as described in 2.3.5 and pre-cleared by tumbling with 50 µl of washed GSH-sepharose for 1 hour at 4 °C. The supernatant was removed from the GST protein coupled beads by centrifugation (2000 g for 1 minute at 4 °C) and equal volumes of pre-cleared cell extract added to each tube. Beads and cell extracts were tumbled together for 2 hours at 4 °C. The beads were then washed a minimum of five times and a maximum of ten times with lysis buffer by centrifugation at 12000 g, 4 °C for 10 seconds and removal of supernatant using a syringe. The proteins were extracted in 4 X NuPAGE® SDS buffer and denatured by heating to 70 °C for 10 minutes. SDS-PAGE and Western blot were performed as described 2.3.10.

2.3.12 Immunoprecipitation using monoclonal anti-HA antibodies and protein A.

A cell extract was prepared as described above in RIPA buffer (Tris-HCl 50 mM, pH 7.4, NP-40 1 %, Na-deoxycholate 0.25 %) with PMSF (1 mM), aprotinin (1 µg/ml), leupeptin (1 µg/ml), pepstatin (1 µg/ml), Na_3VO_4 (1 mM) and NaF (1 mM). The cell extract was pre-cleared by tumbling with 10 mg of washed protein A-sepharose for one hour at 4 °C. A further 3 mg of protein A-sepharose was prepared by washing in 1 ml RIPA buffer and spinning at 12000 g for 10 seconds, RIPA buffer was removed using a syringe and this procedure repeated three times. A sample of the clarified cell extract was taken and the remainder added to washed sepharose beads together with 3 µl of monoclonal anti-HA antibodies (Santa Cruz) and tumbled at 4 °C for 2 hours. The beads were then washed a minimum of five times and a maximum of ten times with RIPA buffer by centrifugation at 12000 g,

4 °C for 10 seconds and removal of supernatant using a syringe. The proteins were extracted in 4X NuPAGE® SDS buffer and denatured by heating to 70 °C for 10 minutes. SDS-PAGE and Western blots were performed as described 2.3.10.

2.3.13 Immunoprecipitation using high affinity rat monoclonal anti-HA antibodies (Roche) and goat anti-rat IgG (whole molecule) agarose.

A cell extract was prepared as described above either in RIPA (Tris-HCl 50 mM, pH 7.4, NP-40 1 %, Na-deoxycholate 0.25 %) with Roche protease inhibitors (Cat. No. 1 697 498) or when tyrosine phosphorylation was being carried out in RIPA with PMSF (1 mM), aprotinin (1 μg/ml), leupeptin (1 μg/ml), pepstatin (1 μg/ml), Na_3VO_4 (1 mM) and NaF (1 mM). The cell extract was pre-cleared by tumbling with 10 μl of washed (RIPA) goat anti-rat IgG (whole molecule) agarose for 1 hour at 4 °C. A further 8 μl of goat anti-rat IgG (whole molecule) agarose was prepared by washing in 1 ml RIPA buffer and spinning at 12000 g for 10 seconds, RIPA buffer was removed using a syringe and this procedure repeated three times. A sample of the clarified cell extract was taken and the remainder added to washed agarose beads together with 4 μl of rat monoclonal anti-HA antibodies (Roche) and tumbled at 4 °C for 2 hours. The beads were then washed seven times with RIPA buffer by centrifugation at 12000 g, 4 °C for 10 seconds and removal of supernatant using a syringe. The proteins were extracted in 4 X NuPAGE® SDS buffer and denatured by heating to 70 °C for 10 minutes. SDS-PAGE and Western blot were performed as described 2.3.10.

2.3.14 Immunoprecipitation of GIPC using goat anti-GIPC antibodies and anti-goat beads.

A cell extract was prepared as described above in RIPA (Tris-HCl 50 mM, pH 7.4, NP-40 1 %, Na-deoxycholate 0.25 %) with Roche protease inhibitors (Cat. No. 1 697 498). The cell extract was pre-cleared by tumbling with 10 µl of washed (RIPA) rabbit anti-goat IgG (whole molecule) agarose for 1 hour at 4 °C. A further 8 µl of rabbit anti-goat IgG (whole molecule) agarose was prepared by washing in 1 ml RIPA buffer and spinning at 12000 g for 10 seconds, RIPA buffer was removed using a syringe and this procedure repeated three times. A sample of the clarified cell extract was taken and the remainder added to washed agarose beads together with 4 µl of goat polyclonal anti-GIPC antibodies (Santa Cruz) and tumbled at 4 °C for 2 hours. The beads were then washed seven times with RIPA buffer by centrifugation at 12000 g, 4 °C for 10 seconds and removal of supernatant using a syringe. The proteins were extracted in 4 X NuPAGE® SDS buffer and denatured by heating to 70°C for 10 minutes. SDS-PAGE and Western blot were performed as described 2.3.10.

2.3.15 Immunoprecipitation using monoclonal anti-HA beads.

A cell extract was prepared as described above either in RIPA (Tris-HCl 50 mM, pH 7.4, NP-40 1 %, Na-deoxycholate 0.25 %) with Roche protease inhibitors (Cat. No 1 697 498) or when tyrosine phosphorylation was being carried out in RIPA with PMSF (1 mM), aprotinin (1 µg/ml), leupeptin (1 µg/ml), pepstatin (1 µg/ml), Na_3VO_4 (1 mM) and NaF (1 mM). Tumbling with 100 µl of Rabbit IgG agarose for 1 hour at 4 °C pre-cleared the cell extract. 40 µl of 1:1 anti-HA agarose was

prepared by washing in 1 ml RIPA buffer and spinning at 12000 g for 10 seconds, RIPA buffer was removed using a syringe and this procedure repeated five times. A sample of the clarified cell extract was taken and the remainder added to washed agarose beads and tumbled at 4 °C for 2 hours. The beads were then washed a minimum of five times and a maximum of ten times with RIPA buffer by centrifugation at 12000 g, 4 °C for 10 seconds and removal of supernatant using a syringe. The proteins were then extracted in 4X NuPAGE® SDS buffer and denatured by heating to 70 °C for 10 minutes. SDS-PAGE and Western blot were performed as described 2.3.10.

2.3.16 Tandem affinity purification.

All procedures were carried out at 4 °C unless otherwise stated. Cultured cells grown on 140 mm diameter tissue culture dishes were washed twice in ice cold PBS. Cells were scraped from each cell culture dishes into 1 ml of PBS. Cells were pelleted (1200 g, 3 minutes) and the pellet lysed by rotation in 1 ml of lysis buffer (50 mM Tris pH 7.4, 150 mM NaCl, 1 mM EDTA, 1 % (v/v) NP-40, 15 % (v/v) glycerol, 1X Roche cocktail of protease inhibitors (Cat. No. 1 697 498), and 1 mM PMSF) for 30 minutes. Cell debris was removed by centrifugation (14000 g, 15 minutes at room temperature). 50 µl samples of the supernatant were retained, and then Rabbit IgG beads (20 µl) were coupled to N-TAP constructs within the remaining supernatant by tumbling at 4 °C for 2 hours. The coupled beads were centrifuged (2000 g, 4 °C, 1 minute) and the supernatant was removed using a syringe. Beads were washed 3 times in 1 ml TBS- (0.05 %)T (50 mM Tris pH 7.4, 150 mM NaCl, 0.5 % (v/v) Tween-20) and twice in 50 µl TEV cleavage buffer

(TCB) (10 mM Tris-HCl pH 8.0, 150 mM NaCl, 0.1 % (v/v) NP-40, 0.5 mM EDTA, 1 mM dithiothreitol). The beads were resuspended in 20µl TEV cleavage buffer and 0.5µl (50U) of TEV protease (Invitrogen) added and tumbled overnight at 4 °C. The supernatant was transferred to a fresh tube and the IgG beads were washed with TCB. Supernatants were combined and supplemented with three volumes of calmodulin binding buffer (CBB) (10 mM Tris-HCl, pH 8.0, 150 mM NaCl, 0.1 % NP-40, 10 mM β-mercaptoethanol, 1 mM imidazole, 1 mM magnesium acetate, 2 mM $CaCl_2$) and a further 3 nM $CaCl_2$. 40 µl of washed calmodulin beads (Stratagene) were added to the supernatants and the beads were rocked for 2 hours to allow the CBP portion of the protein complex to bind the calmodulin beads. The beads were thoroughly washed with CBB, then the remaining protein complex was eluted by four washes of calmodulin elution buffer (10 mM Tris-HCl, pH 8.0, 150 mM NaCl, 0.1 % NP-40, 10 mM β-mercaptoethanol, 1 mM imidazole, 1 mM magnesium acetate, 2 mM EGTA) and one wash of a high salt solution (50 mM Tris-HCl pH 8.0, 1 M NaCl, 2 mM EGTA). These elutes were combined and SDS-PAGE and Western blot were performed as described 2.3.10.

2.3.17 Affinity purification of rabbit NrCAM cytoplasmic terminus antibodies.

3 ml of packed gel, α-amino hexyl sepharose 4B was measure into a 15 ml plastic centrifuge tube and packed by centrifugation at 1200 g for 5 minutes and the alcohol containing supernatant removed. The gel was washed in double its volume of ice-cold PBS, which was removed by centrifugation as described above. This wash step was repeated three times and the washed gel was finally resuspended in 2 ml of PBS. 200 µl of N,N-dimethylformamide (DMF) containing 5 mg of sulfo-MBS (Pierce)

was added to the gel suspension, mixed thoroughly and tumbled at room temperature for 2 hours. The gel was packed and washed three times with two volumes of PBS as already described. 10 mg of NrCAM peptide in 800 µl of 10 mM HCl (pH 6.0 using 0.1 M NaOH) was coupled to the MBS activated gel by tumbling both together overnight at room temperature. The matrix was then washed in two volumes of 1 M Tris-HCl pH 7.6 and then 2 volumes of 0.2 M glycine pH 2.6 and finally 2 volumes of PBS. 5 ml of week-8 NrCAM rabbit anti-serum was added to the packed peptide-matrix and allowed to couple by tumbling overnight at 4 °C. The slurry was added to a 10 ml column and allowed to settle. The column was washed three times with 10 ml of PBS. The antibody was eluted using 2 X 3 volumes of 0.2 M glycine and collected as 0.5 ml fractions in 1.5 ml plastic tubes, already containing 0.5 ml of 1 M Tris-HCl pH 7.6. The fractions most likely containing antibodies were marked as ones that registered a pH drop on litmus paper. The column was washed in 3 volumes of glycine and stored in PBS 0.01 % sodium azide.

2.3.18 Removal of primary and secondary antibodies from a Western blot.

The nitrocellulose membrane was washed three times for ten minutes in 10 mls of distilled water and then incubated for 45 minutes in stripping buffer (0.2M glycine pH 2.2, 0.1% SDS, 1.0% Tween-20) at room temperature. The membrane was then washed a further three times for ten minutes in 10 mls of distilled water and incubated with the primary and secondary antibody previously used as described in section 2.3.10.

2.3.19 PNGAse F treatment of cells.

NrCAM glycosylated protein within crude cell extracts and extracts from immunoprecipitations was denatured in Glycoprotein denaturing buffer (NEB: 0.5% SDS, 1% β-mercaptoethanol) at 100 °C for 10 minutes. Two equal volume samples of denatured protein were then incubated in G7 reaction buffer (NEB: 50 mM Sodium Phosphate, pH 7.5 @ 25 °C) supplemented with 1% NP-40 (NEB). One sample of denatured protein was treated with 500 units of peptide: N-glycosidase F (PNGase F) and the second sample left untreated. Both samples were incubated overnight at 37 °C and analysed by SDS-PAGE and Western blot as described sections 2.3.7 to 2.3.10.

2.4 Yeast and the Yeast two-hybrid Assay.

2.4.1 General care and details on Y190 strain.

All culturing of yeast was done under aseptic conditions unless otherwise stated. Untransfected Y190 were cultured overnight at 30 °C in YPAD (1 % (w/v) yeast extract (Difco), 2 % (w/v) peptone (Difco), 2 % (w/v) glucose, 0.01 % (w/v) adenine hemisulfate) liquid medium or on YPAD agar plates. Transfected Y190 were cultured overnight at 30 °C in omission liquid medium (0.67 % (w/v) Yeast nitrogen base without amino acids (Difco), 2 % (w/v) glucose and 0.067 % synthetic drop out mix) or on omission media agar plates. Drop out mix included all of the following amino acids less the amino acid(s) being selected for: 2.0 g adenine hemisulfate, 2.0 g arginine-HCl, 2.0 g histidine-HCl, 2.0 g isoleucine, 4.0 g leucine, 2.0 g lysine-

HCl, 2.0 g methionine, 3.0 g phenylalanine, 2.0 g serine, 2.0 g threonine, 3.0 g tryptophan, 2.0 g tyrosine, 1.2 g uracil and 9.0 g valine.

2.4.2 Li Acetate method of transformation.

Yeast strain Y190 was co-transformed using the lithium acetate/single-stranded carrier DNA/polyethylene glycol (LiAc/ss-DNA/PEG) protocol developed by the Gietz laboratory (Agatep *et al* 1998). 2.5 x 10^8 yeast cells were inoculated into YPAD medium that was pre-warmed to 30 °C. The cells were incubated at 30 °C and 200 r.p.m until the cell titre reached 2 x 10^7 cells per ml. Cells were harvested by centrifugation at 3000 g for 5 minutes at 21 °C. Cells were washed in 10 ml of sterile distilled water by re-centrifugation and decanting off the supernatant. Cells were resuspended in 1.0 ml of 100 mM lithium acetate, which was allocated in ten 100 µl-aliquots in micro-centrifuge tubes. The cells in each tube were pelleted and the lithium acetate supernatant removed. The following reagents were added in the following order to each cell pellet; polyethylene glycol 3350 (50 % w/v) 240 µl, lithium acetate 1.0 M 36 µl, carrier single stranded DNA (10 µg) 50 µl, sterile distilled water, pAS2-1 bait construct (1 µg) and pACT2 construct (1 µg) 36 µl. The cells were resuspended by vortexing and incubated at 30 °C for 30 minutes. The cells were then heat shocked in a water bath at 42°C for 30 minutes, pelleted at 7000 g on a bench centrifuge and gently resuspended in 1.0 ml of sterile distilled water. 200 µl of each cell suspension was plated onto an agar plate lacking leucine and tryptophan (W^-L^-) and grown at 30°C for 3 to 4 days.

2.4.3 The filter lift assay.

Positive interaction between proteins was tested for β-galactosidase activity by the filter lift assay as described by Parchaliuk *et al* (1999). Sterile 7.5 cm diameter Whatman grade 1 paper was soaked in a solution of 10 ml Z buffer (60 mM $Na_2HPO_4.7H_20$, 40 mM $NaH_2PO_4.H_20$, 10 mM KCL and 1 mM $MgSO_4.7H_20$, pH 7.0), 0.5 ml of 20 mg/ml 5-bromo-4-chloro-3-indolyl-D-galactopyranoside (X-gal) in DMF and 27 µl mercaptoethanol, and placed into an 8.0 cm diameter Petri dish. Clean dry filter paper was placed over the surface of colonies growing on W^-L^- plates using a forceps. The colonies were transferred to the filter paper, which was then placed in liquid nitrogen. After the paper was frozen completely it was removed from the liquid nitrogen and allowed to defrost at room temperature. This freeze thaw cycle was repeated and then the defrosted paper placed on top of the wetted filter paper in the Petri dish. The filter papers were then incubated at 37 °C for 3 hours and then at room temperature (in the dark) for a further 20 hours.

2.4.4 Preparation of glycerol stocks of transformed Y190.

Glycerol stocks were prepared from overnight Y190 cultures. 600 µl of culture were mixed with 400 µl of sterile 50 % glycerol in sterile MQH_2O and stored at – 70 °C.

2.4.5 Extracting DNA from yeast.

Two or three colonies of pACT2 library plasmid expressing were grown overnight in 3 mls of L^- liquid media. This starter culture was inoculated (100 µl) into three

more 3 ml L⁻ cultures and grown overnight. Each one of the three overnight cultures were pelleted in a microfuge tubes, using a bench centrifuge, the supernatants were discarded and 200 µl of yeast lysis buffer (10 mM Tris-HCL, 100 mM NaCl, 1 mM EDTA, 2 % (v/v) Triton X-100, 1 % (w/v) SDS) was added to each pellet. 0.45 µm sterile glass beads were added to just below the liquid level and the microfuge tubes were vortexed for a minimum of 60 seconds. 200 µl of phenol-chloroform mixture were then added to the microfuge tubes and the mixture was vortexed for a further 60 seconds. The aqueous layer was extracted by centrifuging the mixture for two minutes, using a bench centrifuge, and then transferring, by pipetting, the top (aqueous layer) into a fresh clean microfuge tube. This aqueous layer was cleaned a second time using a further 200 µl of phenol- chloroform, centrifugation and transfer steps as previously described. All three aqueous layers were then added to the same Qiagen miniprep column. The manufactures protocols were then followed (described in section 2.1.10). Briefly the columns were centrifuged for one minute in a bench centrifuge and the supernatant was discarded. The column was washed by adding 500 µl of buffer EB and centrifuging for one minute and then discarding the supernatant. The column was washed a second time with buffer PE, using the same procedure. The DNA was eluted from the column using 50 to 100 µl of sterile MQH_2O at 70 °C.

Chapter 3. The Yeast Two-Hybrid Library Screen.

3.0 Introduction: General principles of the yeast two-hybrid library screen.

No protein acts in isolation, most proteins are part of dynamic protein-protein complexes which enable/disable and/or modify the proteins function. Therefore to fully explore NrCAM's functions a first step would be to establish its binding partners. Although several of NrCAM's extracellular binding partners have been published, only one intracellular binding partner (ankyrin) has been shown to date (Davis et al., 1996; Grumet, 1997). Taking into consideration the 100 % amino acid conservation of NrCAM's cytoplasmic terminus from chick to human (Davis and Bennett, 1994; Lane et al., 1996) it is therefore suggested that NrCAM may have as yet unidentified binding partners. To explore this possibility it was decided to screen a cDNA yeast two-hybrid library for potential binding partners.

The yeast two-hybrid assay is a method of detecting interacting proteins in the nucleus of a yeast cell (Fields and Song, 1989). The method takes advantage of the modular nature of transcription factors. Transcription factors can be divided into two distinct domains, a DNA binding domain (BD) and a transcription-activating domain (AD) (Ptashne and Ma, 1988). Both the AD and BD are independently non functional as transcription factors; however, when both domains are brought into close proximity they act as a normally active transcription factor (Fields and Song, 1989; Bartel and Field, 1997; Gietz and Woods, 2002a).

The yeast two-hybrid method used in this thesis is described in Figure 3-1 and is based upon Clontech's MATCHMAKER Two-Hybrid system 2 (http://www.icb.ufmg.br/~prodap/2003/tectrans/dhclontech.pdf). The DNA sequence of the cytoplasmic terminus of NrCAM was cloned in frame into pAS2-1 (Clontech)

(Figure 3-1 (A)), and this was called the bait plasmid. A cDNA library from a rat developing brain was cloned in frame into pACT-2 plasmids Figure 3-1(B) and these plasmids were called the prey plasmids. The bait plasmid encoded for a chimeric protein that consisted of the BD of the yeast GAL4 trans-acting transcription factor N-terminally fused to the relevant NrCAM cytoplasmic terminus. The prey plasmids encoded for the AD of the yeast GAL4 trans acting transcription factor N-terminally fused to potential binding partners of NrCAM (Figure 3-1 (C) and Figure 3-1 (D). Interactions between the BD-bait fusion protein and an AD-prey fusion protein bring the GAL4 AD and GAL4 BD into close proximity, activate the transcription factor and initiate the transcription of reporter gene(s) in the genome (Fields and Song, 1989). If the BD-bait fusion protein and an AD-prey fusion protein do not interact the transcription factor is not activated and the reporter genes are not transcribed. The Y190 yeast strain has two reporter genes HIS3 and LacZ incorporated into its genome (Durfee and et, 1993) (Figure 3-1 (E)). This allows identification of interacting proteins as those that will enable the yeast colonies to both 1) grow on media lacking the amino acid histidine and 2) express functional β-galactosidase that can cleave 5-bromo-4-chloro-3-indolyl-D-galactopyranoside (x-gal) to give a blue product. The general principles of the yeast two-hybrid screen are described in (Bartel and Field, 1997; McAlister-Henn *et al.*, 1999; Gietz and Woods, 2002a).

A. The bait plasmid.

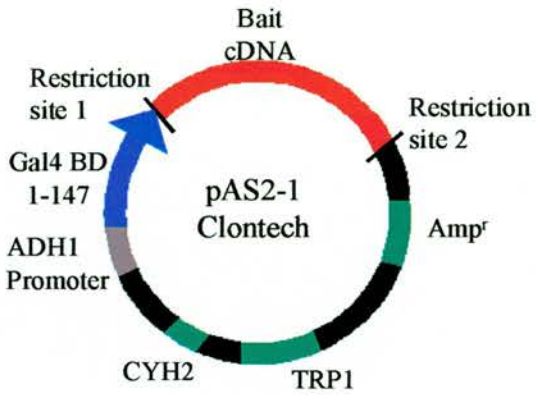

B. The prey plasmid.

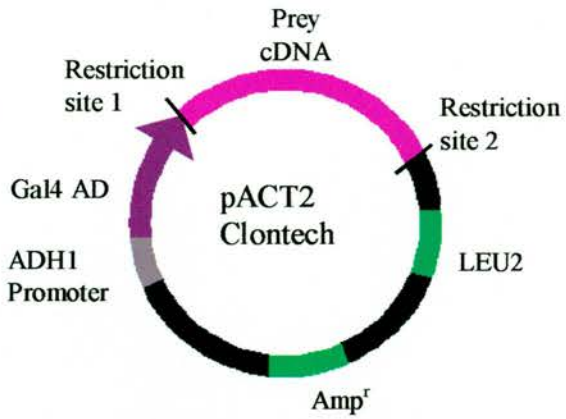

C. The BD-bait fusion protein.

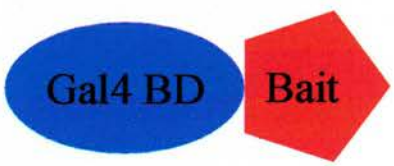

D. The AD-prey fusion protein.

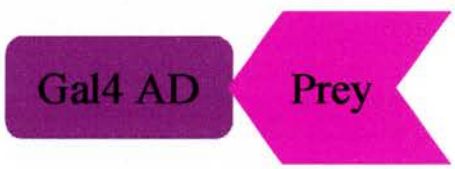

E. Interaction of the BD-bait and AD-prey fusion proteins in the yeast nucleus produce a functional transcription activator. This initiates transcription of reporter genes.

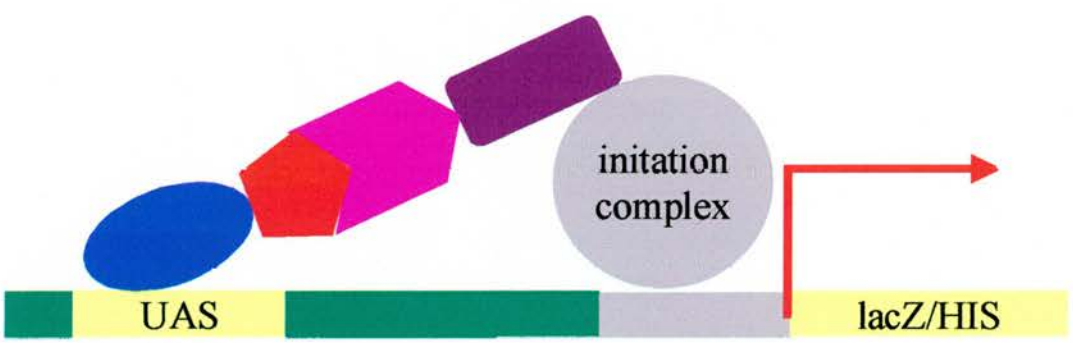

Figure 3-1. General principles of the yeast two-hybrid assay. **A)** The bait plasmid. **B)** The prey plasmid. **C)** A chimeric protein consisting of the BD of GAL4 N-terminally fused to the bait protein. **D)** A chimeric protein of the AD of GAL4 N-terminally fused to the prey protein. **E)** Binding of the bait and prey protein will bring both parts of the GAL4 transcription factor into close proximity and initiate the transcription of reporter genes. See text for details.

3.1 The yeast two-hybrid library screen.

The library screening procedures that were carried out are summarised in Figure 3-2 and are described briefly below.

3.1.1 Cloning of the bait and library plasmids.

3.1.1.1 The NrCAM bait plasmid.

The DNA sequence encoding the intracellular C-terminal region of rat NrCAM (NrCAM-CT) (amino acids 1102-1215; accession number U81037) was amplified by PCR from a developing rat optic nerve library and sub-cloned into pAS2-1 (Clontech) (Figure 3-3).

3.1.1.2 The Library plasmids.

A developing rat brain cDNA library was sub-cloned into the pACT2-AD (Clontech) vector (a gift from Prof. P. Brophy, University of Edinburgh).

3.1.2 Initial testing of the bait.

3.1.2.1 Autonomous reporter activation of bait and yeast cell toxicity.

A number of initial tests are recommended before commencing a large scale library screen (Gietz et al., 1997). pAS2-1 NrCAM CT was tested for toxicity, inappropriate auto-activation and appropriate activation of the LacZ gene using the filter lift assay as previously described (section 2.4.3). Briefly the pAS2-1 NrCAM CT vector together with the appropriate pACT vector were co-transformed into Y190

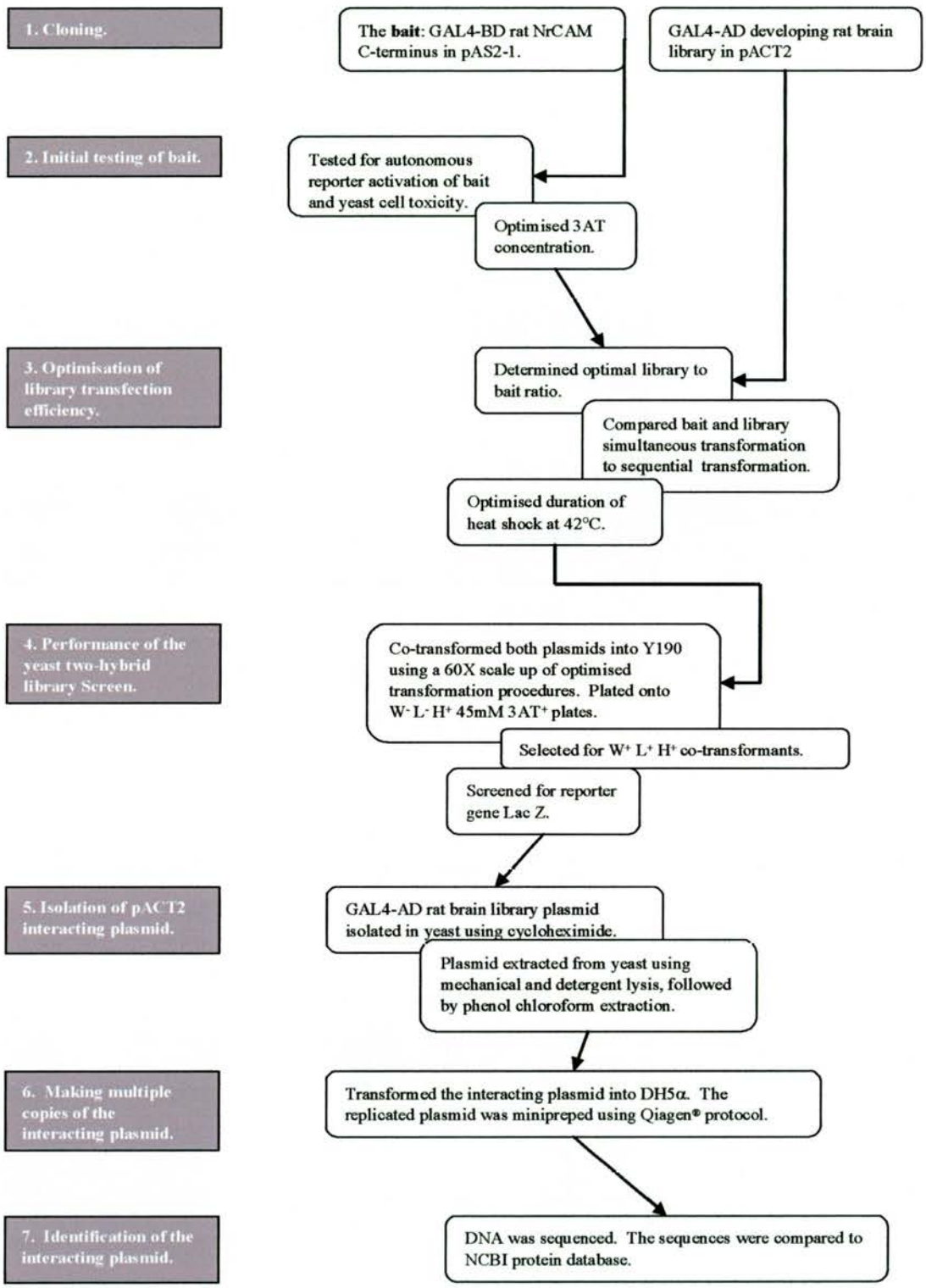

Figure 3-2. A flow chart of the two-hybrid library screen method used in this thesis. Steps 1 to 7 (grey boxes) were carried out in this order. White boxes are more detailed methodologies of each step. Full details are given in the text (3.1)

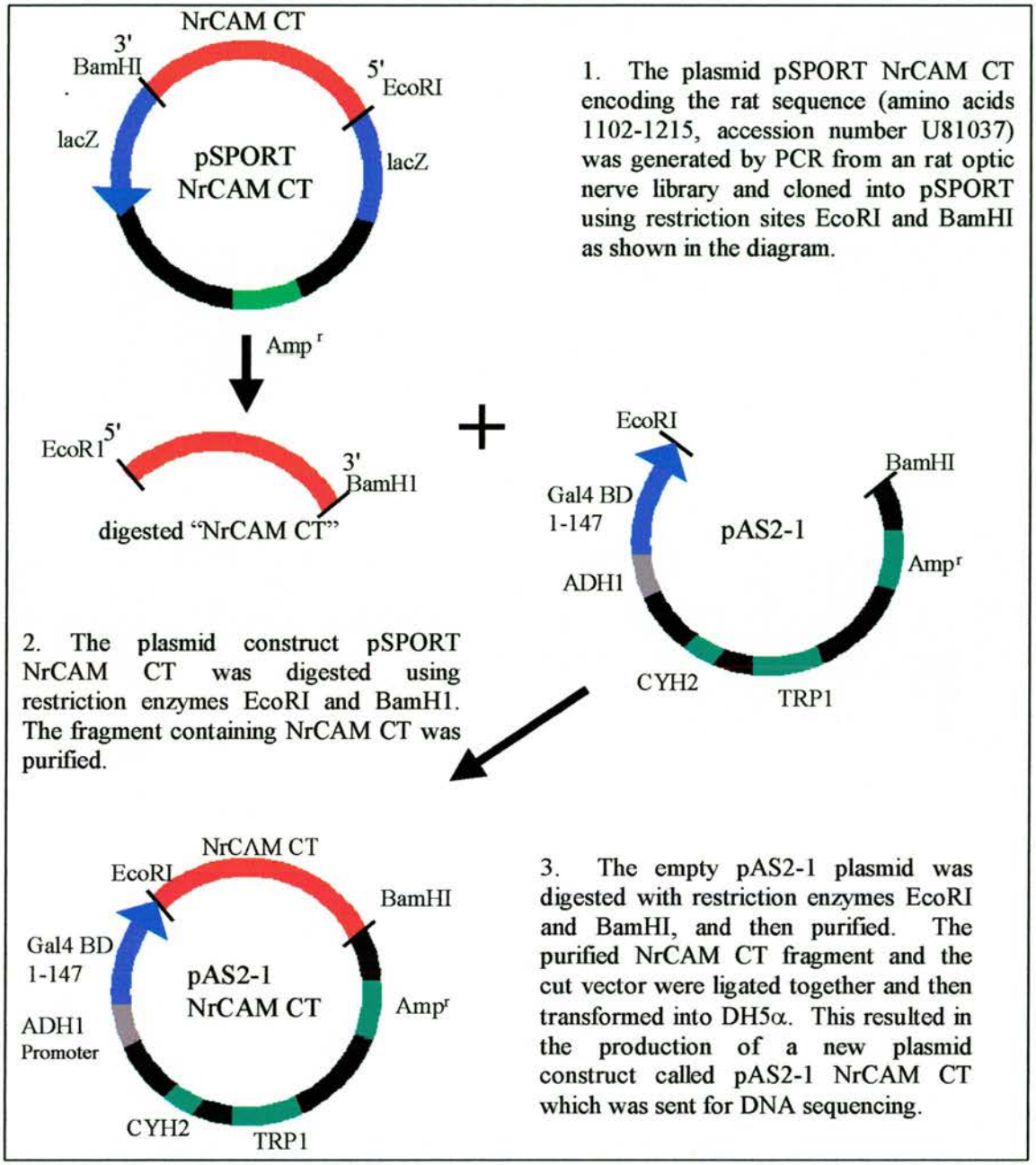

Figure 3-3. Cloning strategy for the production of the plasmid pAS2-1 NrCAM CT. Full details of materials and methods are described in chapter 2 and accompanying text.

and grown on tryptophan and leucine deficient (W^- L^-) agar plates. After three days yeast colonies were transferred on to filter papers, the yeast cell walls were lysed by snap freezing in liquid nitrogen and the lysed yeast were incubated in x-gal

containing buffer. The strength of the interaction of the bait and prey plasmid was assessed as the time taken for β-galactosidase to cleave x-gal to a blue product. A ranking system was introduced as described in Table 3-1

Time taken to go blue	Binding Strength	Ranking
within 30 minutes	very strong	++++
30 to 60 minutes	strong	+++
one to two hours	moderate	++
two to six hours	weak	+
greater than six hours	none	-

Table 3-1. The ranking system in this thesis, to rank binding strengths of interacting proteins in the yeast two-hybrid.

To ensure that NrCAM does not auto-activate, i.e. that the BD-NrCAM CT fusion protein was not sufficient to initiate transcription of the lacZ gene without an interacting AD fusion protein, 1 μg of the pAS2-1 NrCAM CT plasmid was transformed together with 1 μg of empty pACT vector into Y190 and the filter lift assay was performed (section 2.4.3). The expression of the pAS2-1 NrCAM-CT plasmid in the yeast nucleus without an interacting protein did not induce β-galactosidase to cleave x-gal to a blue product and it was concluded that the pAS2-1 NrCAM CT did not auto-activate.

To ensure that NrCAM was expressing correctly in the yeast nucleus and that it interacted normally with an already established cytoplasmic binding partner of NrCAM, 1 μg of ankyrin$_R$ (amino acids 14-515) in pACT (a gift from Prof. P Brophy, University of Edinburgh) was co-transformed into Y190 with 1 μg of pAS2-1 NrCAM CT. Transformed colonies were allowed to grow on W^- L^- agar plates, the

filter lift assay was performed and colonies containing the pAS2-1 NrCAM CT plasmid and the pACT ankyrin$_R$ plasmid went blue within 30 minutes, indicating a strong interaction. Thus it was established that the pAS2-1 NrCAM CT plasmid was expressing correctly and could therefore identify potential cytoplasmic interacting protein partners. These results also confirmed the suitability of the yeast strain Y190 for use with this bait as the LacZ gene had been correctly activated.

3.1.2.2 Choosing a 3AT concentration.

The Y190 strain contains two reporter genes *HIS3* and *lacZ* (Durfee and et, 1993). Yeast colonies that contain interacting BD and AD fusion proteins are able to grow on agar plates lacking the amino acid histidine (H^-) and can express β-galactosidase and cleave x-gal. The design of the library screen requires both of these reporter genes to eliminate non-interacting colonies. The first elimination step disregards colonies not able to grow on H^- plates. The second elimination step eliminates colonies unable to cleave x-gal (Figure 3-2, step 4).

However, the Y190 yeast strain is leaky for HIS3 expression and can grow on H^- plates. The addition of the chemical 3-amino-1,2,4-triazole (3AT) to the yeast's growth medium is necessary to quench the background expression of the *HIS3* gene product (Durfee and et, 1993). Thus the optimal 3AT concentration for Y190 transfected with the NrCAM bait had to be established. The 3AT concentration was optimised by plating Y190 transformed with bait on a series of $W^- H^-$ at 3AT concentrations of 0, 20, 30, 35, 40, 45, 55, 50, 60 and 80 mM. This experiment was performed three times. A 3AT concentration of 45 mM was selected as optimal

because after one week as it allowed only small (<1mm) colonies to grow. This relatively high concentration for 3AT is typical of concentrations found by other groups when using a combination of Y190 and the pAS2-1 vector (Parchaliuk *et al.*, 1999a; Furuyama and Sassa, 2000; Kim *et al.*, 2002).

3.1.3 Determination of library transformation yield and efficiency.

Before performing a large-scale library screen it is recommended that the transformation procedure be optimised for the bait, library and yeast strain being used (Gietz et al., 1997).

3.1.3.1 Optimal library to bait ratio.

The standard high-efficiency transformation protocol described in section 2.4.2 (Agatep et al., 1998; Gietz and Woods, 2002b) was used to co-transform Y190 with 2 μg of bait plasmid together with increasing concentrations of pACT2 rat brain library DNA (0.5 μg, 1 μg and 2 μg). Transformed Y190 were plated onto W^- L^- agar plates and the yeast colonies were counted after three days growth. Transformation efficiencies for the increasing quantities (plus or minus the standard error of the mean (n=3)) of library cDNA were calculated to be $2.3 \times 10^4 \pm 0.1 \times 10^4$, $2.7 \times 10^4 \pm 0.3 \times 10^4$ and $3.0 \times 10^4 \pm 0.09 \times 10^4$ colony forming units per μg of DNA respectively. As library transformation efficiency was not statistically different when using 1 μg or 2 μg of library cDNA it was decided to use 1 μg of library cDNA on economic grounds.

3.1.3.2 Bait and library simultaneous transformation versus sequential transformation.

The efficiency of the sequential transformation of bait plasmid and then library plasmid was compared with the efficiency of co-transformation of bait and library plasmids. The standard high-efficiency transformation protocol (section 2.4.2) (Agatep et al., 1998; Gietz and Woods, 2002b) was used to transform Y190 with 2 μg of bait plasmid. The pAS2-1 NrCAM CT expressing colonies were grown for three days on agar plates lacking the amino acid leucine (L^-). The pAS2-1 NrCAM CT expressing colonies were inoculated into L^- liquid medium and the pAS2-1 NrCAM CT expressing yeast cells were transformed with library plasmids (section 2.4.2) (Agatep et al., 1998). Y190 that had been transformed with both plasmids were plated onto $W^- L^-$ agar plates and the number of colonies that grew after three days were counted. This experiment was repeated twice. On both occasions efficiencies were found to be approximately 100^{th} of co-transformation efficiencies reported above. It was decided that the co-transformation protocol would be used for the library screen to maximise transformation efficiency.

3.1.3.3 Optimisation of duration of 42 °C heat shock.

The standard high-efficiency transformation protocol (section 2.4.2) was used to transform Y190 with 2 μg of bait plasmid and 1 μg of library plasmids with two amendments to the standard protocol:

1) The heat shock at 42 °C was performed on individual transformations for 15 minutes, 30 minutes and 60 minutes.

2) Only 10 µl (normally 200µl) of each transformation mixture was plated on to three 90 mm W^- L^- agar plates.

Yeast colonies were counted three days later. The mean number of colonies (plus or minus the standard error of the mean (n=3)) for increasing heat shock time was found to be 3 ± 1, 10 ± 3 and 35 ± 9 colonies respectively. Thus it was decided to heat shock for one hour when performing the large scale transformation experiment.

3.1.4 Transforming with library DNA.

Once the efficiency tests were completed and an optimal protocol chosen a large-scale library screen was performed. A 60X scale up of the normal transformation procedure was chosen as this was calculated to be sufficient to cover the library once. 120 µg of bait plasmid and 60 µg of library plasmids were co-transformed into Y190 using the standard protocol (section 2.4.2) (Agatep et al., 1998; Gietz and Woods, 2002b). 420 µl of the transformation mixture was plated on to ninety five-150 mm W^- L^- H^- $3AT^+$ agar transformation plates and 10 µl of transforming mixture on to four-90 mm W^- L^- agar efficiency test plates. The efficiency test plates were counted three days after the transformation procedure was carried out and the transformation efficiency of the screen plus or minus the standard error of the mean was calculated to be $5.78 \times 10^4 \pm 0.972 \times 10^4$ colony forming units per µg of DNA. 60 µg of DNA was transfected therefore $3.468 \times 10^6 \pm 0.586 \times 10^6$ clones were transformed. The complexity of the library was 3.3×10^6 independent clones. Therefore, the yeast two-hybrid screen had covered the whole cDNA library at least once. The large transformation plates were incubated at 30 °C for 21 days in loosely fitting bags.

3.1.4.1 Selecting the yeast two-hybrid positives.

Transformation plates were checked for positive colonies after four days of incubation at 30 °C. Positive colonies were chosen that were observed to grow faster than the background growth, the colony was circled and given a library reference number. The circled colonies were further observed every day for the first week and every second day for a further two weeks. When the diameter of the colonies had reached approximately two to three millimetres they were plated in triplicate on to fresh $W^- L^- H^- 3AT^+$ agar plates. In total 519 positive colonies were circled and re-plated on to $W^- L^- H^- 3AT^+$ agar plates. After 3-5 days (depending on the rate of growth) the colonies growing on the fresh $W^- L^- H^- 3AT^+$ agar plates were tested for β-galactosidase activity by filter lift assay (section 2.4.3) (Parchaliuk et al., 1999b). 33 out of 519 positive colonies went blue after the first filter lift assay. These "blue colonies" were plated onto another fresh $W^- L^- H^- 3AT^+$ agar plates and retested using the filter lift assay. Only 31 of the 33 "blue colonies" were still positive for β-galactosidase activity after a second filter lift assay was performed. Of the 31 colonies 18 colonies went blue within 30 minutes and were considered strong interactions.

3.1.5 Isolating the pACT2 interacting plasmid.

3.1.5.1 Cycloheximide selection for colonies that have lost the GAL4 BD-bait plasmid.

The Y190 yeast strain carries the Cyh^r2 mutant allele and so is cycloheximide resistant (Harper et al., 1993). The pAS2-1 plasmid encodes the dominant wild type CH^S2 gene and transformation of the plasmid into Y190 makes the yeast strain sensitive to cycloheximide. Yeast cells containing both plasmids will spontaneously loose the pAS2-1 plasmid while retaining the pACT2 plasmid if plated onto cycloheximide containing media (http://www.icb.ufmg.br/~prodap/2003/ tectrans/dhclontech.pdf). The 31 blue colonies from section 3.1.4 were plated onto cycloheximide containing W^- L^- agar plates. Colonies growing on these plates were picked and re-plated onto both L^- plates and W^- plates. Colonies that grew on L^- but not on W^- plates (i.e. contained the library plasmid only) were stored at 4°C. One colony did not grow on the cycloheximide containing W^- L^- agar plate and 30 out of the 31 yeast colonies were available for DNA extraction in 3.1.6 below. The filter lift assay was used to test the 30 colonies for auto-activation of the pACT2-AD library plasmid as they grew on the L^- agar plates (colonies not expressing a pAS2-1 bait plasmid should not be able to activate the lacZ gene and cleave x-gal). No colonies were found to be auto-activating at this step.

3.1.6 Extracting DNA from yeast and retransformation into DH5α.

DNA was extracted from the 30 yeast colonies (section 2.4.5) and the entire DNA solution was then transformed into super competent DH5α (section 2.1.9). The

replicated DNA was extracted from this *E.coli* strain (section 2.1.10) and 200 ng to 300 ng of the DNA was sent to the Sequencing Service of the University of Dundee for sequencing (http://www.dnaseq.co.uk).

3.1.7 Identification of potential candidate proteins that may bind NrCAM.

Sequences received from the University from Dundee were checked against their Chromas file (http://www.technelysium.com.au/chromas.html) to ensure accuracy. They were then put into the correct frame and the nucleotide sequence translated to an amino acid sequence using the EXPASY translation tool (http://us.expasy.org/tools/dna.html). The resulting translated sequence was then compared against the NCBI database (http://www.ncbi.nlm.nih.gov/) of July/August 2002 and again in March/April 2004. Two of the thirty cDNAs clones did not give a clean DNA sequence despite being sequenced twice. The 28 remaining library clones are described in Table 3-2.

Of these 28 clones, 8 encoded for DNA binding proteins, collagen, viral DNA and short peptides. DNA binding proteins and collagen are common false positives found in most yeast two-hybrid screens (Hengen, 1997). There were two short peptide sequences. One was 34 amino acids and the other 8 amino acids. The sequences of both peptides had no corresponding matches in the BLAST search of the NCBI database and were not considered to be real protein products that could interact with NrCAM. Therefore these eight clones were immediately dismissed as unlikely candidates (Table 3-2).

Matched to protein database		Strength of Interaction <30min	>30min	Unlikely candidate	Auto-activation	Potential Candidates
Ankyrin B	10	9	1			10
SAP102	3	2	1			3
PSD-95	1		1			1
GIPC	2	1	1			2
VHS of GGA1	1	1				1
RanBPM	3	3			3	
DNA binding proteins	4		4	4		
Collagen	1		1	1		
Viral DNA	1		1	1		
Short Peptides	2		2	2		
Total library clones	**28**	**16**	**12**	**8**	**3**	**17**

Table 3-2. Identification of clones selected by the yeast two-hybrid screen. (section 3.1.7).

The remaining 20 clones were subjected to a second test for auto-activation. 1 μg of empty pAS2-1 vector cDNA and 1 μg each library cDNA plasmid was transformed into Y190 using the standard protocol (Agatep et al., 1998; Gietz and Woods, 2002b) (2.4.2) and plated onto W^- L^- agar plates. The colonies were tested for β-galactosidase activity using the filter lift assay protocol. The scoring system used is as described in Table 3-1. The results are given in Table 3-2. All of the RanBPM colonies went blue within the first 15 minutes and were eliminated as false positives. This left a remaining 17 potential candidates (Table 3-2).

3.2 Analysis and description of the potential NrCAM binding candidates.

3.2.1 Ankyrin$_B$.

Ten of the positive clones encoded for the membrane binding sequence of ankyrin$_B$ (ankyrin2). NrCAM's interaction with ankyrin has already been described

(Davis and Bennett, 1994). The best matches in the NCBI database are shown in Table 3-3. Seven of the interactions were selected from $W^- L^- H^- 3AT^+$ agar plates in the first week, two in the second week and one in the third week (Table 3-3). When performing the filter lift assay nine of the colonies went blue within 30 minutes and were considered strong interactions.

3.2.2 SAP102.

Three of the positive clones coded for part of the cDNA of Synapse associated protein 102 (SAP102) and one encoded for the cDNA of postsynaptic density-95 (PSD-95/SAP90). SAP102 and PSD-95 are two members of the membrane-associated guanylate kinase (MAGUK) family (Fujita and Yoshihisa, 2000). MAGUKs are a family of signalling molecules that are characterized by their three PSD95/Dlg/ZO-1 (PDZ) domains, a single src homology 3 (SH3) domain and a guanylate kinase domain (GUK) (Fujita and Yoshihisa, 2000).

Name	Protein accession	Selected	Interaction strength <30 mins.	>30 min.
4A	XP_342338	Week 1	1	
10A	XP_342338	Week 1	1	
16A-1	2003319A	Week 1	1	
4D-1	Q01484	Week 1	1	
22A	Q01484	Week 1	1	
27A	Q01484	Week 1	1	
27B 2A	CAB42644	Week 1	1	
57B-2	Q01484	Week 2	1	
68B-2	Q01484	Week 2	1	
37B	S37431	Week 3		1

Table 3-3. Identification of the ten-ankyrin clones isolated by the yeast two-hybrid screen.

Two of the clones (RL48A(2) and RL29B) had been selected as fast growing colonies on $W^- L^- H^- 3AT^+$ agar plates in week one and were considered strong interactions as colonies went blue within 30 minutes when the filter lift assay was performed. Both of these clones encoded for the three PDZ domains and the SH3 domain of SAP102 (amino acids 54-623 accession number U53367) (Muller et al., 1996) but minus an alternatively spliced region (amino acids 120-137). They did not code for a stop before running into the pAC2-AD vector sequence. Therefore, the expressed protein has an additional seven amino acids before encountering the stop encoded for by the pACT2-AD vector (Figure 3-4).

The third SAP102 clone (RL71D) had been selected as a fast growing colony on a $W^- L^- H^- 3AT^+$ agar plate in week three and was considered a weak interaction as colonies went blue within two hours when the original filter lift assays were performed (section 3.1.4.1). This clone contained three PDZ domains of SAP102 (amino acids 96-533 accession number U53367) (Muller et al., 1996) and a single proline followed by a stop. It included the amino acids of the alternatively spliced region (amino acids 120-137) that were not found in RL48A(2) and RL29B but are reported in accession number U53367 (Figure 3-4).

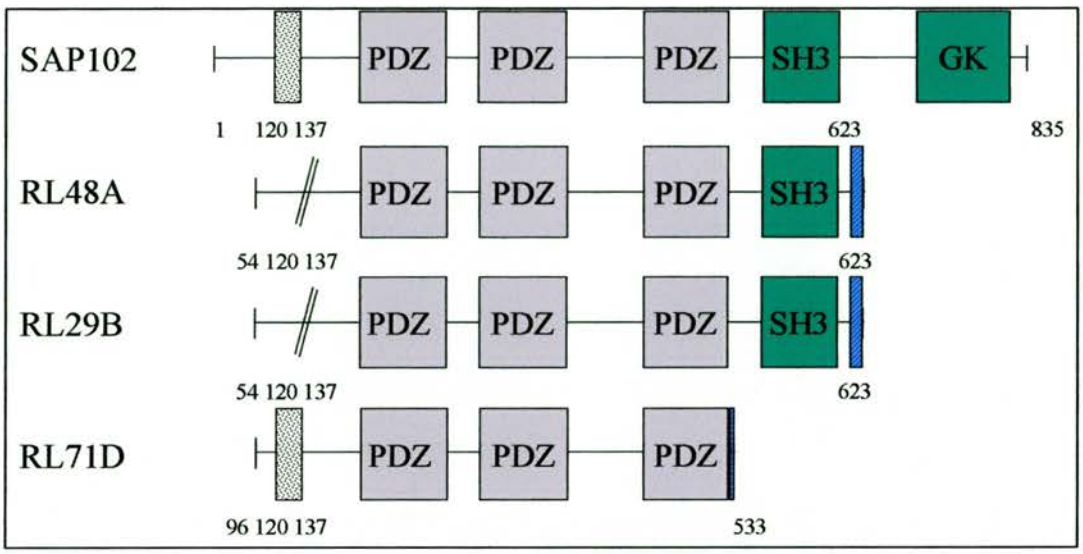

Figure 3-4. Alignment of the protein domains encoded by the rat library cDNA clones RL48A, RL29B and RL71D against the protein domains of full length SAP102 as described by accession number U53367. PDZ domains have been shown in grey, other protein domains have been shown in green. Additional amino acids encoded by the rat library clone not normally encoded by SAP102 DNA are shown in blue.

3.2.3 PSD-95.

The PSD-95 clone (RL65B) had been selected as fast growing colony on a W^- L^- H^- $3AT^+$ agar plate in week two and was considered a moderate interaction as colonies went blue within 60 minutes when the original filter lift assays were performed as described in 3.1.4.1. This clone contained the cDNA coding for the first two PDZ domains of PSD-95 (amino acids 71-258 accession number NP_062567 (Takeuchi et al., 1997) followed by a further six amino acids and then a stop (Figure 3-5).

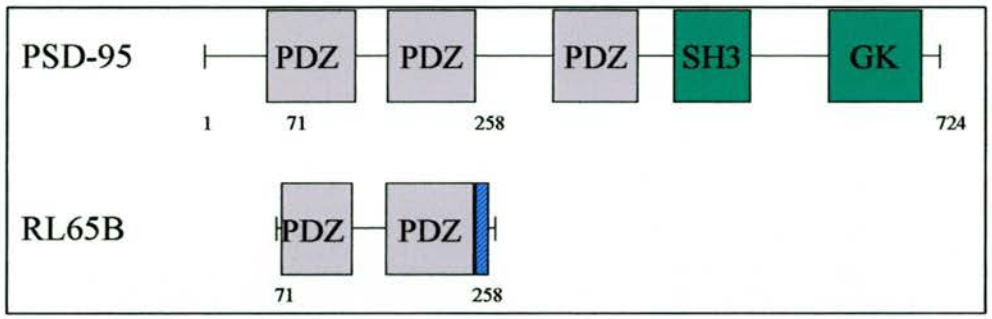

Figure 3-5. Alignment of the protein domains encoded by the rat library cDNA clone RL65B against the protein domains of full length PDS-95 as described by accession number NP_062567. PDZ domains have been shown in grey, other protein domains have been shown in green. Additional amino acids encoded by the rat library clone not normally encoded by PSD-95 DNA are shown in blue.

3.2.4 GIPC.

Two of the positive clones encoded for the cDNA of GAIP interacting protein C terminus 1 (GIPC1). GIPC1 along with GIPC2 and GIPC3 are members of the GIPC family. GIPCs are proteins with a central PDZ domain and GIPC homology (GH1 and GH2) domains (Katoh, 2002) (Figure 3-6). Two of the clones (RL16B(C)(2) and RL6C(2)) had been selected as fast growing colonies on $W^- L^- H^- 3AT^+$ agar plates in week one and week two respectively. RL16B(C)(2) was considered a strong interacting plasmid as colonies went blue within 30 minutes when the filter lift assay was performed and RL6C(2) was originally considered a weak interacting plasmid as colonies went blue after two hours when the filter lift assay was performed (section 3.1.4.1).

RL16B(C)(2) encoded for sequence 5' of the published start of GIPC. This 5' sequence included 36 nucleotides followed by the published promoter of GIPC (accession number NM_053341). The cDNA then encoded for amino acids 1-215 of accession number NP_445793 followed by 22 amino acids to a stop (Figure 3-6)

(Bunn et al., 1999). The pACT-AD vector is designed to express the GAL4 AD followed by all the encoded amino acids to the first stop. Thus the RL16B(C)2 plasmid expressed amino acids not normally expressed by native GIPC such as the promoter sequence (Figure 3-6, blue areas). This was also true for RL6C(2).

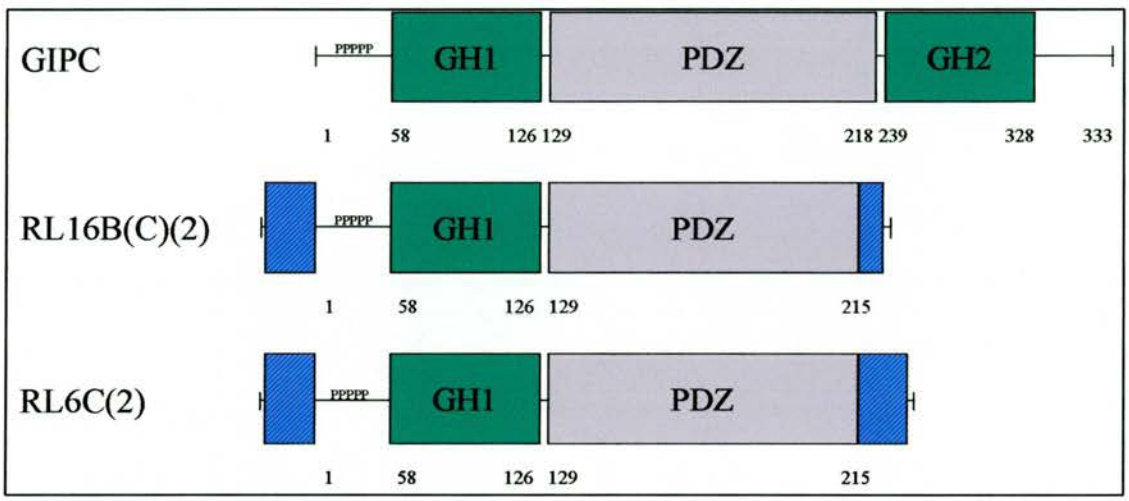

Figure 3-6. Alignment of the protein domains encoded by the rat library cDNA clones RL16B(C)2 and RL6C(2) against the protein domains of full length GIPC as described by accession number NP_445793. PDZ domains have been shown in grey, other protein domains have been shown in green. Additional amino acids encoded by the rat library clone not normally encoded by GIPC DNA are shown in blue.

RL6C(2) encoded for sequence 5' of the published start of GIPC. This 5' sequence included 36 nucleotides followed by the published promoter of GIPC (accession number NM_053341). The cDNA then further encoded for amino acids 1-215 of accession number NP_445793 followed by 126 amino acids to a stop (Figure 3-6).

3.2.5 The VHS domain of GGA1.

The RL68C clone encoded for the Vps27, Hrs and STAM (VHS) domain of Golgi-localized, gamma-ear-containing, Arf binding protein I (GGA1) (amino acids 1-161 of accession number AAF05707 (Boman et al., 2000). GGAs are described in Figure 3-7 and consist of an N-terminal VHS domain, followed by a ~20 amino acid proline rich sequence, which in turn is followed by a GGA and TOM (GAT) domain, an unstructured variable amino acid hinge segment and finally a γ-adaptin ear (GAE) domain (reviewed Boman, 2001; Hirst et al., 2001). The cDNA of RL68C did not code for a stop before running into the pAC2T-AD vector sequence. Therefore, the expressed protein has an additional seven amino acids before encountering the stop encoded for by the pAC2T-AD vector. The RL68C clone had been selected as a fast growing colony on $W^- L^- H^- 3AT^+$ agar plates in week two. RL68C was considered a strong interacting plasmid, as colonies went blue within 30 minutes when the filter lift assay was performed (section 3.1.4.1) (Figure 3-7).

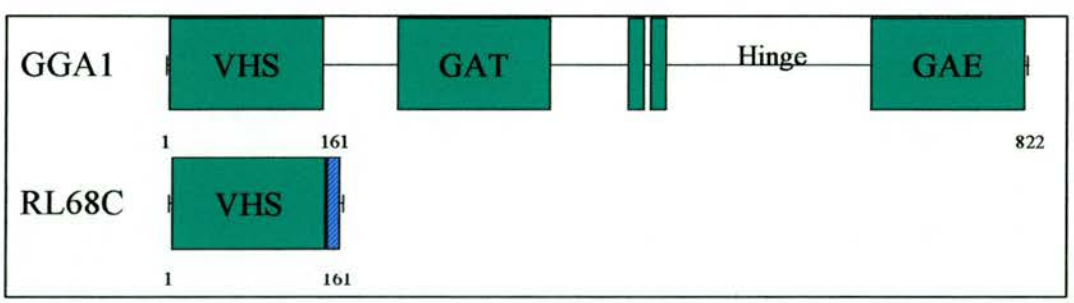

Figure 3-7. Alignment of the protein domains encoded by the rat library cDNA clone RL68C against the protein domains of full length GGA1 as described by accession number AAF05707. Protein domains have been shown in green. Additional amino acids encoded by the rat library clone not usually normally coded for by GGA1 are shown in blue.

3.3 Cloning of new NrCAM and L1-CAM bait plasmids.

The interaction of the clones described in Table 3-2 had been confirmed by two filter lift assays on $W^- L^- H^- 3AT^+$ agar plates (section 3.1.4.1). However there are two potential problems in relying upon these assay results:

1. More than one library plasmid could potentially be transfected into and hence expressed by an individual colony of yeast. Thus the cDNA that was isolated from the yeast colonies in sections 3.1.5 and 3.1.6 may not have been the plasmid coding for the true NrCAM-interacting protein but of a second non-interacting plasmid.

2. The colonies require the continuous interaction of the BD-NrCAM CT and the AD-prey fusion proteins to allow robust growth on media lacking histidine and containing 3AT. This additional selection pressure may have increased LacZ gene expression by the yeast over what may have occurred on a $W^- L^-$ agar plate.

To eliminate these possibilities the relative binding strengths of each of the colonies listed as potential candidates in Table 3-2 were re-tested. 1 μg of the pAS-1 NrCAM CT was co-transformed with 1 μg of each of the seven library clones into Y190 yeast. The transformed yeast were plated onto $W^- L^-$ agar plates and grown for three days after which the filter lift assay was performed (section 2.4.3). This assay was repeated on two separate occasions and the results are shown in Table 3-4. The binding of NrCAM to $ankyrin_R$ plasmid was used as a positive control for the assays. From Table 3-4 only five of the seven library plasmids reconfirmed as an interacting protein, as the shorter SAP102 clone RL71D and the PSD-95 clone RL65B failed to go blue within 6 hours. Of the five remaining interactions, all showed a weaker

binding strength, as measured by the filter lift assay, then had been found on $W^- L^- H^-$ $3AT^+$ agar plates.

Protein	Library Clone	Strength of interaction
$Ankyrin_R$	N/A	++++
SAP102	RL48A(2) and RL29B	+++
SAP102	RL71D	-
PSD-95	RL65B	-
GIPC	RL16B(C)(2) and RL6C(2)	+++
VHS	RL68C	+++

Table 3-4. Re-transformation and re-testing of plasmids isolated by the yeast two-hybrid library screen. The filter lift assay results as reported in section 3.1.9.

3.3.1 Cloning of NrCAM C-terminal deletion bait plasmids.

A set of filter assays were performed on the five remaining library plasmids to establish the region in the cytoplasmic terminus of NrCAM that binds to the library proteins. Three pAS2-1 NrCAM plasmids were designed that would encode for part of the cytoplasmic terminus of NrCAM as described in Figure 3-8 and Figure 3-9. One of these plasmids (pAS2-1 NrCAM 1-22) encoded for the first 86 amino acids of the NrCAM cytoplasmic terminus and included the sequence of the proposed ankyrin-binding site of NrCAM. The second plasmid pAS2-1 NrCAM 20-2 encoded for the last 58 amino acids of the NrCAM cytoplasmic terminus and which include the ankyrin-binding domain. The third plasmid pAS2-1 NrCAM 21-2 encoded the last 28 amino acids of the NrCAM cytoplasmic terminus, which do not include the ankyrin-binding domain. Thus these plasmids would be able to distinguish between binding cytoplasmic binding partners of NrCAM that bound N-terminally and C-

terminally and cytoplasmic binding partners that bound in the region of the ankyrin-binding domain.

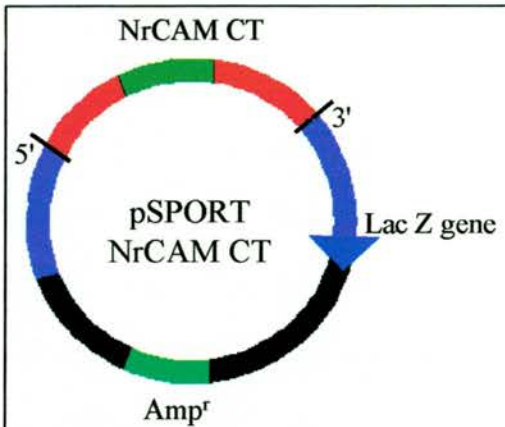

1. The plasmid pSPORT NrCAM CT encoding the rat sequence) amino acids 1102-1215, accession number U81037) was used as a PCR template. The ankyrin-binding domain of NrCAM has been shown in green and the remainder of the cytoplasmic sequence of NrCAM in red.

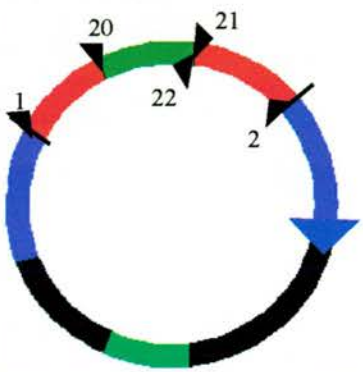

2. PCR sense primers NrCAM 1, NrCAM 20 and NrCAM 21 were designed to add the EcoRI restriction enzyme site to the 5' of the NrCAM encoding sequence. PCR anti-sense primers NrCAM 2 and NrCAM 22 were designed to add the BamH1 restriction enzyme site to the 3' cDNA of the NrCAM encoding sequence (see appendix 4 for primer sequences).

Figure 3-8. Continued on next page.

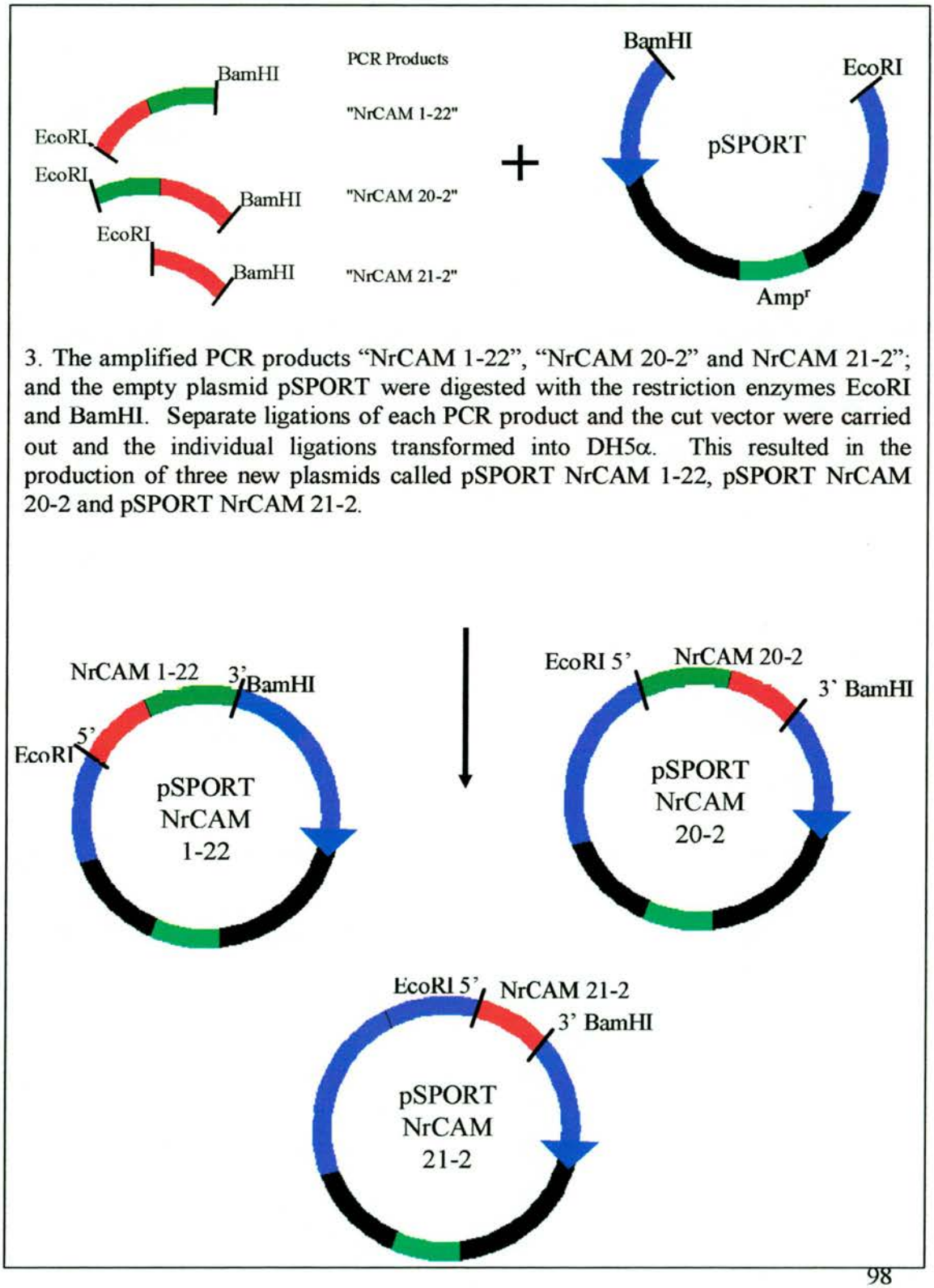

3. The amplified PCR products "NrCAM 1-22", "NrCAM 20-2" and NrCAM 21-2"; and the empty plasmid pSPORT were digested with the restriction enzymes EcoRI and BamHI. Separate ligations of each PCR product and the cut vector were carried out and the individual ligations transformed into DH5α. This resulted in the production of three new plasmids called pSPORT NrCAM 1-22, pSPORT NrCAM 20-2 and pSPORT NrCAM 21-2.

Figure 3-8 Continued on next page.

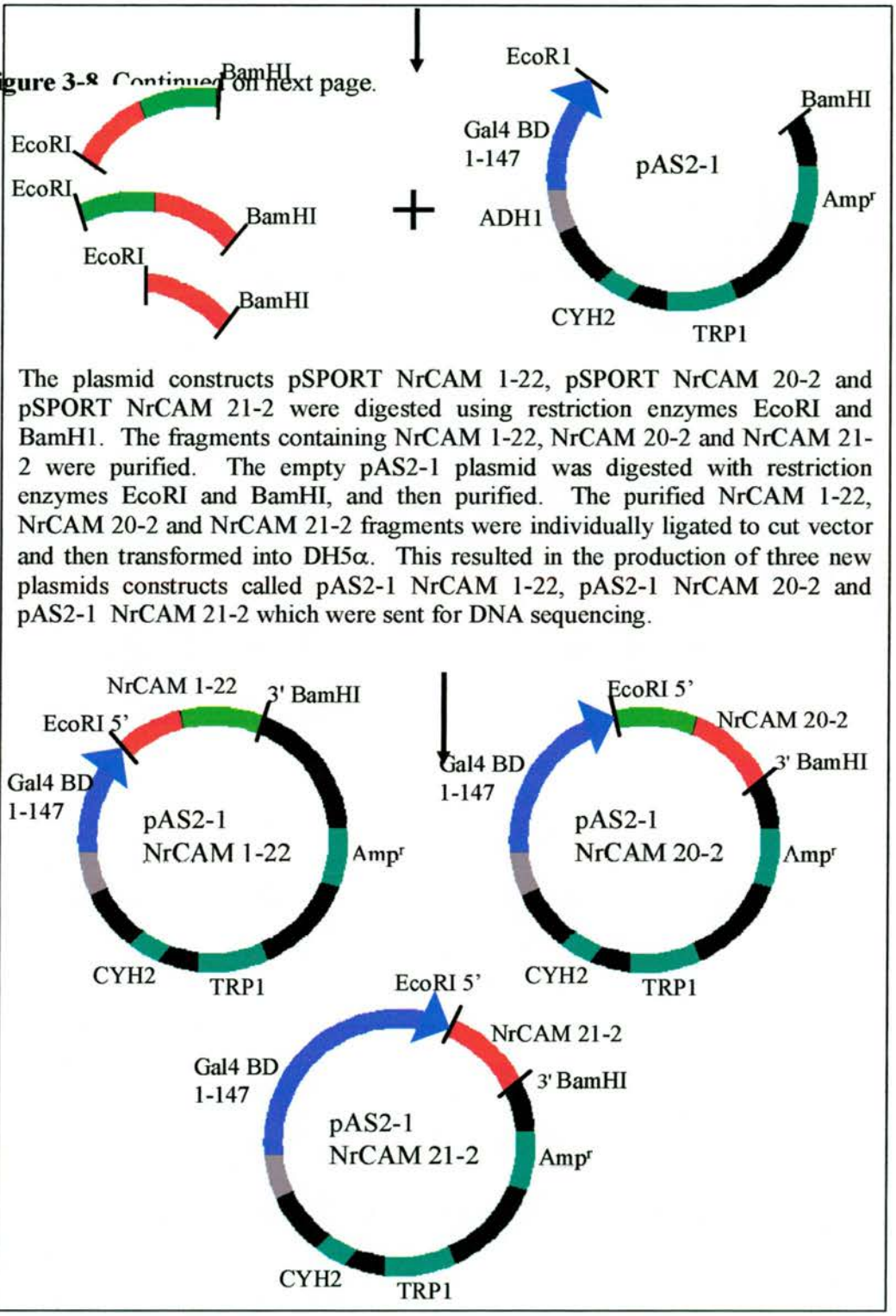

The plasmid constructs pSPORT NrCAM 1-22, pSPORT NrCAM 20-2 and pSPORT NrCAM 21-2 were digested using restriction enzymes EcoRI and BamH1. The fragments containing NrCAM 1-22, NrCAM 20-2 and NrCAM 21-2 were purified. The empty pAS2-1 plasmid was digested with restriction enzymes EcoRI and BamHI, and then purified. The purified NrCAM 1-22, NrCAM 20-2 and NrCAM 21-2 fragments were individually ligated to cut vector and then transformed into DH5α. This resulted in the production of three new plasmids constructs called pAS2-1 NrCAM 1-22, pAS2-1 NrCAM 20-2 and pAS2-1 NrCAM 21-2 which were sent for DNA sequencing.

Figure 3-8. Cloning strategy for the production of the plasmids pAS2-1 NrCAM 1-22, pAS2-1 NrCAM 20-2 and pAS2-1 NrCAM 21-2. Full details of materials and methods are described in chapter 2 and accompanying text.

3.3.2 Cloning of bait plasmid pAS2-1 NrCAM Y86>E.

Dr. F. Davey of the University of St Andrews generated another pAS2-1 NrCAM bait plasmid with a single amino-acid mutation from tyrosine to glutamic acid at position 86 of the cytoplasmic rat sequence (this is amino acid 1187 of accession number U81037). This plasmid substitutes a negatively charged amino acid for the tyrosine of the FIGQY sequence in the ankyrin binding site and is believed to mimic a phosphorylated tyrosine at this position (Zhang *et al.*, 1998a). The plasmid was called pAS2-1 NrCAM Y86>E.

3.3.3 Cloning of bait plasmid pAS2-1 L1 and pAS2-1 neurofascin.

It was also decided to test the various plasmids against other members of the L1-CAM family. The cytoplasmic domain of human L1 (L1-CT, amino acids 1143-1257; accession number NP_000416) was generated by PCR from a human image clone (image:6569796) supplied by the IMAGE consortium and cloned in frame into pAS2-1. The intracellular portion of neurofascin (neurofascin CT amino acids 1065-1175 of neurofascin 155; accession number AY061639) was cloned in frame into pAS2-1 by Dr F. Gunn-Moore, University of St Andrews.

3.4 Analysis of the potential binding partners to NrCAM C-terminal deletions and to other members of the L1-CAM family.

The binding of the different C-terminal deletions of NrCAM and of full length neurofascin CT and full length L1 CT to the potential binding partners (Ankyrin, SAP102, GIPC, VHS) was tested using the filter lift assay (section 2.4.3). The

binding of all of the proteins to Ankyrin$_R$ was used as a positive control. Figure 3-9 summarizes the results of these potential interactions.

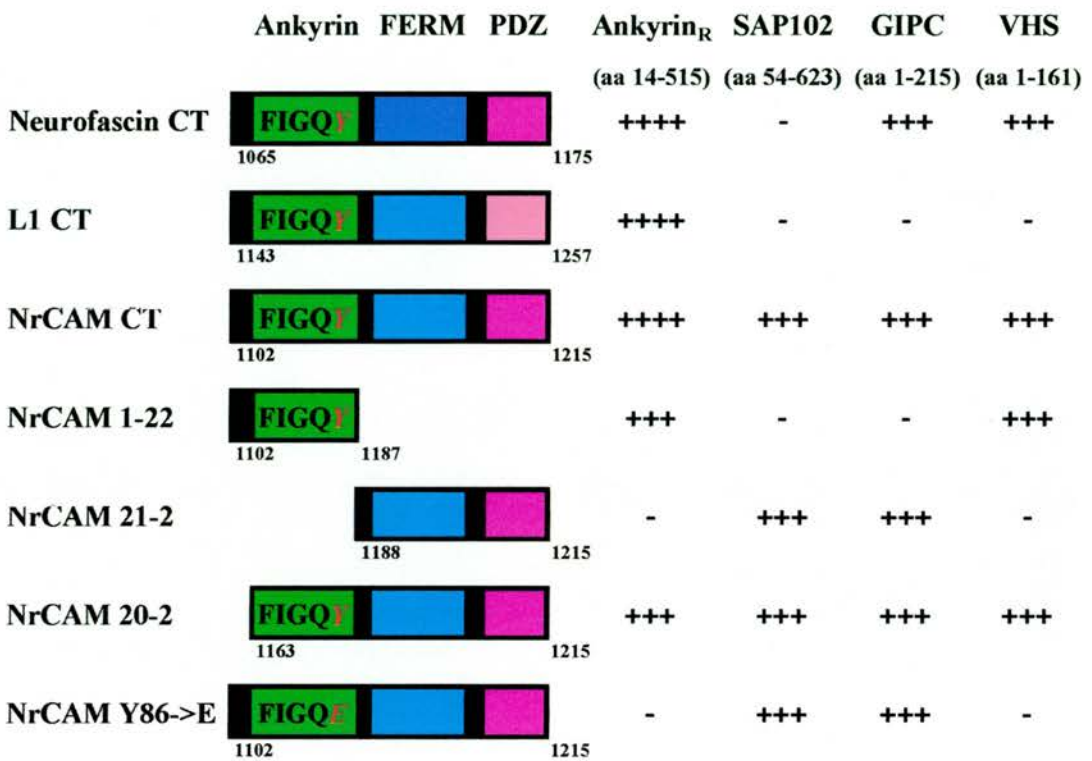

Figure 3-9. Testing of the library plasmids against differing L1-CAM baits. Ankyrin$_R$ in pAS2-1 was used as a positive control. The L1-CAM plasmids and NrCAM plasmids have been shown diagrammatically. Green boxes represent the ankyrin domain. The dark blue box is the FERM binding domain in neurofascin and the paler blue boxes are the equivalent amino acids in L1 and NrCAM. The dark pink boxes are the PDZ domains of neurofascin and NrCAM. The paler pink box is the equivalent amino acids in L1. Binding strengths were scored using the system outlined in Table 3-1.

3.4.1 Ankyrin binding.

Ankyrin$_R$ bound to L1, neurofascin and NrCAM as was expected (Davis and Bennett, 1994). pAS2-1 NrCAM 1-22 and pAS2-1 NrCAM 20-2 both encode for the amino acids defined as being the ankyrin binding site (Figure 3-9, green highlight)

and both plasmids bound to ankyrin as expected. pAS2-1 NrCAM 21-2 does not include the ankyrin binding site and showed no interaction with ankyrin as expected. Furthermore the substitution of a glutamate for the essential tyrosine in the FIGQY amino acid sequence of the NrCAM ankyrin-binding domain abolished the binding of ankyrin to NrCAM. Thus the pAS2-1 plasmids were behaving as would be expected with respect to ankyrin binding and were suitable for testing the binding preferences of the library plasmids.

3.4.2 SAP102.

RL48A(2) and RL29B encoded for the same amino acids of SAP102 (Figure 3-4) and these two plasmids gave indistinguishable filter lift assay results from each other. Therefore, both have been included in Figure 3-9 under SAP102. The SAP102 proteins did not bind to either neurofascin CT or L1 CT but did show a strong interaction with NrCAM CT (Figure 3-9). When comparing the binding of the various different length NrCAM plasmids to SAP102 it can be seen that all NrCAM plasmids bound strongly to SAP102 except for the plasmid which does not code for the C-terminal 28 amino acids of NrCAM (pAS2-1 NrCAM 1-22). Notably a plasmid consisting of only the C- terminal 28 amino acids of NrCAM (pAS2-1 NrCAM 21-2) did bind to SAP102. Thus showing that the last 28 amino acids of NrCAM are sufficient and necessary for binding of SAP102.

3.4.3 GIPC binding.

The two RL16B(C)(2) and RL6C(2) clones encoded for the same amino acids of GIPC (Figure 3-6) and these two plasmids gave indistinguishable filter lift assay results from each other. Therefore both have been included in Figure 3-9 under GIPC. The binding of these GIPC clones to NrCAM and to the other L1-CAMs was notably similar and dissimilar when compared to the binding of the SAP102 clones to NrCAM. Like SAP102 both GIPC clones showed a strong interaction (as measured by the filter lift assay) with the full NrCAM CT but did not bind to L1 CT. Unlike SAP102 however the GIPC clones showed a strong interaction with neurofascin CT. When comparing the binding of the various different length NrCAM plasmids to GIPC the results where similar to SAP102. The plasmid, which does not encode for the C-terminal 28 amino acids of NrCAM (pAS2-1 NrCAM 1-22) did not bind to GIPC, however a plasmid consisting of only the C- terminal 28 amino acids (pAS2-1 NrCAM 21-2) did bind. Thus showing that the last 28 amino acids of NrCAM are sufficient and necessary for GIPC-NrCAM binding.

3.4.4 VHS domain binding.

The binding of the VHS domain of GGA1 (RL68C) to NrCAM and to the other L1-CAMs was notably similar and dissimilar to the binding of the ankyrin$_R$ to NrCAM. Like ankyrin$_R$ the VHS clone showed a strong interaction with NrCAM CT and neurofascin CT. Unlike ankyrin$_R$ however the VHS clone did not appear to interact with L1 CT. When comparing the binding of the various different length NrCAM plasmids to the VHS clone the results where similar to ankyrin$_R$. pAS2-1

NrCAM 1-22 and pAS2-1 NrCAM 20-2 both encode for the amino acids defined as being the ankyrin binding site (Figure 3-9, green highlight) and both plasmids bound to the VHS domain. pAS2-1 NrCAM 21-2 does not include the ankyrin binding site and showed no interaction with the VHS. Furthermore the substitution of a glutamate for the essential tyrosine in the FIGQY amino acid sequence of the NrCAM ankyrin-binding domain abolished the binding of the VHS domain to NrCAM. Thus it would appear that the VHS site binds to the ankyrin binding domain of NrCAM and that the substitution of a negatively glutamate for a tyrosine at position 86 in NrCAM inhibits VHS binding.

3.5 Analysis and description of the published binding partners of SAP102 and GIPC.

It was noted from the results above that the final 28 amino acids of NrCAM were sufficient to bind to both SAP102 and GIPC. An analysis of SAP102's and GIPC's other published binding partners highlighted the residues within NrCAM to which both proteins may be binding. Table 3-5 and Table 3-6 show all of SAP102's and GIPC's published binding partners. As can be seen from both tables the majority of proteins that bind to both SAP102 and GIPC bind via the last four amino acids of their cytoplasmic termini. These last four amino acids bind to the PDZ domains of SAP102 or GIPC and are called PDZ binding motifs (Bezprozvanny and Maximov, 2001). The most important residues of the PDZ binding motifs are the most C-terminal residue (called P0) and the third to last residue (called P-2) (Bezprozvanny and Maximov, 2001).

Protein that binds to SAP102					Reference(s):
Receptors - Class 1 PDZ	**P-3**	**P-2**	**P-1**	**P0**	
NR2B subunit of the NMDA receptor	E	S	D	V	(Lau et al., 1996; Muller et al., 1996; Sans et al., 2000)
ErbB4	N	T	V	V	(Huang et al., 2002)
Inward rectifier potassium channel Kir2.2	E	S	E	I	(Leonoudakis et al., 2004)
Megalin	D	S	E	V	(Larsson et al., 2003; Lim et al., 2002)
Plasma membrane calcium ATPase isoform PMCA4b	E	T	S	V	(DeMarco and Strehler, 2001)
Serotonin receptor 5HT2C	I	S	S	V	(Becamel et al., 2004)
Cytoplasmic - Class 1 PDZ	**P-3**	**P-2**	**P-1**	**P0**	
Stargazin	T	T	P	V	(Ives et al., 2004)
CRIPT	Q	T	S	V	(Lim et al., 2002)
Cypin	S	S	S	V	(Firestein et al., 1999)
P51-nedasin (isoform S)	S	S	S	V	(Kuwahara et al., 1999)
Sec8	I	T	T	V	(Sans et al., 2003)
SynGAP.	Q	T	R	V	(Kim et al., 1998)
APC	V	T	S	V	(Makino et al., 1997)
SH3 interactions					
PyK2					(Seabold et al., 2003)
Calmodulin					(Masuko et al., 1999)
To the GK domain of PSD95					(Masuko et al., 1999; Shin et al.,
To the GK domain of SAP102					(Shin et al., 2000)
GK interactions					
Guanylate kinase associated protein (GKAP)					(Kim et al., 1997)
Receptors - associating					
Kainate receptor subunit Glur6 and KA2					(Garcia et al., 1998)

Table 3-5. Published binding partners of SAP102. Binding partners have been analysed under the regions in SAP102 to which they bind. P-0, P-1, P-3, P-4 are the C-terminal amino acids in SAP102's binding partner that are known to bind to the PDZ domain of SAP102.

Protein that binds to GIPC					Reference(s):
Receptors: PDZ binding	**P-3**	**P-2**	**P-1**	**P0**	
HTVL-1 Tax oncoprotein	E	T	E	V	(Rousset et al., 1998)
HTVL-1 Tax oncoprotein	E	T	E	A	(Rousset et al., 1998)
RGS-GAIP	S	S	E	A	(De Vries et al., 1998)
GLUT1	D	S	Q	V	(Bunn et al., 1999)
a-actinin-1	E	S	D	L	(Bunn et al., 1999)
KIF-1B	E	T	T	V	(Bunn et al., 1999)
M-SemF	S	S	E	A	(Wang et al., 1999)
Neuropilin 1	Y	S	E	A	(Cai and Reed, 1999)
Syndecan-4	E	F	Y	A	(Gao et al., 2000)
gp75	Q	S	V	V	(Liu et al., 2001)
Integrin a 6A	T	S	D	A	(Tani and Mercurio, 2001)
Integrin a 6B	E	S	Y	S	(Tani and Mercurio, 2001)
Integrin a 5	T	S	D	A	(Tani and Mercurio, 2001)
Type III receptor	S	S	T	A	(Blobe et al., 2001)
5T4	N	S	D	V	(Awan et al., 2002)
Megalin	S	S	E	V	(Lou et al., 2002)
B1 Adrenergic receptors	E	S	K	V	(Hu et al., 2003)
LDH	Y	T	E	C	(Hirakawa et al., 2003)
Dopamine receptor D2	I	L	H	C	(Jeanneteau et al., 2004)
Dopamine receptor D3	I	L	S	C	(Jeanneteau et al., 2004)
CD93	G	T	D	C	(Bohlson et al., 2004)
Other PDZ					
TrkA					(Lou et al., 2001)
Non PDZ binding partners					
Dopamine receptor D2					(Jeanneteau et al., 2004)
Dopamine receptor D3					(Jeanneteau et al., 2004)
Myosin VI					(Bunn et al., 1999)
GIPC					(Bunn et al., 1999)

Table 3-6. Published binding partners of GIPC. Binding partners have been analysed under the regions in GIPC to which they bind. P-0, P-1, P-3, P-4 are the C-terminal amino acids in GIPC's binding partners that are known to bind to the PDZ domain of GIPC.

3.6 Testing whether the last three amino acids of NrCAM are necessary for NrCAM to bind to SAP102 and/or GIPC.

Like the majority of SAP102's and GIPC's binding partners NrCAM also has a C-terminal PDZ binding motif namely –NSFV-COOH. As shown in Figure 3-9 the NrCAM clone that does not have this motif (pAS2-1 NrCAM 1-22) is the only NrCAM clone not to bind to SAP102 and GIPC. It was therefore decided to test if the binding of SAP102 and GIPC to NrCAM depended on the presence of NrCAM's PDZ binding motif. A plasmid was designed that had the P0 (S), P-1 (F) and P-2 (V) residues of NrCAM deleted. This should eliminate a functional PDZ binding domain as described by (Bezprozvanny and Maximov, 2001). The cloning of this plasmid is described by Figure 3-10 .

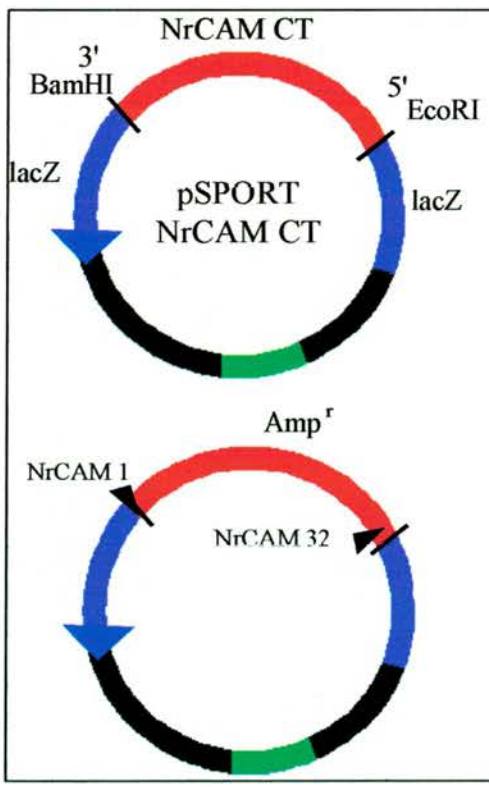

1. The plasmid pSPORT NrCAM CT encoding the rat sequence (amino acids 1102-1215, accession number U81037) was used as a PCR template.

2. PCR primers NrCAM 1 and NrCAM 32 were designed 1) eliminate the coding sequence for the last three amino acids of the NrCAM and 2) to add the EcoRI restriction enzyme and the BamH1 restriction enzyme site to the NrCAM encoding sequence (see appendix 4 for primer sequences).

Figure 3-10 Continued on next page

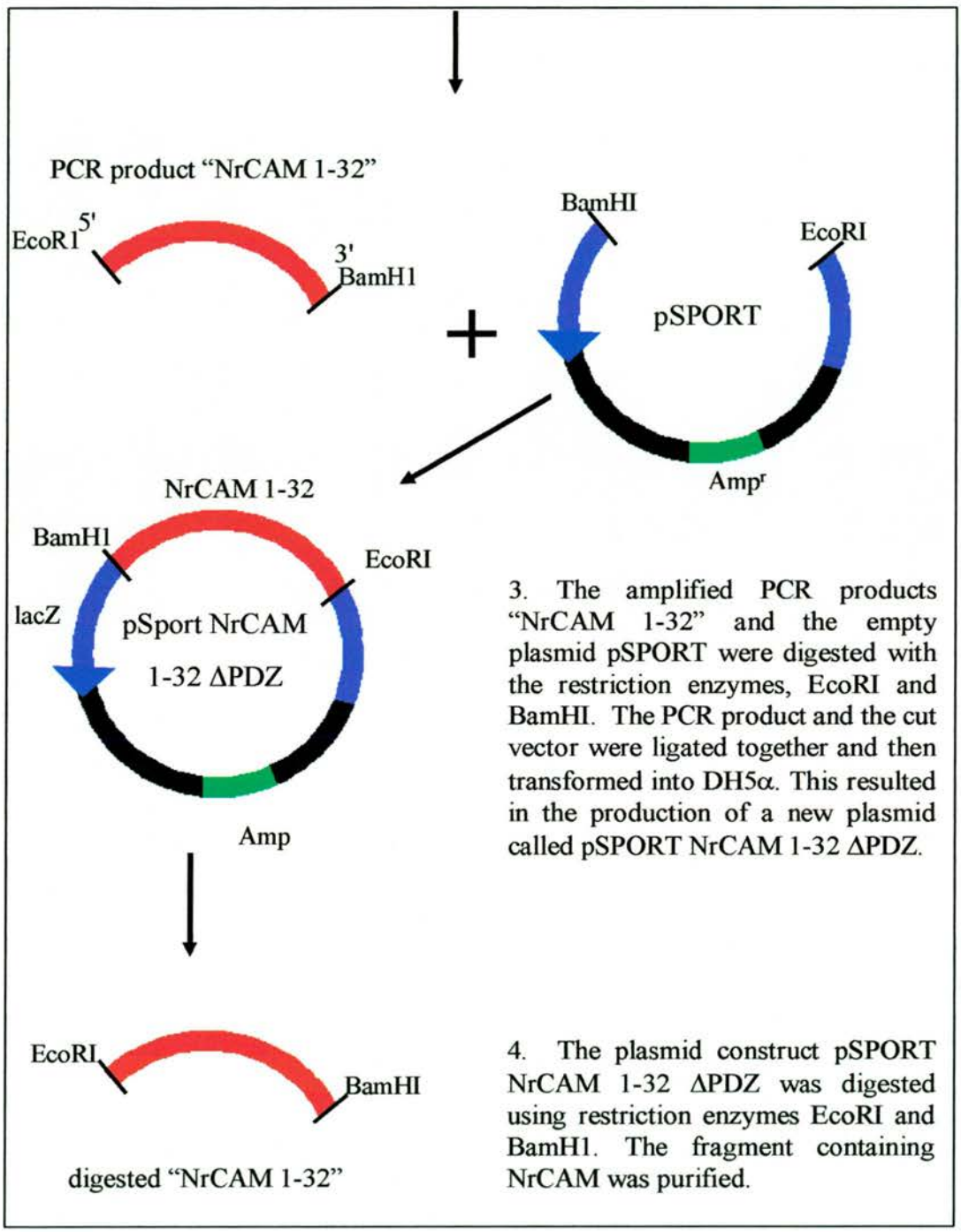

Figure 3-10 Continued on next page

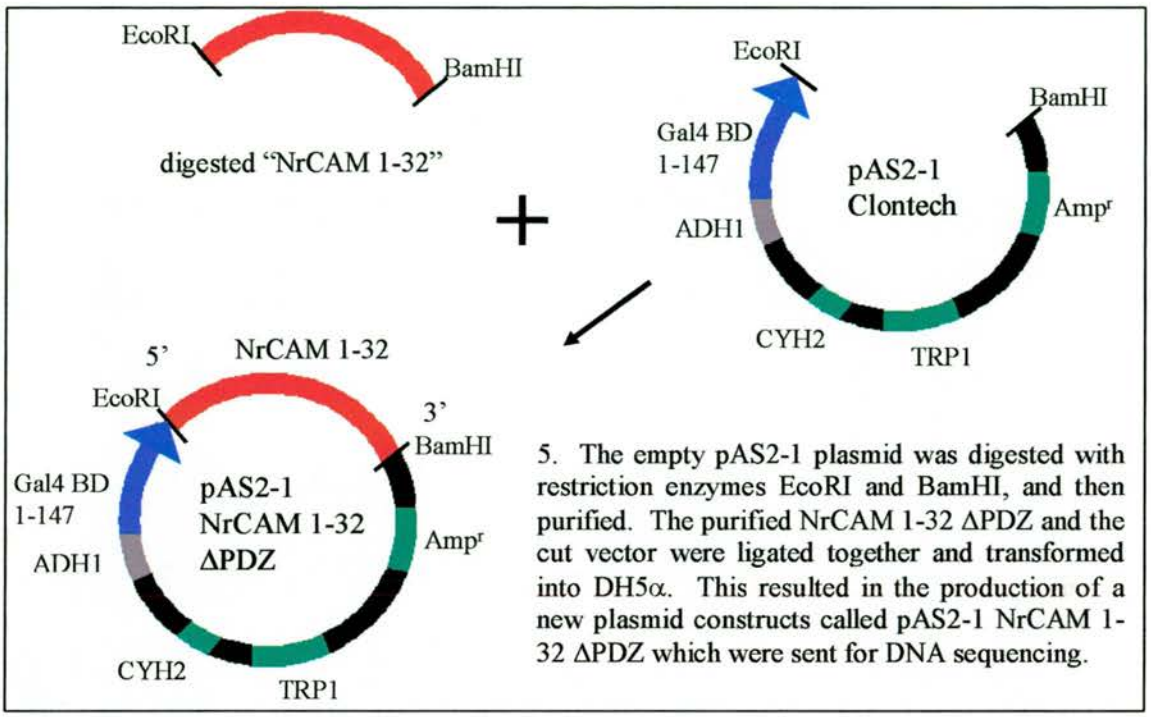

Figure 3-10. Cloning strategy for the production of the plasmid pAS2-1 NrCAM 1-32 ΔPDZ. Full details of materials and methods are described in chapter 2 and accompanying text.

The pAS2-1 NrCAM 1-32 ΔPDZ plasmid did not encode a functional PDZ binding domain. Therefore, if NrCAM CT bound to the PDZ domains of SAP102 and GIPC then NrCAM 1-32 ΔPDZ would not show any binding. This was tested using the filter lift assay as described in 2.4.1. The results are shown in Figure 3-11.

NrCAM CT bound to both SAP102 and GIPC as before. However, the cytoplasmic terminus of NrCAM without its terminal three amino acids (SFV-COOH) did not show any binding to SAP102 or GIPC. L1 CT, which does not have a PDZ domain, did not bind to SAP102 or GIPC. Neurofascin CT, which has the

three C-terminal acids, SLA bound to GIPC but not to SAP102. Thus the binding of NrCAM to SAP102 and GIPC was dependent of the last three amino acid residues.

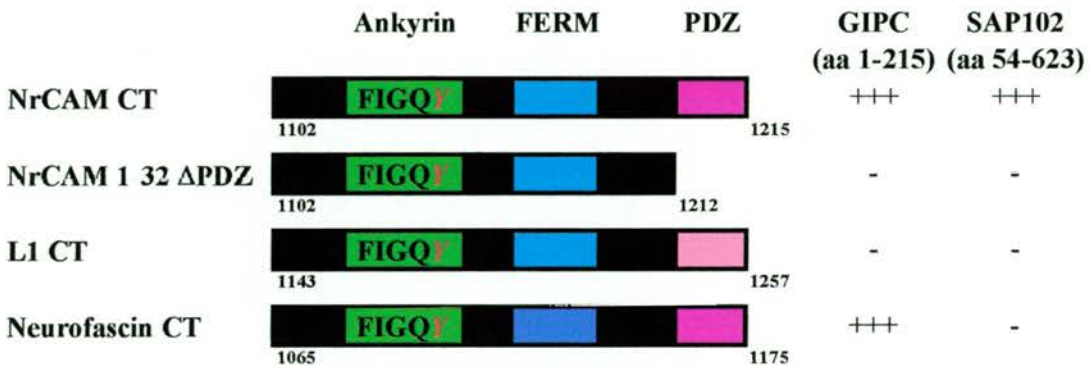

Figure 3-11. Testing of the library plasmids against an NrCAM bait without a PDZ binding domain. The L1-CAM plasmids and NrCAM plasmids have been shown diagrammatically. Green boxes represent the ankyrin domain. The dark blue box is the FERM binding domain in neurofascin and the paler blue boxes are the equivalent amino acids in L1 and NrCAM. The dark pink boxes are the PDZ domains of neurofascin and NrCAM. The paler pink box is the equivalent amino acids in L1. Binding strengths were scored using the system outlined in Table 3-1.

3.7 Discussion of results.

A developing rat brain cDNA library of 3.3×10^6 independent clones was screened for interaction with the cytoplasmic terminus of NrCAM. 17 potentially interacting clones were isolated from the library as potential binding partners. Ten clones encoded for the membrane-binding region of ankyrin$_B$, four clones encoded for PDZ domain containing regions of two members of the MAGUK family, SAP102 and PSD-95, two clones encoded for the PDZ domain containing region of GIPC and one clone encoded for the VHS domain of GGA1.

3.7.1 Ankyrin binding.

The majority of the interacting clones contained the membrane-binding region of cDNA of ankyrin$_B$ (Table 3-2). NrCAM together with the rest of the L1-CAM family had already been reported as associating with ankyrins (Davis and Bennett, 1994) and it is known that the membrane-binding domain of ankyrins has two high affinity binding sites for L1-CAMs (Michaely and Bennett, 1995; Bennett and Chen, 2001). Ankyrin$_B$ is the most abundantly expressed ankyrin molecule in the nervous system (Bennett and Chen, 2001) and it has been suggested that the NrCAM-ankyrin$_B$ interaction is important for the correct development of the lens in mice (More et al., 2001). Thus the abundance of ankyrin$_B$ clones isolated by the library screen was an expected result. Interestingly no ankyrin$_G$ or ankyrin$_R$ clones were isolated. Full length ankyrin$_R$ has been shown to bind to the NrCAM bait (Table 3-4, Figure 3-9f) however ankyrin$_R$ is only found at very low expression levels within the nervous system (Bennett and Chen, 2001). Therefore there may have been no ankyrin$_R$ cDNA clone in the library. However ankyrin$_G$ is reported to be an abundantly expressed protein in the developing nervous system (Bennett and Chen, 2001) and to associate with NrCAM at the node of Ranvier (Lambert *et al.*, 1997; Lustig *et al.*, 2001; Custer *et al.*, 2003) and at initial segments (Jenkins and Bennett, 2001). It is not known why no ankyrin$_G$ clones were isolated.

Ankyrins bind to neurofascin at a highly conserved amino acid motif in their cytoplasmic termini that ends with the amino acid motif FIGQY (Garver et al., 1997; Zhang et al., 1998a). Figure 3-9 shows that this same motif is also required for the NrCAM and ankyrin binding. If the tyrosine residue of FIGQY is phosphorylated

ankyrin biding to neurofascin and L1 is abolished (Garver *et al.*, 1997; Tuvia *et al.*, 1997; Gil *et al.*, 2003). Similarly when the tyrosine was mutated to a negatively charged amino acid, glutamate, ankyrin binding to neurofascin was abolished (Zhang et al., 1998b). A similar mutation of the NrCAM CT has shown the same effect. In Figure 3-9 pAS2-1 NrCAM Y86>E failed to bind to ankyrin$_R$. Additionally a library screen performed by Dr. F. Davey of the University of St Andrews using the pAS2-1 NrCAM Y86>E plasmid as bait did not select any ankyrin clones. The phosphorylation of NrCAM at this tyrosine and its interaction with ankyrin will be examined further in chapter six.

3.7.2 GIPC binding.

GAIP Interacting Protein C terminus (GIPC) (rat) (De Vries et al., 1998) was cloned by several independent groups in the late 1990s and subsequently has several names including Tax Interacting Protein –2 (TIP-2) (human) (Rousset et al., 1998), GLUT1 C-terminal Binding Protein (GLUT1CBP) (rat) (Bunn et al., 1999), Neuropilin-1 Interacting Protein (NIP-1) (rat) (Bunn et al., 1999), M-SemF cytoplasmic domain associated protein (SEMCAP-1) (mouse) (Wang et al., 1999) and synectin (mouse) (Gao et al., 2000). The Xenopus sequence was cloned in 2001 and is called Kermit (Tan et al., 2001). The GIPC family consists of three known members GIPC (GIPC1), GIPC2, GIPC3. All three proteins have a central PDZ domain and two conserved GIPC homology domains GH1 and GH2 (Katoh, 2002) (Figure 3-6).

The PDZ domain of GIPC is the only protein domain of known function within the molecule. Table 3-6 shows the currently known binding partners of GIPC. 21 out of 25 of the binding partners interact with the PDZ domain of GIPC via their terminal four amino acids. The consensus motif of these amino acids is X-S/T-X-V/A/L-COOH (Table 3-6). From the PDZ classification system described by Harris and Wendell this is a class 1 PDZ domain although a slightly atypical one in that it prefers smaller hydrophobic residues at P0 such as alanine and valine and not the bulkier residue of isoleucine (Harris and Wendell, 2001). Importantly GIPC does not necessarily require a hydrophobic residue at P0. This is illustrated by the integrin subunit $\alpha 6\beta$ where the P0 amino acid is a serine (Tani and Mercurio, 2001) (El Mourabit et al., 2002) and the LDH receptor, the Dopamine receptors D_2 and D_3 and the CD93 receptor where the P0 amino acid is a cysteine. The P-2 residue shows a similar promiscuity yet selectivity. In 18 out of 21 proteins it is a hydroxyl containing serine or threonine residue but in Syndecan –4 the P-2 residue is a bulky hydrophobic phenylalanine (Gao et al., 2000) and in the dopamine receptor it is a leucine (Jeanneteau et al., 2004).

The part length GIPC clones selected from the library both possessed a PDZ domain. Furthermore these clones appear to bind to the C-terminal end of the NrCAM cytoplasmic terminus (Figure 3-9). The three most C-terminal amino acids of NrCAM NSFV-COOH are described as a typical class I PDZ domain binding motif (Bezprozvanny and Maximov, 2001; Harris and Wendell, 2001; Sheng and Sala, 2001). The NSFV-COOH motif is also consistent with the amino acid motif X-S/T-X-V/A/L-COOH that is preferred by the PDZ domain of GIPC. It was investigated whether the GIPC library clones bound other L1 family members. The

cytoplasmic portion of both rat L1 and rat neurofascin (Figure 3-9) were tested against GIPC cDNA. GIPC did not interact with L1 however GIPC did interact with neurofascin. L1 does not possess a PDZ domain-binding motif, as its C-terminal amino acids are VALE-COOH. Neurofascin has a PDZ domain binding motif YSLA-COOH and has been reported to bind to syntenin a PDZ domain containing protein (Koroll et al., 2001). Furthermore this motif is in agreement with the amino acid motif X-S/T-X-V/A/L-COOH that GIPC normally prefers. Taken together these results suggest that NrCAM may be binding to PDZ domain found in the GIPC clones. To confirm this the last three residues of the NrCAM cytoplasmic segment were deleted. This prevented NrCAM from binding to GIPC (Figure 3-11). It was decided to further investigate the interactions of NrCAM with GIPC by co-localisation studies and pull-down assays. These results will be discussed in full in chapter four.

3.7.3 SAP102 binding.

SAP102 is a member of the membrane associated guanylate kinase family proteins (MAGUKs) that are composed of three tandem N-terminal PDZ domains followed by a src homology 3 (SH3) domain and C-terminal guanylate kinase domain (GK). The most characterised SAP102 interaction has been with the NR2B subunit of the NMDA receptor. All three PDZ domains of SAP102 interact with the C-terminal (E)S/TXV/I/L-COOH amino acids of the NR2B subunits in vitro (Lau et al., 1996; Muller et al., 1996). Phosphorylation of the serine in the NMDA receptor C-terminal motif interferes with SAP102 binding and reduces NMDA receptor expression at the

cell surface (Chung et al., 2004). The first two PDZ domains (and to a certain extent the third) of SAP102 bind to Sec8, a member of the exocyst complex (Sans et al., 2003) and the SAP102/Sec8 interaction may have a role in trafficking the NMDA receptor to the plasma membrane (Sans et al., 2003). The majority of the other published binding partners of SAP102 are also to one or more of its PDZ domains and all of these proteins have an XS/TXV/I/L-COOH consensus motif in their cytoplasmic segments (Table 3-5).

The part length SAP102 clones selected by the library screen possessed all three PDZ domains of SAP102. Furthermore these clones appear to bind to the C-terminal end of the NrCAM cytoplasmic terminus (Figure 3-9). The four most C-terminal amino acids of NrCAM are NSFV-COOH and are consistent with an S/TXV/I/L-COOH consensus motif. It was investigated whether SAP102 library clones bound other L1 family members (Figure 3-9). Neither L1 nor neurofascin interacted with SAP102. Neurofascin also has a PDZ domain binding motif of YSLA-COOH (Koroll et al., 2001) that is not consistent with the S/TXV/I/L-COOH consensus motif preferred by SAP102. This is due to an alanine substitution at the P0 position for the larger valine, leucine or isoleucine residues. L1's C-terminal amino acids are VALE-COOH and therefore it does not possess a PDZ domain-binding motif. Taken together these results suggest that NrCAM may be binding to one or more PDZ domains found in SAP102. Deletion of the terminal SFV-COOH residues of NrCAM confirmed this, as all binding to SAP102 was abolished (Figure 3-11). Therefore it would appear that NrCAM is binding to one or more PDZ domains of SAP102.

However it was noted that a plasmid of SAP102 (RL71D) that had all three PDZ domain of SAP102 but no SH3 or GK domain (Figure 3-4) failed to interact with

NrCAM in the experiment described by Table 3-4. This is surprising if all that NrCAM needs to interact with SAP102 are functional PDZ domain. Notably RL71D did not encode amino acids 534 to 623 of SAP102 that were encoded by the RL48A and RL29B plasmids that did interact with NrCAM (Figure 3-4). These amino acids code for the SH3 domain of SAP102. It is therefore possible that SH3 domain of SAP102 is necessary for NrCAM and SAP102 binding. It is also possible that the amino acids 534 to 623 were necessary for the correct folding of the SAP102 PDZ domains and that misfolding of RL71D had occurred.

It was decided to further investigate the interactions of NrCAM with SAP102 by co-localisation studies and pull-down assays. These results will be discussed in full in chapter four.

3.7.4 The binding of the VHS domain of GGA1.

The library screen also identified the VHS domain of the GGA1 protein as a potential interaction with the NrCAM cytoplasmic terminus. There are three GGAs in humans, GGA1, GGA2 (Vear) and GGA3 (Boman et al., 2000; Dell'Angelica et al., 2000; Hirst et al., 2000). The GGAs are localised to the trans Golgi network (TGN) and vesicles in the cytoplasm (reviewed Boman, 2001) and deletion of the two GGA genes found in yeast result in trafficking defects from the TGN to early/and or later endosomes (reviewed Boman, 2001). Thus the GGA proteins are believed to function mainly in the trafficking receptors from the trans Golgi network (TGN) to the early/late endosome (Bonifacino, 2004). All three human GGAs have been

highly conserved throughout evolution and are believed to bind to and traffic the same receptors (Boman, 2001; Bonifacino and Traub, 2003).

The VHS domain of the GGAs are essential for their trafficking function (Hirst et al., 2001) and recognise DXXLL (where D is an essential aspartate, X can be any amino acid and LL are two hydrophobic residues (normally both leucine)) amino acid motifs in cytoplasmic terminus of receptors (Bonifacino, 2004). These signals are present in several transmembrane proteins and cargo proteins that cycle between the trans Golgi network (TGN) and the endosome. Mannose-6-phosphate receptors (M 6-Ps) and sortilin are receptors for newly synthesised acidic hydrolases and neurotensin respectively (Nielsen *et al.*, 2001; Bonifacino and Traub, 2003). Both receptors have a DXXLL motif in their cytoplasmic termini and the VHS domain of GGAs is thought to sort receptors from the TGN to the endosome (Nielsen *et al.*, 2001; Puertollano *et al.*, 2001; Bonifacino and Traub, 2003).

Three rules for recognition of the VHS domain of amino acids in the cytoplasmic segment of receptors have been defined by (Bonifacino, 2004):

1. The cytoplasmic terminus of the receptor must contain an "acidic cluster dileucine" or DXXLL sequence (Bonifacino, 2004). There are two notable features of this motif: a.) the dileucine repeat can sometimes be replaced by other hydrophobic residues for example in SorLA the dileucine is replaced by a methionine and a valine (i.e. DXXMV not DXXLL) (Jacobsen et al., 2002). b.) the essential aspartate of the DXXLL is often found near a cluster of acidic residues (Bonifacino, 2004).

2. Serine residues are often found within or one to three positions N-terminal to DXXLL signals. For example the VHS domain of GGA1 binds to the DISLL sequence of BACE, the serine of which can be phosphorylated. Phosphorylation of

the serine increases the affinity of GGAs for the BACE protease (He et al., 2003; Shiba et al., 2004; von Arnim et al., 2004).

3. The sequence is usually located near to the carboxyl terminus of the receptor (reviewed Bonifacino, 2004). However this is not always true, for example both GGA1 and GGA3 have a DXXLL motif in their hinge domain. These sequences can bind to the VHS domain of the same protein and both of these sequences are significantly upstream of the C-terminal end of the GGA protein (Doray et al., 2002).

If you apply these rules to L1-CAMs there are two potential "acidic cluster dileucine" sequences in their ankyrin binding domains as shown by Figure 3-12. The first is a DXXLV/A motif and the second is a DXXFI motif (Figure 3-12). All of these motifs have essential aspartate residues in acidic clusters (D and E residues are shown in yellow). All of the potential motifs have a serine (shown in red font) within the DXXLL sequence (number 64 and 81 for NrCAM) and the first potential DXXLL has a serine one amino acid N-terminal to the DXXLL sequence (number 61 for NrCAM). Interestingly an aspartate residue that may provide a COOH group that mimics the C-terminal of a chain of amino acids follows the first DXXLV/A amino acid sequence. Thus both of these sequences would satisfy the criteria described by (Bonifacino, 2004) above.

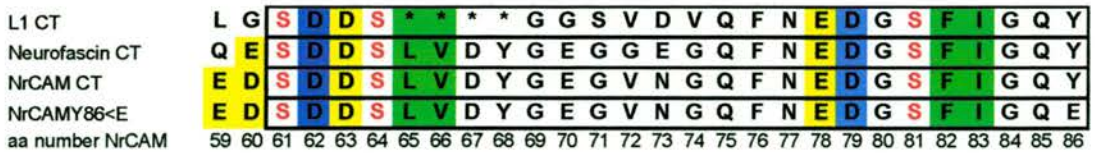

****Normally L1 would have LADY in this position.

Figure 3-12. The potential GGA-VHS binding amino acid sequences of the L1-CAM family plasmids used in this thesis. Boxed are the ankyrin binding domains. Highlighted in blue are essential aspartates. Highlighted in green are dileucine like repeats. Highlighted in yellow are acidic clusters. Potentially important serine residues are shown in red font. Numbers are the amino acid position of the residue in the cytoplasmic terminus of rat NrCAM (without RSLE). See text for details.

The NrCAM and neurofascin plasmids used in Figure 3-9 both have a DXXLV motif in their cytoplasmic terminus and both bound to the VHS plasmid (Figure 3-12). The L1 cytoplasmic terminus used in this assay was missing the normal LADY amino acid sequence found in the cytoplasmic terminus of most L1 isoforms and did not have the first DXXLA sequence normally found. This sequence did not bind to the VHS of GGA1 (Figure 3-9 and Figure 3-12). Thus there is some evidence that the DXXLV/A sequence may be necessary for VHS binding. However pAS2-1 NrCAM Y86<E has a normal DXXLV sequence but did not bind to the VHS plasmid. It is unclear as to why a substitution of a glutamic acid for a tyrosine should interfere with VHS binding. Perhaps the negative residue causes a conformational change in the ankyrin-binding domain?

Thus, it is concluded that the highly conserved ankyrin bind site of the L1-CAM family has the potential to bind to the VHS domain of the GGAs. The possible functions of the VHS domain binding to NrCAM interaction are discussed in Chapter 7.

Chapter 4. The examination of the potential interactions between NrCAM and GIPC/ SAP102.

4.0 Introduction: The potential cytoplasmic binding partners of NrCAM.

In Chapter 3, three putative NrCAM binding partners were identified GIPC, SAP102 and the VHS domain of GGA1. Both GIPC and SAP102 interacted with the C-terminal class 1 PDZ binding motif of NrCAM, and the VHS domain interacted with the ankyrin-binding domain of NrCAM. The amino acid sequences within the cytoplasmic tail of NrCAM to which GIPC, SAP102 and the VHS domain bound, were consistent with similar conserved amino acid sequences in the cytoplasmic tails of other membrane proteins already known to interact with GIPC, SAP102 and the VHS domain. Mutation studies of the NrCAM cytoplasmic tail showed that there were essential amino acids in for these interactions, the elimination/mutation of which prevented the NrCAM/putative binding partner interaction. The case for NrCAM binding was further strengthened as the putative interacting proteins all had different binding profiles among the L1-CAM family and the binding appeared dependent on certain conserved amino acids.

However, it remained to be shown whether these interactions were biologically relevant. Therefore, a set of experiments was designed to establish whether NrCAM was expressed at the same time and place as the putative binding partners thus making biological interactions between the proteins possible. A second set of experiments were attempted to reconfirm the interaction within mammalian cell extracts. It was hoped that the times and locations within the brain/cell that the NrCAM putative binding partner interaction occurs, as established by these experiments, would suggest the biological role of these interactions.

As both the GIPC and SAP102 interactions with NrCAM were likely to be similar (they were both interacting with the last three amino acids of NrCAM's cytoplasmic tail) they were further analysed first.

4.1 Are NrCAM and the potential binding partners expressed at the same time in brain development?

4.1.1 Western blot analysis of early brain development.

To ensure that it is feasible for NrCAM to bind to the PDZ proteins both NrCAM and the respective PDZ protein should be expressed in the brain at the same time. Brains were dissected from rat embryos/pups at embryonic day 14 (E14), E16 and E20 and postnatal day 7 (P7). It had been previously reported that SAP102 did not readily solubilise in most detergents (Muller et al., 1996) therefore freshly prepared rat brains were homogenised by sonication and solubilised in 2 % sodium dodecyl sulfate (SDS) as described in (2.3.6). 100 μg of brain samples were separated on two 10 % SDS-PAGE gels (for NrCAM and SAP102 immunostaining) and one 12 % SDS-PAGE gel (for GIPC immunostaining) and transferred onto nitrocellulose transfer membrane. The membranes were probed with antibodies for NrCAM, GIPC and SAP102 as described in section (2.3.10) and appendix (3).

NrCAM showed increased expression in the rat brain during embryonic and postnatal development (Figure 4-1). The biggest change in NrCAM expression occurred between E14 and E16. A minimum of two bands was seen at all stages of development from E20 onwards. One was a lower molecular weight band of approximately 110 kDa. A large diffuse band of approximately 160 kDa to 200 kDa was much more strongly expressed. At P7 there was a third NrCAM band of

approximately 116 kDa. The multiple protein sizes of NrCAM may reflect either N-linked glycosylation of the extracellular domains or furin protease like cleavage within the third fibronectin like (FNIII-like) domain of NrCAM. Both of these possibilities are examined in Chapter 6. However it was noted at this stage that the larger molecular weight of NrCAM was predominant in all brain samples and was expressed from E16 onwards.

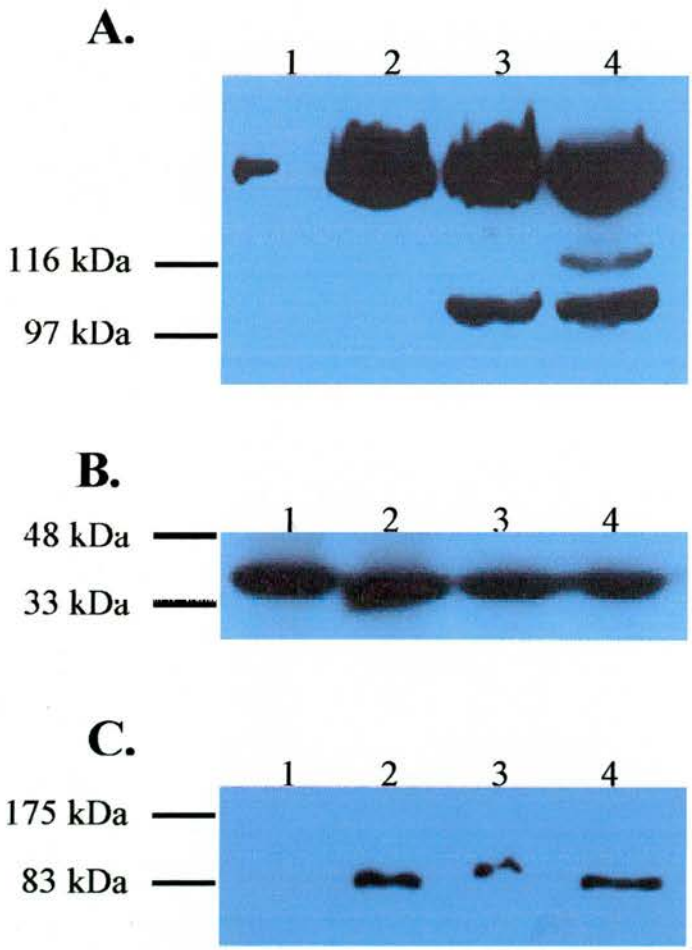

Figure 4-1. NrCAM, GIPC and SAP102 expression in developing brain.
A) NrCAM expression in rat developing brain. **B)** GIPC expression in rat developing brain. **C)** SAP102 expression in rat developing brain. Lanes 1 to 4 are 100 µg of rat brain homogenates of various ages: Lane 1 is E14, lane 2 is E16, lane 3 is E20 and lane 4 is P7. For methods see section 2.3.10 and appendix 3.

GIPC did not show changes in expression level during embryonic and postnatal development. One band of approximately 39 kDa was seen for all brain developmental stages tested (Figure 4-1). SAP102 was not detectable on Western blot at E14 (Figure 4-1). At E16 SAP102 was detected as a single band of approximately 100 kDa. SAP102 expression levels remained at the E16 expression level at E20 and P7.

Therefore in summary both NrCAM and GIPC were expressed at all developmental stages tested. GIPC expression levels remain constant while NrCAM expression levels greatly increased at E16. SAP102 was not expressed at a detectable level until E16, which coincides with NrCAM's rapid increase in expression levels. Thus it appears that SAP102 but not GIPC may be developmentally regulated in whole brain in a similar manner to NrCAM. In order for NrCAM to interact with either GIPC or SAP102 both proteins must be expressed in the same subset of neurons/glial cells. Therefore it was decided to see if GIPC and SAP102 were expressed in a particular neuronal population that was already known to express NrCAM.

4.1.2 NrCAM and the PDZ proteins are expressed in the same neurons.

NrCAM was found in cerebellar granule cells (CGCs) where it has an important role in granule cell migration and development (Krushel *et al.*, 1993; Faivre-Sarrailh *et al.*, 1999; Sakurai *et al.*, 2001). Hence it was decided to see if GIPC and SAP102 were also present in CGCs. CGCs were extracted from P7 mouse pups and cultured on poly-D-lysine coated 90 mm dishes. The CGCs were cultured for up to seven days and cell extracts were prepared by solubilising the cells in 1 % Triton-X100 in

the presence of protease inhibitors as described in section (2.3.6). 90 μg CGC samples were separated on two NuPAGE® Novex 6-12% Bis-Tris Gels (for GIPC and SAP102 immunostaining) and one NuPAGE® Novex 3-8% Tris-Acetate gel (for NrCAM immunostaining) and transferred onto nitrocellulose transfer membrane (see section 2.3.9). The membranes were probed for NrCAM, GIPC and SAP102 as described in section 2.3.10 and appendix 3.

NrCAM did not show changes in expression level during development of CGCs *in vitro* (Figure 4-2). A minimum of two bands was seen at all stages of development. One was a lower molecular weight band of approximately 130-140 kDa the second band was approximately 180 kDa. At later stages of development there was a third band of approximately 170 kDa. The NuPAGE® Novex 3-8% Tris-Acetate together with HiMark™ protein markers gives an accurate measurement of high molecular weight proteins when compared to other SDS-PAGE gels and markers (http://www.invitrogen.com) and thus the sizes of NrCAM on this gel were considered more accurate than the sizes shown in Figure 4-1. This will be discussed further in Chapter 6. Unlike the whole brain samples in Figure 4-1 the lower molecular weight bands of NrCAM were more heavily expressed than the larger molecular weight bands.

GIPC expression in CGCs increased after three days *in vitro* but did not show changes in expression level thereafter. One band of approximately 39 kDa was seen for all CGC developmental stages tested (Figure 4-2). SAP102 expression in CGCs did not show changes in expression level for up to seven days in vitro. One band of approximately 100 kDa was seen for all CGC developmental stages tested (Figure 4-2).

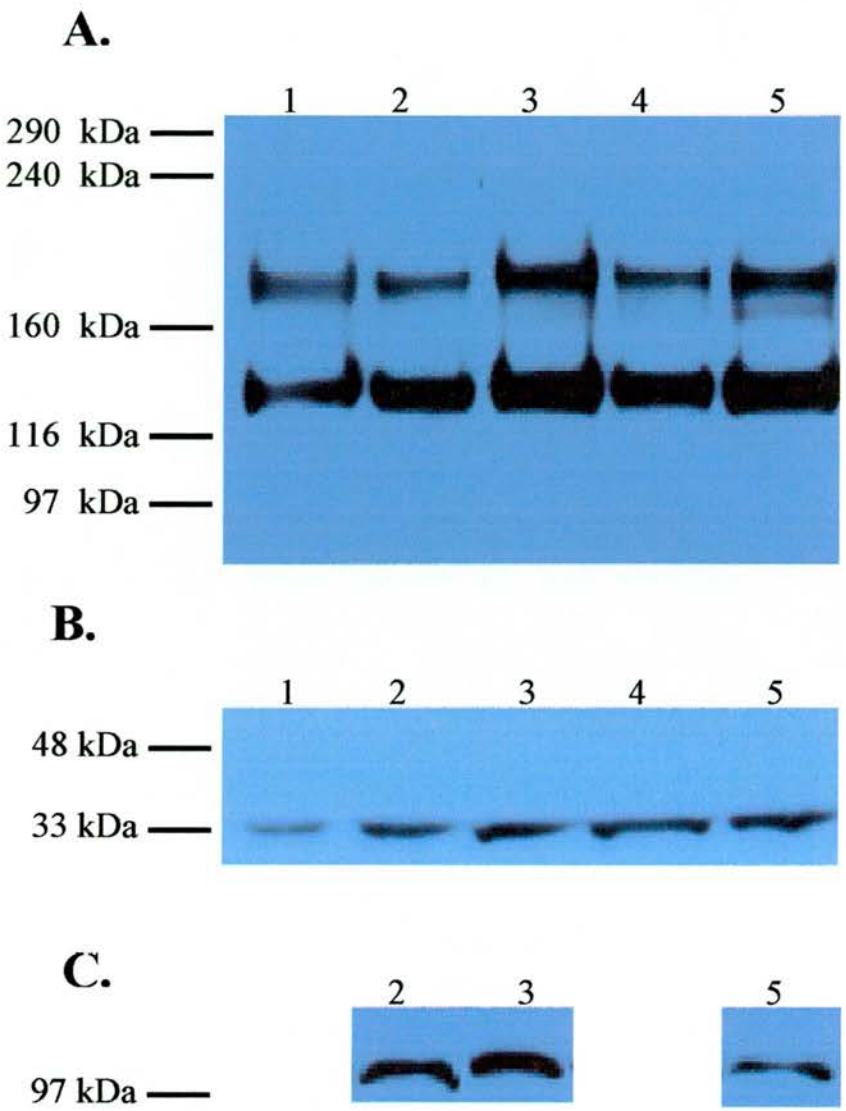

Figure 4-2. NrCAM, GIPC and SAP102 expression in CGCs. **A)** NrCAM expression in CGCs. **B)** GIPC expression in CGCs. **C)** SAP102 expression in CGCs. Lanes 1 to 6 are 90 μg CGC extracts of various days *in vitro* (DIV): Lane 1 one DIV, lane 2 is two DIV, lane 3 is four DIV, lane 4 is five DIV and lane 6 is seven DIV. For methods see section 2.3.10 and appendix 3.

In summary NrCAM, GIPC and SAP102 were expressed by CGCs that were cultured for up to 7 DIV. At 3 DIV, all three proteins were at their maximum expression levels and this expression remained constant up to 7 DIV.

4.2 Sub-cellular location of NrCAM, GIPC and SAP102.

Thus both GIPC and SAP102 were expressed in CGCs cultured *in vitro*. However if NrCAM interacts with one or both of the PDZ proteins, both NrCAM and the PDZ protein should be expressed in the same part of the cell at the same times. Ideally CGCs would be immunostained for endogenous levels of NrCAM, GIPC and SAP102 and areas of co-localisation would be identified as areas where the two proteins could potentially interact within the cell.

4.2.1 GIPC co-localisation studies.

4.2.1.1 HA-NrCAM and endogenous GIPC co-localisation in HEK293 cells.

A kind gift of a plasmid vector encoding for HA-NrCAM was received from Dr. Faivre-Sarrailh, Marseille, France. It encoded for the signal peptide of NrCAM followed by the HA epitope (YPYAVPDYA) followed by the full-length rat NrCAM sequence (as published Davis et al., 1996). The vector encoding for HA-NrCAM cDNA was transfected into Human Embryonic Kidney 293 (HEK293) cells and the cells that stably expressed the vector were selected by G418 antibiotic containing media as described in section 2.2.8. Figure 4-3 shows a Z-section of the upper surface of a single HEK293 cell stably expressing HA-NrCAM. It shows a punctate HA-NrCAM immunostaining in the plasma membrane, as Z-sections below this image showed decreasing HA-NrCAM immunostaining except at the edges of the cell (not shown). Therefore, GIPC immunostaining shown in Figure 4-3 is near to or just below the plasma membrane. GIPC immunostaining was punctate in its appearance as had been previously reported (Lou et al., 2001) and in contrast to HA-NrCAM,

punctate GIPC immunostaining was seen throughout the cytoplasm in lower Z-section (not shown). As indicated by arrows in Figure 4-3 (C), HA-NrCAM and GIPC showed areas of co-localisation in the plasma membrane.

4.2.1.2 HA-NrCAM and endogenous GIPC co- localisation in B104 cells.

To determine whether this co-localisation was cell type specific, B104 neuroblastoma cells stably expressing the same HA-NrCAM construct were also immunostained for NrCAM and GIPC expression (HA-NrCAM stably transfected B104 cells were a kind gift from Dr. Faivre-Sarrailh, University of Marseille, France). As indicated in Figure 4-4 GIPC co-localised with stably expressed HA-NrCAM at the plasma membrane in regions of HA-NrCAM expression. Thus, GIPC co-localisation with stably expressed HA-NrCAM was not cell type specific.

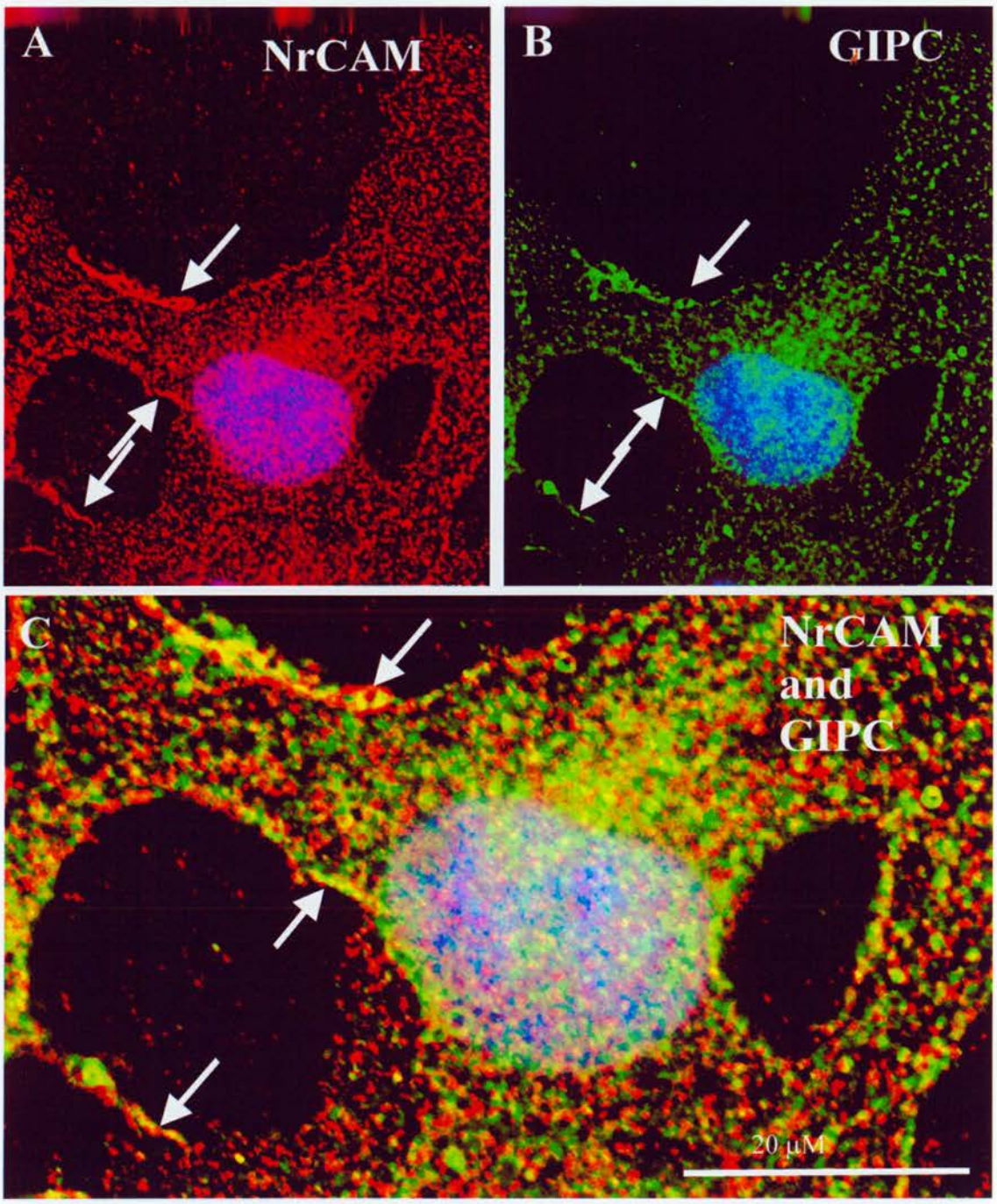

Figure 4-3. A Z Section of a HEK293 cell stably expressing HA-NrCAM. **A**) HA-NrCAM immunostaining was performed using an anti-HA rat monoclonal antibody and anti-mouse Alexa 568 conjugated antibody and is shown in red. **B**) Endogenous GIPC immunostaining was performed using a goat antibody to the N-terminus of GIPC and an anti goat FITC conjugated antibody and is shown in green. **C**) Co-localisation between both proteins occurs were HA-NrCAM is most highly expressed (arrows). The nucleus of the cell has been stained with DAPI and is shown in blue. See methods 2.2.10.

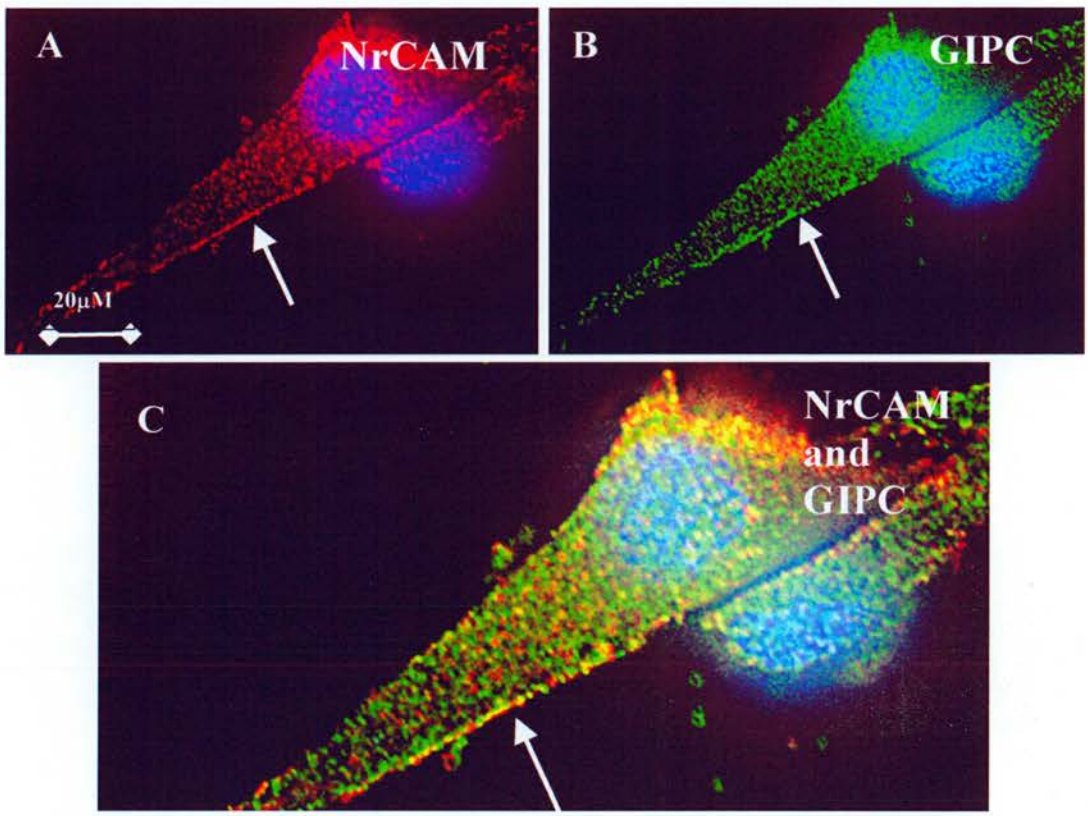

Figure 4-4. A Z Section of a B104 cell stably expressing HA-NrCAM. **A**) HA-NrCAM immunostaining was performed using an NrCAM rabbit polyclonal antibody and anti-rabbit Alexa 568 conjugated antibody and is shown in red. **B**) Endogenous GIPC immunostaining was performed using a goat antibody to the N-terminus of GIPC and an anti goat FITC conjugated antibody and is shown in green. **C**) Co-localisation between both proteins occurs at (arrow). The nucleus of the cell has been stained with DAPI and is shown in blue. See methods 2.2.10, appendix 3B.

4.2.1.3 Co-localisations studies of $GIPC_{1-3}GFP$ with HA-NrCAM.

The partial co-localisation of GIPC and NrCAM suggested that this interaction could be transient. Therefore, it was decided to explore real time imaging as a means of investigating this further. To make live imaging possible it was therefore decided to C-terminally tag the part length GIPC clone, selected from the cDNA library in Chapter 3, with Green Fluorescence Protein (GFP). The cloning of this construct is shown in Figure 4-5 and was called $GIPC_{1-3}$-GFP. The $GIPC_{1-3}$-GFP construct was

designed to remove any sequence 5' or 3' not normally translated from the cDNA encoded for by GIPC library construct (Figure 4-5 for details).

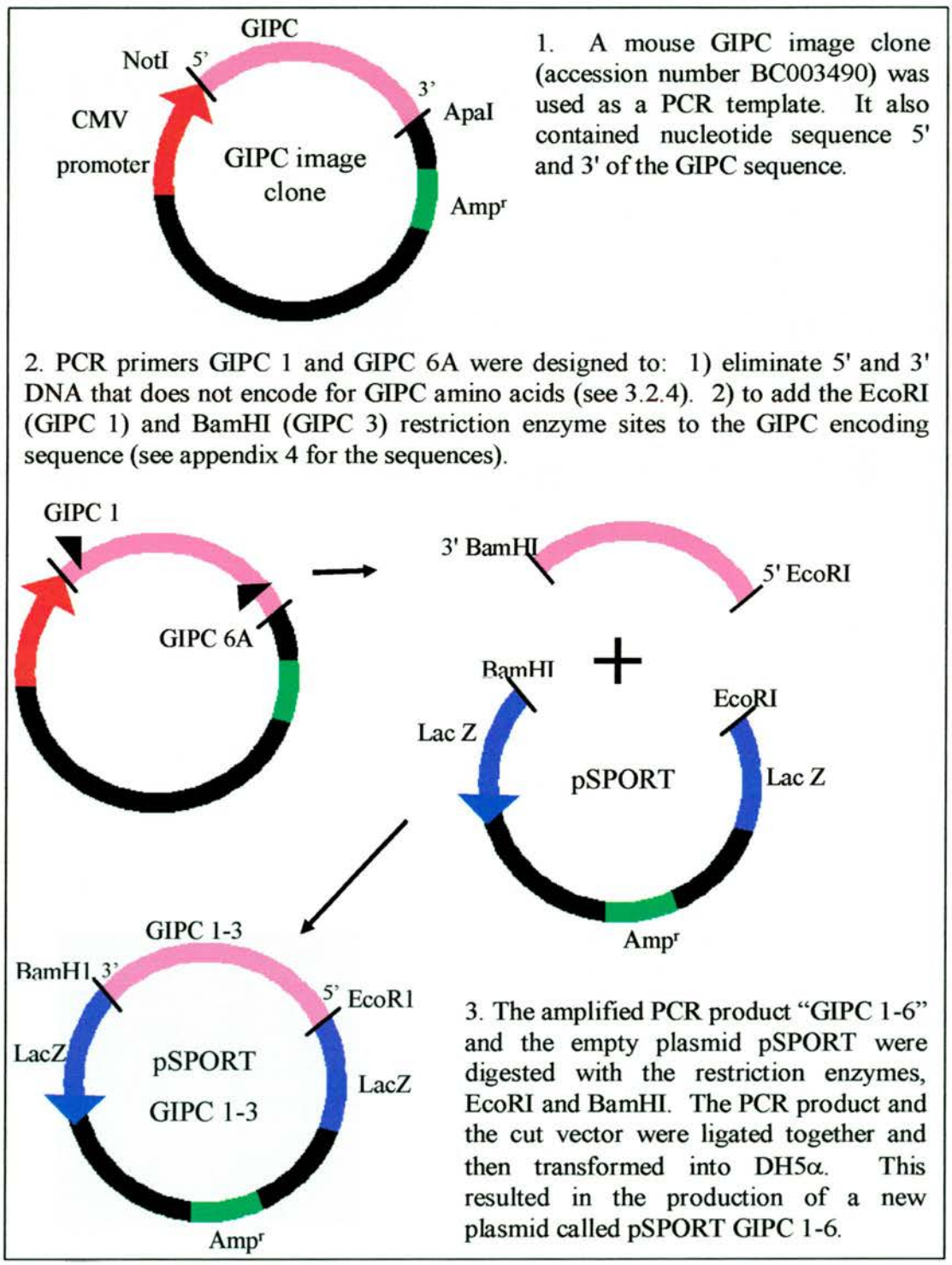

Figure 4-5. Continued on next page.

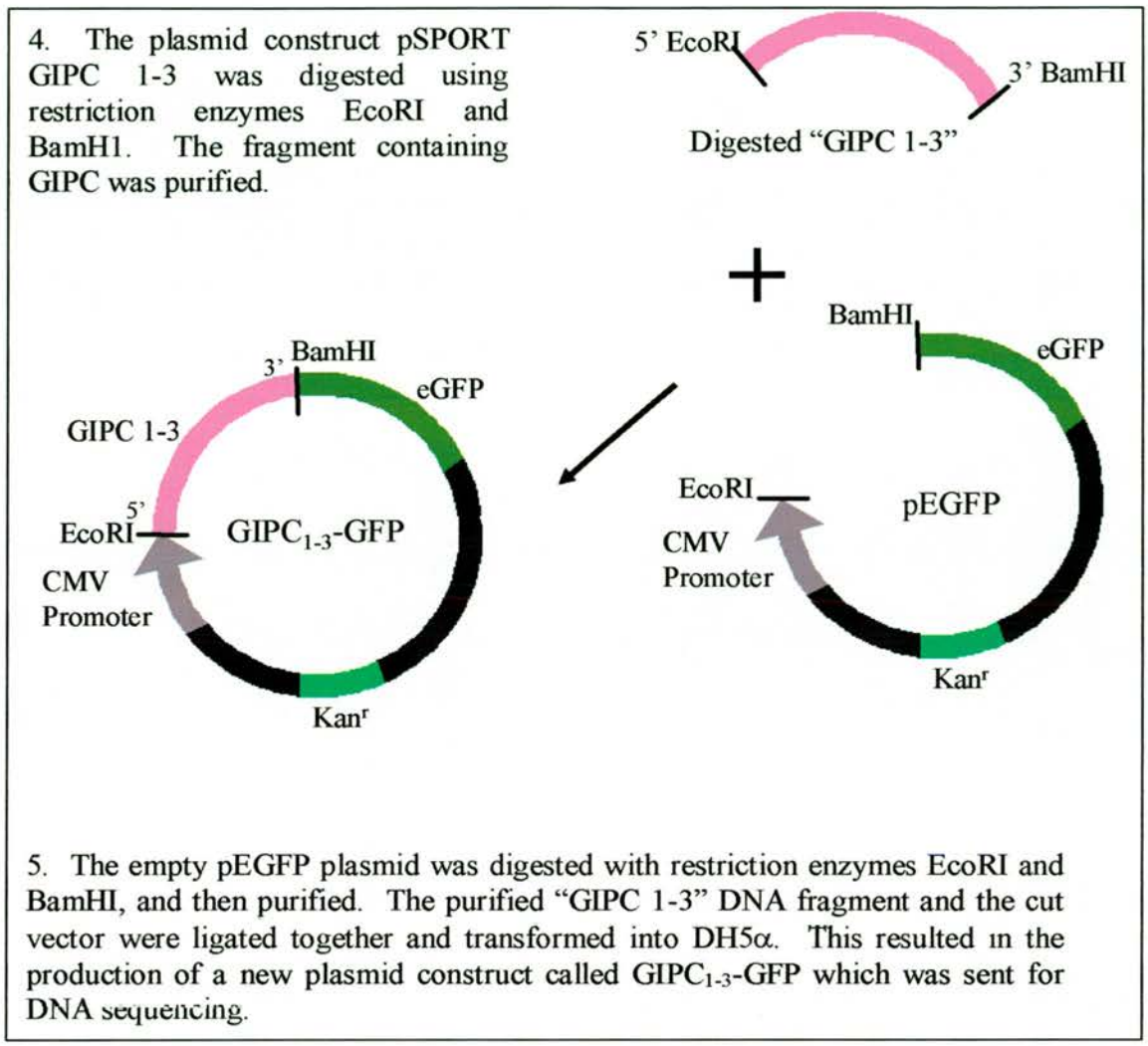

Figure 4-5. Cloning strategy for the production of the plasmid $GIPC_{1-3}$-GFP. Detail of material and methods are described in Chapter 2 and accompanying text.

The $GIPC_{1-3}$-GFP construct was transfected into COS-7 cells, HEK293 cells and B104 cells (section 2.2.5). In all of the cell-lines examined, $GIPC_{1-3}$-GFP expression was not punctate (as had been recorded for endogenous GIPC (Figure 4-3 and Figure 4-4)) but was diffuse throughout the cytoplasm and nucleus of the cell. An example of $GIPC_{1-3}$-GFP in a COS-7 cell can be seen at Figure 4-6.

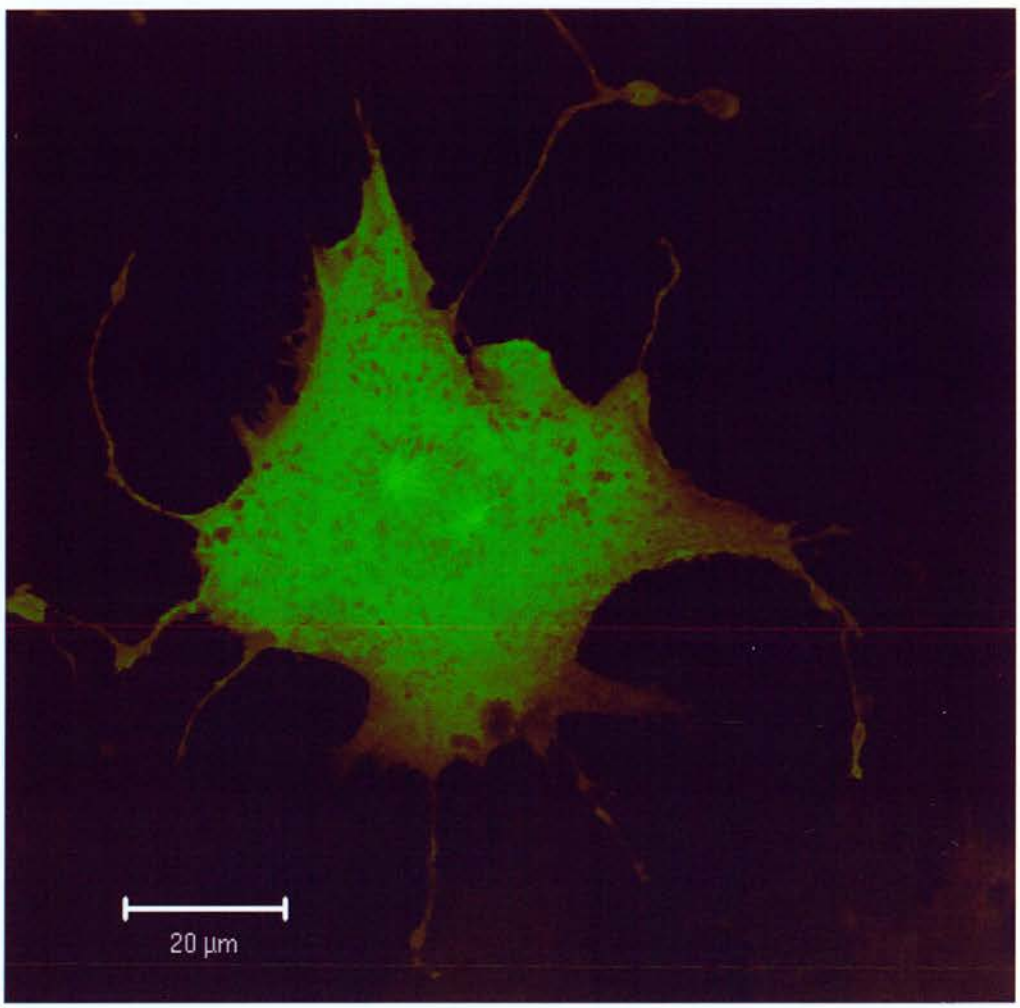

Figure 4-6. The expression pattern of $GIPC_{1-3}$-GFP in a COS7 cell.

Despite this observation, the co-expression of NrCAM may have influenced the distribution of $GIPC_{1-3}$-GFP or vice versa. To test this HEK293 and COS-7 were co-transfected with full length NrCAM (a kind gift from Prof. Vann Bennett, Howard Hughes Medical Institute, Maryland, USA) and $GIPC_{1-3}$-GFP. However, co-expression of NrCAM and $GIPC_{1-3}$-GFP did not show any detectable change in either NrCAM or $GIPC_{1-3}$-GFP distribution when compared to cells expressing either NrCAM or $GIPC_{1-3}$-GFP individually (image not shown). Thus, it was concluded

that the $GIPC_{1-3}$-GFP construct was not showing normal GIPC expression patterns and did not show any distinguishable association with NrCAM.

4.2.1.4 Co-localisations studies of $GIPC_{1-6}$-GFP with HA-NrCAM

It had been noted when carrying other experiments discussed in Chapter 6 that a partial length clone of ankyrin-GFP occasionally mistargeted to the nucleus and whereas a full-length clone of ankyrin-GFP did not localise to the nucleus and co-localised with NrCAM expression. Furthermore, the $GIPC_{1-3}$-GFP clone codes for amino acid 1 to 215 of rat GIPC. Amino acid 215 is the last amino acid of the PDZ domain and tagging a GFP protein to it may have interfered with correct folding of the PDZ domain. It was also possible that amino acids 216 to 333 may be required for the correct targeting of the protein to vesicles. Hence, it was decided to C-terminally tag a full length GIPC construct with GFP and examine its cellular localisation.

The cloning of this construct is shown in Figure 4-7 and the plasmid codes for full length murine GIPC (accession number BC003490) obtained from a mammary tumour library supplied by the IMAGE consortium (Lennon et al., 1996) followed by the GFP protein. This plasmid construct was called $GIPC_{1-6}$-GFP and was transfected into COS-7 cells and HEK293 cells (See Figure 4-8 for an example of a COS-7 cell).

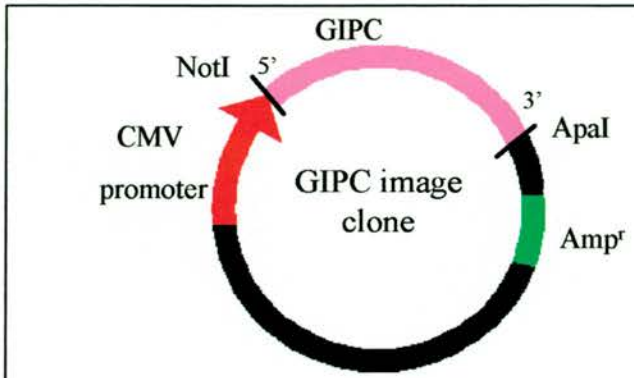

1. A mouse GIPC image clone (accession number BC003490) was used as a PCR template. It also contained nucleotide sequence 5' and 3' of the GIPC sequence.

2. PCR primers GIPC 1 and GIPC 6A were designed to: 1) eliminate 5' and 3' DNA that does not encode for GIPC amino acids (see 3.2.4). 2) to add the EcoRI (GIPC 1) and BamHI (GIPC 3) restriction enzyme sites to the GIPC encoding sequence (see appendix 4 for the sequences).

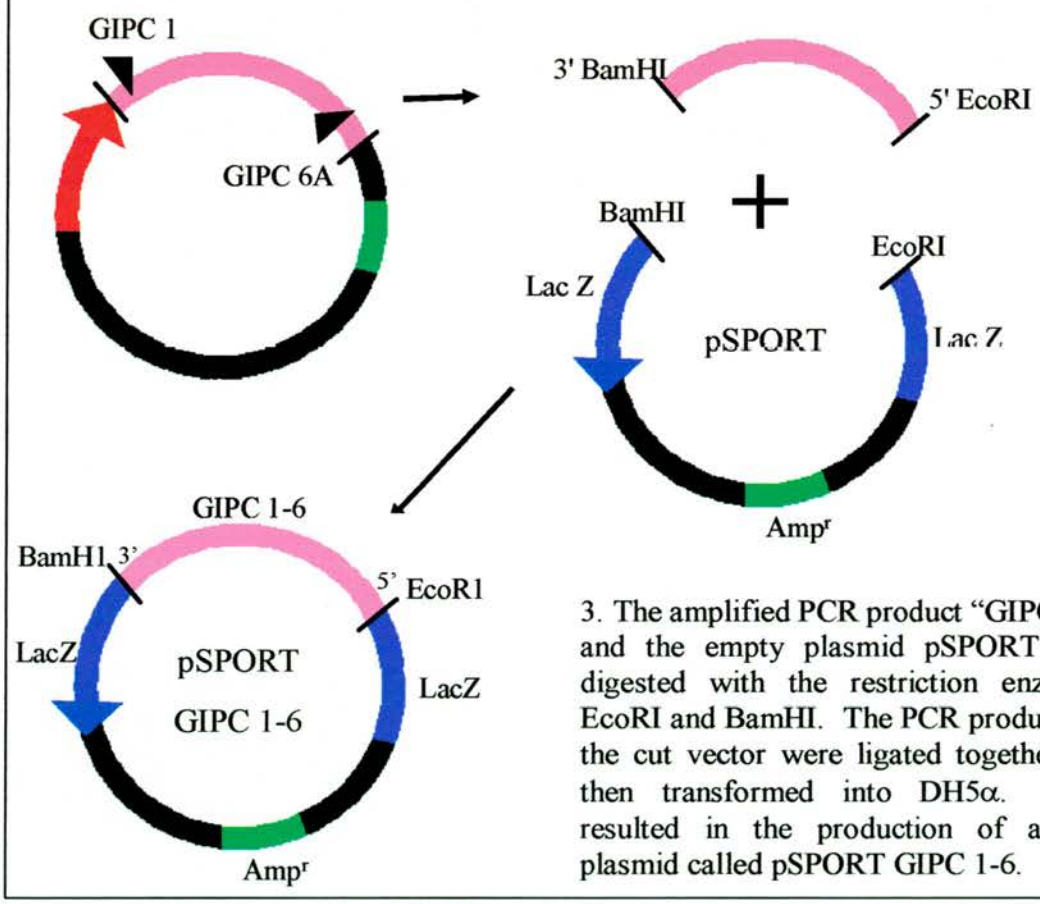

3. The amplified PCR product "GIPC 1-6" and the empty plasmid pSPORT were digested with the restriction enzymes, EcoRI and BamHI. The PCR product and the cut vector were ligated together and then transformed into DH5α. This resulted in the production of a new plasmid called pSPORT GIPC 1-6.

Figure 4-7. Continued on next page.

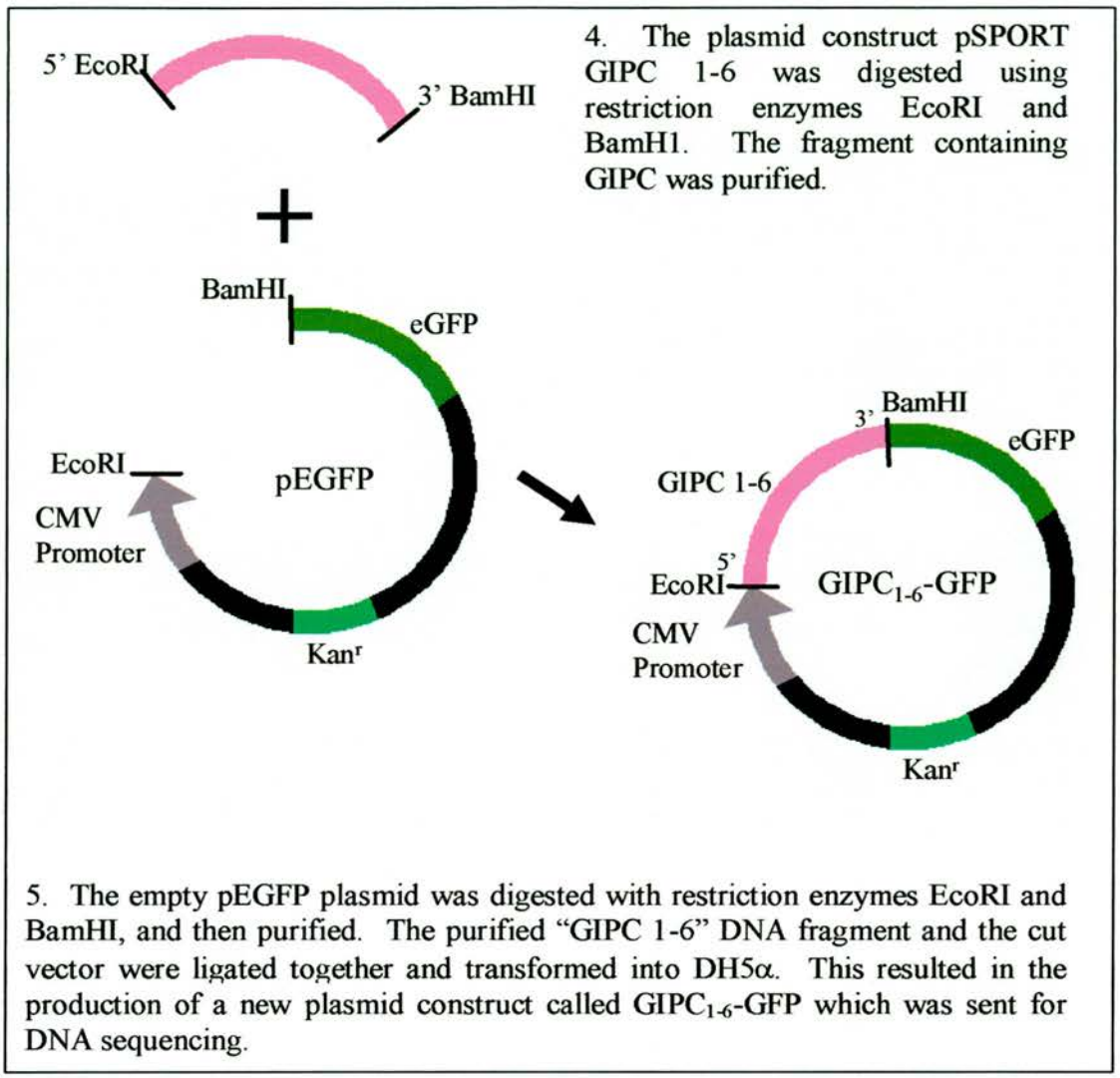

Figure 4-7. Cloning strategy for the production of the plasmid $GIPC_{1-6}$-GFP. Details of material and methods are described in Chapter 2 and accompanying text.

$GIPC_{1-6}$-GFP showed a cytoplasmic expression pattern similar to that which was observed with the truncated $GIPC_{1-3}$-GFP construct. However, in at least 50 % of both COS-7 and HEK293 cells examined it was excluded from the nucleus (data not shown). Unfortunately, no punctate immunostaining of $GIPC_{1-6}$-GFP was evident in any cell examined. Co-transfection of full-length rat NrCAM with $GIPC_{1-6}$-GFP also

did not change either proteins expression pattern in either HEK293 or COS-7 cells (Figure 4-8).

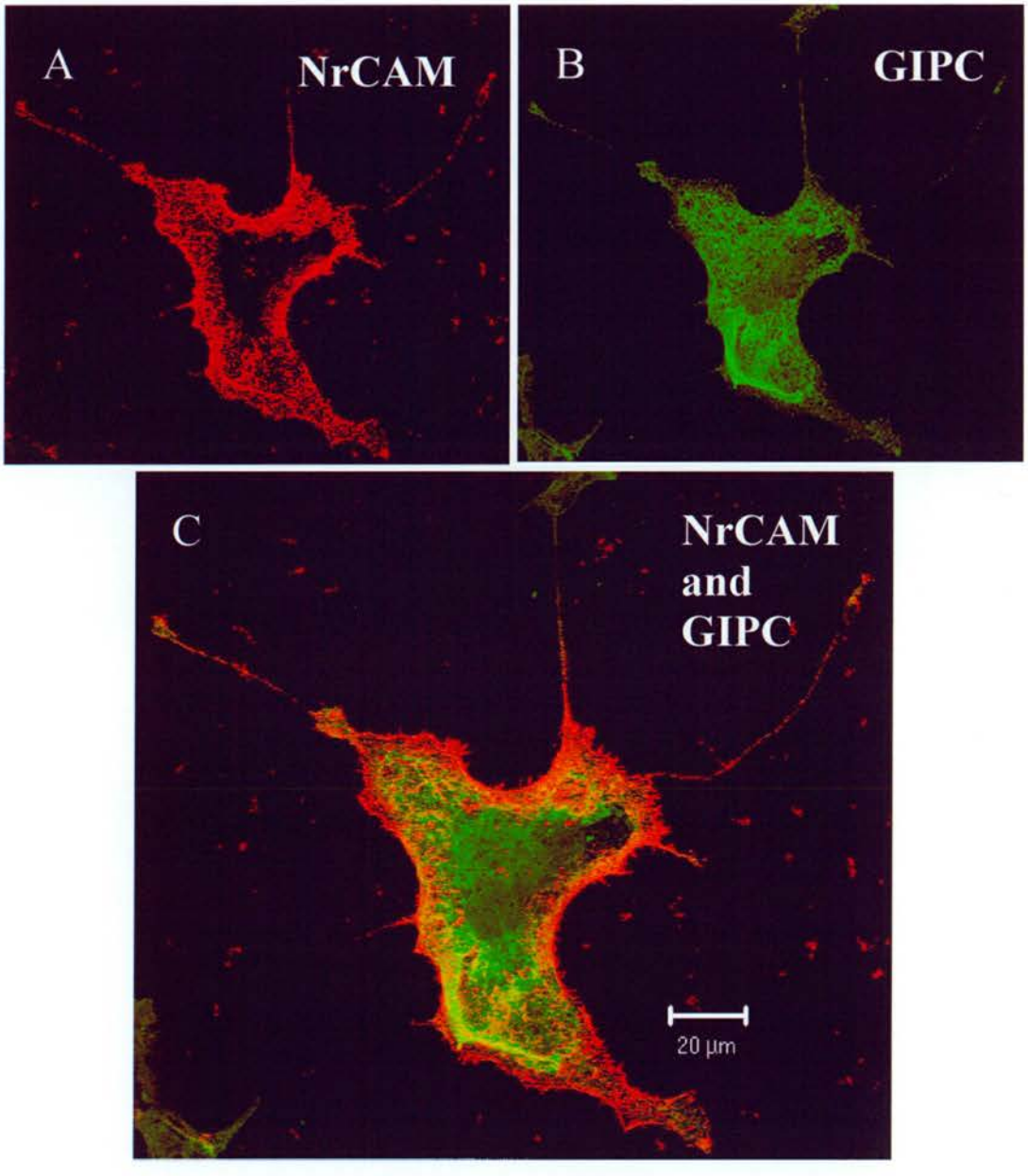

Figure 4-8. Transient expression in a COS-7 cell of NrCAM and $GIPC_{1-6}$-GFP. **A**) Full-length rat NrCAM (NrCAM immunostaining was performed using an NrCAM rabbit polyclonal antibody and anti-rabbit Alexa 568 conjugated antibody and is shown in red). **B**) full-length murine $GIPC_{1-6}$-GFP (green). **C**) Co-localisation between both proteins did not occur. See methods 2.2.10.

4.2.2 SAP102 co-localisation studies.

4.2.2.1 GFP-SAP102 transfected cells.

As there was no antibody suitable for the immunocytochemistry of SAP102 it was therefore decided to perform co-localisation of HA-NrCAM transfected cells with full length rat SAP102 N-terminally tagged with GFP (a kind gift from Dr. N. Sans, National Institute in Deafness and other Communication Disorders, Maryland, USA.). This cDNA construct was transfected into both COS-7 cells and CGCs by Dr F. Davey of the University of St Andrews. Unfortunately, Dr. Davey reported that this construct mistargeted. This mistargeting could have been due to the large size of the GFP proteins at the N-terminal end of the SAP102 protein. Therefore, it was decided to N-terminal tag SAP102 with the smaller FLAG epitope (DYKDDDDKG).

4.2.2.2 Cloning and transfection of the FLAG-SAP102 plasmid construct.

A FLAG-tagged SAP102 construct (FLAG-SAP102) was generated by sub-cloning the SAP102 cDNA isolated in the rat brain library screen (RL29B), into pCMV-Tag 2A (Stratagene) by Dr F. Davey of the University of St Andrews (Davey *et al.*, 2005).

This construct was co-transfected with HA-NrCAM into COS-7 cells grown on glass cover-slips as described in section 2.2.5. The cells were immunostained for HA-NrCAM and FLAG-SAP102 using monoclonal antibodies to the N-terminal epitopes as described in section 2.2.10. Figure 4-9 shows a Z-section of a single COS-7 cell. Patches of co-localisation of HA-NrCAM and FLAG-SAP102 was seen at or near the membrane of most COS-7 cells. However it was most noticable in a small percentage of cells that had HA-NrCAM localised to "microvilli like"

membrane protrusions (Figure 4-9). The localisation of HA-NrCAM to the membrane protrusions occurred when SAP102 was not transfected and was therefore not dependent on the presence of SAP102. Similarly, the localisation of SAP102 to the membrane protrusions occasionally occurred when HA-NrCAM was not transfected and was therefore not dependent on the presence of NrCAM in the cells. Therefore, transiently expressed HA-NrCAM and FLAG-SAP102 co-localise at regions of intense HA-NrCAM immunostaining in the plasma membrane of COS-7 cells. To show that this was not cell type specific and that this could also occur in neurons. CGCs were also transiently transfected by Dr F. Davey of the University of St Andrews with HA-NrCAM and FLAG-SAP102. She reported punctate co-localisation of both proteins at the cell body, along the axon and notably at the endings of the neurons (Davey et al., 2005). Thus, FLAG-SAP102 co-localisation with transiently expressed HA-NrCAM was not cell type specific.

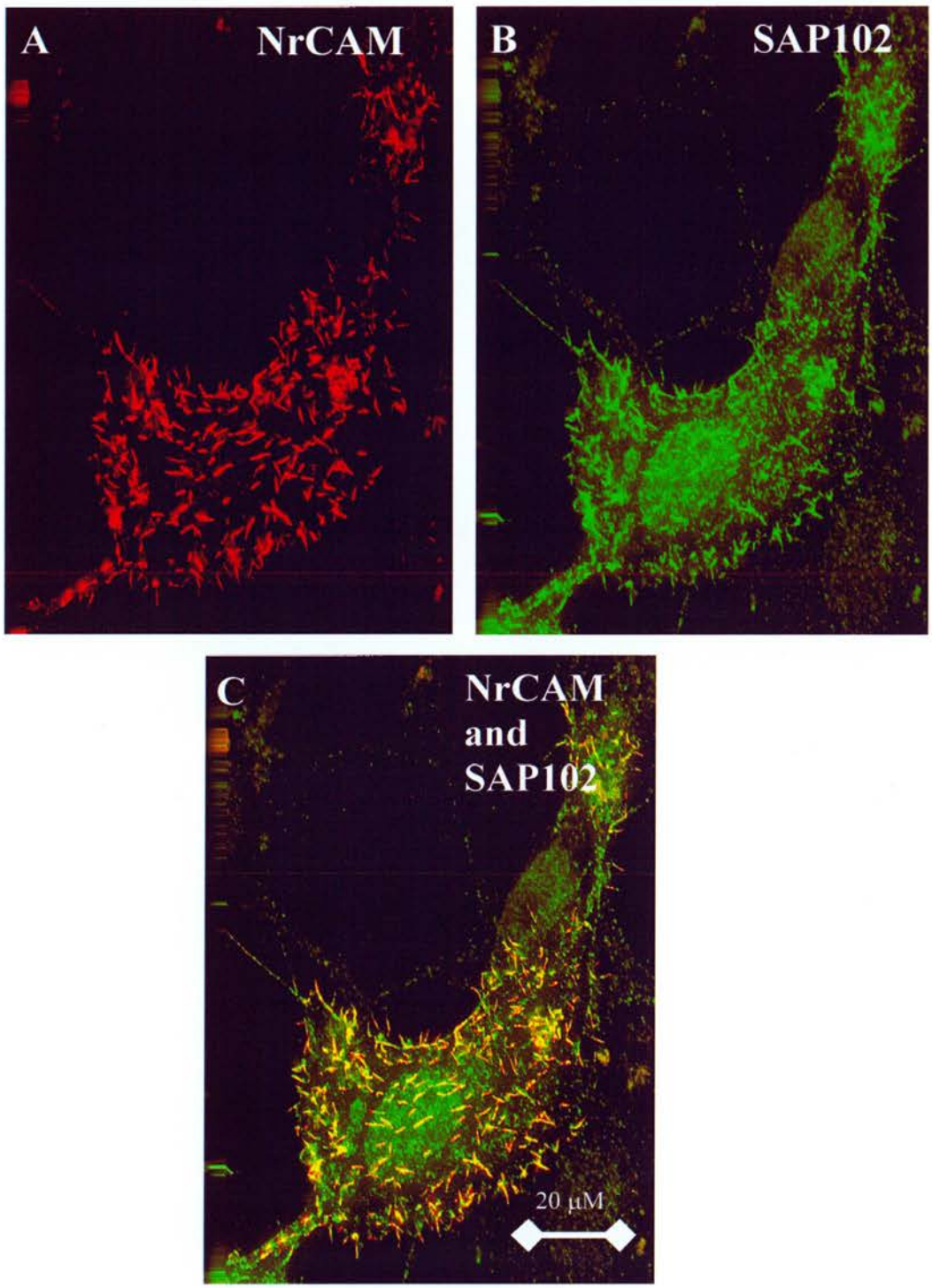

Figure 4-9. Transient expression in a COS-7 cell of HA-NrCAM and FLAG-SAP102. **A**) HA-NrCAM and **B**) FLAG-SAP102. HA-NrCAM immunostaining was performed using an anti-HA rat monoclonal antibody and anti-mouse Alexa 568 conjugated antibody and is shown in red. FLAG-SAP102 immunostaining was performed using a mouse monoclonal antibody to the N-terminal FLAG epitope of FLAG-SAP102 and an anti-mouse antibody conjugated to FITC and is shown in green **C**) Co-localisation between both proteins occurs close to the membrane (yellow). See methods 2.2.10.

4.3 Immunoprecipitation studies.

4.3.1 Immunoprecipitations.

It had been shown that both GIPC and SAP102 could be expressed at the same place and time as NrCAM. However to confirm that these proteins interact further biochemical assays were necessary.

4.3.1.1 Immunoprecipitation of HA-NrCAM using protein A.

As the antibody to the extracellular portion of NrCAM was unsuitable for immunoprecipitation (personal communication Dr. Faivre-Sarrailh, University of Marseille, France) it was therefore decided to target the HA epitope of the HA-NrCAM construct for immunoprecipitation. B104 cells stably expressing HA-neurofascin had been successfully used to immunoprecipitate neurofascin (Garver et al., 1997). It was therefore decided to try immunoprecipitating HA-NrCAM from B104 cells stably expressing rat HA NrCAM.

Initially an immunoprecipitation of HA-NrCAM and its binding partner(s) was attempted using anti-HA antibodies complexed to protein A bound in turn to sepharose beads as described in 2.3.12. This method is described diagrammatically by Figure 4-10 (A). This assay was attempted several times. However, it was never possible to immunoprecipitate out detectable levels of NrCAM using this method. A typical blot is shown in Figure 4-10 (B).

A. Immunoprecipitation

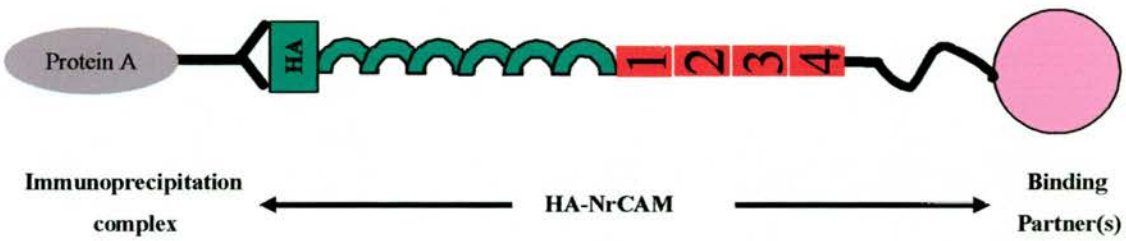

B. NrCAM

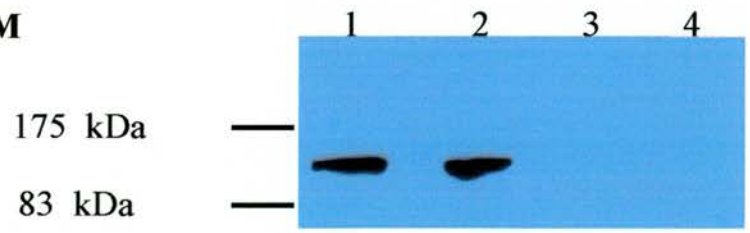

Figure 4-10. Immunoprecipitation of HA-NrCAM using protein A.**A)** A diagrammatic representation of the immunoprecipitation of HA-NrCAM using protein A and antibodies to the HA epitope. **B)** A Western blot of an unsuccessful attempt to immunoprecipitate HA-NrCAM using a polyclonal anti-HA anti body and protein A. Lanes 1 and 2 are 75 μg of cell extract of B104 cells stably expressing HA-NrCAM and lanes 3 and 4 are the proteins immunoprecipitated from cell extract 1 and 2 respectively. The blot was probed with an anti-HA rat monoclonal antibody as described in section 2.3.10 and appendix 3.

4.3.1.2 Immunoprecipitations of HA-NrCAM using anti-rat IgG beads.

Another approach was made to immunoprecipitate out HA-NrCAM and its binding partner(s) using rat monoclonal anti-HA antibodies bound by anti-rat IgG complexed in turn to agarose beads. This method is described diagrammatically by Figure 4-11 (A) and is described in section 2.3.13. Briefly approximately 4 mg of protein extract from B104 cells stably expressing HA-NrCAM extract was tumbled with 4 μl rat monoclonal anti-HA antibodies and 8 μl of anti-rat IgG agarose beads. Detectable levels of HA-NrCAM were immunoprecipitated using this method as shown in Figure 4-11 (B). A 38 kDa band was present in the crude cell extract when

the blot was probed with an anti-GIPC antibody (Figure 4-11 (C)). Two strong bands of approximately 25 kDa and 49 kDa were present in the immunoprecipitated extract probed with an anti-GIPC antibody (Figure 4-11 (C)). These bands were probably the result of the secondary anti-mouse-HRP conjugated antibody binding to the light and heavy chains of the anti-HA rat monoclonal antibody used in the immunoprecipitation experiment. Between the IgG bands of lane 4 there were two weaker bands of approximately 39 kDa and 42 kDa. As the lower of these two bands could possibly be immunoprecipitated GIPC it was therefore decided to repeat the experiment as before except the amount of HA-NrCAM expressing B104 cell extract was increased to 7.5 mg. A 4-12% gel was run using a MES buffer as this favoured the greater separation of lower molecular weight proteins (http://www.invitrogen.com). Proteins were transferred to nitrocellulose and probed for GIPC initially, stripped of antibodies and then probed for NrCAM (Figure 4-12).

As indicated by Figure 4-12, a 38 kDa band was present in the crude cell extract when the blot was probed with an anti-GIPC antibody. Two strong bands of approximately 25 kDa and 49 kDa were again present in the immunoprecipitated extract probed with an anti-GIPC antibody, representing the light and heavy chains of the anti-HA rat monoclonal antibody used in the immunoprecipitation experiment. Between the IgG bands there were two weaker bands of approximately 30 kDa and 40 kDa. As it was possible that the 40 kDa band was GIPC it was decided to confirm the HA-NrCAM-GIPC interaction by immunoprecipitating GIPC and looking for associated GIPC.

A. Immunoprecipitation

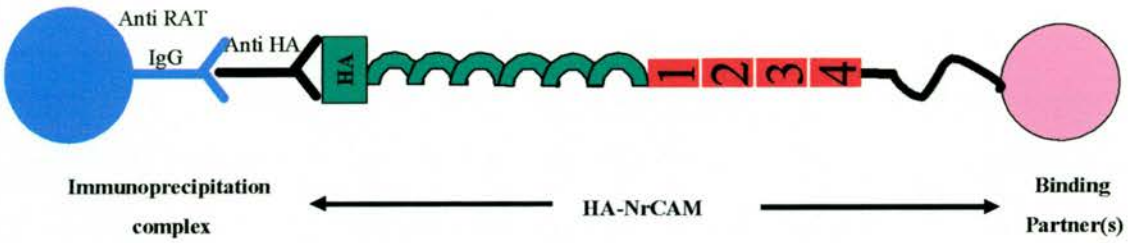

B. NrCAM

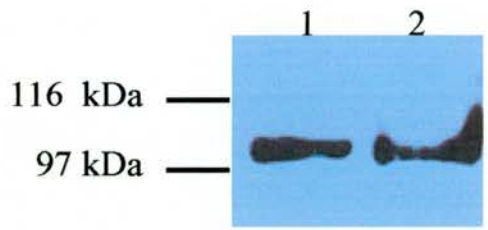

C. GIPC

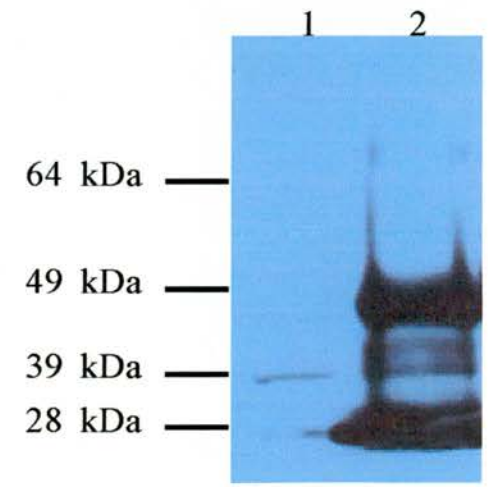

Figure 4-11. Immunoprecipitations of HA-NrCAM using anti-rat IgG beads **A)** A diagrammatic representation of the immunoprecipitation of HA-NrCAM using protein Anti-rat IgG agarose beads and anti-HA rat antibodies.
B) A Western blot of an immunoprecipitatation of HA-NrCAM. Lane 1 is 75 µg of cell extract of B104 cells stably expressing HA-NrCAM and lanes 2 is HA-NrCAM immunoprecipitated from cell extract 1. HA- NrCAM was probed using an anti-HA rat monoclonal antibody. **C)** The Western blot shown in **(B)** stripped of primary and secondary antibodies and reprobed for GIPC. GIPC was probed using a goat GIPC antibody. See Section 2.3 for methods and appendix 3.

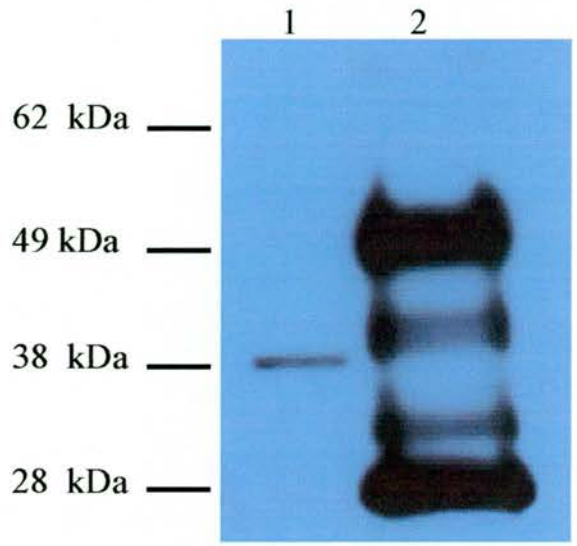

Figure 4-12. A Western blot of immunoprecipitated HA-NrCAM probed for GIPC. Lane 1 is 75 μg of cell extract of B104 stably expressing HA-NrCAM and lane 2 is all of the proteins immunoprecipitated from the cell extract in lane 1. GIPC was probed using an N-terminal GIPC antibody. See section 2.3 for methods and appendix 3.

4.3.1.3 Immunoprecipitations of GIPC using anti-GIPC antibodies.

Approximately 75 mg of HA-NrCAM expressing B104 cell extract was prepared as described in 2.3.5. This extract was divided into two. One-half was tumbled with 8 μl anti Goat IgG conjugated agarose beads and 4 μl goat anti-GIPC antibody. The second half was tumbled with 8 μl anti-mouse agarose beads and 4 μl monoclonal mouse anti-c-Myc antibody. Immunoprecipitations were carried out as described in 2.3.14. The immunoprecipitated products of both fractions were separated on a NuPAGE® Novex 6-12% Bis-Tris gel. The gels was transferred onto nitrocellulose membrane and probed for HA-NrCAM using a rabbit polyclonal antibody to the IgG regions of NrCAM. The membrane was stripped of primary and secondary antibodies and reprobed using a goat anti-GIPC antibody (section 2.3 for methods and Figure 4-13 for results).

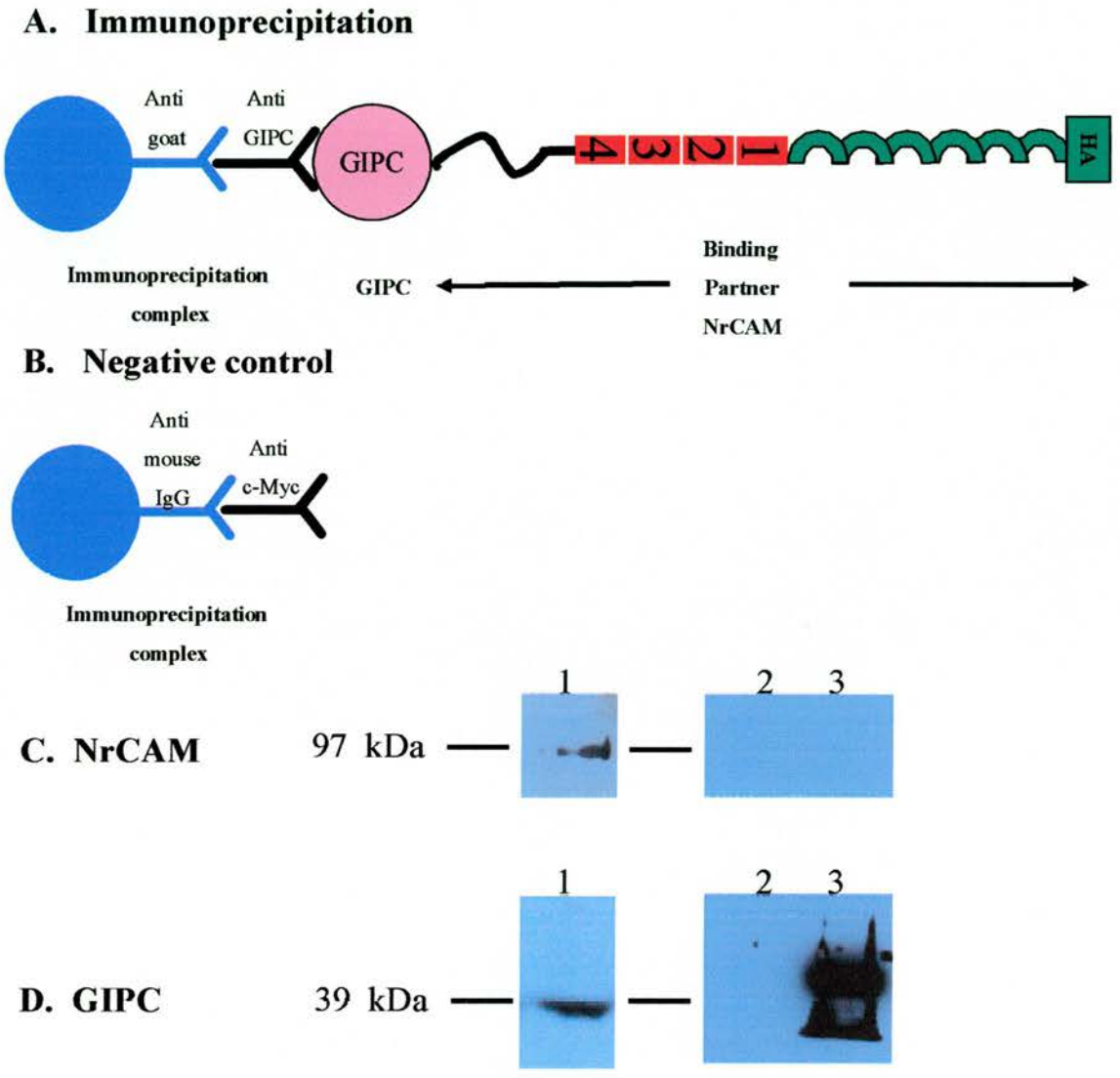

Figure 4-13 Immunoprecipitations of GIPC using anti-GIPC antibodies.
A) A diagrammatic representation of the immunoprecipitation of GIPC using anti-goat IgG agarose beads and anti-GIPC antibodies raised in goat. **B)** A negative control of anti c-Myc antibodies. **C)** and **D**) Western blots of 75 µg of crude cell extract of HA-NrCAM expressing B104 cells (lane 1) and of proteins immunoprecipitated using anti c-Myc antibodies (lane 2) and anti-GIPC antibodies (lane 3). **C)** was probed using a polyclonal anti-NrCAM. **D)** is the same blot as **C)** stripped of anti-NrCAM antibody and reprobed for GIPC using a goat anti-GIPC antibody. See section 2.3 for methods and appendix 3.

As shown in Figure 4-13 (C) HA-NrCAM was present as a single band in the crude cell extract (lane 1), it was not immunoprecipitated using anti c-Myc antibodies (lane 2) or anti-GIPC antibodies (lane 3). The membrane was stripped and reprobed with anti-GIPC antibodies (lanes 4 and 5). Strong bands of approximately 25 kDa and 55 kDa were present in the immunoprecipitated extract of lane 5 but not lane 4. These bands were the result of the secondary anti goat-HRP conjugated antibody binding to the light and heavy chains of the anti-GIPC goat antibody used in the immunoprecipitation experiment. These bands were highly immunoreactive and masked any potential signal at 39 kDa from immunoprecipitated GIPC. Therefore, using this approach it was not possible to determine whether GIPC had been successfully immunoprecipitated.

4.3.2 The effect of furin cleavage on the immunoprecipitation of NrCAM.

It has been reported that NrCAM, unlike neurofascin, can be cleaved within the extracellular domain by furin like proteases (Grumet, 1997), thereby making immunoprecipitation studies difficult for NrCAM. This was a possible explanation for the two/three protein bands seen for NrCAM expression in brain extracts (Figure 4-1 (A)) and CGCs (Figure 4-2 (A)). If NrCAM is furin cleaved it may still associate with itself (at its third FNIII-like domain) and it may be possible to immunoprecipitate out cytoplasmic binding partners using an antibody to the extracellular membrane region (Figure 4-14 (B)). For example it was possible to immunoprecipitate both furin cleaved segments of tractin (the L1 family member in leech) (Xu et al., 2003). However, if NrCAM is furin cleaved and does not associate with itself then antibodies to the extracellular domain N terminal of the FNIII-like

domain will not immunoprecipitate out the cytoplasmic region of NrCAM. Therefore, it will not immunoprecipitate any potential cytoplasmic binding partners (Figure 4-14(C)). In all of the immunoprecipitations attempted above only one band was seen for HA-NrCAM in B104 cells. It was important to establish whether this band represented full-length HA-NrCAM or HA-NrCAM that had been furin cleaved and this was studied in detail in Chapter 6. From this study, a HA-NrCAM construct that did not contain the third FNIII-like domain was engineered and named HA-NrCAM ΔFN2&3. HA-NrCAM ΔFN2&3 cannot be furin cleaved and was used to design the immunoprecipitation experiment described by Figure 4-15(A).

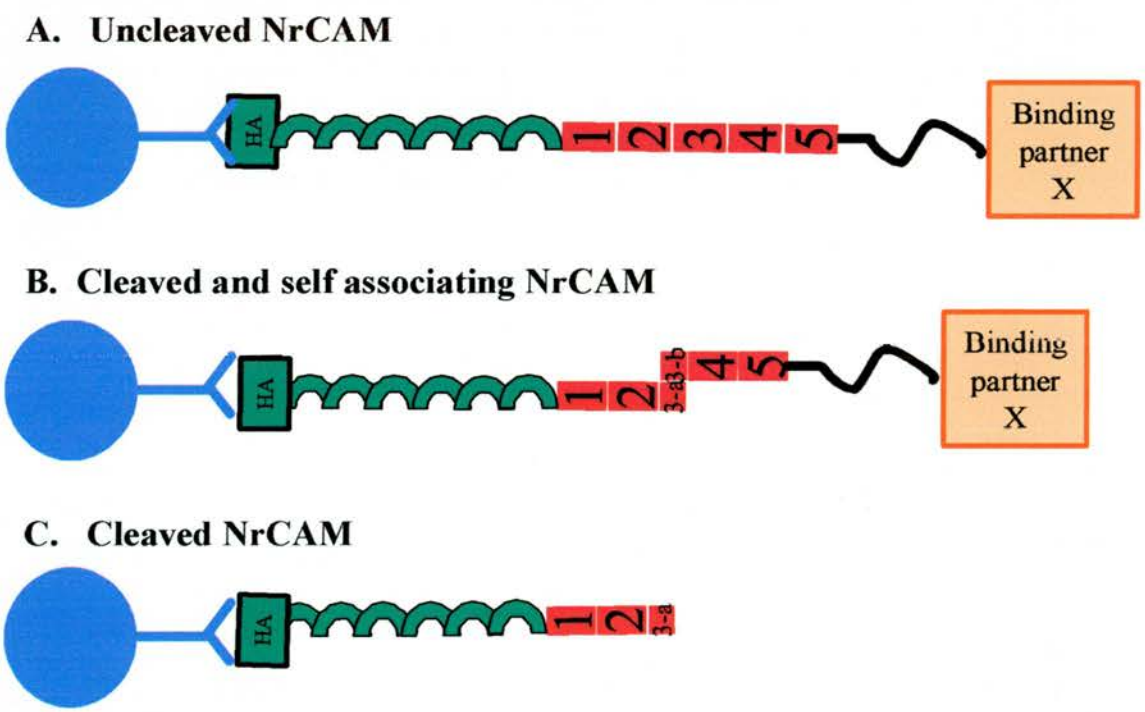

Figure 4-14. Immunoprecipitations of cleaved and uncleaved HA-NrCAM. Anti-HA antibodies and beads can be used to precipitate HA-NrCAM and its cytoplasmic binding partners when **A)** NrCAM is not furin cleaved or **B)** NrCAM is cleaved but still associated with itself at is third FNIII-like domain. However if **C)** NrCAM is cleaved by furin but does not associate with itself, antibodies to HA will not immunoprecipitate the cytoplasmic terminus of NrCAM or any of its binding partners.

4.3.2.1 Immunoprecipitations of HA-NrCAM ΔFN2&3 using anti-HA beads.

HEK293 cells were transiently transfected with the HA-NrCAM ΔFN2&3 construct as described in section 2.2.5. Approximately 8 mg of transfected HEK293 cell extract was prepared as described in 2.3.5. This extract was divided in two. One-half was tumbled with 40 µl anti-HA IgG conjugated agarose beads. The other half was tumbled with 40 µl anti-mouse agarose beads. Immunoprecipitations were carried out as described in 2.3.15. The immunoprecipitated products of both halves were separated by SDS PAGE electrophoresis and a Western blot carried out using a goat anti-GIPC antibody. The membrane was stripped and reprobed for HA-NrCAM ΔFN2&3 using a rat anti-HA monoclonal antibody (see section 2.3). As shown in Figure 4-15 (C) lane 5, HA-NrCAM ΔFN2&3 was successfully immunoprecipitated as a single diffuse band of protein between 100 and 160 kDa. A negative control using anti-mouse beads showed no immunoprecipitated protein as would be expected (Figure 4-15 (C) lane 6). GIPC was present in the crude cell extract (Figure 4-15 (C) lane 1 but was not immunoprecipitated with HA-NrCAM ΔFN2&3 (Figure 4-15 (C) lane 3). Therefore GIPC had not been successfully immunoprecipitated with HA-NrCAM ΔFN2&3 using the conditions tested. It was therefore decided to try a different biochemical approach to confirm the GIPC-NrCAM interaction.

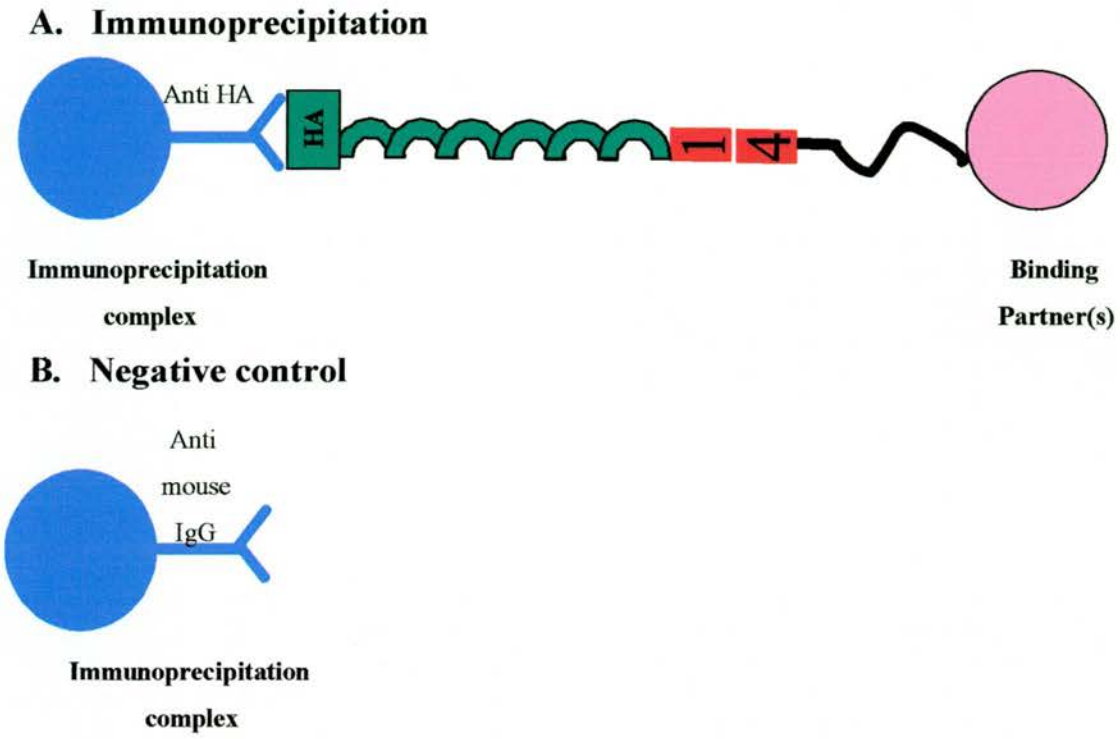

Figure 4-15. Immunoprecipitation of HA-NrCAM ΔFN2&3 using anti-HA beads. **A)** A diagrammatic representation of the immunoprecipitation of HA-NrCAM ΔFN2&3 using agarose beads conjugated to monoclonal anti-HA antibodies. **B)** A negative control were agarose beads conjugated to anti-mouse IgG antibodies do not bind to HA-NrCAM ΔFN2&3 and so do not precipitate any of HA-NrCAM ΔFN2&3's binding partners. **C)** Western blots of extracted cells and immunoprecipitation products. Lane 1 and 2 are 100 μg of crude cell extract of HA-NrCAM ΔFN2&3 expressing HEK293 cells probed for GIPC. Lane 4 and 6 are proteins immunoprecipitated using beads conjugated to anti-HA antibodies. Lanes 5 and 7 are the negative controls of just beads conjugated to anti-mouse antibodies. 1 to 4 were probed for GIPC using a goat anti-GIPC antibody. 5 and 6 is the same blot as 3 and 4 stripped of primary and secondary antibodies and reprobed for HA-NrCAM ΔFN2&3 using a rat monoclonal anti-HA antibody. For methods see section 2.3.10 and appendix 3.

4.4 GST pull-down experiments

Despite various approaches the immunoprecipitation of NrCAM with a potential binding partner had proven unsuccessful. Therefore it was decided to use a variation of the technique called a GST pull-down. In a GST pull-down, the target protein is fused to the enzyme glutathione S-transferase (GST). Beads coated with glutathione select the hybrid GST-protein and its associated binding partners. This assay is illustrated by Figure 4-16.

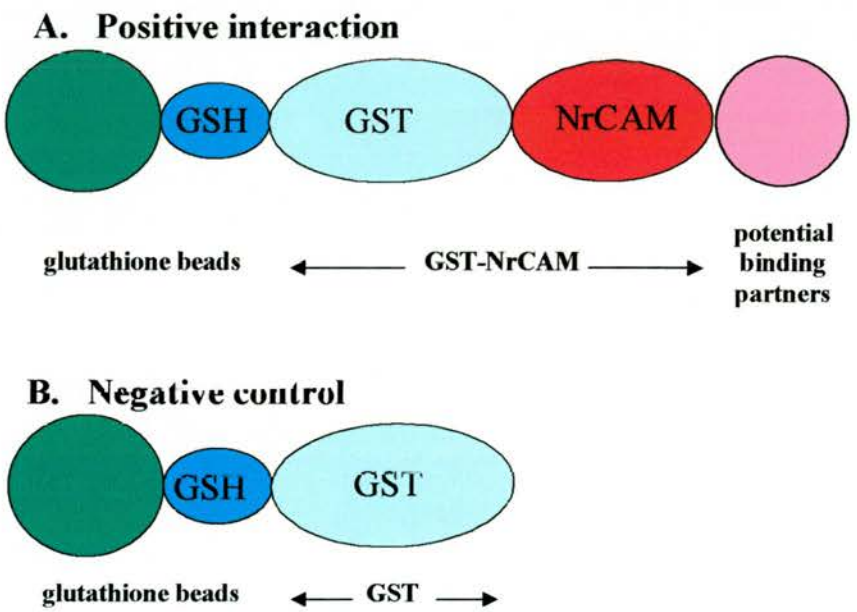

Figure 4-16. A diagrammatic representation of the GST pull-down assay using GST-NrCAM and glutathione coated beads. This compares to a negative control were glutathione beads are coupled to GST only and subsequently do not bind to any binding partners of the cytoplasmic terminus of NrCAM.

4.4.1 Construction of GST-NrCAM

The DNA sequence encoding the intracellular C-terminal region of NrCAM (amino acids 1102-1215 of accession number U81037) was amplified by PCR from a developing rat optic nerve library and sub-cloned into pGEX-KG C-terminal to the GST protein by Dr F. Davey of the University of St Andrews. The empty pGEX-KG vector encoded for the cDNA of GST alone and was used as a negative control. Both proteins were expressed in BL21 C+ *E.coli* and purified using an affinity matrix column of glutathione beads as described in section 2.3.2.

4.4.2 Effect of increasing GIPC expression.

The immunocytochemistry data (Figure 4-3 and Figure 4-4) suggested that only a small proportion of GIPC may be binding to NrCAM. Therefore, to increase the expression of GIPC in the cell and thereby increase the amount available to bind to NrCAM, the GIPC image clone (Figure 4-7, step 1) was transfected into HEK293 cells (section 2.2.5). A Western blot of extracted proteins from these transfected cells indicated an increase in GIPC expression level (Figure 4-17).

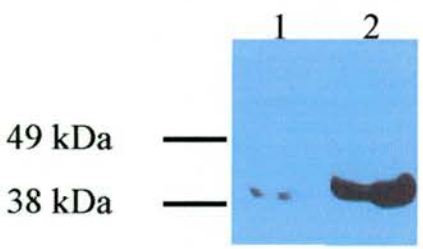

Figure 4-17. A Western blot of 90 μg of crude cell extract of HEK293 cells. Lane 1 are untransfected cells. Lane 2 are cells transfected with murine GIPC cDNA. Lane 1 to 2 was probed using a goat anti-GIPC antibody. For methods see section 2.3.10 and appendix 3.

It was also necessary to show that the over-expressed GIPC had a normal punctate distribution in cells before using it in GST pull-down experiments. Murine GIPC transfected B104 cells, that stably expressed HA-NrCAM, showed a punctate staining pattern for GIPC as expected (Figure 4-18). HA-NrCAM and GIPC co-localised as before (Figure 4-18)). Similar images were seen for HEK293 cells stably expressing HA-NrCAM and transiently transfected with the cDNA from the image clone of GIPC (not shown). Thus, it was shown that transfected murine GIPC was expressing as expected within the cell.

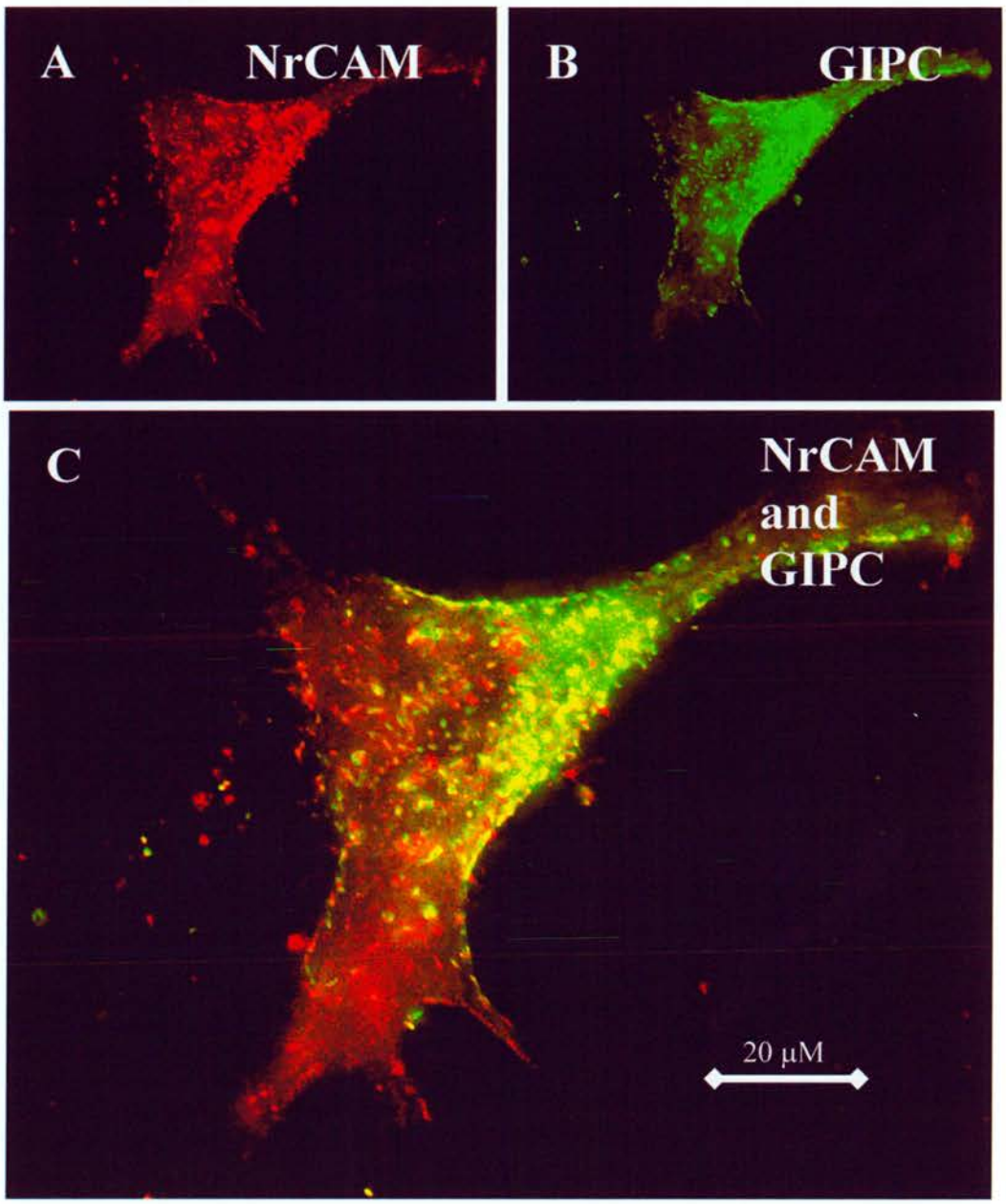

Figure 4-18. Stable expression of HA-NrCAM and transient expression of murine GIPC expressed in a B104 cell. **A**) HA-NrCAM immunostaining was performed using an NrCAM rabbit polyclonal antibody and anti-rabbit Alexa 568 conjugated antibody and is shown in red. **B**) Endogenous GIPC immunostaining was performed using a goat antibody to the N-terminus of GIPC and an anti goat FITC conjugated antibody and is shown in green. **C**) Co-localisation between both proteins occurs in localised areas. See methods 2.2.10, appendix 3B.

4.4.3 NrCAM GST pull-down experiments.

50-60 % confluent 90 mm dishes of HEK293 cells were transfected with the murine GIPC cDNA (to increase GIPC expression) as described in section 2.2.5 and cell extracts prepared in various extraction buffers as described in section 2.3.5. These cell extracts were used to perform the GST pull-down assays as described section 2.3.11. Briefly 10 μg GST or 10 μg GST-NrCAM was coupled to glutathione beads and tumbled in murine GIPC transfected HEK293 cell extract. The GST-beads and GST-NrCAM-beads were washed five to ten times in the extraction buffer and separated on a SDS-PAGE gel, transferred to nitrocellulose and probed by Western blot analysis. Both the buffer used to extract the HEK293 cells and the amount of times the beads were washed was varied to find optimal GST-NrCAM GIPC binding conditions.

The first GST pull-down experiment used radio-immunoprecipitation assay (RIPA) buffer as the extraction buffer (tris-HCL 50 mM pH 7.4, 150 mM NaCl, 1 % NP-40 (v/v), 0.25% Na-deoxycholate). Beads were washed five times and the results are shown in Figure 4-19.

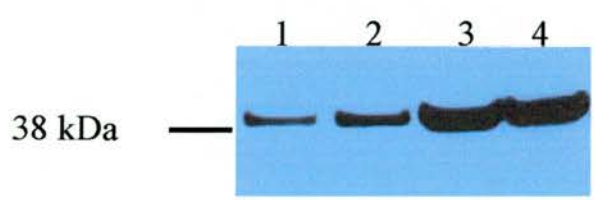

Figure 4-19. A Western blot of a GST pull-down experiment. Lane 4 is 80 μg of crude cell extract of murine GIPC transfected HEK293 cells. Lane 3 is 80 μg of the same cell extract in lane 4 after being pre-cleared with glutathione beads for one hour. Lane 2 is GIPC bound to GST glutathione beads and lane 4 is GIPC bound to GST-NrCAM glutathione beads. Lanes 1 to 4 were probed using a goat anti-GIPC antibody. For methods, see section 2.3.10 and appendix 3.

More GIPC bound to GST alone than bound to GST-NrCAM under these conditions. Therefore it was decided to repeat the experiment using the same RIPA buffer but to increase the washes from five times to ten times. It was hoped that this would eliminate unspecific binding to the GST protein and retain specific binding between GIPC and NrCAM. The results are shown in Figure 4-20.

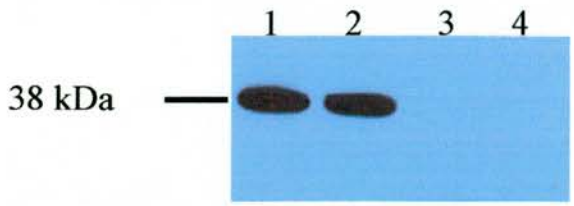

Figure 4-20. A Western blot of a GST pull-down experiment. Lane 1 is 80 μg of crude cell extract of murine GIPC transfected HEK293 cells. Lane 2 is 80 μg of the same cell extract as in lane 1 after being pre-cleared with glutathione beads for one hour. Lane 3 is GIPC bound to GST glutathione beads and lane 4 is GIPC bound to GST-NrCAM glutathione beads. Lanes 1 to 4 were probed using a goat anti-GIPC antibody. For methods, see section 2.3.10 and appendix 3.

Under these conditions, no GIPC bound to either GST alone or GST-NrCAM. This implied that all of the GIPC that bound in Figure 4-19 was unspecific binding to the beads.

It was possible that the ionic strength of the 0.25 % (v/v) Na-deoxycholate detergent used in the RIPA buffer was to too strong to allow a GIPC-NrCAM interaction. Therefore, a series of RIPA buffers of varying Na-deoxycholate strength between 0 and 0.2 % (v/v) were prepared and used to lyse the GIPC transfected HEK293 cells. The beads were washed ten times. However, GIPC did not bind to GST-NrCAM under any of these conditions (Figure 4-21).

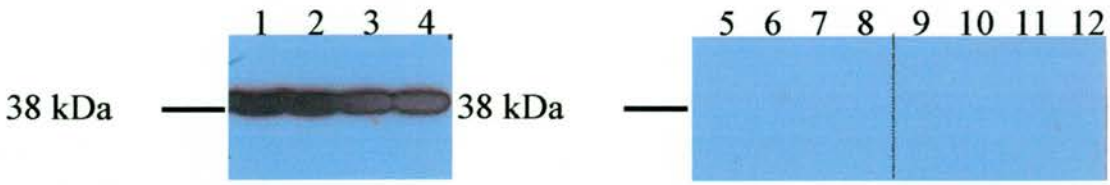

Figure 4-21. A Western blot of GST pull-down experiments. Lanes 1 to 4 are 80 µg of crude cell extracts of murine GIPC transfected HEK293 cells lysed in RIPA buffer containing 0 %, 0.5 %, 0.15 % and 0.2 % (v/v) Na-deoxycholate respectively. Lanes 5 to 8 are GIPC bound to GST glutathione beads when Na-deoxycholate concentrations were 0 %, 0.5 %, 0.15 % and 0.2 % (v/v) respectively and lane 9 to 12 are GIPC bound to GST-NrCAM glutathione beads when Na-deoxycholate concentrations were 0 %, 0.5 %, 0.15 % and 0.2 % (v/v) respectively. Lanes 1 to 12 were probed using a goat anti-GIPC antibody. For methods see section 2.3.10 and appendix 3.

Three different buffers that had been used in the literature to perform GST pull-downs with different GIPC binding partners were tested next (Cai and Reed, 1999; Wang *et al.*, 1999; Lou *et al.*, 2001). These buffers are described in full in Appendix 2. The first buffer called GBH1 is a phosphate buffer and contains three different ionic detergents 1 % Triton X-100, 0.2 SDS, 0.5 % Na-deoxycholate. The second buffer GBH2 was a phosphate buffer without any detergent. The third buffer GBH3 was a tris buffer with 1 % NP-40 non-ionic detergent. All three buffers including buffer GBH2 extracted GIPC protein. However only buffer GBH1 suggested GIPC specifically binding to GST-NrCAM beads. No other bands were seen on the blot (Figure 4-22).

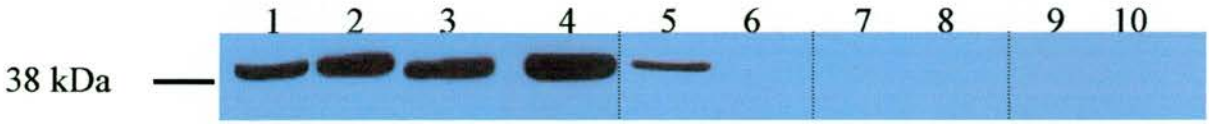

Figure 4-22. A Western blot of GST pull-down experiment varying extraction buffer conditions. Three different buffers were used to extract murine GIPC from transfected HEK293 cells and couple it to GST-NrCAM. Lane 1 is a 100 μg sample of rat brain extract at embryonic day 20. Lane 2 is 80 μg of HEK293 cell extract using buffer GBH1, lane 3 is 80 μg of HEK293 cell extract using buffer GBH2 and lane 4 is 80 μg of cell extract using buffer GBH3. Lanes 5 and 6 are the results of the GST-pull-down assay using GBH1 with 5 being the GST-NrCAM lane and 6 being the GST only lane. Lanes 7 and 8 are the results of the GST-pull-down assay using GBH2 with 7 being the GST-NrCAM lane and 8 being the GST only lane. Lanes 9 and 10 are the results of the GST-pull-down assay using GBH3 with 9 being the GST-NrCAM lane and 10 being the GST only lane. Lanes 1 to 10 were probed using a goat anti-GIPC antibody. For methods see section 2.3.10 and appendix 3.

Due to this potential positive result, instead of HEK293 cells 240 μg of mouse cerebellum was extracted in GHB1 buffer. An additional negative control was added which consisted of GST-NrCAM beads tumbled in 500 μl of GBH1 buffer only (i.e. in the absence of cellular proteins) (Figure 4-23).

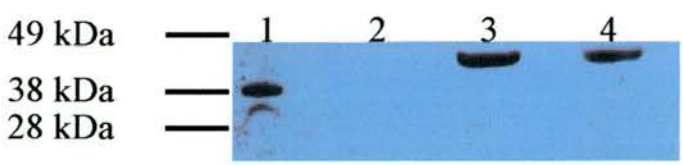

Figure 4-23. A Western blot of a GST pull-down experiment. Lane 1 is 45 μg of cerebellum extracted in buffer GBH1. Lanes 2 and 3 are the results of the GST pull-down assay with 2 being the GST only lane and 3 being the GST-NrCAM lane. Lane 4 is 10μl GST-NrCAM beads tumbled in GBH1 buffer only. Lanes 1 to 4 were probed using a goat anti-GIPC antibody. For methods see section 2.3.10 and appendix 3.

In this experiment, no protein of 39 kDa molecular weight, appeared to have bound to GST-NrCAM (Figure 4-23, lane 3) and thus it was concluded that cerebellar GIPC was not binding to GST-NrCAM. Also noted was a 45 kDA molecular weight protein band that was present in both lanes 3 and 4 of Figure 4-23. As lane 4 is GST-NrCAM beads tumbled in buffer without any extracted proteins, it was evident that the 45 kDA band was the GIPC antibody binding unspecifically to GST-NrCAM.

4.4.4 The production of a FLAG-GIPC construct.

The unspecificity of the GIPC antibody was disappointing. To try to overcome this, it was decided to add an N-terminal FLAG epitope to the murine GIPC cDNA. The cloning was carried out as described in Figure 4-24.

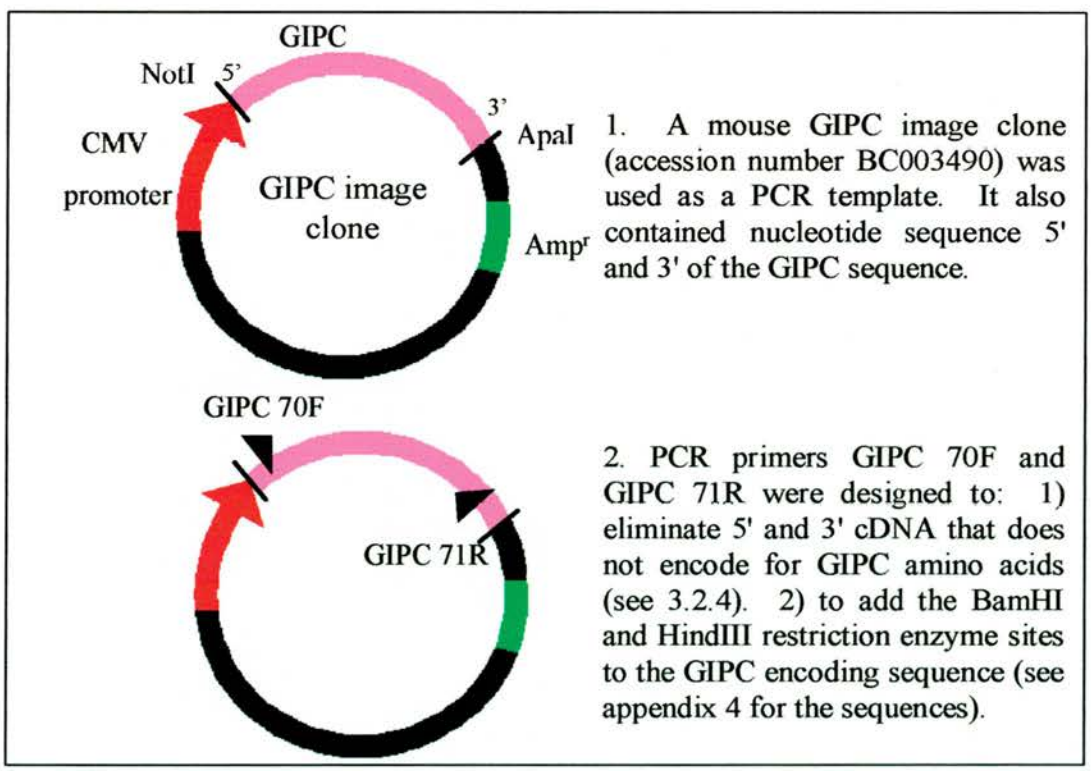

1. A mouse GIPC image clone (accession number BC003490) was used as a PCR template. It also contained nucleotide sequence 5' and 3' of the GIPC sequence.

2. PCR primers GIPC 70F and GIPC 71R were designed to: 1) eliminate 5' and 3' cDNA that does not encode for GIPC amino acids (see 3.2.4). 2) to add the BamHI and HindIII restriction enzyme sites to the GIPC encoding sequence (see appendix 4 for the sequences).

Figure 4-24. Continued on next page.

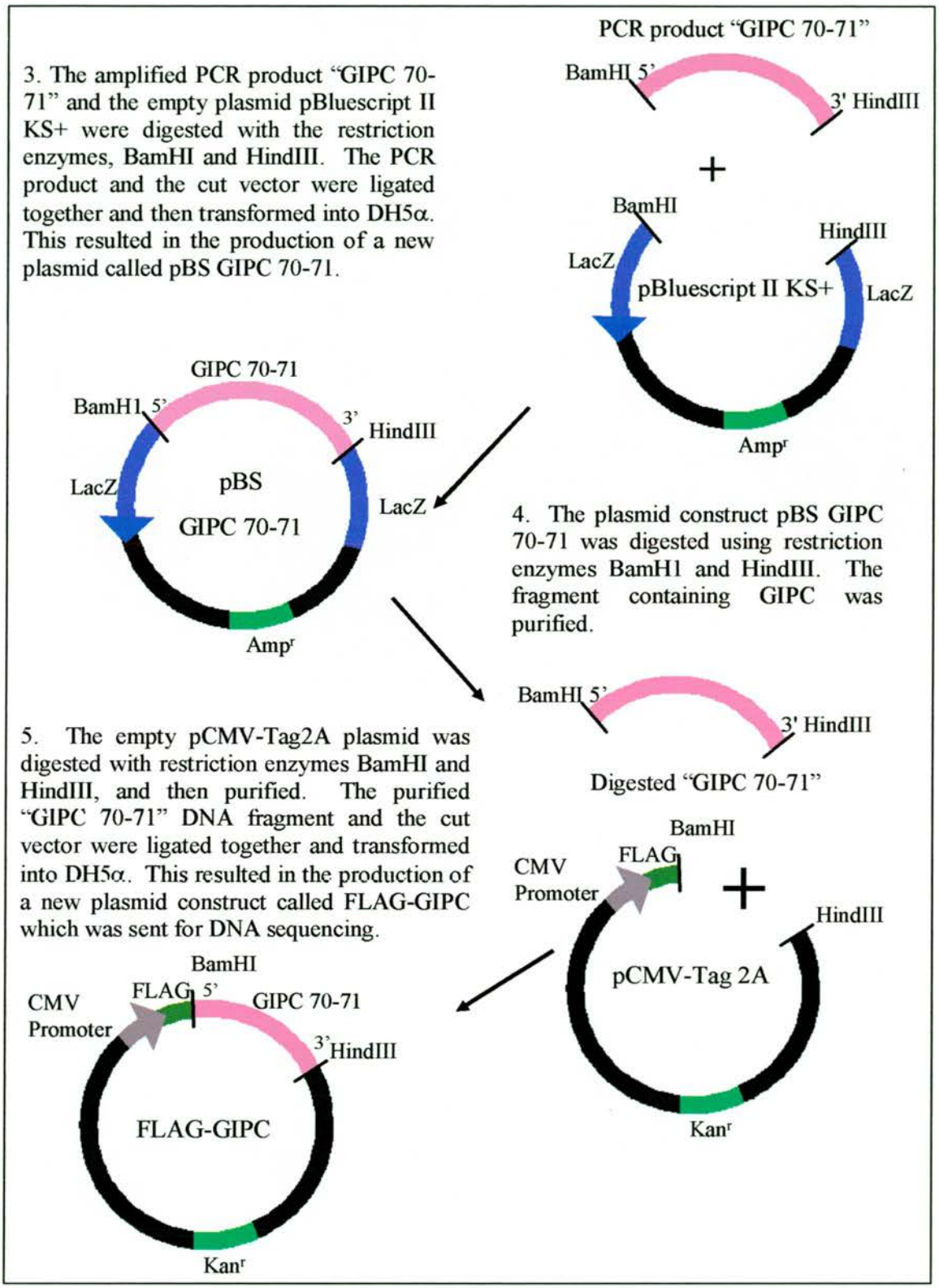

Figure 4-24. Cloning strategy for the production of the plasmid FLAG-GIPC. Details of material and methods are described in Chapter 2 and accompanying text.

This FLAG-GIPC cDNA construct and the murine GIPC cDNA were both transfected into HEK293 cells and the GST-pull-down procedure was carried out as before. Protein samples were separated on an NuPAGE® Novex 6-12% Bis-Tris gel, transferred to a nitroceullose membrane and subsequently probed using an anti-FLAG monoclonal antibody. The membrane was then stripped of its primary and secondary antibodies and reprobed with the anti-GIPC antibody. Results are shown in Figure 4-25.

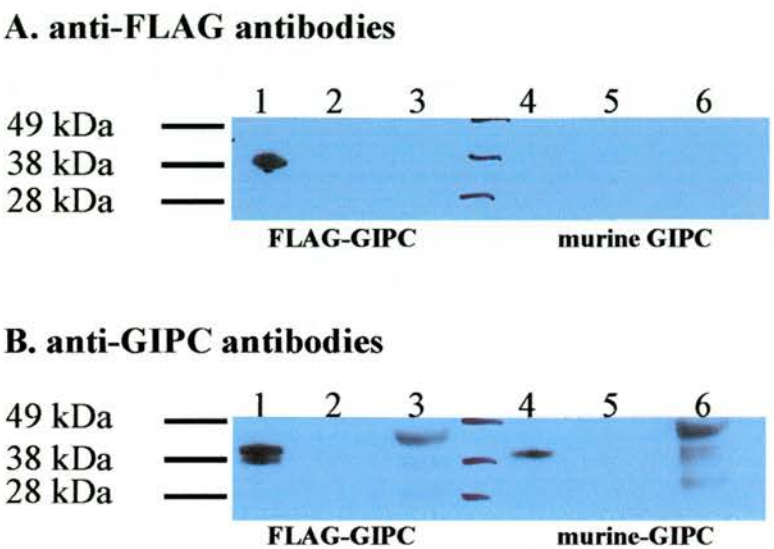

Figure 4-25. A Western blot of two GST pull-down experiments. Lanes 1 to 3 is a GST pull-down experiment carried out on cell extracts from FLAG-GIPC expressing HEK293 cells. Lanes 4 to 6 is a GST pull-down experiment carried out on cell extracts from murine GIPC expressing HEK293 cells. **A)** This membrane was probed using an anti-FLAG antibody. **B)** The membrane in (A) was stripped of primary and secondary antibodies and re probed with a goat anti-GIPC antibody. Lane 1 and lane 4 are 90µg of cell extract of FLAG-GIPC expressing HEK293 cells and murine GIPC expressing cells respectively. Lane 2 and Lane 5 are proteins that bound to GST. Lane 3 and Lane 6 are proteins that bound to GST-NrCAM. For methods see section 2.3.10 and appendix 3.

As expected the anti-FLAG antibodies showed a single band in the FLAG-GIPC transfected cell extract (Figure 4-25 (A) lane 1) but no bands in the murine GIPC

cDNA transfected cell extract (Figure 4-25 (A), lane 4). Unfortunately, no FLAG-GIPC bound to GST-NrCAM. The membrane was stripped of primary and secondary antibodies and reprobed with an anti-GIPC anti-body in Figure 4-25(B). The FLAG-GIPC cell extract showed two bands, with the higher molecular weight band being FLAG-GIPC and the lower molecular weight band being endogenous GIPC (Figure 4-25 (B), lane 1). As before there were no protein bands seen in the GST lanes (Figure 4-25, lane 2 and lane 5). However Figure 4-25 (B) lane 3 and lane 6 (the GST-NrCAM lanes) showed three protein bands. One was the 45 kDa band seen before, one the 39 kDa seen in transfected HEK293 samples and the other a new band of approximately 33 kDa was observed for the first time. This assay was repeated with similar results (blots not shown). However, the three bands in the GST-NrCAM lanes (Figure 4-25 (B) lane 3 and lane 6) were non-specific binding of the GIPC antibody binding to GST-NrCAM and its breakdown products. To illustrate this 5 μg of GST-NrCAM was separated on a NuPAGE® Novex 6-12% Bis-Tris gel, transferred to nitrocellulose and probed with an antibody to the cytoplasmic terminus of NrCAM (Figure 4-26). GST-NrCAM produced both a 45 kDa and a 39 kDa band, suggesting that the 39 kDa band observed in Figure 4-25 is a breakdown product of GST-NrCAM and not GIPC.

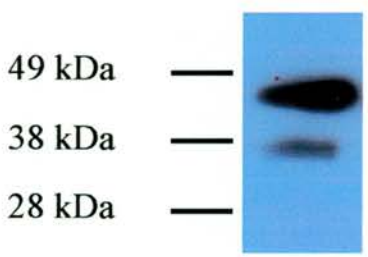

Figure 4-26. A Western blot of GST-NrCAM using an antibody to the cytoplasmic terminus of NrCAM. For methods see section 2.3.10 and appendix 3.

4.4.5 The confirmation of endogenous SAP102 binding with NrCAM but not endogenous GIPC, using Tandem Affinity Purification analysis.

Dr. F. Davey of the University of St Andrews confirmed the binding of SAP102 using the Tandem Affinity Purification Assay (Davey *et al.*, 2005). The DNA sequence encoding the intracellular C-terminal region of NrCAM (amino acids 1102-1215 of accession number U81037) was amplified by PCR from a developing rat optic nerve library and sub-cloned into a pCMV5/TAP vector (a gift from Prof. R. Hay, University of St Andrews). This vector inserts a TAP tag on the N-terminal region of the NrCAM construct, consisting of two IgG binding domains of protein A from *Staphylococcus aureus*, a cleavage site for the tobacco etch virus (TEV) protease, and a calmodulin-binding peptide. The TAP-tagged NrCAM protein was transiently expressed in COS-7 cells and subjected to two successive purification steps. The first purification step involves binding of the protein A tag to beads conjugated to mouse IgG. TAP-NrCAM and the complexes of proteins that bind to it are eluted from the IgG beads using TEV protease. The purified TAP-NrCAM protein complexes were bound to calmodulin beads to remove TEV protease and contaminants and eluted by adjusting the concentration of calcium ions with chelating reagents. The highly purified TAP-NrCAM protein complexes were separated on an SDS-PAGE gel and subjected to Western blot.

It was therefore decided to repeat this experiment using the NrCAM and SAP102 interaction as a positive control to see if the NrCAM and GIPC interaction could also be shown using this method. The method is described in full in 2.3.16. Briefly ten 140 mm plates of COS-7 cells were each transiently transfected with 10 μg TAP-NrCAM cDNA or as a control the empty TAP vector cDNA as described 2.2.5. After

48 hours the cells were lysed in 1ml lysis buffer (50 mM Tris-HCl pH 7.4, 150 mM NaCl, 1 mM EDTA, 1% NP40, 15% glycerol, 1 mM PMSF, a mixture of protease inhibitors). Cell debris was removed by centrifugation and 50 µl of crude cell extract retained. The remaining cell extract was coupled to Rabbit IgG conjugated beads. They were washed five times and the TAP protein complexes eluted using TEV protease. The TAP protein complexes were resuspended in calmodulin binding buffer (CBB) (10 mM Tris-HCl pH 8, 150 mM NaCl, 0.1% NP40, 10 mM β-mercaptoethanol, 1 mM imidazole, 1 mM magnesium acetate, 2 mM $CaCl_2$) and a further 3 mM $CaCl_2$ and coupled to 40 µl of washed calmodulin beads. The beads were thoroughly washed with CBB, then the remaining protein complex was eluted by four washes of calmodulin elution buffer (10 mM Tris-HCl pH 8, 150 mM NaCl, 0.1% NP40, 10 mM β-mercaptoethanol, 1 mM imidazole, 1 mM magnesium acetate, 2 mM EGTA) and one wash of a high salt solution (50 mM Tris-HCl pH 8, 1 M NaCl, 2 mM EGTA). These elutes were combined and immunoblotted.

As shown in Figure 4-27(A) endogenous SAP102 expressed in COS-7 cell extracts (lanes 1 and 2), only associated with TAP-NrCAM (lane 3) and not TAP (lane 4) expressing cells. As shown in Figure 4-27 (B), endogenous GIPC expressed in COS-7 cell extracts (lanes 1 and 2) but did not associate with either TAP-NrCAM (lane 3) or TAP expressing COS-7 cells (lane 4). Thus SAP102 but not GIPC binding has been confirmed by a second biochemical technique.

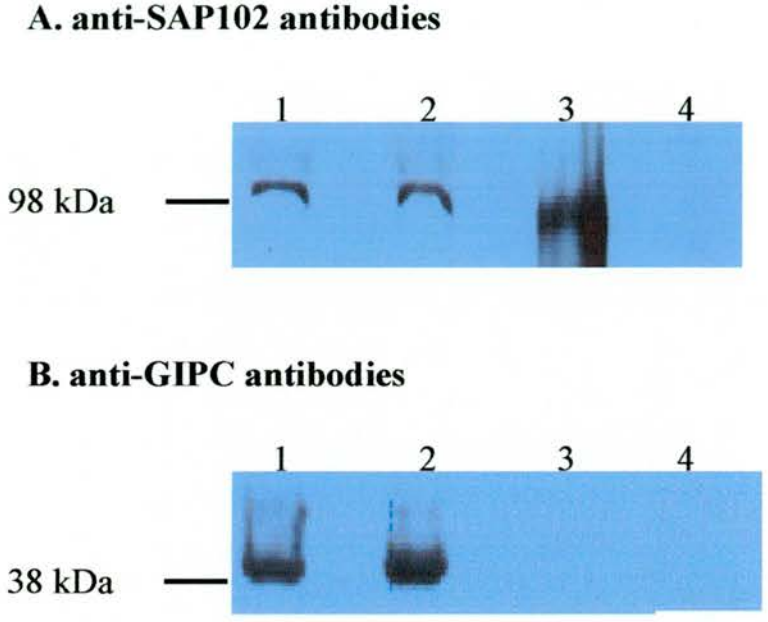

Figure 4-27. A Western blot of a Tandem Affinity Purification Assay. **A)** The membrane was probed using an anti-SAP102 antibody. **B)** The membrane was probed using an anti-GIPC antibody. Lane 1 is the crude cell extract of COS-7 cells transfected with empty TAP vector. Lane 2 is the crude cell extract of COS-7 cells transfected with empty TAP vector. Lane 3 are the proteins eluted with TAP-NrCAM. Lane 4 are the proteins eluted with TAP.

4.5 Retesting of full-length GIPC and SAP102 against NrCAM CT and other members of the L1-CAM family, using the yeast two-hybrid technique.

4.5.1 Cloning of full length GIPC and SAP102 constructs.

Full-length cDNA encoding for GIPC and SAP102 had not been available when the original yeast two-hybrid experiments were performed in Chapter 3. However, it was important to show that the cytoplasmic terminus of NrCAM could bind to the full-length of both of the PDZ domain containing proteins. Therefore, full-length

murine GIPC cDNA and rat full-length SAP102 cDNA were both sub-cloned into the plasmid pACT2-AD as described by Figure 4-28 and Figure 4-29.

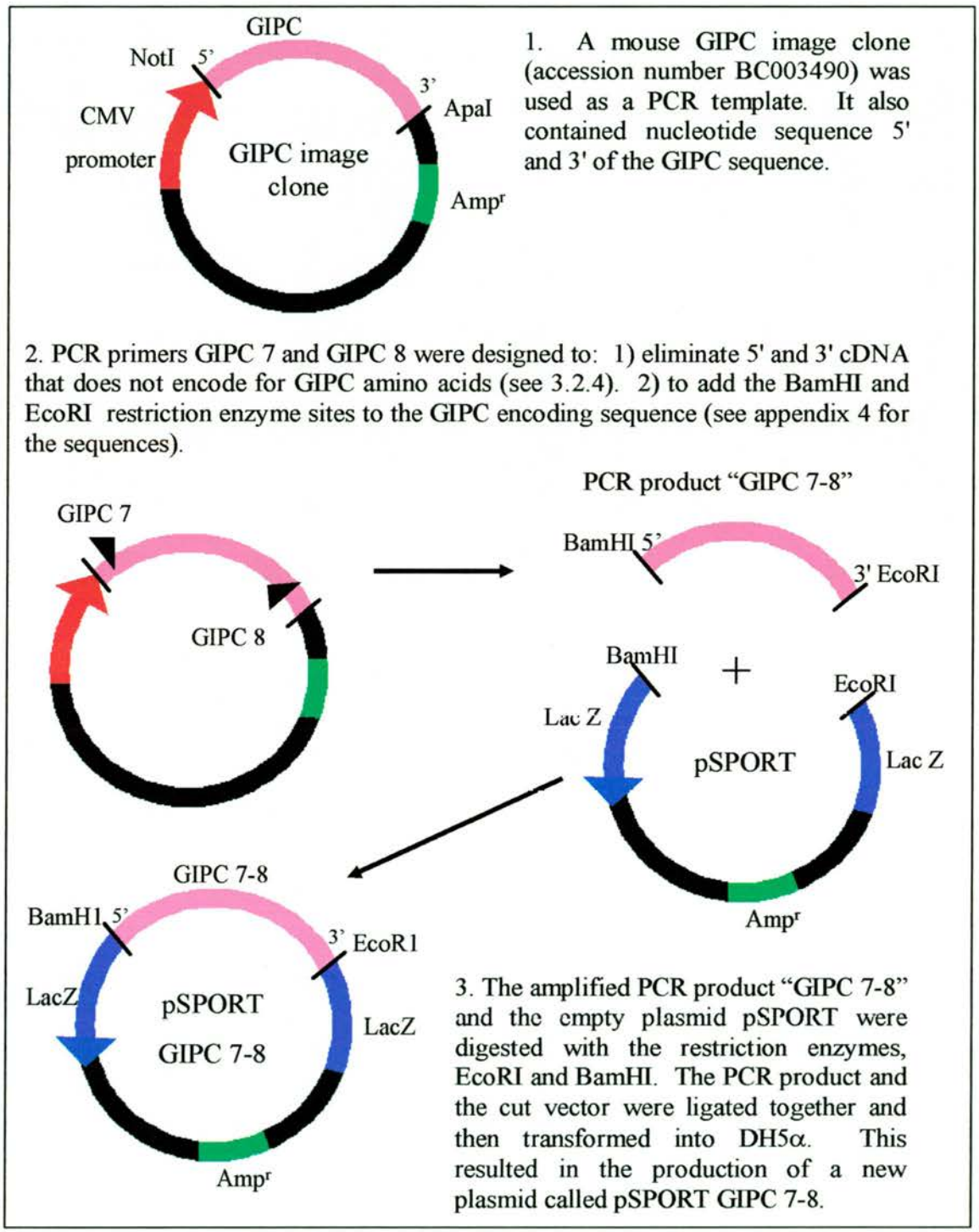

Figure 4-28. Continued on next page.

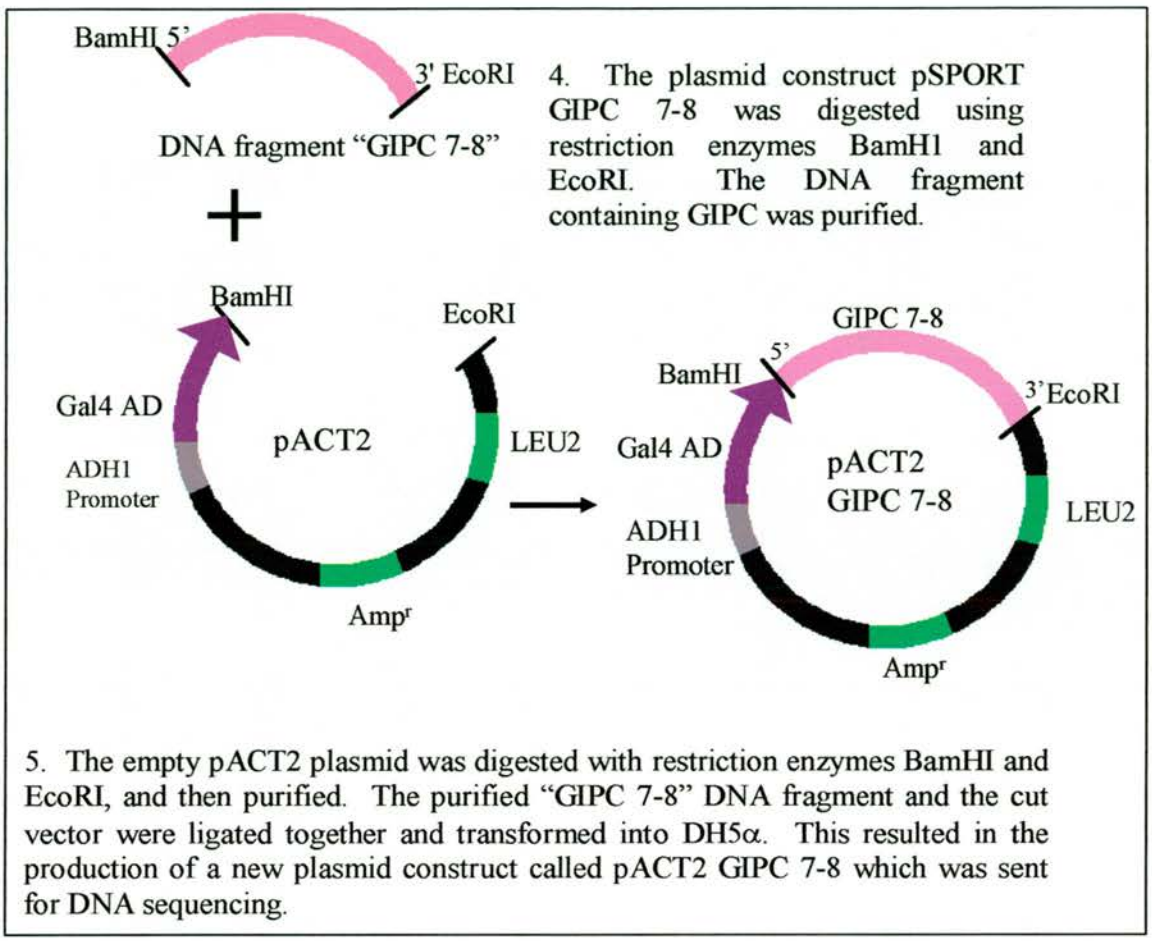

Figure 4-28. Cloning strategy for the production of the plasmid pACT2 GIPC 7-8. Details of material and methods are described in Chapter 2 and accompanying text.

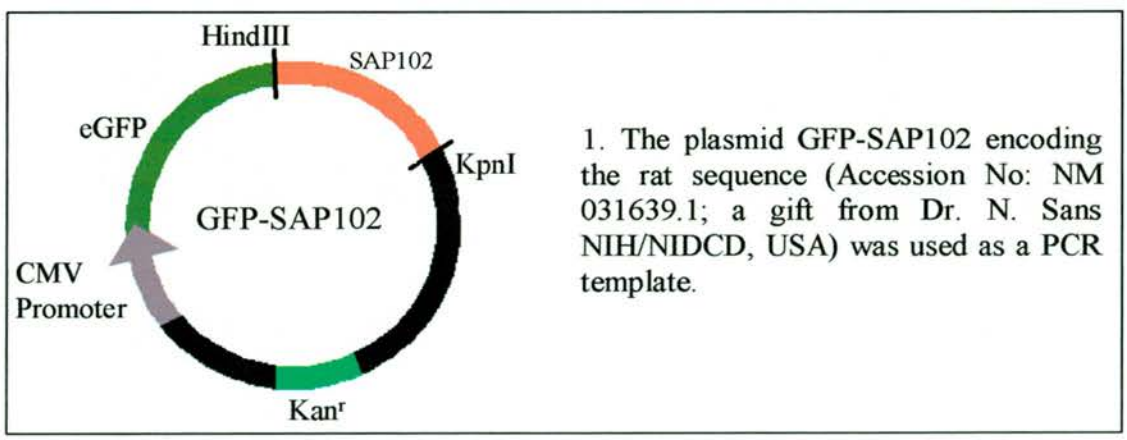

Figure 4-29. Continued on next page.

2. PCR primers (SAP102H and SAP102I: were used to incorporate EcoRI restriction enzyme sites to the ends of the SAP102 coding sequence (see appendix 4 for the sequences).

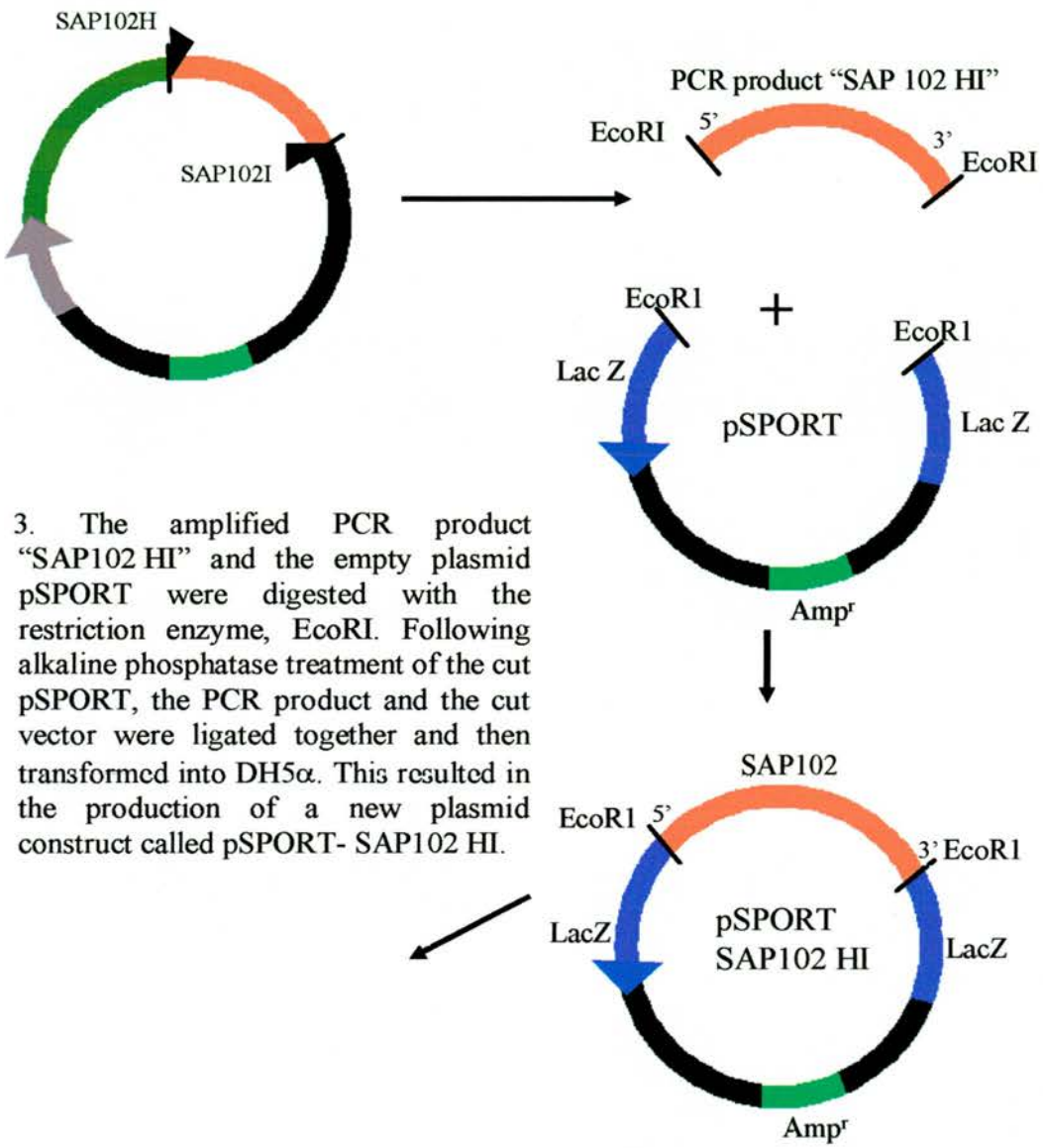

3. The amplified PCR product "SAP102 HI" and the empty plasmid pSPORT were digested with the restriction enzyme, EcoRI. Following alkaline phosphatase treatment of the cut pSPORT, the PCR product and the cut vector were ligated together and then transformed into DH5α. This resulted in the production of a new plasmid construct called pSPORT- SAP102 HI.

4. The plasmid construct, pSPORT-SAP102 HI was digested using the restriction enzyme, EcoRI. The fragment containing SAP102 was purified.

Figure 4-29. Continued on next page.

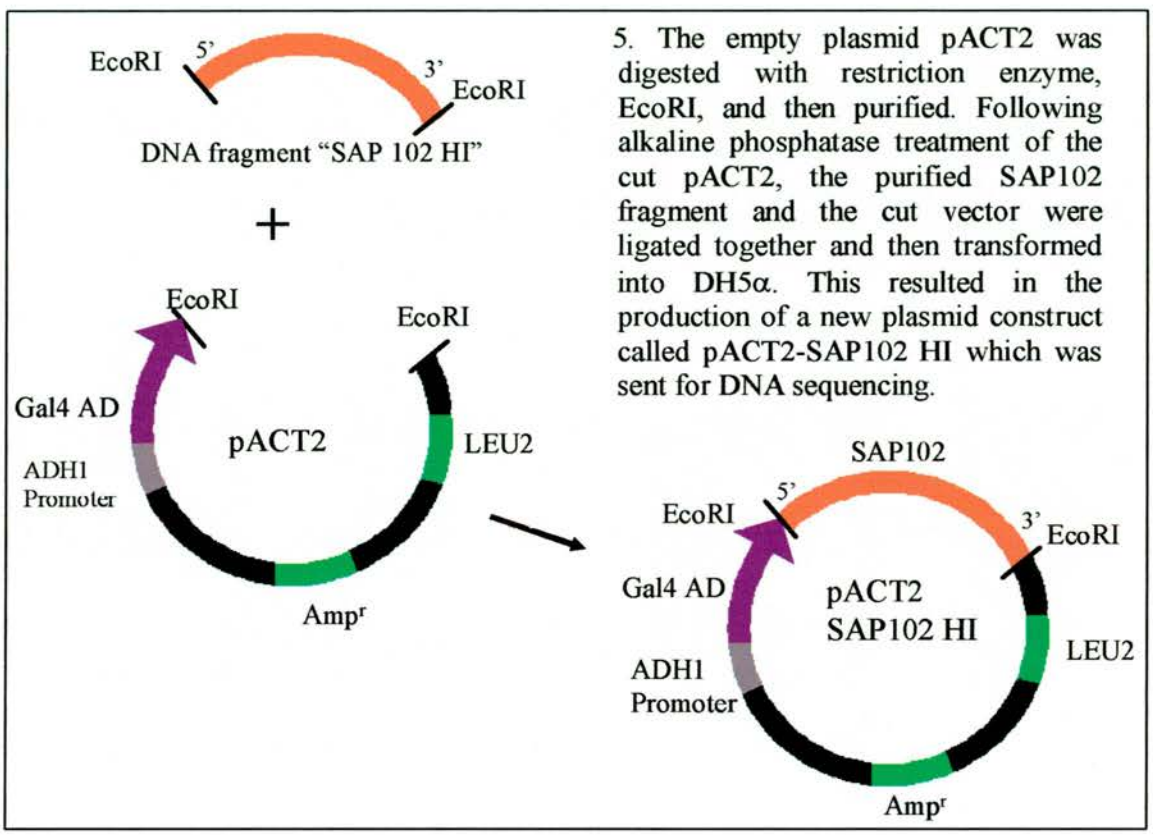

Figure 4-29. Cloning strategy for the production of the plasmid pACT2 SAP102 HI. Details of material and methods are described in Chapter 2 and accompanying text.

4.5.2 Testing of full-length GIPC and SAP102 binding to NrCAM CT.

One μg of bait plasmid (pAS2-1 NrCAM CT, pAS2-1 NrCAM 1-32 ΔPDZ, pAS2-1 neurofascin CT or pAS2-1 L1 CT) was transformed together with one μg of prey plasmid (pACT2 GIPC RL16B(C)2, pACT2 GIPC7-8, pACT2 SAP102 RL29B2 or pACT2 SAP102 HI) into Y190 yeast and the filter lift assay was performed as previously described in Chapter 3. The results are recorded in Figure 4-30.

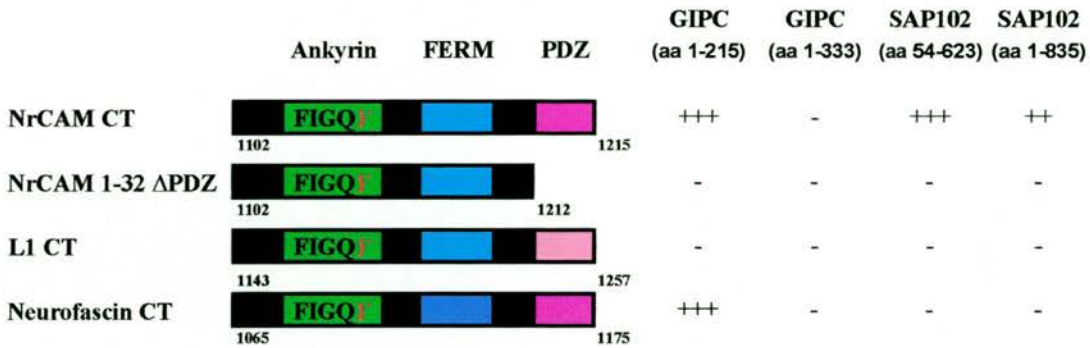

Figure 4-30. Testing of L1-CAM binding to the full length murine GIPC and full-length rat SAP102 proteins using the yeast two-hybrid filter lift assay. The L1-CAM plasmids and NrCAM plasmids have been shown diagrammatically. Green boxes represent the ankyrin binding domain. The dark blue box is the FERM binding domain in neurofascin and the paler blue boxes are the equivalent amino acids in L1 and NrCAM. The dark pink boxes are the PDZ binding domains of neurofascin and NrCAM. The paler pink box is the equivalent amino acids in L1. Binding strengths were scored using the system outlined in Table 3-1.

As shown in Figure 4-30 the cytoplasmic terminus of NrCAM and neurofascin both bound strongly to the GIPC clone, selected by the library screen in Chapter 3, that coded for amino acids 1-215 of rat GIPC. Unexpectedly however neither NrCAM nor neurofascin bound to the full-length murine GIPC protein (amino acids 1-333). This experiment was repeated several times with similar results.

As shown in Figure 4-30 the cytoplasmic terminus of NrCAM bound strongly to the SAP102 clone, selected by the library screen in Chapter 3, which coded for amino acids 54-623 of rat SAP102. The cytoplasmic terminus of NrCAM also bound moderately to the full-length rat SAP102 protein (amino acids 1-835).

4.6 Discussion of results.

The expression levels of NrCAM, GIPC and SAP102 in developing rat brain and CGC cells grown *in vitro* were tested by Western blot for E14, E16, E20 and P7. Both GIPC and NrCAM were expressed at all stages tested and SAP102 was present from E16. Thus NrCAM is developmentally regulated in a similar manner to both of the PDZ proteins.

Co-localisation of stably expressed HA-NrCAM and endogenous GIPC only occurred at small, localised areas of the plasma membrane. Co-localisation of HA-NrCAM and FLAG-SAP102 also occurred at localised areas of the plasma membrane. Thus, only a small percentage of NrCAM can be interacting with a small percentage of GIPC or SAP102 at any one time. This is perhaps unsurprising as both GIPC and SAP102 bind to numerous binding partners (see Table 3-5 and Table 3-6) and are multifunctional proteins.

Various biochemical techniques were attempted to confirm the NrCAM and GIPC interaction. Co-immunoprecipitations of NrCAM with GIPC and GIPC with NrCAM were attempted but were difficult to prove due to the secondary antibody used in the Western blot procedure cross reacting with one of the IgG domains of one of the antibodies used in the immunoprecipitation. This was further complicated as NrCAM may be furin cleaved in its third FN-III-like domain (Kayyem *et al.*, 1992; Grumet, 1997) and though this may not necessary impair its ability to be immunoprecipitated (Xu *et al.*, 2003) this was difficult to prove without a specific antibody to the cytoplasmic terminus of NrCAM (see Chapter 6). Therefore an attempt was made to co-immunoprecipitate GIPC with an HA-tagged NrCAM protein that did not contain

the third FNIII-like domain (NrCAM ΔFN2&3). This was unsuccessful and thus it has been concluded that endogenous GIPC had not been successfully co-immunoprecipitated with either HA-NrCAM or HA-NrCAM ΔFN2&3.

Because of the difficulties experienced with the immunoprecipitation procedure, I tried verifying the NrCAM and GIPC interactions using a different biochemical technique. The cytoplasmic terminus of rat NrCAM was N-terminally tagged with GST and GST pull-downs attempted. One out of several buffering conditions tested appeared to show that over expressed murine GIPC could bind to GST-NrCAM. However, the validity of this result is questionable as the GIPC antibody appeared to be binding to GST-NrCAM and one of the breakdown products of the GST-NrCAM protein is 39kDa. To overcome the problem GIPC was N-terminally tagged with the FLAG epitope, thus allowing the use of monoclonal antibodies to probe for GIPC. FLAG-GIPC expressed at levels equal to endogenous levels of GIPC but unfortunately failed to bind to GST-NrCAM and so it was concluded that the GIPC-NrCAM interaction could not be shown using GST pull-downs.

Meanwhile the binding of NrCAM to endogenous SAP102 had been shown by TAP analysis. This experiment was repeated and both of the NrCAM-SAP102 and NrCAM-GIPC interactions were tested. The binding of NrCAM to SAP102 was reconfirmed. However, NrCAM did not bind to endogenous GIPC.

The yeast two-hybrid analysis showed similar results. Full-length rat SAP102 bound to NrCAM (though with a more moderate binding strength than between the part-length library clone of SAP102 and NrCAM). Full-length murine GIPC however did not show any binding to NrCAM.

Proposed roles for NrCAM-SAP102 binding and whether NrCAM is believed to be binding to GIPC are discussed further in Chapter 7.

Chapter 5. The different binding abilities of NrCAM, L1 and neurofascin to members of the 4.1 Superfamily family.

5.0 Introduction. Members of the 4.1 superfamily of proteins may link NrCAM to the cytoskeleton in the axonal growth cone.

The neuronal growth cone advances when external substrate cues physically anchor growth cone plasma membrane receptors to the internal actin retrograde flow (Lin and Forscher, 1995). Both NrCAM and L1 are known to be coupled to the actin retrograde flow of the growth cone (Faivre-Sarrailh et al., 1999; Kamiguchi and Yoshihara, 2001) but it is not yet fully understood how this coupling takes place. One possibility is that NrCAM and L1 bind to the retrogradely moving actin cytoskeleton via ankyrin. NrCAM has an ankyrin-binding motif in its cytoplasmic terminus and, at the node of Ranvier, NrCAM is linked to the actin cytoskeleton via ankyrin$_G$ (Davis et al., 1996). However ankyrin$_G$ is not found in the growth cone and ankyrin$_B$ is only found at the proximal region of the growth cone (Nishimura et al., 2003). Furthermore ankyrin$_B$-binding to L1 has been shown to inhibit its retrograde movement and to promote stationery behaviour (Gil et al., 2003). Thus, it is likely that a protein(s) other than ankyrin is/are coupling NrCAM and L1 to retrogradely moving actin filaments in the growth cone

Candidate proteins that may fulfil this role belong to the 4.1 superfamily. FERM family proteins link membrane receptors to the actin cytoskeleton both directly and indirectly (Bretscher et al., 2000). Direct interactions occur when the 4.1 ezrin radixin moesin (FERM) domain of the protein binds to a cytoplasmic domain of the membrane protein (Figure 5-1 (A)). Indirect interactions occur when the cytoplasmic terminus of a membrane receptor binds to an adaptor protein such as EBP50 that in turn binds to a member of the 4.1 superfamily member (Figure 5-1 (B)).

There is some evidence that suggest that 4.1 superfamily members suggests binding to NrCAM in the growth cone. For example two members of the family, radixin and moesin, are essential for neuronal growth cone motility and neurite extension (Paglini et al., 1998) (Castelo and Jay, 1999) and NrCAM co-localises with another family member, ezrin, at the membrane protrusions of renal carcinoma cells (Conacci-Sorrell et al., 2002).

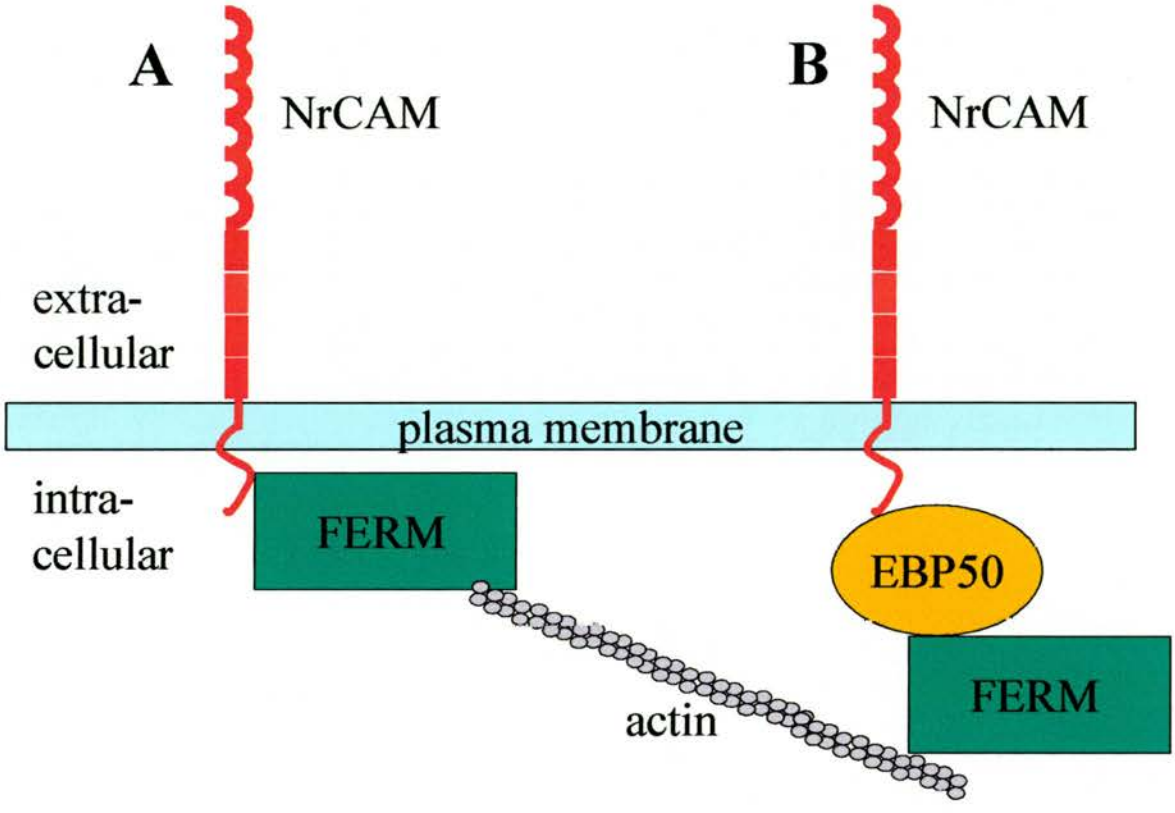

Figure 5-1. A diagrammatic representation of how proteins of the 4.1 superfamily may link NrCAM and other members of the L1-CAM family to the actin cytoskeleton. **A)** Shows a direct interaction between NrCAM and the FERM domain containing protein. An amino acid sequence in the cytoplasmic terminus of NrCAM binds to the FERM domain of the 4.1 superfamily protein, which in turn binds to actin filaments via a C-terminal motif. **B)** Shows an indirect interaction between NrCAM and the 4.1 superfamily protein. An amino acid sequence in the cytoplasmic terminus of NrCAM binds to the PDZ domain of the EBP50 protein, which in turn binds to a 4.1 superfamily protein, which then binds to actin filaments. This Figure was adapted from (Bretscher et al., 2000).

The strongest suggestion that NrCAM may bind to 4.1 superfamily members has come from studies on neurofascin. The neurofascin cytoplasmic terminus has been shown to bind to two members of the 4.1 superfamily by a yeast two-hybrid screen performed by Dr. F. Gunn-Moore of the University of St Andrews. The first clone identified was ezrin (amino acids 1 to 482) and the second clone identified was a novel member of the 4.1 superfamily that has been termed willin (amino acids 1-342). It is predicted that the last 28 amino acids of neurofascin bind to the FERM domains of both clones (Gunn-Moore unpublished results). Within these 28 amino acids is a 14 amino acid sequence that is a FERM binding consensus sequence (Figure 5-2). Importantly NrCAM codes for 10 out of 14 of these amino acids see Figure 5-2.

Neurofascin	(aa 1148-1161)	R K D K E E T E G N E S S E
NrCAM	(aa1190-1203)	K K E K E P A E G N E S S E
Consensus		+ K - K E X X E G N E S S E

Figure 5-2. An alignment of the amino acids of the proposed FERM binding domain of neurofascin and the equivalent amino acids in NrCAM. When the equivalent amino acids of NrCAM and neurofascin are of the same charge at physiological pH their charge has been written in the amino acid sequence as a + or -. Only two amino acids are significantly different in NrCAM when compared to neurofascin and have not been included in the consensus sequence.

5.1 Results.

5.1.1 Do NrCAM and ezrin co-localise?

NrCAM must first co-localise with a member of the 4.1 superfamily in cells in order for binding to occur. Therefore NrCAM and ezrin co-localisation was tested in

various cell types. Dr F. Gunn-Moore of the University of St Andrews generated a FLAG-tagged ezrin construct that coded for amino acid 1-482 of ezrin, N-terminally tagged by the FLAG epitope (FLAG-ezrin). This construct was co-transfected with HA-NrCAM into COS-7 cells growing on glass coverslips as described in section 2.2.5 and immunostained for HA-NrCAM and FLAG-ezrin using monoclonal antibodies to the N-terminal epitopes as described in section 2.2.10. Figure 5-3 shows a Z-section of two COS-7 cells.

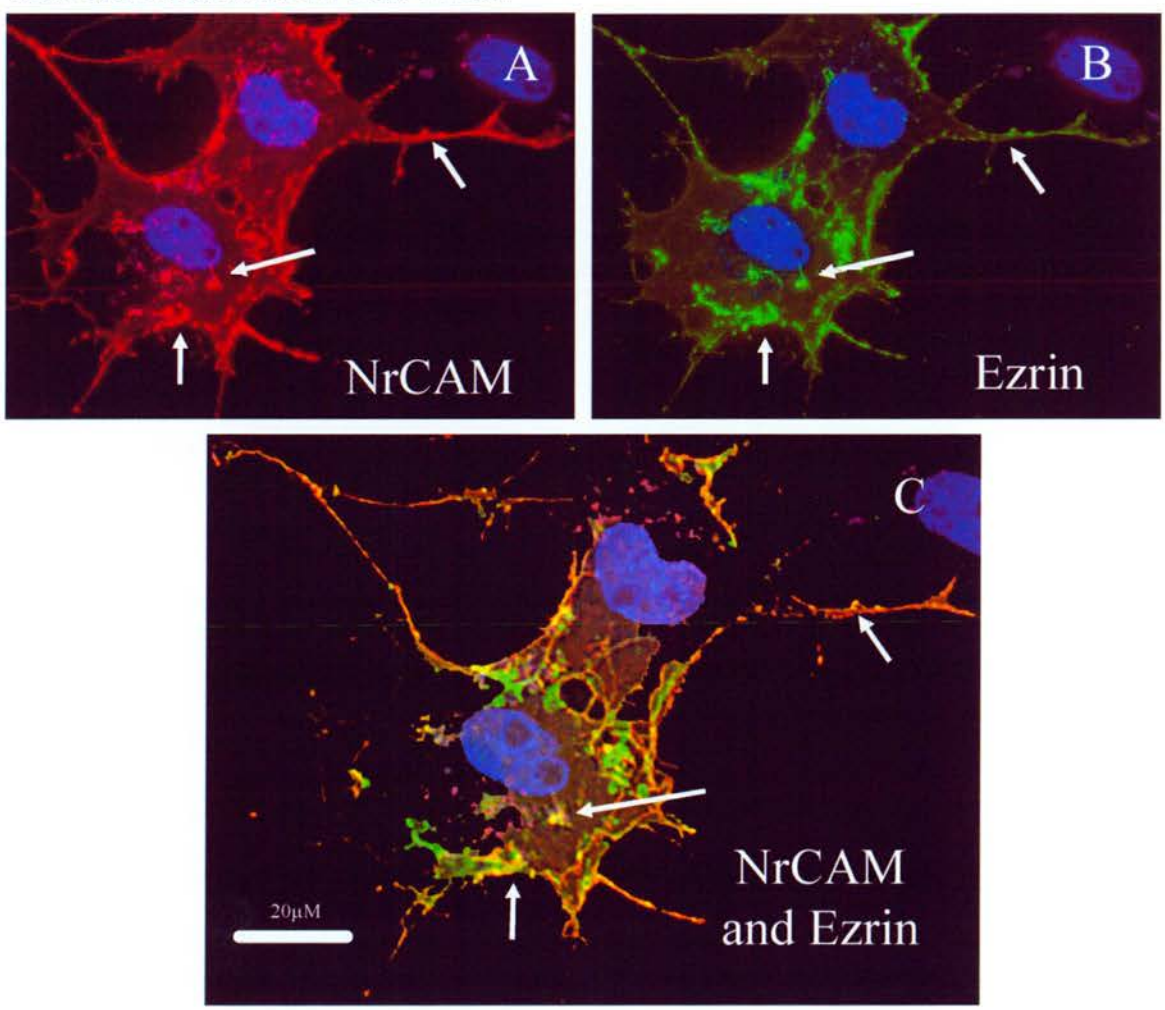

Figure 5-3. An image of transient expression of both HA-NrCAM and FLAG-ezrin in COS-7 cells. **A**) HA-NrCAM immunostaining was performed using an anti-HA rat monoclonal antibody and anti-mouse Alexa 568 conjugated antibody and is shown in red. **B**) FLAG-ezrin immunostaining was performed using a mouse monoclonal antibody to the N-terminal FLAG epitope of FLAG-ezrin and an anti-mouse FITC conjugated antibody and is shown in green. C) Co-localisation of both proteins occur at the plasma membrane (indicated by arrows). The nuclei of the cells have been stained with DAPI and are shown in blue. See methods 2.2.10, appendix 3B.

Co-localisation of HA-NrCAM and FLAG-ezrin occurred at the points within plasma membrane of COS-7 cells (Figure 5-3 (C)). To show that this co-localisation was not cell type specific and that it could occur in neurons, CGCs were also transiently transfected by Dr F. Davey of the University of St Andrews with HA-NrCAM and FLAG-ezrin. Transfected CGCs that had been growing on cover slips for 4 days (i.e. 4 DIV) were immunostained for HA-NrCAM and FLAG-ezrin using monoclonal antibodies to the N-terminal epitopes as described in section 2.2.10. Figure 5-4 shows a Z section of a CGC transfected with HA-NrCAM and FLAG-ezrin. Punctate HA-NrCAM staining was observed on the cell body, plasma membrane and along the axon (Figure 5-4(A)). FLAG-ezrin was also expressed in the cell body membrane and along the axon (Figure 5-4(B)). Co-localisation of both proteins occurred in patches evenly distributed down the axon (Figure 5-4(C)). Thus, HA-NrCAM and FLAG-ezrin can co-localise in both COS-7 cells and CGCs.

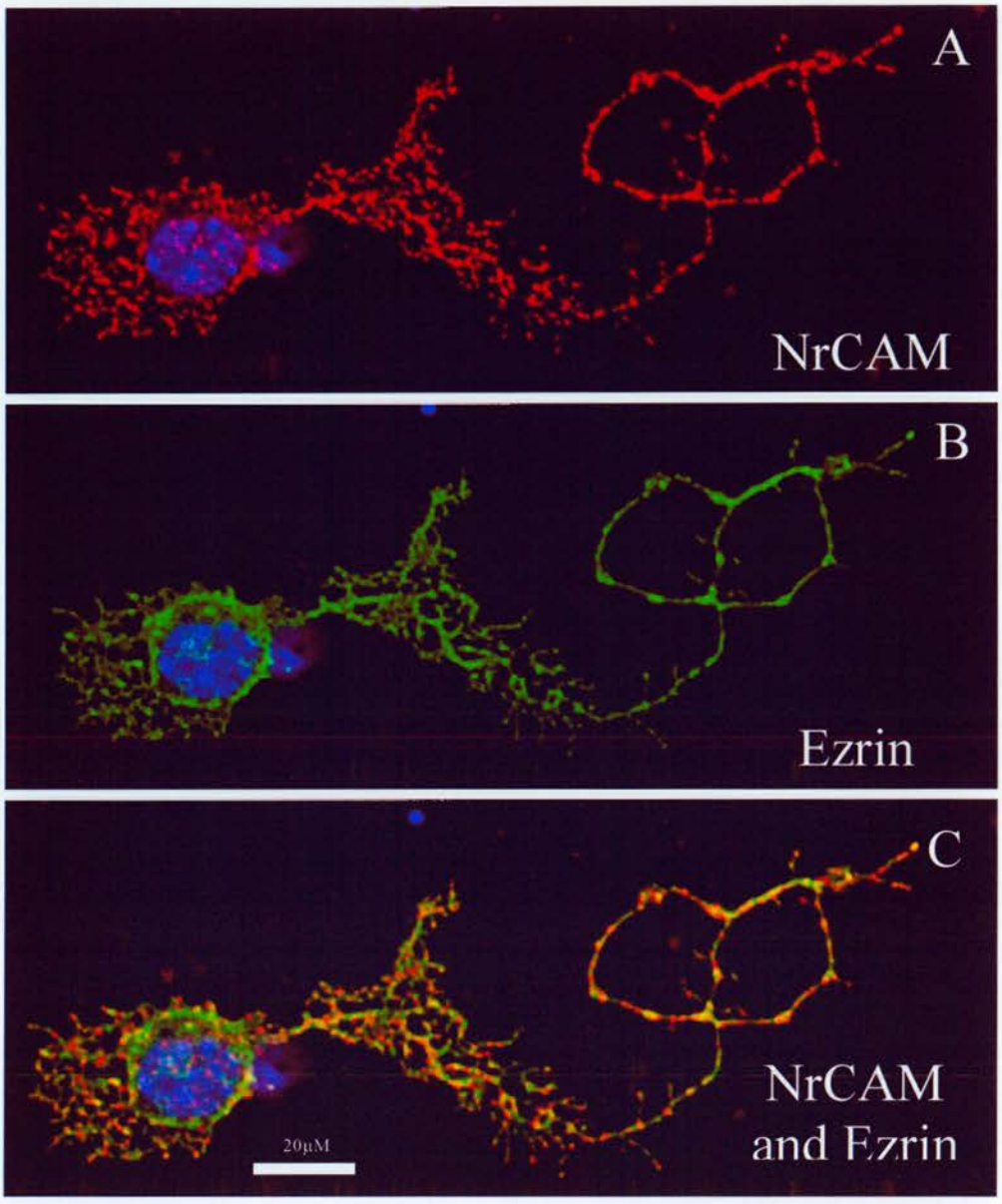

Figure 5-4. An image of transient expression of both HA-NrCAM and FLAG-ezrin in a CGC. **A**) HA-NrCAM immunostaining was performed using an anti-HA rat monoclonal antibody and anti-mouse Alexa 568 conjugated antibody and is shown in red. **B**) FLAG-ezrin immunostaining was performed using a mouse monoclonal antibody to the N-terminal FLAG epitope of FLAG-ezrin and an anti-mouse FITC conjugated antibody and is shown in green. **C**) Co-localisation of both proteins occur patches evenly distributed down the axon. The nucleus of the cell has been stained with DAPI and is shown in blue. See methods 2.2.10.

5.1.2 Does NrCAM bind to ezrin?

It was therefore decided to verify if NrCAM interacts with ezrin using the yeast two-hybrid technique. A bait plasmid that encoded for the neurofascin cytoplasmic terminus (neurofascin CT) (amino acids number 1065 to 1175) was cloned in frame into the pAS2-1 plasmid and a prey plasmid that encoded for ezrin (amino acids 1-482) that was in frame into the pACT2 plasmid by Dr F. Gunn-Moore. The interaction of neurofascin CT and ezrin was used as a positive control. The cloning of a bait plasmid NrCAM CT, that encoded for the rat NrCAM cytoplasmic terminus (amino acids 1102- to 1215), in frame into the pAS2-1 plasmid is described in Chapter 3. A prey plasmid that encoded for ankyrin$_R$ (amino acids 14-515) that had been cloned in frame into the pACT2 plasmid was a kind gift from Prof. P. Brophy of the University of Edinburgh. The interaction of NrCAM CT and ankyrin$_R$ was used as a second control. The interactions of all proteins were tested using the filter lift assay as described in section 2.4.3. As shown Figure 5-5, neurofascin bound to both ankyrin$_R$ and ezrin. However, NrCAM bound to ankyrin$_R$ but showed no binding to ezrin. This was surprising considering the immunocytochemistry results in Figure 5-1 and Figure 5-2. Therefore, using this technique NrCAM does not appear to bind to ezrin; however, it was still possible that it may be able to bind to another protein with a FERM domain. Therefore, two other members of the 4.1 superfamily were tested for their interaction with NrCAM. In particular, radixin was tested as it is implicated in growth cone motility (Paglini *et al.*, 1998; Castelo and Jay, 1999). Willin was tested as hybridisation data had shown strong expression of the protein in the cerebellum (Gunn-Moore, unpublished data), as occurs for NrCAM (Chapter 4).

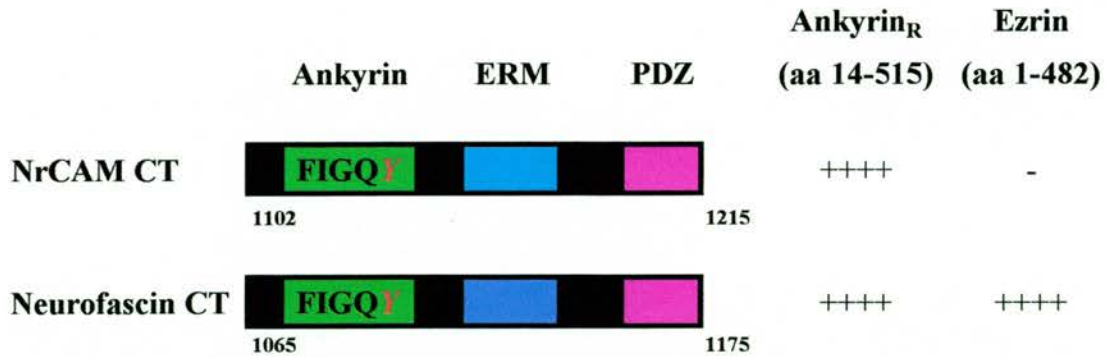

Figure 5-5. Testing of NrCAM binding to ezrin using the yeast two-hybrid assay. Neurofascin binding to ezrin was used as a positive control. NrCAM and neurofascin binding to ankyrin$_R$ was used as second positive control. The NrCAM and neurofascin proteins have been shown diagrammatically. Green boxes represent the ankyrin domain. The dark blue box is the proposed FERM binding domain in neurofascin and the paler blue box is the equivalent amino acids in NrCAM. The dark pink boxes are the PDZ domains. Binding strengths were scored using the system outlined in Table 3-1.

5.1.3 Does NrCAM bind to radixin or willin?

A prey plasmid that encoded for radixin (amino acids 166 to 1575) had been cloned in frame into the pACT2 plasmid, and was provided by Dr F. Davey. A prey plasmid that encoded for willin (amino acids 1-341), that had been cloned in frame into the pACT2 plasmid, was provided by Dr F. Gunn-Moore. The interactions of the proteins were tested using the filter lift assay as described in section 2.4.3. As shown in Figure 5-6 neurofascin showed a strong reaction with willin as had been expected.

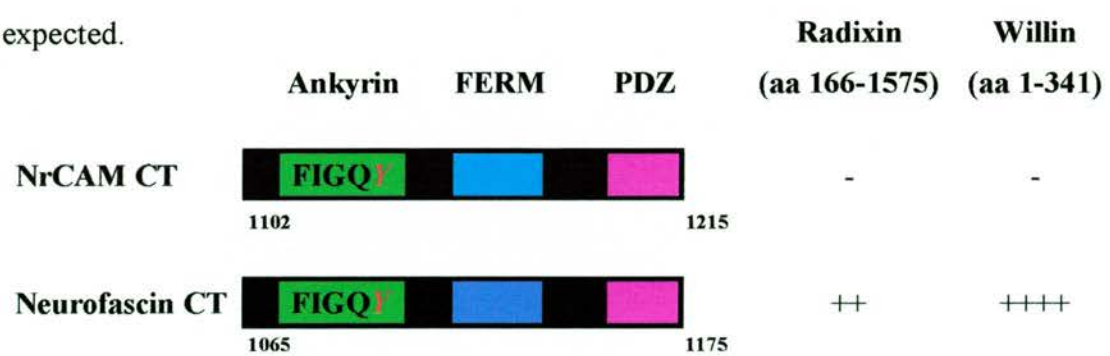

Figure 5-6. Testing of NrCAM binding to radixin and willin using the yeast two-hybrid assay. The NrCAM and neurofascin proteins have been shown diagrammatically. Green boxes represent the ankyrin domain. The dark blue box is the proposed FERM domain in neurofascin and the paler blue box is the equivalent amino acids in NrCAM. The dark pink boxes are the PDZ domains. Binding strengths were scored using the system outlined in Table 3-1.

Neurofascin's binding to radixin had not been tested previously. Therefore, it was notable that the strength of neurofascin's interaction with radixin was moderate when compared to its interaction with the other 4.1 superfamily member ezrin. Thus, neurofascin shows different binding abilities with different members of the 4.1 superfamily. NrCAM did not bind to either radixin or willin. Thus, NrCAM and neurofascin showed different binding preferences for members of the 4.1 superfamily.

When comparing the predicted FERM domain binding sequence of neurofascin to the equivalent NrCAM sequence two important amino acid substitutions were noted (Figure 5-7). From the yellow highlighted section of Figure 5-7 neurofascin has a large polar threonine that has been substituted with a small neutral alanine in NrCAM but perhaps more significantly neurofascin has a small negatively charged glutamic acid that has been substituted with a proline by NrCAM. Proline is a cyclic secondary amino acid that has conformational constraints imposed by the cyclic nature of its pyrrolidine side group (Voet and Voet, 1995). This proline substitution effectively puts a kink in the amino acid chain of NrCAM in the middle of the proposed FERM binding site. Thus, the proline amino acid substitution alone could account for the different binding abilities of NrCAM and neurofascin for the FERM family members.

Neurofascin	(aa 1148-1161)	R K D K E E T E G N E S S E
NrCAM	(aa1190-1203)	K K E K E P A E G N E S S E
Consensus		+ K - K E X X E G N E S S E

Figure 5-7. An alignment of the amino acids of the proposed FERM binding domain of neurofascin and the equivalent amino acids in NrCAM as already described by Figure 5-2. Only two amino acids are significantly different in NrCAM when compared to neurofascin and these residues have been highlighted in yellow for clarity.

As shown in Figure 5-8, the majority of the FERM binding residues in neurofascin have been conserved in L1. Importantly it does not have a proline at position 6 but an alanine. Like NrCAM, L1 had been reported as associating with FERM domain containing proteins (Mintz et al., 2003). Therefore, it was decided to investigate whether L1 could bind to FERM domain containing proteins using this motif.

L1	(aa 1231-1244)	K	K	E	K	E	A	A	G	G	N	D	S	S	G
Neurofascin	(aa 1148-1161)	R	K	D	K	E	E	T	E	G	N	E	S	S	E
NrCAM	(aa1190-1203)	K	K	E	K	E	P	A	E	G	N	E	S	S	E
Consensus		+	K	-	K	E	X	X	X	G	N	-	S	S	X

Figure 5-8. An alignment of the amino acids of the proposed FERM binding domain of neurofascin and the equivalent amino acids in NrCAM and L1. The two amino acids that are significantly different in NrCAM when compared to neurofascin (see figure 5-7) have been highlighted in yellow.

5.1.4 Does L1 bind to ezrin, radixin or willin?

The bait plasmid that encoded for the cytoplasmic terminus of L1 (L1-CT, amino acids 1143-1257; accession number NP_000416) was cloned in frame into pAS2-1. (provided by Dr F. Gunn-Moore). L1 binding to FERM domain-containing proteins was tested against the ezrin, radixin and willin prey clones using the yeast two-hybrid technique and filter lift assay. L1 binding to ankyrin$_R$ was used as a positive control. As shown in Figure 5-9, L1 bound to ankyrin as expected. However, it did not bind to ezrin or radixin and only showed a weak interaction with willin. Therefore, L1 also shows different binding ability for FERM domain containing proteins when compared to neurofascin. Furthermore, the lack of interaction between FERM domain containing proteins and NrCAM cannot be explained simply by the conformational change to the amino acid chain imposed by the proline

substitution in NrCAM. Thus, from these studies it seemed that only neurofascin could bind to members of the 4.1 superfamily.

Figure 5-9. Testing of L1 binding to ezrin, radixin and willin using the yeast two-hybrid assay. The L1 protein has been shown diagrammatically. The green box is the ankyrin binding domain. The pale blue box is the equivalent amino acids of the proposed FERM binding domain of neurofascin. The pale pink box is the equivalent amino acids of the proposed PDZ binding domain of NrCAM and neurofascin. Binding strengths were scored using the system outlined in Table 3-1.

5.1.5 Does the presence of an RSLE motif allow NrCAM to bind to ezrin, radixin or willin?

During the course of these experiments it was shown independently that ezrin could bind to a specific isoform of the L1 cytoplasmic terminus that contained a RSLE motif (Dickson et al., 2002). This RSLE motif is normally spliced out of the cytoplasmic portion of L1, but when present it is essential for both the sorting of L1 to the growth cone and for the AP2 protein mediated endocytosis of L1 (Kamiguchi et al., 1998). Like L1, the human NrCAM gene encodes the RSLE amino acids and also as with L1, these amino acids are normally spliced out (Dry et al., 2001). This suggested that NrCAM containing an RSLE motif might also bind to ezrin. To see if naturally occurring isoforms of NrCAM retain the RSLE motif a search was made of the NCBI database (http://www.ncbi.nlm.nih.gov). No sequences containing the RSLE motif had been reported for rat or murine NrCAM. However a human sequence was identified that contained the RSLE motif (accession number AAF22282). Interestingly all chick NrCAM sequences contained the RSLE amino acids. Therefore, it was decided to: 1) Test a L1 clone with the RSLE sequence to

independently reconfirm the Dickinson et al results; 2) Test an NrCAM clone with a naturally occurring RSLE sequence to establish if NrCAM could bind to ezrin via this motif.

The L1 clone with the RSLE motif for the Dickinson et al paper was a kind gift from Dr. Salton, the Mount Sciani School of Medicine, New York. This construct was sub-cloned in frame into the pAS2-1 vector as described by Figure 5-10.

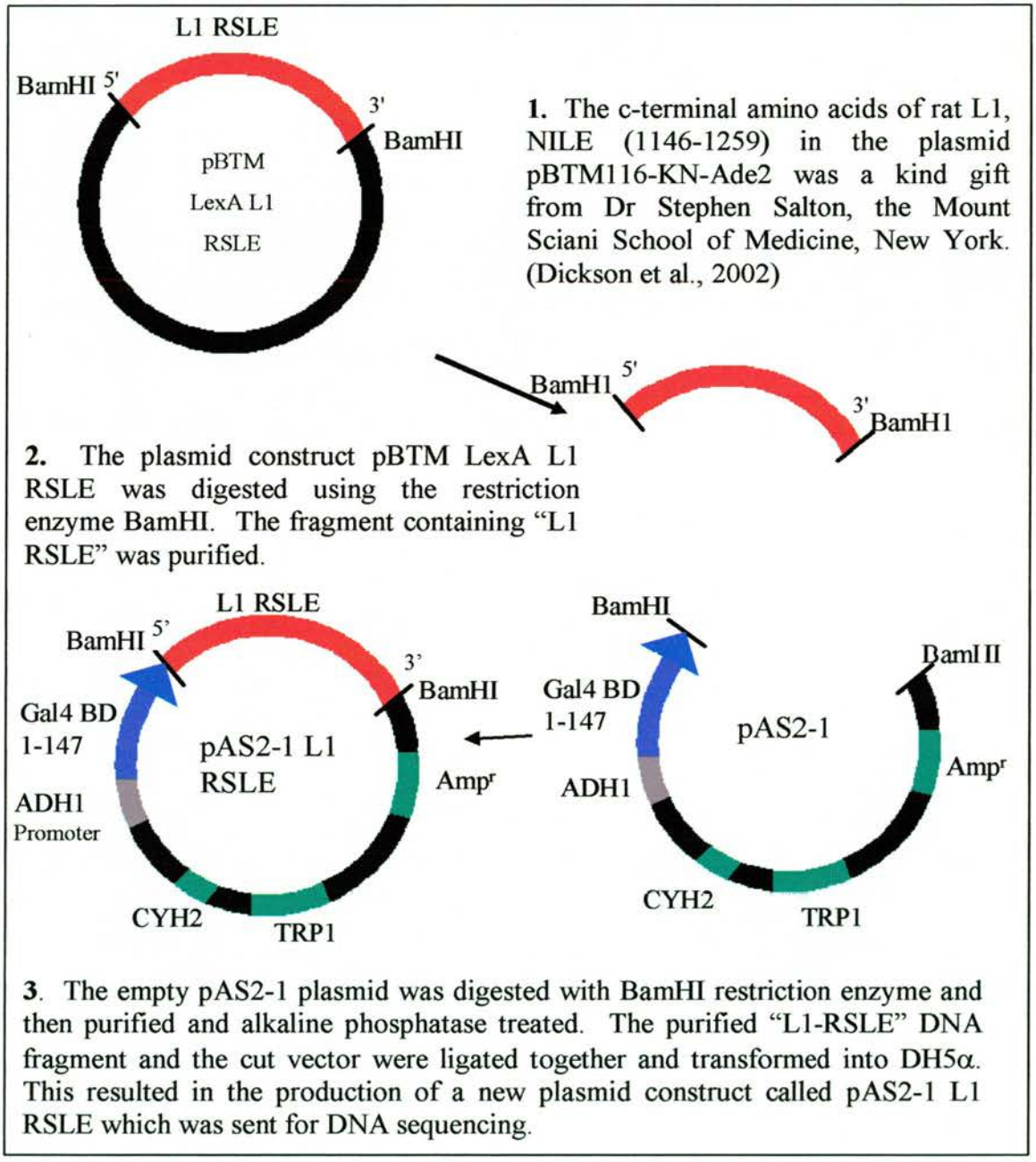

Figure 5-10. Cloning strategy for the production of the plasmid pAS2-1 L1 RSLE. Details of material and methods are described in chapter 2 and accompanying text.

No human NrCAM clones containing the RSLE sequence were available, however the amino acid sequence of the cytoplasmic portion of NrCAM has been 100% conserved from chick to human (Davis and Bennett, 1994; Lane et al., 1996). Therefore, a chick EST clone was purchased from Ark-Genomics, the Roslin Institute and cloned in frame into pAS2-1 as described by Figure 5-11. This clone codes for amino acids 1166 to 1260 of accession number P35331, which is the entire cytoplasmic sequence of the chick NrCAM with the exception of the C-terminal 24 amino acids.

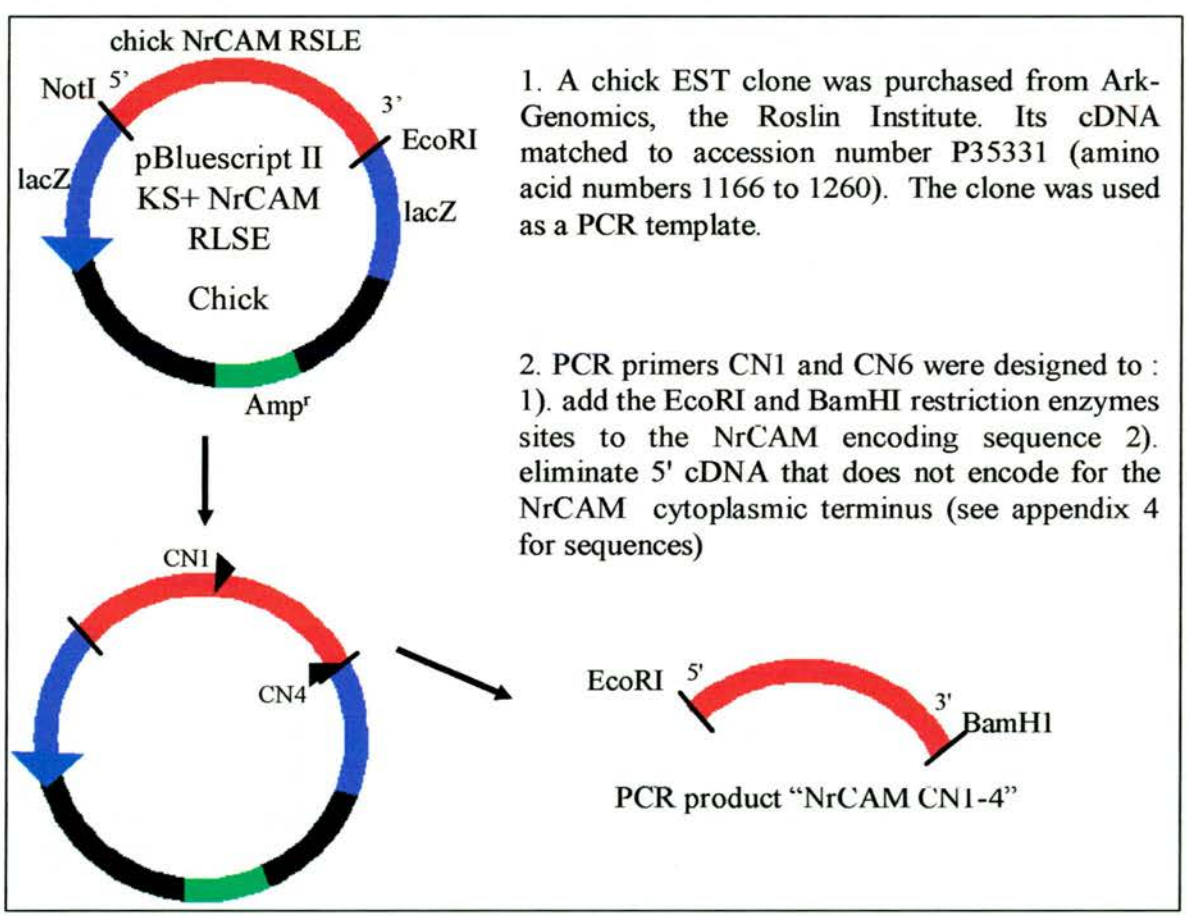

Figure 5-11. Continued on next page.

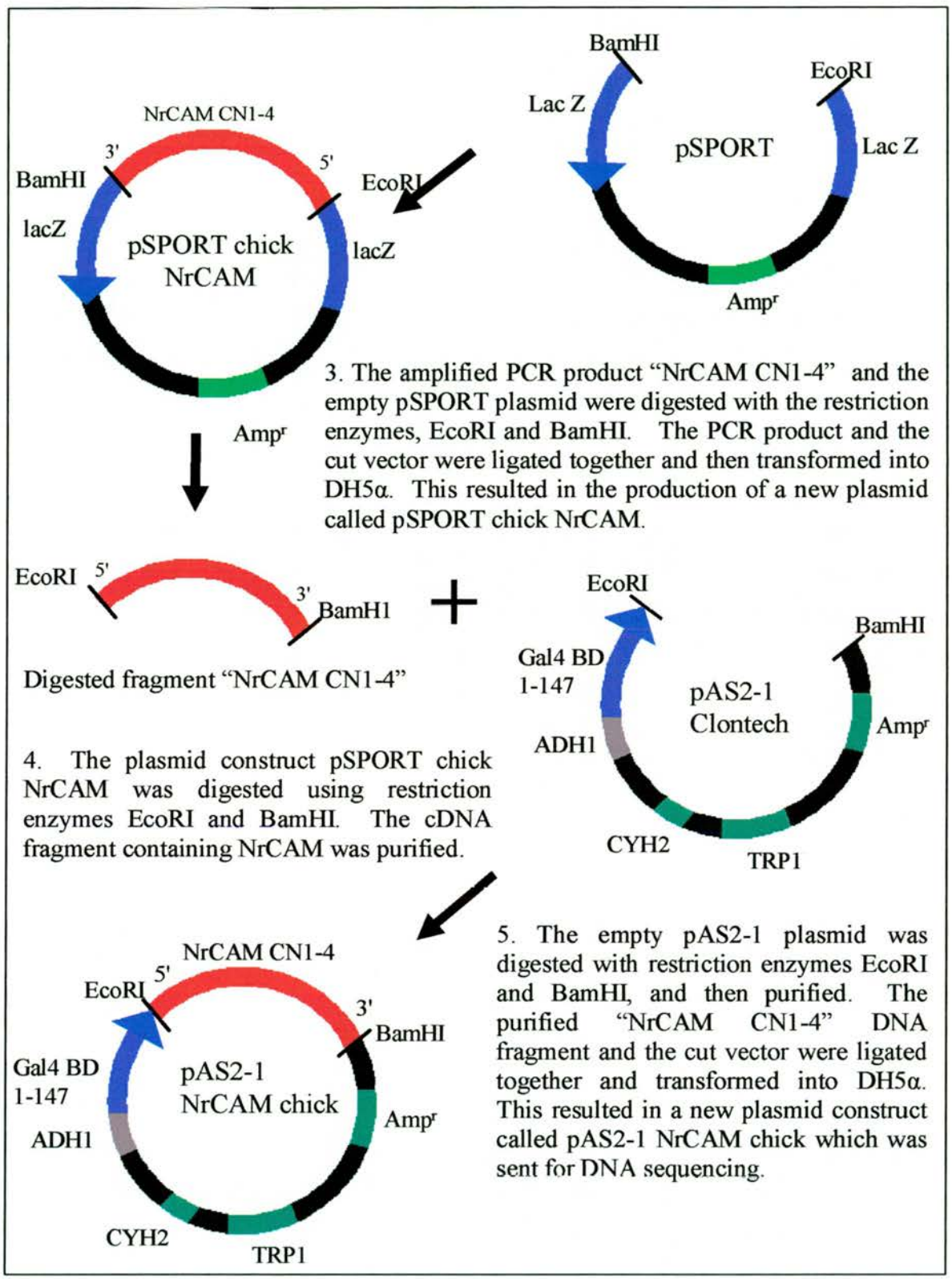

Figure 5-11. The cloning strategy for the production of the plasmid pAS2-1 NrCAM chick. Details of material and methods are described in chapter 2 and accompanying text.

As L1 RSLE and Chick NrCAM were both new baits they first needed to be tested to ensure that they:

1. Did not auto-activate.
2. Behaved normally when binding to a known binding partner such as ankyrin.

Thus, both clones were tested against empty pACT2 vector and ankyrin$_R$. The interactions were tested using the filter lift assay as described in section 2.4.3. As shown in Figure 5-12, L1 showed weak auto-activation but interacted strongly with ankyrin. Therefore, this clone was suitable for testing proteins that strongly interact with L1 RSLE only. The Chick NrCAM protein did not auto-activate and bound to ankyrin$_R$ strongly.

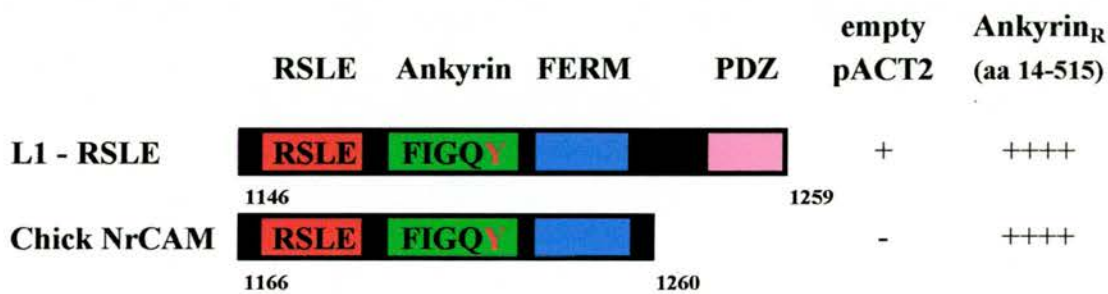

Figure 5-12. Testing of L1-RSLE and chick NrCAM for auto-activation and normal binding to full-length ankyrin$_R$. The L1 and NrCAM proteins have been shown diagrammatically. The red box indicates the presence of an alternatively spliced RSLE motif. Green boxes represent the ankyrin domain. The blue box is the equivalent amino acids of the FERM domain in neurofascin present in NrCAM and L1. The pink box is the equivalent amino acids of the PDZ domain of NrCAM present in L1. The chick NrCAM construct did not encode a PDZ domain. Binding strengths were scored using the system outlined in Table 3-1.

L1 RSLE and Chick NrCAM were then tested against the FERM domain containing prey clones ezrin, radixin and willin. The interactions were tested using the filter lift assay as described in section 2.4.3. As shown in Figure 5-13, L1-RSLE interacted strongly with ezrin, moderately with radixin but interactions with willin

could not be distinguished over auto-activation levels. Chick NrCAM did not appear to interact with any of the 4.1 superfamily proteins.

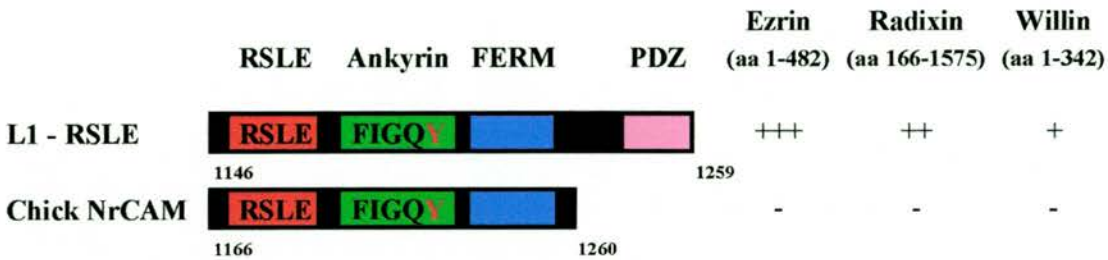

Figure 5-13. Testing of L1-RSLE and chick NrCAM binding to ezrin, radixin and willin. The L1 and NrCAM proteins have been shown diagrammatically. Green boxes represent the ankyrin domain. The red box indicates the presence of an alternatively spliced RSLE motif. The blue box is the equivalent amino acids of the FERM domain in neurofascin present in NrCAM and L1. The pink box is the equivalent amino acids of the PDZ domain of NrCAM present in NrCAM. The chick NrCAM construct did not encode a PDZ domain. Binding strengths were scored using the system outlined in Table 3-1.

5.1.6 Does NrCAM to bind to EBP50?

Chapter 3 and 4 demonstrated the importance of the PDZ binding domain of NrCAM. Ezrin binding protein 50 (EBP-50) has an ezrin-binding site in its first 28 residues and is recruited to regions in the cell where ezrin is activated and associated with F-actin through its C-terminal F-actin binding site. It has two PDZ domains and it may be involved in tethering membrane receptors to the cytoskeleton (Bretscher et al., 2000) (see figure 5-13). Thus, it was decided to see if EBP50 could bind to NrCAM via its PDZ binding domain.

A FLAG-tagged ezrin construct that coded for EBP50 N-terminally tagged by the FLAG epitope (FLAG-EBP50) was generated by Dr. F. Gunn-Moore (aa 1-716). This construct was co-transfected with HA-NrCAM into COS-7 cells growing on glass cover-slips as described in section 2.2.5 and immunostained for HA-NrCAM

and FLAG-EBP50 using monoclonal antibodies to the N-terminal epitopes as described in section 2.2.10. Figure 5-14 shows a Z-section of a single COS-7 cell. HA-NrCAM staining was seen predominantly in the membrane and membrane protrusions of COS-7 cells (Figure 5-14 (A)). FLAG-EBP50 was also seen at the plasma membrane as wells as in cytoplasmic regions of the cell (Figure 5-14 (B)). Co-localisation of both proteins occurred in the membrane and membrane protrusions of the COS-7 cells (Figure 5-14 (C)). Thus, transiently expressed HA-NrCAM and FLAG-EBP50 did co-localise at the plasma membrane of COS-7 cells.

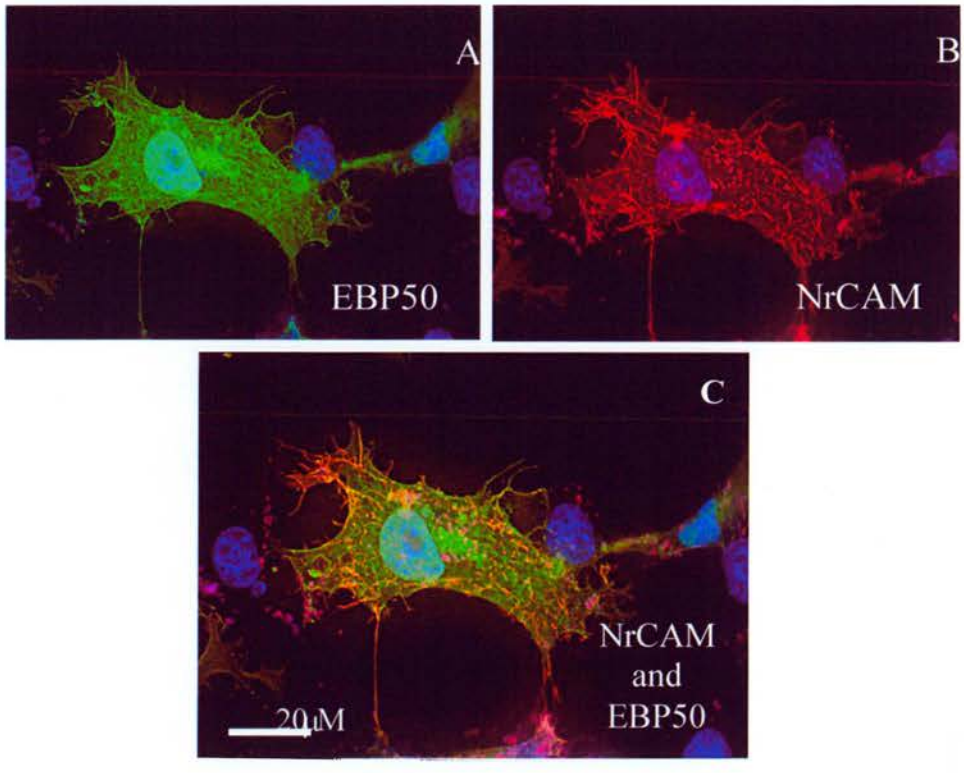

Figure 5-14. An image of transient expression of both HA-NrCAM and FLAG-EBP50 in a COS-7 cell. **A**) FLAG-ezrin immunostaining was performed using a mouse monoclonal antibody to the N-terminal FLAG epitope of FLAG-EBP50 and an anti-mouse FITC conjugated antibody and is shown in green. **B**) HA-NrCAM immunostaining was performed using an anti-HA rat monoclonal antibody and anti mouse Alexa 568 conjugated antibody and is shown in red. **C**). Co-localisation of both proteins occur at localised areas of the plasma membrane. The nucleus of the cell has been stained with DAPI and is shown in blue. See methods 2.2.10, appendix 3B.

As the EBP50 construct could co-localise with NrCAM it was decided to test whether EBP50 was binding directly to NrCAM. A prey plasmid that encoded for EPB50 (amino acids 1-716), which had been cloned in frame into the pACT2 plasmid, was provided by Dr F. Gunn-Moore. The EBP50 prey plasmid was tested against the NrCAM CT bait, the neurofascin CT bait, the L1 CT bait and the L1-RSLE bait using the filter lift assay with the result that EBP50 did not bind to NrCAM or L1 but did bind to neurofascin (Figure 5-15).

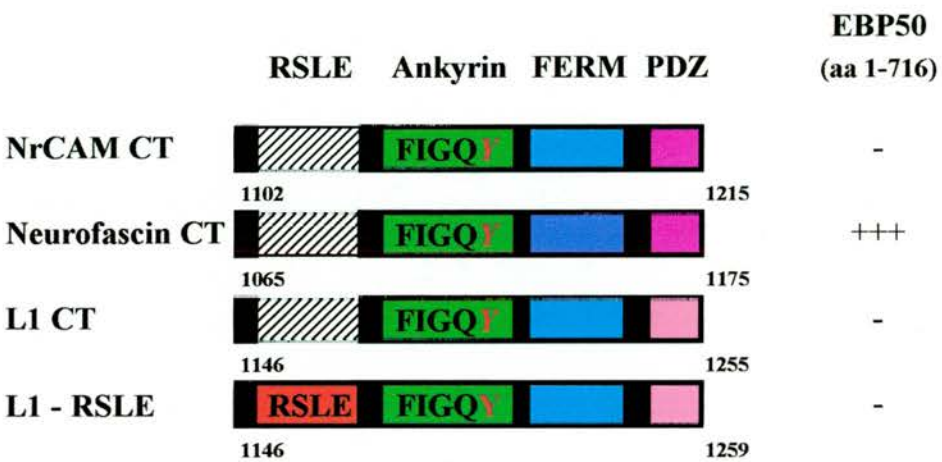

Figure 5-15. Testing of the binding of various L1-CAM constructs to EBP50. The L1-CAM proteins have been shown diagrammatically. The red box indicates the presence of an alternatively spliced RSLE motif. Green boxes represent the ankyrin domain. The dark blue box is the proposed FERM binding domain of neurofascin. The pale blue box is the equivalent amino acids of the FERM domain in neurofascin present in NrCAM and L1. The dark pink boxes are the PDZ binding domains of NrCAM and neurofascin. The pale pink box is the equivalent amino acids of the PDZ domain of NrCAM present in L1. Binding strengths were scored using the system outlined in Table 3-1.

5.1.7 Does NrCAM bind to the cytoplasmic terminus of any other L1-CAMs?

It is also possible that NrCAM binds indirectly to the FERM family members by first binding to neurofascin or L1 RSLE, which then recruits the required binding partner. It is already known that the ectodomains of NrCAM can bind to the IgG

domains of neurofascin (Volkmer et al., 1996). However, it was not known whether NrCAM binds to the cytoplasmic domains of either L1 or neurofascin. Therefore the full-length cytoplasmic terminus of rat NrCAM (without the RSLE sequence) was cloned in to the pACT2 vector as described by Figure 5-16 and was called pACT2 NrCAM 33-34.

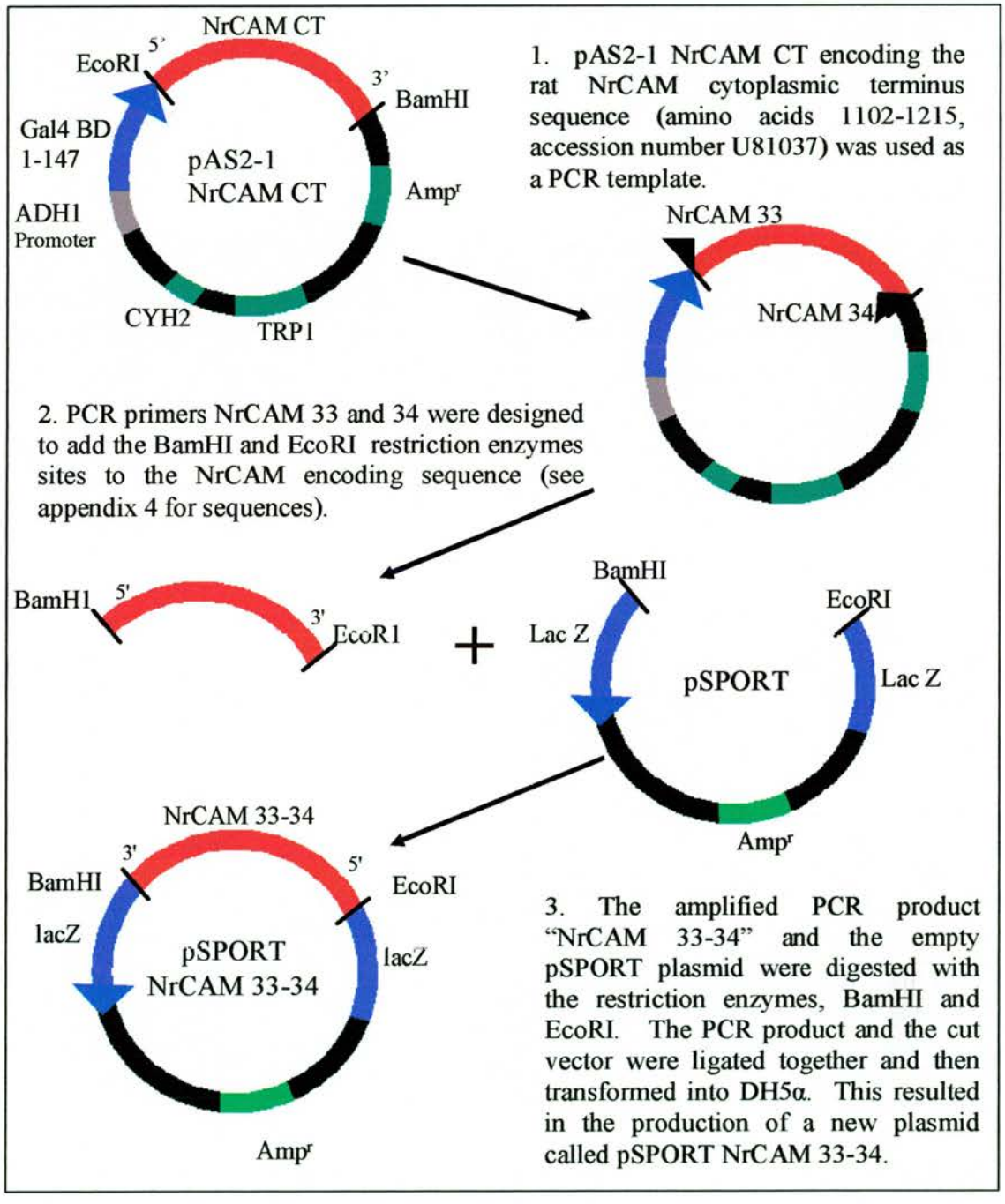

Figure 5-16. Continued on next page.

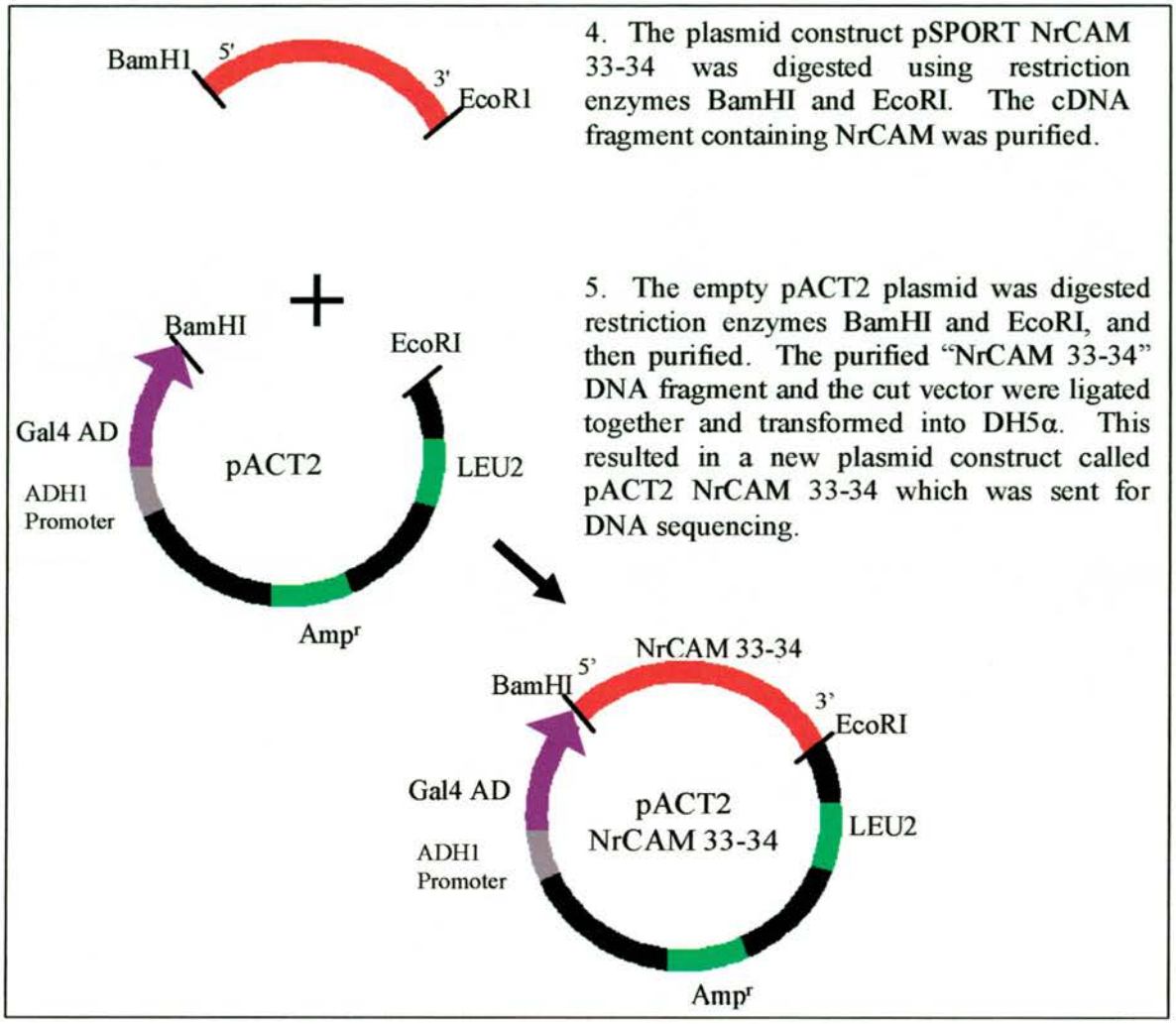

Figure 5-16. The cloning strategy for the production of the plasmid pACT2 NrCAM 33-34. Details of material and methods are described in chapter 2 and accompanying text.

This new prey plasmid was tested against the NrCAM CT bait, NrCAM chick bait, the L1 CT bait, L1-RSLE bait and neurofascin CT bait using the filter lift assay. As shown in Figure 5-17 the cytoplasmic terminus of NrCAM did not appear to bind to itself or to L1 but did show moderate binding to neurofascin.

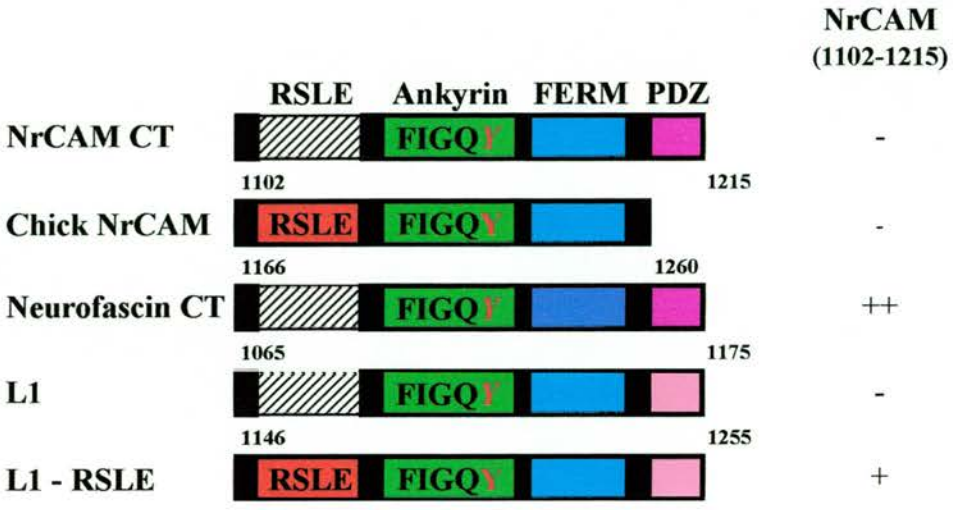

Figure 5-17. Testing of the binding of various L1-CAM constructs to NrCAM's cytoplasmic terminus. The L1-CAM constructs have been shown diagrammatically. The red box indicates the presence of an alternatively spliced RSLE motif. The green boxes represent the ankyrin domain. The dark blue box is the proposed FERM binding domain of neurofascin. The pale blue box is the equivalent amino acids of the FERM domain in neurofascin present in NrCAM and L1. The dark pink boxes are the PDZ binding domains of NrCAM and neurofascin. The pale pink box is the equivalent amino acids of the PDZ domain of NrCAM present in L1. Binding strengths were scored using the system outlined in Table 3-1.

5.2 Discussion of the results.

From section 5.1.1 transiently expressed NrCAM and ezrin co-localise in COS-7 cells and CGCs. This finding agrees with studies that have shown the co-localisation of NrCAM and ezrin in other cell lines (Conacci-Sorrell et al., 2002). It therefore seemed likely that the two proteins would interact. However the yeast two-hybrid results performed here suggest that NrCAM does not interact with ezrin, radixin or willin directly, nor can NrCAM interact indirectly with members of the 4.1 superfamily via an adaptor protein such as EBP50 (5.1.6).

These results are in contrast to studies performed on neurofascin and L1, both of which have been shown to interact directly with the FERM domain containing proteins. For example neurofascin interacts with ezrin and willin via the last 28 amino acids which contains a 14 amino acid motif that has strong similarity to FERM domain binding sequences (Brophy, 2001). L1 has been shown to bind to ezrin via amino acids N-terminal to its ankyrin binding motif, and also only when a RSLE motif is present (Dickson et al., 2002). Both the neurofascin and the L1 results were confirmed here. Additionally in the current studies it was shown that neurofascin and L1 both bind to radixin, though this interaction appears to be weaker than the L1-ezrin and neurofascin-ezrin interactions. Interestingly neurofascin binds strongly to willin but the other L1-CAMS do not, whilst neurofascin also binds to EBP50 while the other L1-CAMs do not. Thus, it appears that all L1-CAM family members show different abilities to interact with members of the 4.1 superfamily.

Chapter 6. Investigations into the tyrosine phosphorylation of the cytoplasmic terminus of NrCAM and its effect on binding to ankyrin.

6.0 Tyrosine phosphorylation inhibits ankyrin binding to L1-CAMs.

Members of the L1-CAM family have four highly conserved tyrosine residues on their cytoplasmic termini. Studies involving neurofascin show that all four tyrosine residues of the neurofascin cytoplasmic terminus are subject to phosphorylation and dephosphorylation by protein tyrosine kinases and protein phosphatases (Garver *et al.*, 1997). However, the principle site of tyrosine phosphorylation is the tyrosine of the highly conserved amino acid sequence phenylalanine–isoleucine-glycine-glutamine-tyrosine (FIGQY) that makes up part of the ankyrin binding site (Garver *et al.*, 1997). Importantly the phosphorylation of the tyrosine residue of the FIGQY sequence has been shown to prevent ankyrin binding both to L1 and to neurofascin (Garver *et al.*, 1997; Tuvia *et al.*, 1997; Jenkins *et al.*, 2001).

NrCAM's interaction with ankyrin was first described by (Davis and Bennett, 1994) and until recently ankyrin was NrCAM's only known cytoplasmic binding partner (Davey *et al.*, 2005). NrCAM has all of the four tyrosine residues that are subject to tyrosine phosphorylation in neurofascin (see Figure 6-1, red font) and the tyrosine phosphorylation of NrCAM is developmentally regulated (Garver *et al.*, 1997), implying a developmental role for tyrosine phosphorylation of NrCAM in brain development. However, it had not been reported whether the phosphorylation of the tyrosine of the FIGQY sequence in NrCAM affects the receptor's ability to bind to ankyrin.

Figure 6-1. The amino acid sequence of the cytoplasmic terminus of NrCAM. Highlighted in green are the amino acids that make up the ankyrin binding site. In red font are the tyrosine residues that are equivalent to the tyrosine residues which are phosphorylated in neurofascin (Garver *et al.*, 1997). The amino acids RSLE, surrounded by a broken line, are present in some isoforms of NrCAM. Amino acids highlighted in grey were selected as a suitable target for a new cytoplasmic antibody (see results section 6.3 for details).

6.1 Immunoprecipitations of HA-NrCAM from B104 cells.

The immunoprecipitation of HA-neurofascin from B104 neuroblastoma cells has been successfully used to study the upstream pathways involved in the tyrosine phosphorylation of neurofascin (Garver *et al.*, 1997). Therefore, it was decided to test whether this assay could also be used to study the NrCAM phosphorylation pathways. Immunoprecipitation of HA-NrCAM with GIPC (as discussed in Chapter 4) was attempted more or less simultaneously and Chapter 4 describes many of the initial experiments. Briefly immunoprecipitation of HA-NrCAM from B104 cells stably expressing HA-NrCAM was not possible using protein A beads but was achieved using anti-rat IgG beads coupled to rat monoclonal anti-HA-antibodies (see Figure 4-10 and Figure 4-11 in chapter 4).

6.1.1 Immunoprecipitation of HA-NrCAM from B104 cells treated with a protein tyrosine phosphatase inhibitor.

Tyrosine phosphorylation of neurofascin in B104 cells has been achieved using the protein tyrosine phosphatase inhibitor sodium orthovanadate (Garver *et al.*, 1997). It was decided to see if tyrosine phosphorylated NrCAM could also

be induced by sodium orthovanadate. The activation of sodium orthovanadate and the treatment of the cells with sodium orthovanadate have been described previously 2.3.3 and 2.3.4. Briefly, B104 cells stably expressing HA-NrCAM were serum starved for two to six hours. Activated sodium orthovanadate was added to half of the dishes of cells to be tested. The remaining dishes of cells had an equal volume of sterile water added (vehicle) and were negative controls. After a five-minute incubation at 37 °C each dish was extracted in ice-cold radio-immunoprecipitation assay (RIPA) buffer in the presence of protease inhibitors and phosphatase inhibitors. The immunoprecipitation was carried out at 4°C as described in 2.3.13. The proteins were transferred onto nitrocellulose by Western blot and probed with an anti-phosphotyrosine antibody (Upstate) as described by 2.3.10. The nitrocellulose membrane was stripped of primary and secondary antibodies as described by 2.3.18 and reprobed using an anti-HA or an anti-NrCAM antibody.

The results are shown in Figure 6-2. Crude protein samples of sodium orthovanadate treated cells showed numerous bands of tyrosine-phosphorylated proteins and these protein bands ranged in size from 39 kDa to over 191 kDa (see Figure 6-2 lane 2). There were two bands of tyrosine-phosphorylated proteins in vehicle treated samples and these protein bands were approximately 60 kDa and 100 kDa (see Figure 6-2, lane 1). NrCAM was successfully immunoprecipitated as a band of approximately 100 kDa as shown by NrCAM immunostaining of a Western blot (see Figure 6-2 lane 7-8). However, NrCAM immunostaining also showed a second band of approximately 55 kDa in size in (Figure 6-2, lanes 5-8). It was unclear whether this band represented the unspecific binding of the NrCAM antibody to an unknown protein or the binding of the antibody to

cleaved NrCAM. There were no proteins immunoprecipitated in vehicle treated cells (Figure 6-2, lane 3); however, there was a 100 kDa protein immunoprecipitated from the sodium orthovanadate treated cell extract (Figure 6-2, lane 4). The size of this band corresponded to NrCAM. Thus, it would appear that the 100 kDa band represents immunoprecipitated tyrosine phosphorylated NrCAM.

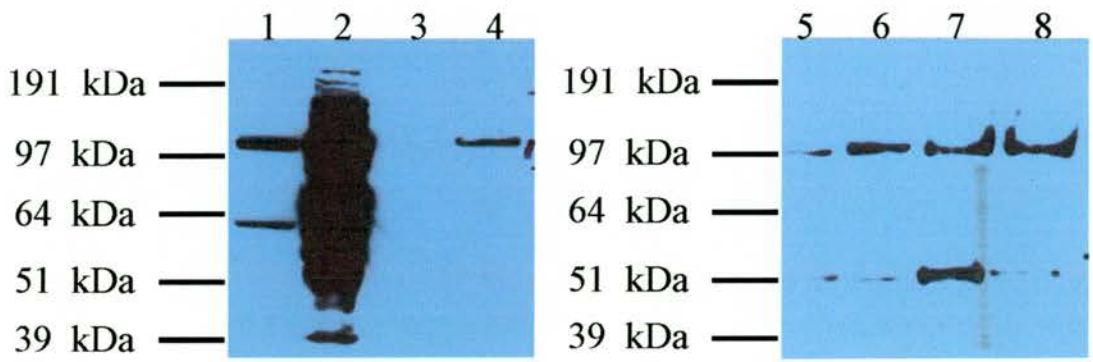

Figure 6-2. Immunoprecipitation of HA-NrCAM from B104 cells treated with a protein tyrosine phosphatase inhibitor. Western blots of 75 μg of crude cell extract of B104 cells stably expressing HA-NrCAM (1-2,5-6) and of proteins immunoprecipitated using anti-HA antibodies (3-4,7-8). Lanes 1 to 4 were probed using a monoclonal anti-phosphotyrosine antibody. Lanes 5 to 8 are the same blot as lanes 1 to 4, stripped of anti-phosphotyrosine antibody and reprobed for NrCAM using a rabbit polyclonal antibody to the extracellular IgG domains of NrCAM. Lane 1/5 is a 75 μg protein sample of vehicle treated, HA-NrCAM expressing B104 cells. Lane 2/6 is a 75 μg protein sample of sodium orthovanadate treated HA-NrCAM expressing B104 cells. Lane 3/7 is the immunoprecipitated proteins from the vehicle treated HA-NrCAM expressing B104 cells. Lane 4/8 is the immunoprecipitated proteins from sodium orthovanadate treated, HA-NrCAM expressing B104 cells. See section 2-3 for methods and appendix 3.

6.2 Furin cleavage of NrCAM.

The 75 μg crude protein sample in Figure 6-2 (lanes 5 and 6) showed a 100 kDa NrCAM band. However, when a 120 μg sample of the HA-NrCAM expressing B104 crude cell extract was separated by SDS-PAGE electrophoresis and probed by Western blot using an antibody to the extracellular region of HA-NrCAM, then two bands of HA-NrCAM were observed, (see Figure 6-3 (A)). One was a highly expressed band of approximately 100 kDa and a second band between 111 kDa and 210 kDa. These two bands have been previously reported (Kayyem *et al.*, 1992; Grumet, 1997). The two NrCAM bands could be the result of differential glycosylation of NrCAM or two different isoforms of NrCAM but are generally believed to be the result of furin protease cleavage in the extracellular third fibronectin type III-like (FNIII-like) domain of NrCAM (Kayyem *et al.*, 1992).

Furin cleavage in the extracellular third FNIII-like domain is postulated to result in a situation demonstrated diagrammatically by Figure 6-3 (B and C). If NrCAM is uncleaved as described by Figure 6-3 (B1) then it would appear as one single high molecular weight band on an SDS PAGE gel (Figure 6-3 (C, lane 1)). If NrCAM is cleaved and self-associating as described by Figure 6-3 (B2) it would appear as two lower molecular weight bands on an SDS-PAGE gel (Figure 6-3 (C, lane 2)). The majority of NrCAM is believed to be cleaved by furin and the minority of NrCAM is believed to remain uncleaved and therefore there should be three protein bands when samples of NrCAM are run on SDS-PAGE gels as shown in Figure 6-3 (C, lane 3) (Kayyem *et al.*, 1992). Antibodies raised to targets in the cytoplasmic terminus of NrCAM theoretically

would give rise to a Western blot as described by Figure 6-3 (C, lane 4). Unfortunately, there have been no reports of a successful antibody raised to the cytoplasmic terminus of NrCAM to test this hypothesis. Antibodies raised to targets in the extracellular domain of NrCAM that are N-terminal to the third FNIII-like repeat would therefore give a staining pattern as demonstrated by Figure 6-3 (C, lane 5).

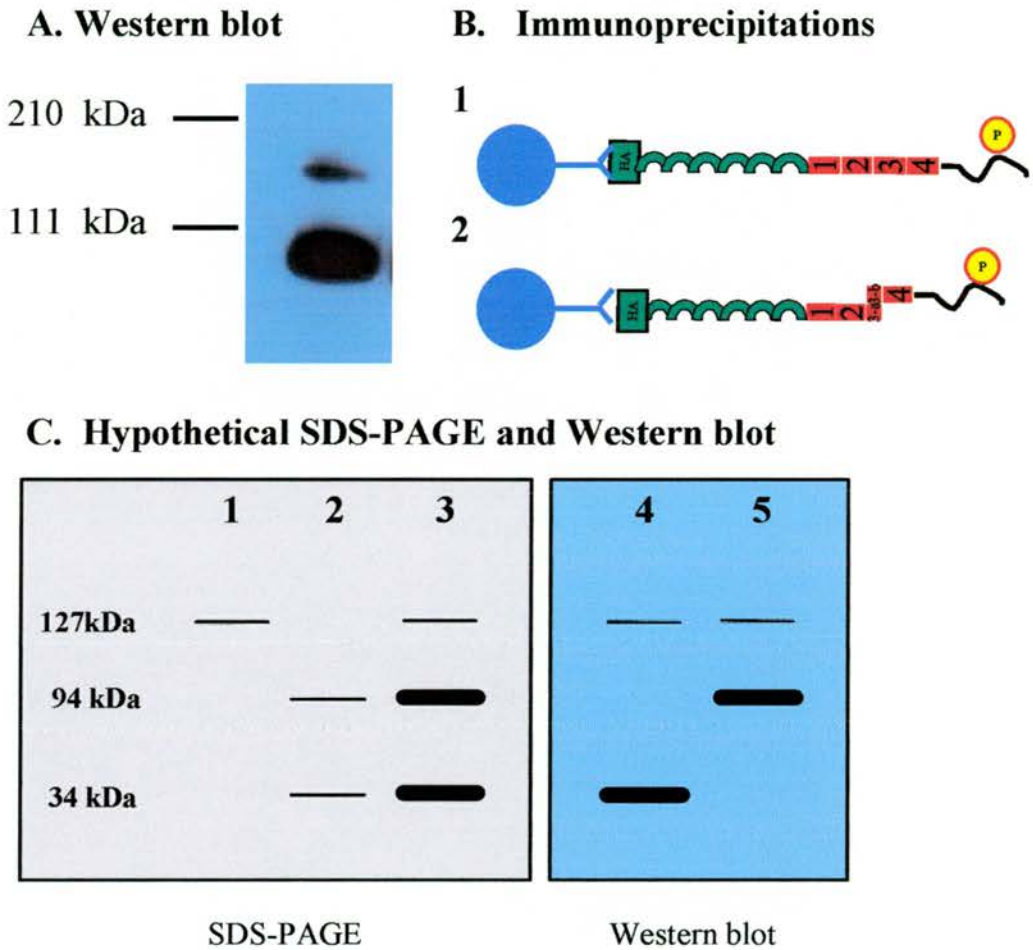

Figure 6-3. A diagrammatical representation of the current theory regarding NrCAM protease cleavage. **A)** A Western blot of a 120 µg sample of HA-NrCAM expressing B104 cells. **B)** Diagrammatical representations of immunoprecipitations of HA-NrCAM that has been 1) uncleaved and 2) furin cleaved and self associating at the third FNIII-like domain. **(C)** A hypothetical SDS-PAGE gel and Western blot. Protein sizes are before post-translational modifications. Lane 1 are the proteins which would be immunoprecipitated by B1, Lane 2 are the proteins which would be immunoprecipitated by B2. Lane 3 represents the approximate proportion of proteins expected from immunoprecipitations in B1 and B2. Lane 4 represents the bands from lane 3 that would be selected by an antibody to the cytoplasmic terminus of NrCAM. Lane 5 are the bands in lane 3 that would be selected by an antibody to the extracellular domain of NrCAM and N-terminal to the third FNIII-like of NrCAM.

The results in Figure 6-2 showed that the extracellular antibody recognised bands of approximately 100 kDa and approximately 55 kDa of which only the 100 kDa band was tyrosine phosphorylated NrCAM, therefore suggesting that the cytoplasmic terminus of NrCAM was not present. To try to overcome this problem it was decided to raise an antibody to the cytoplasmic terminus of NrCAM to both reconfirm this observation and to produce an antibody that could immunoprecipitate out the C-terminus of NrCAM that could then be probed for tyrosine phosphorylation.

6.3 Design and testing of a peptide antibody to the cytoplasmic terminus of NrCAM.

An antibody was designed to the cytoplasmic terminus of NrCAM. The cytoplasmic terminus of NrCAM was examined for a ten amino acid sequence that was both hydrophilic and contained a low sequence homology to other members of the L1-CAM family. Hydrophilicity was tested by manually checking the amino acid sequence of NrCAM's cytoplasmic terminus (Figure 6-1). The homology of different peptide sequences to other known protein sequences was checked using the BLAST search facility at NCBI protein database (www.ncbi.nlm.nih.gov/). The sequence KKGSRTPSDR (given in single letter amino acid code) was chosen as the best sequence at filling both criteria. The N-acetylated KKGSRTPSDR peptide was manufactured and coupled to Keyhole limpet hemocyanin and then immunised into two rabbits by ResGen™, Invitrogen. Serum from bleeds at 4 weeks, 8 weeks, 10 weeks and the final bleeds were obtained from each rabbit. The different serums were tested by Western blot analysis against either 0.5 μg of Glutathione S-transferase (GST) or

0.5 μg of GST coupled to the cytoplasmic terminus of NrCAM (GST-NrCAM). Week 8 was selected for further analyses as this serum gave the strongest reaction with GST-NrCAM at dilutions from 1/1000 to 1/2000. The Week 8 serum from both rabbits was affinity purified as described by 2.3.17. The affinity-purified antibodies were both tested against Western blots of GST and GST-NrCAM. Dilutions from 1/50 to 1/100 of affinity-purified antibodies were sufficient to select and bind GST-NrCAM but not to bind to GST alone.

Most cell lines do not express NrCAM. The antibodies were tested against proteins samples from untransfected cell lines and cell lines that were transfected with various plasmids encoding full length rat NrCAM, HA-NrCAM and a HA-NrCAM construct missing the C-terminal 11 amino acids of the cytoplasmic terminus of NrCAM (HA-NrCAM Δ11CT) (a kind gift from Dr. Catherine Faivre Sarrailh, Marseille, France). Some typical results are described by Figure 6-4.

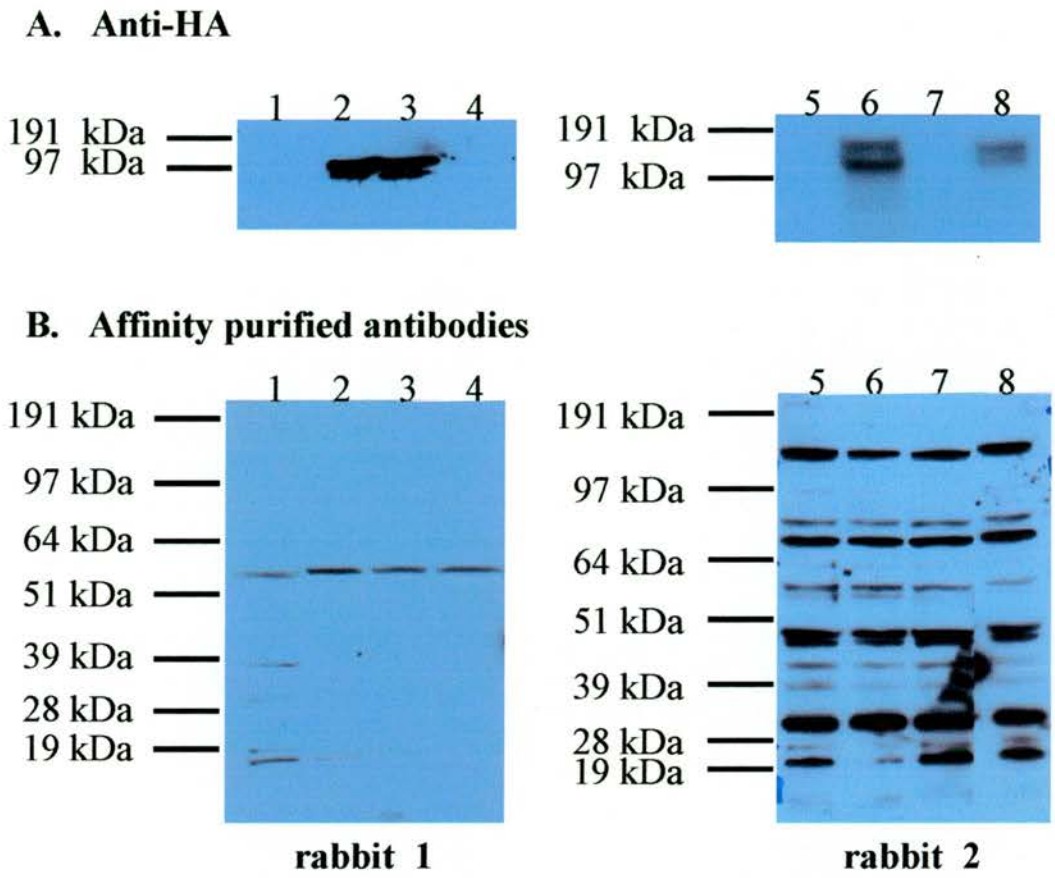

Figure 6-4. Western blots showing the testing of antibodies raised to the cytoplasmic terminus of NrCAM. **A)** Blots were probed with an anti-HA antibody. **B)** The same protein samples as the blots in (A) were probed with a 1/50 dilution of affinity purified antibody from rabbit 1 and rabbit 2 as indicated. Lanes 1 to 4 are 75 μg protein samples of transiently transfected CHO cells. Lane 1 was untransfected, lane 2 was transfected with HA-NrCAM Δ11CT, lane 3 was transfected with HA-NrCAM, lane 4 was transfected with full-length NrCAM. Lanes 5 to 8 are 75μg protein samples of transiently transfected CHO cells. Lane 5 was untransfected, lane 6 was transfected with HA-NrCAM, lane 7 was transfected with full length NrCAM, lanes 8 was transfected with HA-NrCAM Δ11CT. See section 2-3 and appendix 3 for methods.

As shown in Figure 6-4, antibodies raised to this peptide of NrCAM were either non-specific or gave no response. The antibodies picked up numerous protein bands from approximately 20 kDa to 150 kDa. Unfortunately, no antibody picked up a band in NrCAM transfected cells that did not also appear in

the untransfected cells. Therefore it was concluded that the attempt to make a cytoplasmic antibody to NrCAM was unsuccessful.

6.4 Accurate sizing of NrCAM fragments.

In the absence of an antibody to the cytoplasmic terminus of NrCAM it became important to use a Western blot system that showed accurate sizing of molecular weight proteins. The NuPAGE® Novex 3-8% Tris-Acetate together with HiMark™ protein markers gives an accurate measurement of high molecular weight proteins up to 500 kDa when compared to other SDS-PAGE gels and markers (http://www.invitrogen.com) and thus this system was adopted for all of the following experiments. Apparent molecular weight of protein bands were calculated using the HIMark™ Molecular Weight Calculator at www.invitrogen.com.

The predicted molecular weight was 127 kDa for full length NrCAM, 94 kDa for the extracellular region to the furin cleavage site and 34 kDa from the furin cleavage site to the C-terminal end of the cytoplasmic terminus (Figure 6-5). The molecular weights of the molecules are before post-translational modifications such as glycosylation.

The size of HA-NrCAM on Western blots was next determined using the HIMark™ Molecular Weight Calculator. N-terminally HA tagged neurofascin (isoform 186) (a kind gift from Dr Vann Bennett. Howard Hughes Medical Institute, USA) was used as a positive control. Neurofascin does not have a furin cleavage site (Hortsch, 1996) and therefore any band appearing on a Western blot should not be furin cleaved. HA-NrCAM and HA-neurofascin cDNA was

transfected into CHO cells as described by 2.2.5 and after 24 hours the immunoprecipitation experiments were carried out using anti-HA antibodies conjugated to sepharose beads as described by 2.3.15 The results are shown in Figure 6-5.

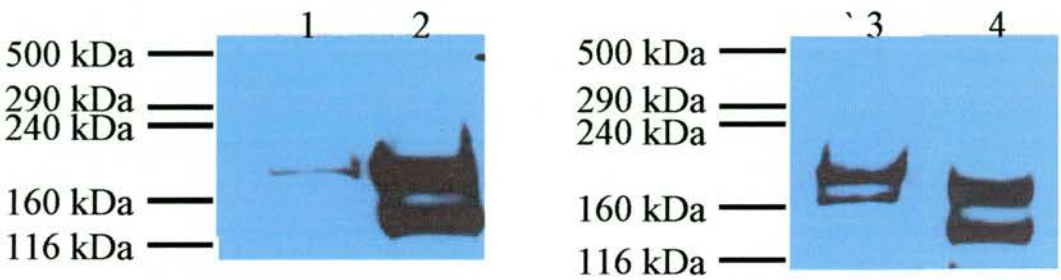

Figure 6-5. Western blots of 80 μg of crude cell extract of CHO cells. Lane 1 are cells transfected with HA-neurofascin. Lane 2 are cells transfected with HA-NrCAM. Lane 3 is the immunoprecipitation of HA-neurofascin. Lane 4 is the immunoprecipitation of HA-NrCAM. Lanes 1 to 4 were probed using a monoclonal anti-HA antibody. See section 2-3 and appendix 3 for methods.

As shown in Figure 6-5 (lane 1) HA-neurofascin did not express as well as HA-NrCAM and its size was approximately 185 kDa as previously reported (Volkmer *et al.*, 1992). HA-NrCAM was detected as two bands (Figure 6-5 (lane 2)). The higher band was between the 240 kDa and 160 kDa marker and was calculated to be approximately 180 kDa (Figure 6-5 (2)). The lower band was between the 160 kDa and 116 kDa markers and was calculated to be approximately 140 kDa (Figure 6-5 (2)). Native NrCAM is normally reported as being 140 kDa in brain extracts (Kayyem *et al.*, 1992; Davis *et al.*, 1996) and this is believed to be the furin cleaved form (Kayyem *et al.*, 1992; Grumet, 1997). Interestingly the 140 kDa protein band from the CHO cell extract was of approximately equal expression level when compared to the 180 kDa band. The lower band was usually more highly expressing in other cell types (Chapter 4, and Figure 6-3 (A) in this chapter). However, in all experiments done using

CHO cells the band was of approximately equal expression (see also Figure 6-4 (A)). This indicates that the expression levels of both isoforms are cell type specific.

The immunoprecipitation of HA-NrCAM gave the same two bands already observed in the crude cell extract. Surprisingly the immunoprecipitation of HA-neurofascin also showed two protein bands. The higher band appears to be the band of approximately 185 kDa already seen in the crude cell extract. However, a band of approximately 175 kDa was also present. Neurofascin does not have a furin cleavage site and is therefore unlikely to be furin cleaved (Hortsch, 1996). Therefore, it was thought possible that both protein bands for neurofascin may be due to differential post-translational modification of a percentage of the protein. Neurofascin has been reported to be subject to both N-linked and O-linked glycosylation (Volkmer *et al.*, 1992). If the two proteins bands for neurofascin were the results of different glycosylation of the proteins then the two protein bands for NrCAM could also be the results of different glycosylation and not cleavage as previously thought. It was therefore decided to test whether the HA-NrCAM protein used in the immunoprecipitations above was subject to N-linked glycosylation .

6.4.1 Examination of the N-linked glycosylation of NrCAM.

To examine N-linked glycosylation, protein extracts of HA-NrCAM were treated with N-glycosidase F (PNGase F), which enzymatically removes N-glycans (Maley *et al.*, 1989) (2.3.19). The protein samples were run on NuPAGE® Novex 3-8% Tris-Acetate gels with HiMark™ protein markers and

the sizes of the glycosylated and de-glycosylated proteins were compared. A typical example is shown in Figure 6-6.

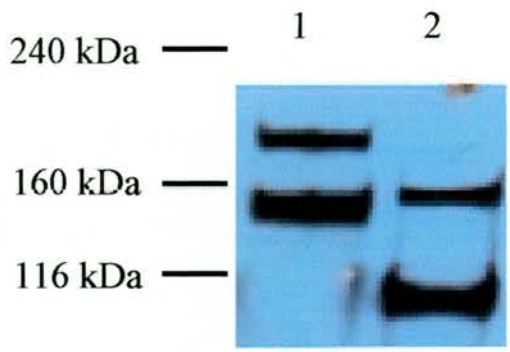

Figure 6-6. Studying the effects of N-linked glycosylation on the size of HA-NrCAM. Lanes 1 to 2 are HA-NrCAM immunoprecipitated from HEK293 cells. Lane 1 was an untreated sample and lane 2 was treated with PNGase F. Lanes 1 to 2 were probed using a monoclonal anti-HA antibody. See section 2-3 and appendix 3 for methods.

Untreated samples, and therefore potentialy glycosylated showed the two bands of molecular weight 180 kDa and 140 kDa as previously observed (Figure 6-6 (lane 1)). However, the addition of PNGase F resulted in a decrease in both sizes to molecular weight 155 kDa and 105 kDa, indicating that there had been a decrease of 25-30 kDa. Therefore, it would appear that both protein bands for HA-NrCAM are glycosylated. The size difference between the two bands must therefore be due to a different post-translational modification.

6.4.2 Examination of HA-NrCAM in the human carcinoma cell line, LoVo.

The human carcinoma cell line LoVo does not express a functional furin protease (Logeat *et al.*, 1998) and has been used successfully to study the effects of furin cleavage on Tractin (the L1-CAM family member in leech) (Xu *et al.*, 2003). Therefore, HA-NrCAM was transiently transfected into LoVo cells as

described in section 2.2.5. Western blots were carried out and the size of HA-NrCAM in LoVo cells was compared to the size of HA-NrCAM in human embryonic kidney (HEK293) cells. The results are shown in Figure 6-7.

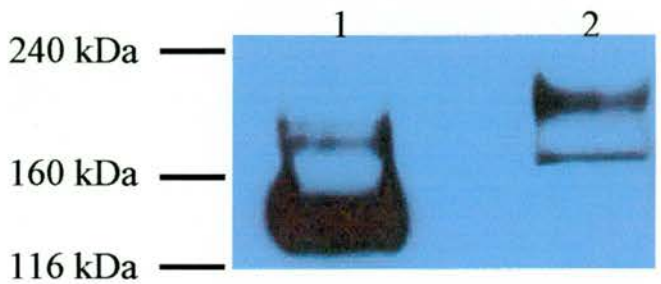

Figure 6-7. Studying the effects of furin cleavage on the size of HA-NrCAM. Lanes 1 is a 80 μg cell extract of HA-NrCAM expressing HEK293 cells. Lane 2 is a 80 μg cell extract of HA-NrCAM expressing LoVo cells. Lanes 1 to 2 were probed using a monoclonal anti-HA antibody. See section 2-3 and appendix 3 for methods.

In HEK293 cells, NrCAM is expressed as two protein bands of approximately 180 kDa and 140 kDa. In LoVo cells NrCAM is expressed as two protein bands of approximately 210 kDa and 170 kDa. Therefore, both protein bands of HA-NrCAM have increased in apparent molecular weight by approximately 30 kDa. The molecular weight of the cleaved fragment of NrCAM from the third FNIII-like domain to the cytoplasmic tail is estimated to be 34 kDa (see Figure 6-3(C)). This finding suggested that both fragments of HA-NrCAM may be furin cleaved and that the cytoplasmic terminus of HA-NrCAM may not be present in any of the immunoprecipitations in the other cell lines. Unfortunately, LoVo cells did not express HA-NrCAM at high enough levels to make immunoprecipitation possible from this cell line. As the cytoplasmic terminus is necessary for both the tyrosine phosphorylation experiments being attempted above and the co-immunoprecipitation experiments

attempted in Chapter 4 it was decided to design a HA-NrCAM clone that could not be furin cleaved. This was done by removing the third FNIII-like repeat from HA-NrCAM.

6.5 Cloning and analysis of HA-NrCAM ΔFN2&3.

The second and third FNIII-like repeats of HA-NrCAM were deleted by PCR and a new construct that coded for HA-NrCAM without the 2nd and 3rd FNIII-like repeat (HA-NrCAM ΔFN2&3) was created as described by Figure 6-8.

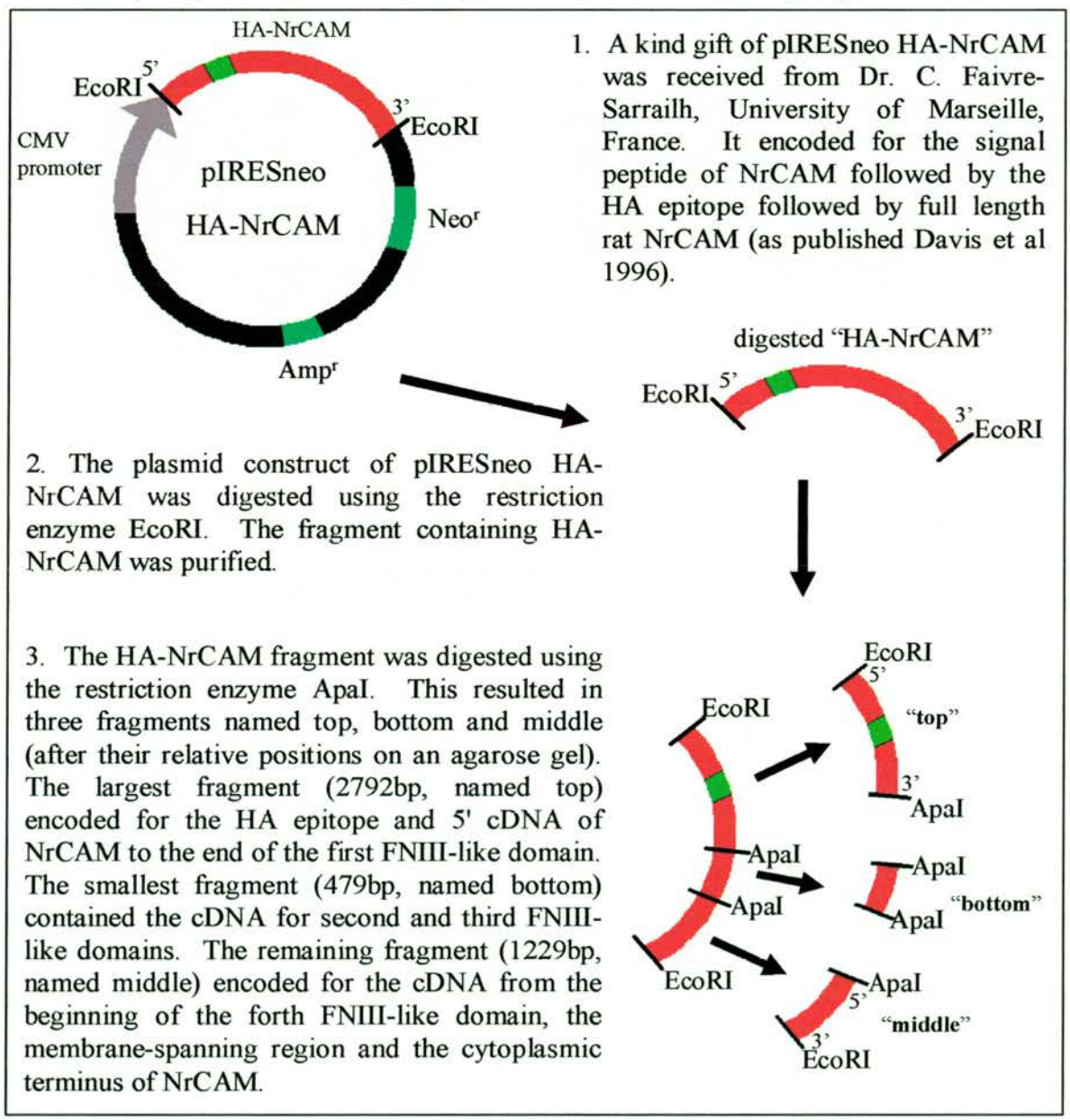

Figure 6-8. Continued on next page.

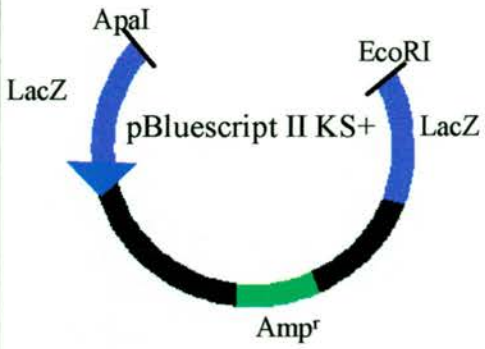

4. pBluescript a was digested with EcoRI and ApaI restriction enzymes, alakine phosphatase treated, then ligated together with either the "top" NrCAM cDNA fragment or the "middle" NrCAM cDNA fragment. The ligations were transformed into DH5α for amplification.This resulted in the production of two new plasmid called pBluescript top and pBluescript middle.

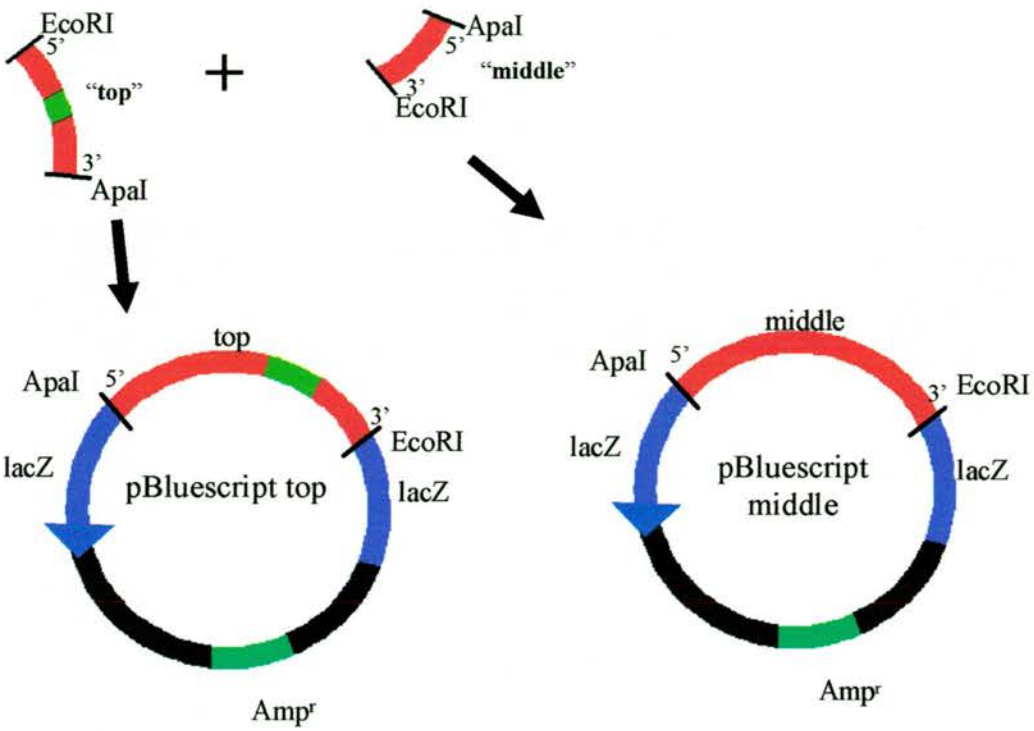

5. The plasmid construct pBluescript middle was not the correct frame2. PCR primers NrCAM F1 and NrCAM F2 were designed to: 1) put the NrCAM cDNA into the correct frame 2) to retain the ApaI and EcoRI restriction enzyme sites to the NrCAM encoding sequence (see appendix 4 for the sequences).

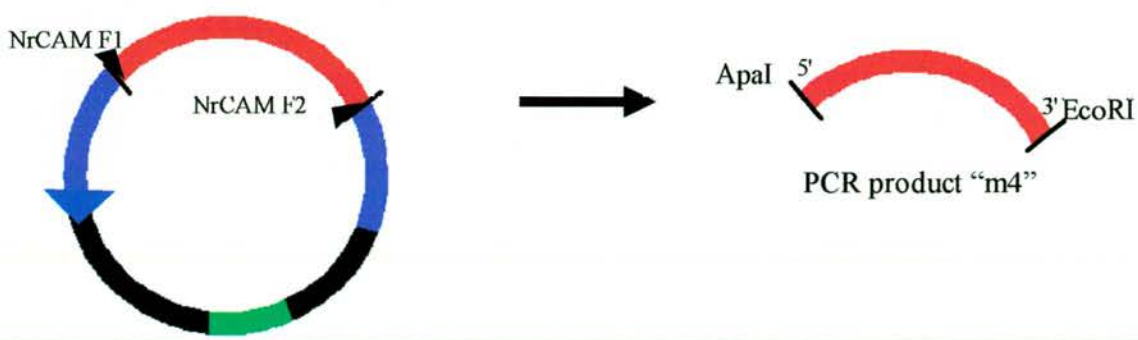

Figure 6-8. Continued on next page.

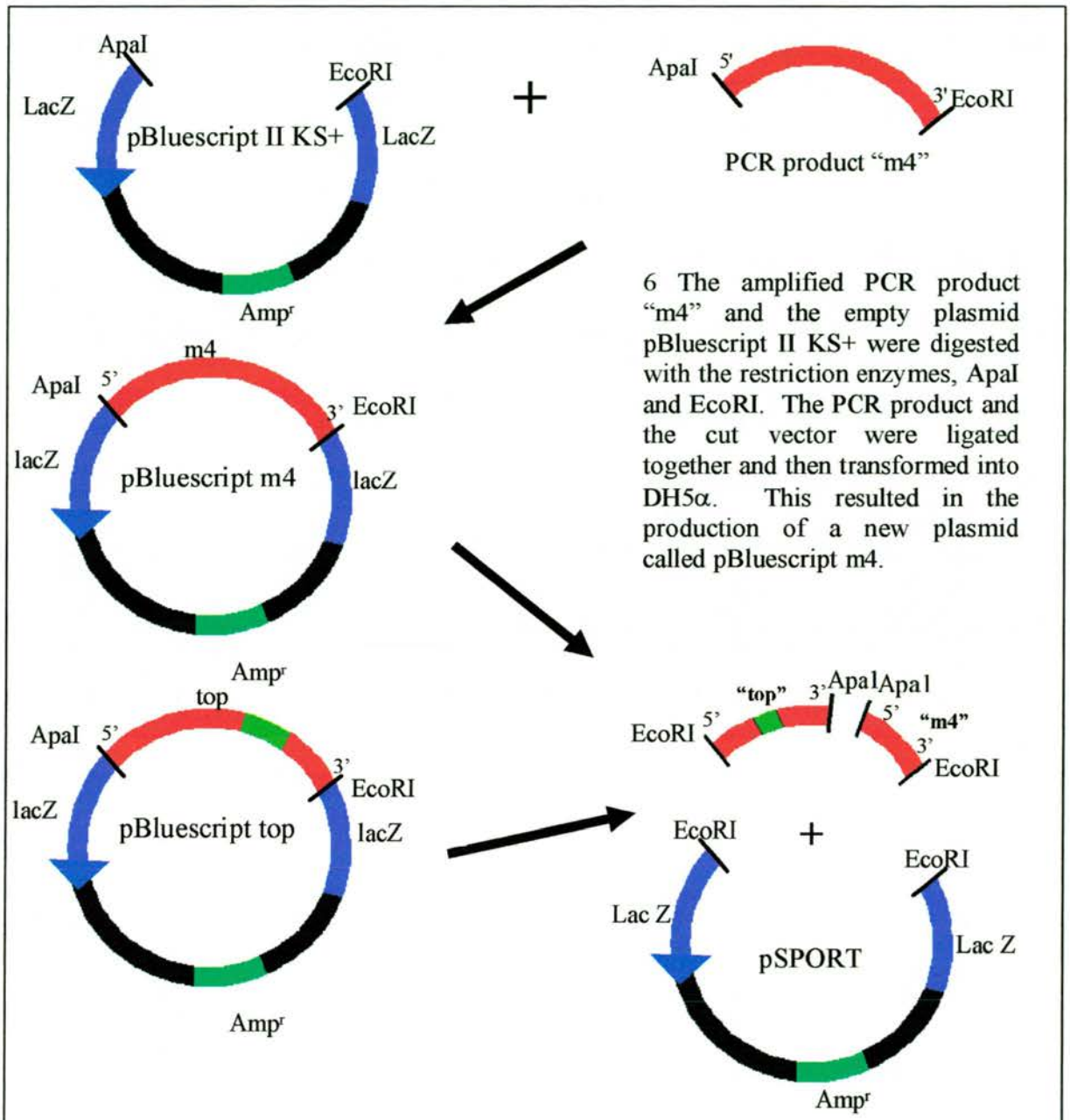

7. The plasmid constructs pBluescript top and pBluescript m4 were digested using restriction enzymes ApaI and EcoRI. The two fragment containing NrCAM were purified. The empty pSPORT plasmid was digested with the restriction enzymes EcoRI, purified and alkaline phosphatases treated. The purified "top" and "m4" cDNA fragments and the cut vector were ligated together and transformed into DH5α. This resulted in the production of a new plasmid construct called pSPORT HA-NrCAM ? FN2&3.

Figure 6-8. Continued on next page.

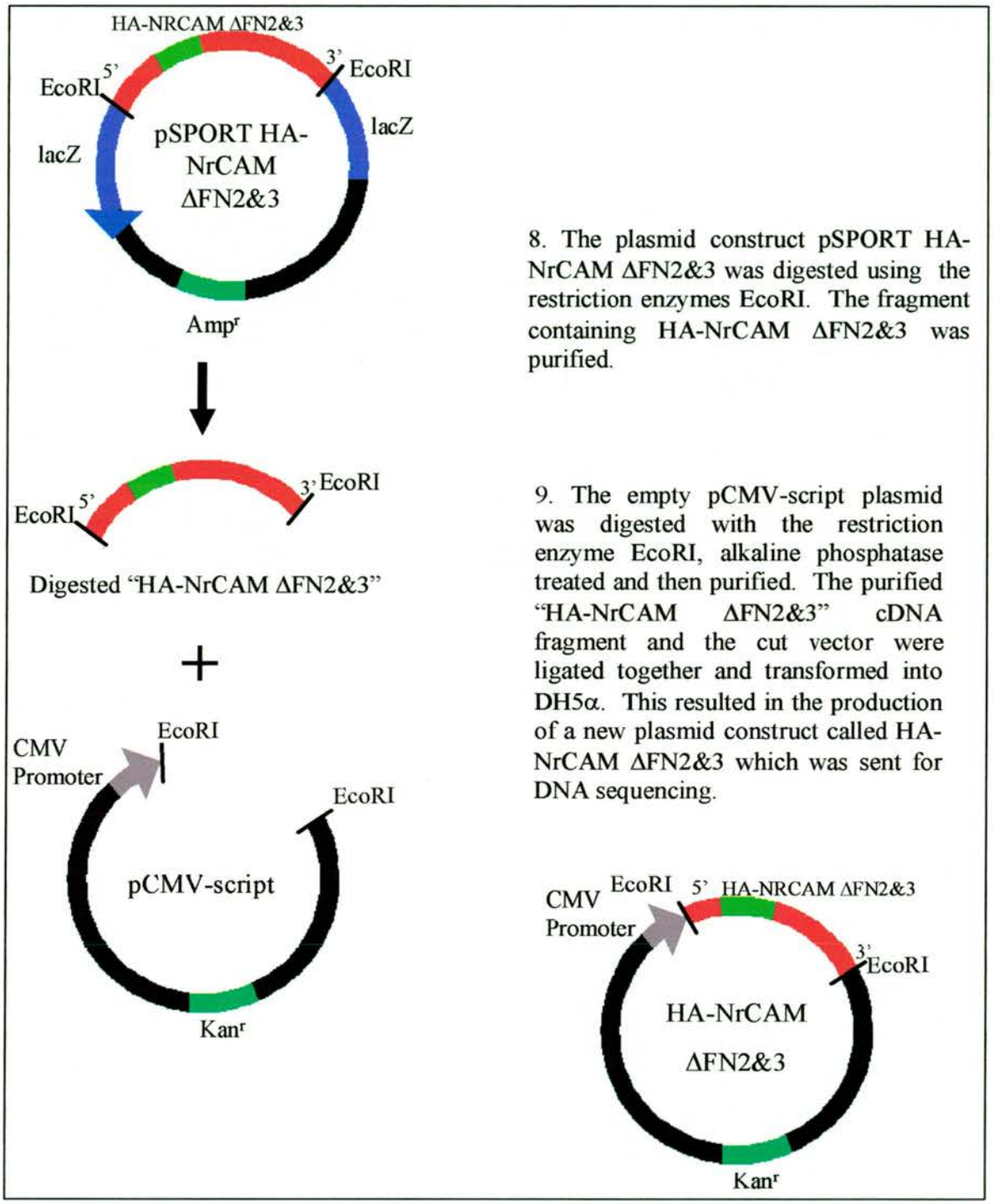

Figure 6-8. The cloning strategy for the production of the plasmid HA-NrCAM ΔFN2&3. Details of material and methods are described in chapter 2 and accompanying text.

6.5.1 HA-NrCAM ΔFN2&3 expression and glycosylation.

HA-NrCAM and HA-NrCAM ΔFN2&3 plasmids were transfected into HEK293 cells as described by 2.2.5. Crude cell extracts were prepared and run on NuPAGE® Novex 3-8% Tris-Acetate and a Western blot performed.

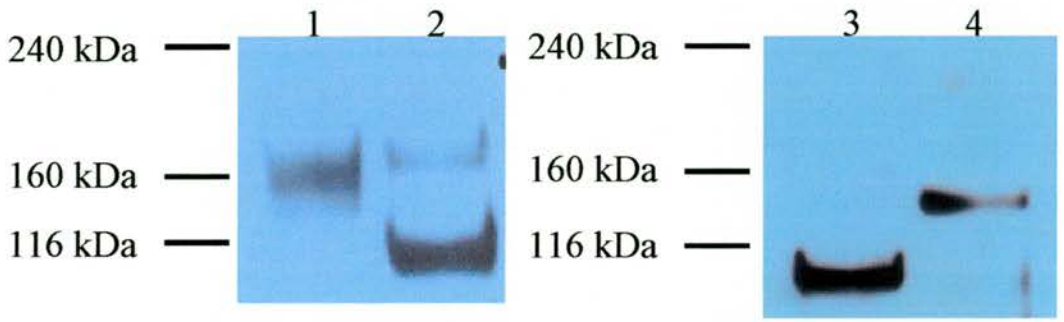

Figure 6-9. Expression of the HA-NrCAM ΔFN2&3 construct in HEK293 cells. Lane 1 is a 80 μg crude cell extract of HA-NrCAM ΔFN2&3 expressing HEK293 cells. Lane 2 is a 80 μg crude cell extract of HA-NrCAM expressing HEK293 cells. Lanes 3 to 4 are HA-NrCAM ΔFN2&3 immunoprecipitated from HEK293 cells. Lane 3 was treated with PNGase F and lane 4 was left untreated. Lanes 1 to 4 were probed using a monoclonal anti-HA antibody. See section 2-3 and appendix 3 for methods.

As shown in Figure 6-9 crude cell extracts of HA-NrCAM ΔFN2&3 appeared as a diffuse band from approximately 180 kDa to 140 kDa. To examine whether this truncated form of NrCAM underwent N-linked glycosylation, HA-NrCAM ΔFN2&3 cDNA was again transiently transfected into HEK293 cells, immunoprecipitated, and then treated with or without PNGase F. The protein samples were run on a NuPAGE® Novex 3-8% Tris-Acetate gel and sizes of the glycosylated and de-glycosylated HA-NrCAM ΔFN2&3 proteins were compared. The results are shown in Figure 6-9 (lanes 3 and 4). Untreated HA-NrCAM ΔFN2&3 immunoprecipitated from a HEK293 cells as a single band of

approximately 140 kDa. Deglycosylation reduced the apparent molecular weight of HA-NrCAM ΔFN2&3 by 30 kDa to approximately 100 kDa. This was similar to the molecular weight reduction found for HA-NrCAM. Importantly the 100 kDa weight was close to the 110 kDa weight predicted for the HA-NrCAM ΔFN2&3 protein. Therefore, HA-NrCAM ΔFN2&3 appeared to be uncleaved. Three attempts were then made to transiently transfect HA-NrCAM ΔFN2&3 cDNA into LoVo cells. However, the HA-NrCAM ΔFN2&3 protein was not expressed at a detectable levels (not shown). As HA-NrCAM ΔFN2&3 appears to be uncleaved it was therefore decided to investigate whether the tyrosine-phosphorylated protein could be immunoprecipitated from orthovanadate treated HEK293 cells.

6.5.2 Immunoprecipitation of HA-NrCAM ΔFN2&3 protein from HEK293 cells treated with a protein tyrosine phosphatase inhibitor.

HEK293 cells were transiently transfected with HA-NrCAM ΔFN2&3. After 24 hours the HEK293 cells were treated with either sterile water (vehicle) or sodium orthovanadate as described previously. The immunoprecipitation was carried out as described by 2.3.15 and Western blots were carried out. The procedure was repeated on four separate occasions. Figure 6-10 is a typical blot of one such experiment.

Immunostaining for HA-NrCAM ΔFN2&3 normally appeared as a band of approximately 100 kDa (Figure 6-9, lane 3). As shown in Figure 6-10 (B, lanes 3 and 4) a band of this weight appeared in the immunoprecipitated extract when it was reprobed with an anti-HA antibody. However, no 100 kDa tyrosine phosphorylated protein band was seen when probing with the anti-tyrosine

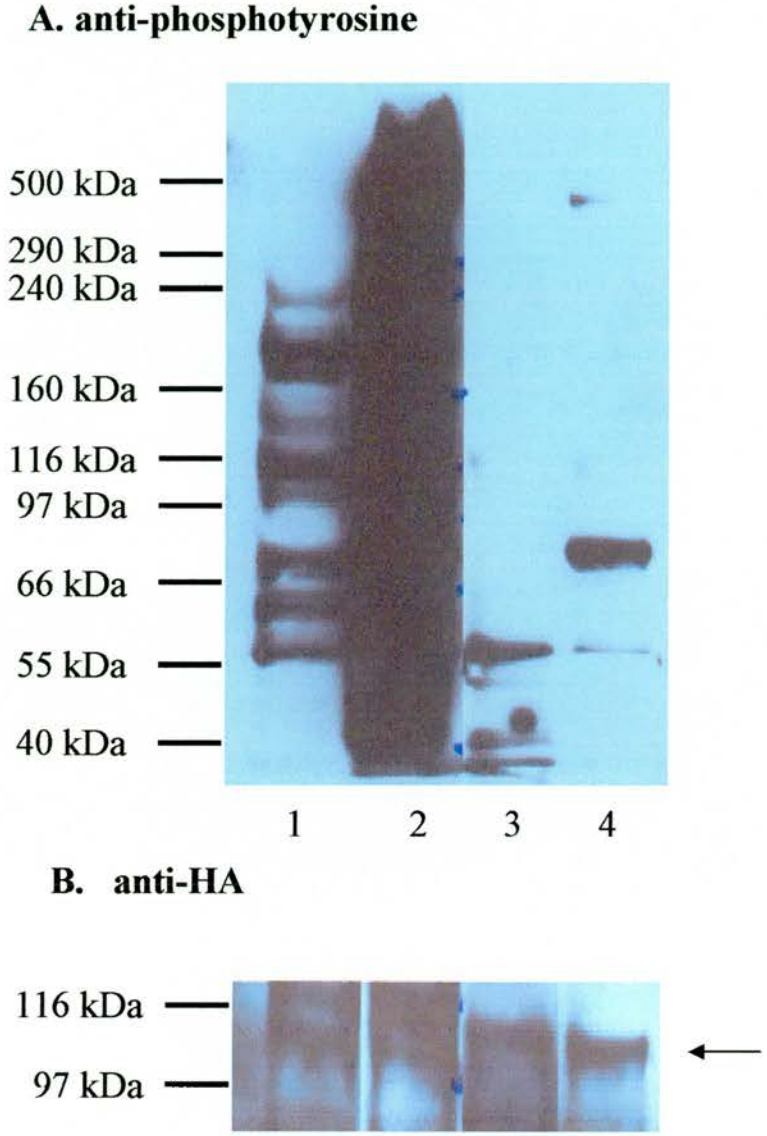

Figure 6-10. Immunoprecipitation of HA-NrCAM ΔFN2&3 from sodium orthovanadate treated HEK293 cells. **A)** Western blots (probing with a monoclonal anti-phosophotyrosine anibody) of 80 μg of crude cell extract of HEK293 cells transfected with HA-NrCAM ΔFN2&3 (lanes 1-2) and of proteins immunoprecipitated from the HEK293 cells using anti-HA antibodies (lanes 3-4). Lane 1 and lane 3 were the vehicle treated sample. Lane 2 and lane 4 were the orthovanadate treated sample. **B)** The blot in (A) was stripped of primary and secondary antibodies and reprobed with anti-HA antibodies. Arrow indicates immunoprecipitated HA-NrCAM See section 2.3 and appendix 3 for methods.

antibody (Figure 6-10 (A, lane 4). Thus it would appear that immunoprecipitated HA-NrCAM ΔFN2&3 was not phosphorylated. However, two novel phosphorylated bands were seen in Figure 6-10 (A, lane 4). A band of approximately 80 kDa (that appeared in all of the immunoprecipitation attempts of HA-NrCAM ΔFN2&3) and a second large molecular weight protein band of approximately 400 kDa (that was visible in this immunoprecipitation attempt only).

6.6 Ankyrin-GFP binding to NrCAM.

As the immunoprecipitations of various tyrosine phosphorylated NrCAM had been unsuccessful it was decided to try a different assay to study the effects of the tyrosine phosphorylation of the NrCAM cytoplasmic terminus. The assay was based upon the ability of both neurofascin and L1 to recruit the normally cytoplasmic protein ankyrin-GFP to the plasma membrane of HEK293 cells (Zhang *et al.*, 1998b; Needham *et al.*, 2001). It was decided to test whether this assay could be used to show both the binding of ankyrin-GFP to NrCAM and examine the effects of tyrosine phosphorylation on the ankyrin-GFP-NrCAM interaction.

A plasmid encoding full-length ankyrin$_G$ C-terminally tagged with GFP (ankyrin-GFP) was a kind gift from Dr Vann Bennett, Howard Hughes Medical Institute, USA. HEK 293 cells were grown overnight to approximately 50% confluence on standard glass cover slips. The HEK 293 cells were transfected with 2.5 μg of ankyrin-GFP plasmid only, or 2.5 μg ankyrin-GFP plasmid and 2.5 μg of HA-NrCAM plasmid (2.2.5). The transfected cells were allowed to grow for a further 24 hours, fixed, immunostained and imaged (section 2.2.10)

Typical transfected HEK293 cells are shown in Figure 6-11 (A to E). Ankyrin-GFP shows a cytoplasmic distribution in cells that are not expressing NrCAM (Figure 6-11 (A and B)). However, expression of HA-NrCAM in HEK293 cells recruited ankyrin-GFP to the plasma membrane (Figure 6-11 (D to F)), thus suggesting that the two proteins are interacting. This was then tested in other cell types such as CHO cells, B104 cells and COS-7 cells. However intriguingly, the recruitment of ankyrin-GFP to the membrane only occurred in the HEK293 cell line. This concurred with previous results for neurofascin and ankyrin-GFP (Zhang *et al.*, 1998a).

Despite the successful recruitment of ankyrin-GFP to the membrane Figure 6-11 (F to H) demonstrated a technical problem. Namely, the expression level of both proteins was critical to the recruitment of ankyrin-GFP. In Figure 6-12 (F) the ankyrin-GFP plasmid is over expressed and while it has been noticeably recruited to the plasma membrane, some of it has remained in the cytoplasm. A similar situation occured when the expression level of NrCAM was low. It was therefore difficult to score the effectiveness of NrCAM's ability to recruit ankyrin-GFP under different phosphorylation conditions in a mixed population of NrCAM/HA-NrCAM and ankyrin-GFP transfected cells. An attempt was made at cloning out HEK293 cells that stably expressed HA-NrCAM to overcome this difficulty. However, these clones, though expressing HA-NrCAM at high level, had lost their contact inhibition and failed to grow as a monolayer, making them difficult to image and thus unsuitable for phosphorylation studies planned.

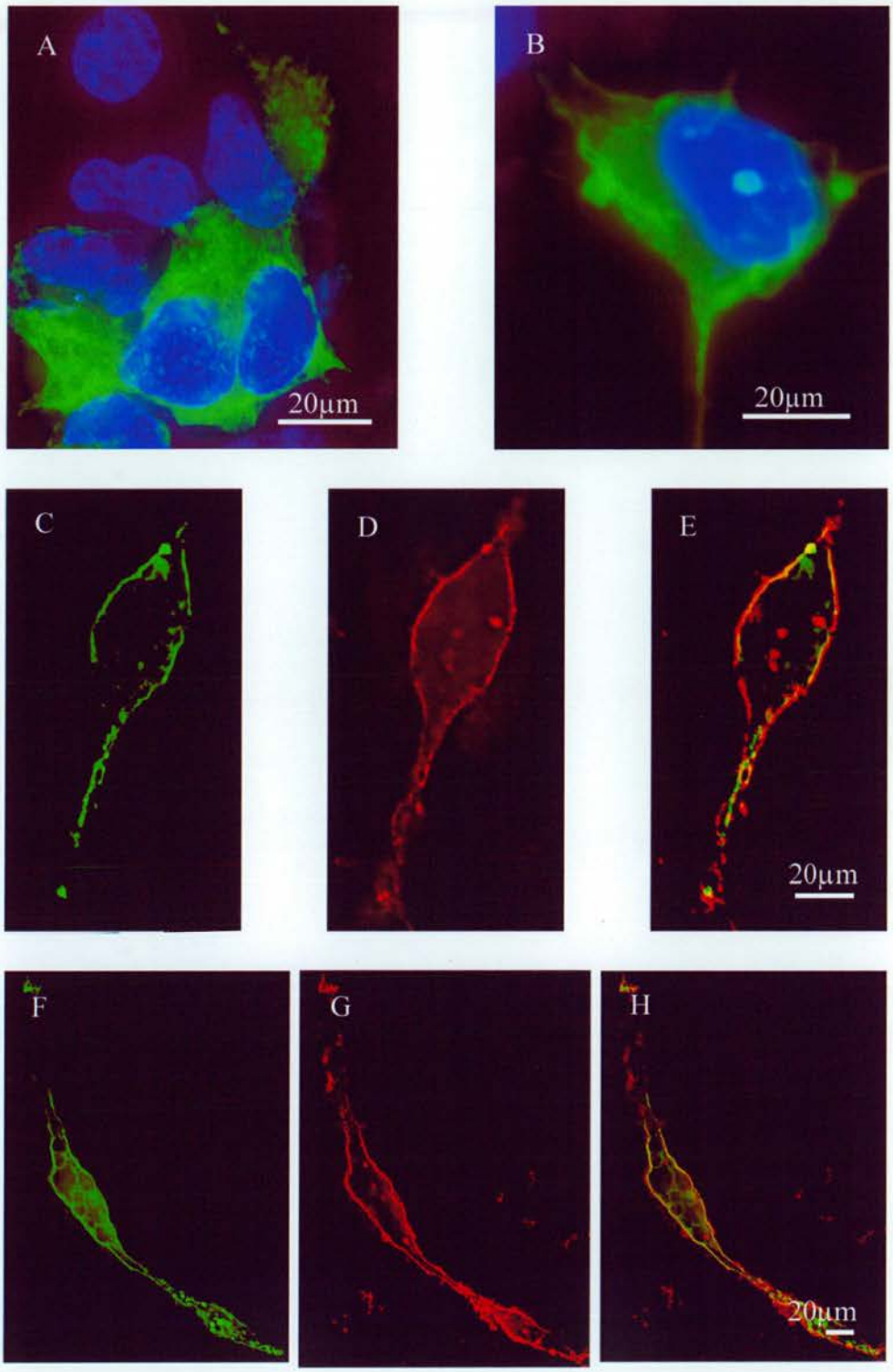

Figure 6-11. Ankyrin-GFP expression in HEK293 cells. **A**) and **B**) are HEK293 cells transfected with ankyrin-GFP only. **C**), **D**) and **E**) is a HEK293 transfected with both HA-NrCAM and ankyrin–GFP. **F**), **G**) and **H**) is a HEK293 transfected with both HA-NrCAM and ankyrin–GFP. Ankyrin-GFP is shown in green (C,F). HA-NrCAM immunostaining was performed using an anti-HA rat monoclonal antibody and anti-mouse Alexa 568 conjugated antibody and is shown in red (D, G). Overlay of both ankyrin-GFP and HA-NrCAM (E,H). See methods section 2.2.10..

It was therefore decided to study individually transfected cells by live imaging. Cells were to be treated with various growth factors to see if this could influence the recruitment of ankyrin-GFP to the plasma membrane by HA-NrCAM. Cells were transfected with both HA-NrCAM and ankyrin-GFP and left in serum free media. However, it was noted that the transport of these cells to the microscope caused ankyrin-GFP to move to the cytoplasm. The HA-NrCAM and ankyrin-GFP transfected cells were then left at 37 °C in 5% CO_2 on the microscope for approximately one hour and it appeared that most of the ankyrin-GFP had returned to the membrane. However another technical problem arose as imaging the transfected cells using the Zeiss Axiovert S100 2TV Delta-Vision Restoration microscope proved impossible, as the process of shining the laser on a cell seemed to cause the ankyrin-GFP to return once more to the cytoplasm.

6.7 Discussion of results.

Previous chapters have shown that the NrCAM cytoplasmic terminus can bind to ankyrin using the yeast two-hybrid system and that this binding occurred when a 26 amino acid motif was present that ended in FIGQY. The mutation of the tyrosine residue of the FIGQY motif to glutamate abolished ankyrin binding to NrCAM and it was believed that this might mimic the phosphorylation of NrCAM. Thus, there was evidence that NrCAM may be phosphorylated at the FIGQY tyrosine in a similar manner to L1 and neurofascin and that this phosphorylation may prevent ankyrin binding. It was therefore decided to study the tyrosine phosphorylation of NrCAM using other phosphorylation

experiments. It was hoped that the immunoprecipitations experiments could be used to establish whether tyrosine phosphorylation occurred mainly at the FIGQY tyrosine (as for neurofascin) and to study the pathways involved in the phosphorylation by the use of various growth factors, phosphatase inhibitors and kinase inhibitors.

One immunoprecipitation experiment appeared to have been successful in showing the tyrosine phosphorylation of NrCAM (Figure 6-2). It was notable that this attempt was made on cell extracts of B104 cells that had grown to 100% cell density and that attempts made at lower cell densities had been unsuccessful. This could imply that at high levels of cell-to-cell contact either more NrCAM is available for phosphorylation or there was more of a particular kinase available to phosphorylate NrCAM. Similar findings have been found in investigations into integrin signalling, where different kinases and phosphatases are present at the points of cell-to-cell contact of fibroblasts grown in 3D cultures than in 2D cultures and the phosphorylation of $\alpha 5\beta 1$ was effected (DeMali *et al.*, 2003).

The blot shown in Figure 6-2 has a band of approximately 100 kDa in the unstimulated crude cell extract and that may indicate that a proportion of stably expressed HA-NrCAM may always be constitutively phosphorylated. A similar finding was also identified for stably expressed HA-neurofascin in B104 cells (Garver *et al.*, 1997). Therefore, it would appear that at a proportion of NrCAM and neurofascin may always remain phosphorylated. It would be interesting to identify which sub-population of NrCAM/neurofascin remains phosphorylated even under serum starvation conditions. One possibility is that NrCAM/neurofascin are being transported to sites at the plasma membrane in which they remain phosphorylated until reaching their final destination. Here it

is then dephosphorylated by an unknown phosphatase and becomes available for ankyrin binding. Another possibility is that there are always two pools of NrCAM/neurofascin in the plasma membrane. One pool is unphosphorylated and binds to ankyrin and the other pool is phosphorylated as has been reported for the L1 receptor (Gil *et al.*, 2003). A third possibility is that tyrosine phosphorylation is necessary for the binding of NrCAM to an as yet unidentified protein. For example neurofascin has been reported to bind to doublecortin but only when it is phosphorylated on its FIGQY tyrosine (Kizhatil *et al.*, 2002).

It is normally believed within the literature that the majority of NrCAM is furin cleaved (Kayyem *et al.*, 1992; Davis *et al.*, 1996). As the antibodies used in this experiments were N-terminal to the furin cleavage site any immunoprecipitated furin cleaved NrCAM would not have a cytoplasmic terminus. An attempt was therefore made to raise antibodies to the cytoplasmic terminus of NrCAM, so that these antibodies could be used to both verify the results in 6-2 and for immunoprecipitation experiments. Despite initial positive indications these antibodies failed to detect expression of NrCAM transfected into mammalian cells. A second attempt to make antibodies to a different target in the NrCAM cytoplasmic terminus has also been unsuccessful and has failed to show convincing binding to NrCAM constructs (personal communication Dr. F. Davey, University of St Andrews).

As no cytoplasmic antibody was available it was necessary to confirm that the 100 kDa tyrosine phosphorylated immunoprecipitated band in Figure 6-2 contained the cytoplasmic terminus of NrCAM using other methods. The appearance of two bands for the immunoprecipitated HA-neurofascin isoform 186 (which does not have a furin cleavage site in its third FNIII-like domain)

suggested that there may be another post-translational modification other than furin cleavage that could explain the second band of neurofascin. The primary post-translational modification studied in neurofascin has been N- and O-linked glycosylation (Volkmer *et al.*, 1992). NrCAM has two potential O-linked glycosylation sites (NetOGlyc 3.1; http://www.cbs.dtu.dk/services/NetOGlyc/) and has 16 potential N-linked glycosylation sites (NetNGlyc 1.0; http://www.cbs.dtu.dk/services/NetNGlyc/). O-linked glycosylation has not been found to result in a large difference in the molecular mass of neurofascin (Volkmer *et al.*, 1992). Therefore, NrCAM was tested for potential N-linked glycosylation. If the two NrCAM bands could be explained by differently glycosylated NrCAM populations then the removal of N-linked glycans from NrCAM would result in a single band of the same molecular weight. However, both NrCAM bands were reduced in size by approximately 25 to 30 kDa thus suggesting that both bands were subject to equivalent N-linked glycosylation.

This indicated that the lower band of HA-NrCAM was due to furin cleavage. If the lower band of HA-NrCAM was furin-cleaved, and the higher band was uncleaved NrCAM, then the expression of NrCAM in a cell line deplete in functional furin should result in the higher molecular weight band of NrCAM only. This had already been reported for Tractin (the L1-CAM in leech) (Xu *et al.*, 2003). While cleavage products of Tractin were found in HEK293T cells no cleavage products of Tractin were found in LoVo cells (a cell line without functional furin) (Xu *et al.*, 2003). However, when HA-NrCAM was expressed in LoVo the apparent size of both NrCAM protein bands increased by 30 kDa. The molecular weight of the cytoplasmic portion of cleaved NrCAM was estimated to be 34 kDa. Therefore, it would appear that both protein bands of

NrCAM in HEK293 cell represented furin-cleaved NrCAM and hence would not contain the C-terminus.

To confirm if both bands of NrCAM are furin cleaved a future experiment could be to add the furin enzyme to LoVo cell extracts containing HA-NrCAM. If NrCAM is furin cleaved both bands should decrease by approximately 30 kDa when compared to bands from LoVo extracts untreated by furin.

At this stage, it had been determined that all of the expressed NrCAM was cleaved in all cell lines except the LoVo cell line. However, the LoVo cell line was not suitable for immunoprecipitation experiments (because of low expression levels). Therefore, HA-NrCAM cDNA that did not encode for the second or third FNIII-like domains of NrCAM was cloned into a mammalian expression vector (HA-NrCAM ΔFN2&3). The furin cleavage site is within the third FNIII-like repeat of NrCAM and so HA-NrCAM ΔFN2&3 should not be furin cleaved. Indeed, the HA-NrCAM ΔFN2&3 protein appeared as a single diffuse band in most Western blots and so did not appear to be furin cleaved. Several attempts were made to immunoprecipitate out tyrosine-phosphorylated HA-NrCAM ΔFN2&3 from HEK293 cells. Unfortunately, despite expression and immunoprecipitation of HA-NrCAM ΔFN2&3, no phosphorylated protein was observed. However, two new tyrosine-phosphorylated proteins were seen in immunoprecipitations of orthovanadate treated cells. The first protein was approximately 80 kDa in size and highly expressed and it was seen in all four attempts at immunoprecipitation of HA-NrCAM ΔFN2&3. The second protein was between 260 kDa and 500 kDa in size and appeared only in one immunoprecipitation attempt. Both of these proteins could be proteins that were

binding unspecifically to the beads and/or antibodies used for the immunoprecipitation. However, both proteins could also be potential binding partners of NrCAM that were co-immunoprecipitated with the HA-NrCAM ΔFN2&3 protein. For example ankyrin can be tyrosine phosphorylated (Woroniecki et al., 2002) and isoforms of ankyrin range from 26 kDa to 480 kDa (Mohler *et al.*, 2002). Thus both proteins immunoprecipitated with HA-NrCAM ΔFN2&3 in Figure 6-10 could be ankyrins.

The recruitment of ankyrin-GFP to the plasma membrane of HEK293 cells by NrCAM and HA-NrCAM confirms the interaction of ankyrins and NrCAM already shown in Chapter 3. Viewing the cells live appeared to indicate that this interaction was highly dynamic as stresses such as moving the cells, or even use of a laser abolished the NrCAM-ankyrin interaction causing ankyrin-GFP to move back to the cytoplasm. Re-incubating the cells under normal growth conditions did appear to result in a return of ankyrin-GFP to the membrane. This phenomenon has implications for its role in dynamic structures such as the growth cone. It is interesting to speculate that kinases could be phosphorylating NrCAM in responses to stresses (resulting in reduced ankyrin binding) and that phosphatases remove the phosphate groups under normal growth conditions (resulting in increased ankyrin binding).

Chapter 7. Overall discussion.

7.0 Introduction and aims.

NrCAM is a cell adhesion molecule of the L1-CAM family and together with the other L1-CAMs is important for the development of the mammalian nervous system (Hortsch, 1996). Within the neuron, NrCAM is expressed at initial segments, the node of Ranvier, growth cones, post and pre-synaptic densities (Jenkins and Bennett, 2001; Custer *et al.*, 2003; Falk *et al.*, 2004; Petralia *et al.*, 2005).

At the start of this project, NrCAM's only known cytoplasmic binding partner was ankyrin (Davis *et al.*, 1996), a protein that couples membrane receptors to the actin cytoskeleton via spectrin (Bennett and Chen, 2001). Ankyrin binding was common to all the L1-CAMs and ankyrin binding to both NrCAM and neurofascin was known to play an important role in the development of the initial segment and the node of Ranvier (Davis *et al.*, 1996). However, ankyrin binding to NrCAM and L1 could not fully explain their behaviours in the growth cone and many authors believed that another family of proteins may be binding to NrCAM and L1 (Gil *et al.*, 2003a). Therefore, it was decided to both investigate whether NrCAM had any other cytoplasmic binding partners and to investigate the effects of phosphorylation on the dynamics of the ankyrin-NrCAM interaction. The strategy taken was three pronged. Firstly, novel candidate binding partners of NrCAM were investigated using a yeast two-hybrid library screen (Chapter 3). Potential interactions were re-confirmed, where possible, and the function of the NrCAM-candidate interaction investigated (Chapter 4). Secondly, proteins of the 4.1 superfamily, that were already suspected to bind to NrCAM, were investigate#d as potential binding

partners (Chapter 5). Thirdly, an attempt was made to investigate the tyrosine phosphorylation of NrCAM and the effects on ankyrin binding.

7.1 Identification of novel binding partner to NrCAM.

To identify cytoplasmic binding partners of NrCAM, a developing rat cDNA library was screened using the yeast two-hybrid technique (Chapter 3). The screen identified three potential binding partners of NrCAM.

The first binding partner contained the Vps27, Hrs, STAM (VHS) domain of Golgi-localized, gamma-ear-containing, Arf binding protein 1 (GGA1). The VHS domain is present in several proteins and is known to bind to membrane receptors (Lohi *et al.*, 2002). The GGA1 protein is thought to sort bound membrane receptors from the trans Golgi network to the endosome (Bonifacino, 2004). The VHS clone selected by the library screen appeared to be binding to amino acid residues that make up the ankyrin binding domain of NrCAM. Furthermore, the VHS clone bound to a neurofascin clone that also contained the highly conserved ankyrin binding domain. Interestingly the amino acid substitution of a glutamate residue for a tyrosine in NrCAM's ankyrin binding domain or the deletion of the amino acids LVDY from L1's ankyrin binding domain eliminated VHS binding. This appeared to be consistent with other reports of important residues in VHS domain/receptor binding (Bonifacino, 2004). Thus, it has been concluded that the VHS domain of GGA1 is binding to NrCAM at the ankyrin binding site. Unfortunately time

constraints did not allow for further investigation of the full length GGA1 (GGA2, and GGA3) interactions with NrCAM in the work done for this thesis.

The two other potential binding partners were GAIP interacting protein C terminus (GIPC) and synapse associated protein 102 (SAP102). GIPC is found on both coated and uncoated intracellular vesicles and is thought to be involved in endocytosis and intracellular trafficking of receptors (Dance *et al.*, 2004). Importantly it also potentially links these receptors to G-protein signalling pathways (De Vries *et al.*, 1998). SAP102 is a member of the membrane-associated guanylate kinase (MAGUK) family and is expressed early in brain development (Fujita and Yoshihisa, 2000; Sans *et al.*, 2000). It is involved in modulation of NMDA receptors, anchoring of transmembrane proteins by multi protein complexes and trafficking of NMDA receptors to the plasma membrane of the post-synaptic density (Lau *et al.*, 1996; Sans *et al.*, 2000; Sans *et al.*, 2003). Both the GIPC and the SAP102 proteins selected by the yeast two-hybrid screen contained PDZ domains and appeared to be binding to the last 28 amino acids of NrCAM. Further investigation showed that the last three amino acids of NrCAM were necessary for binding and thus it has been concluded that SAP102 and GIPC are binding to the class 1 PDZ binding site of NrCAM. Both GIPC and SAP102 are expressed at similar times of development of the brain and neuron as NrCAM and both PDZ proteins co-localised with NrCAM in the localised areas of the plasma membrane of cells. Although the NrCAM-GIPC binding was not successfully reconfirmed the NrCAM-SAP102 interaction was, using the Tandem Affinity Procedure (TAP). NrCAM-SAP102 binding has been subsequently further reconfirmed a third time

using the GST pull-down technique by Dr F. Davey (Davey *et al.*, 2005). The results of Chapter 3 and 4 have been summarised by Figure 7-1.

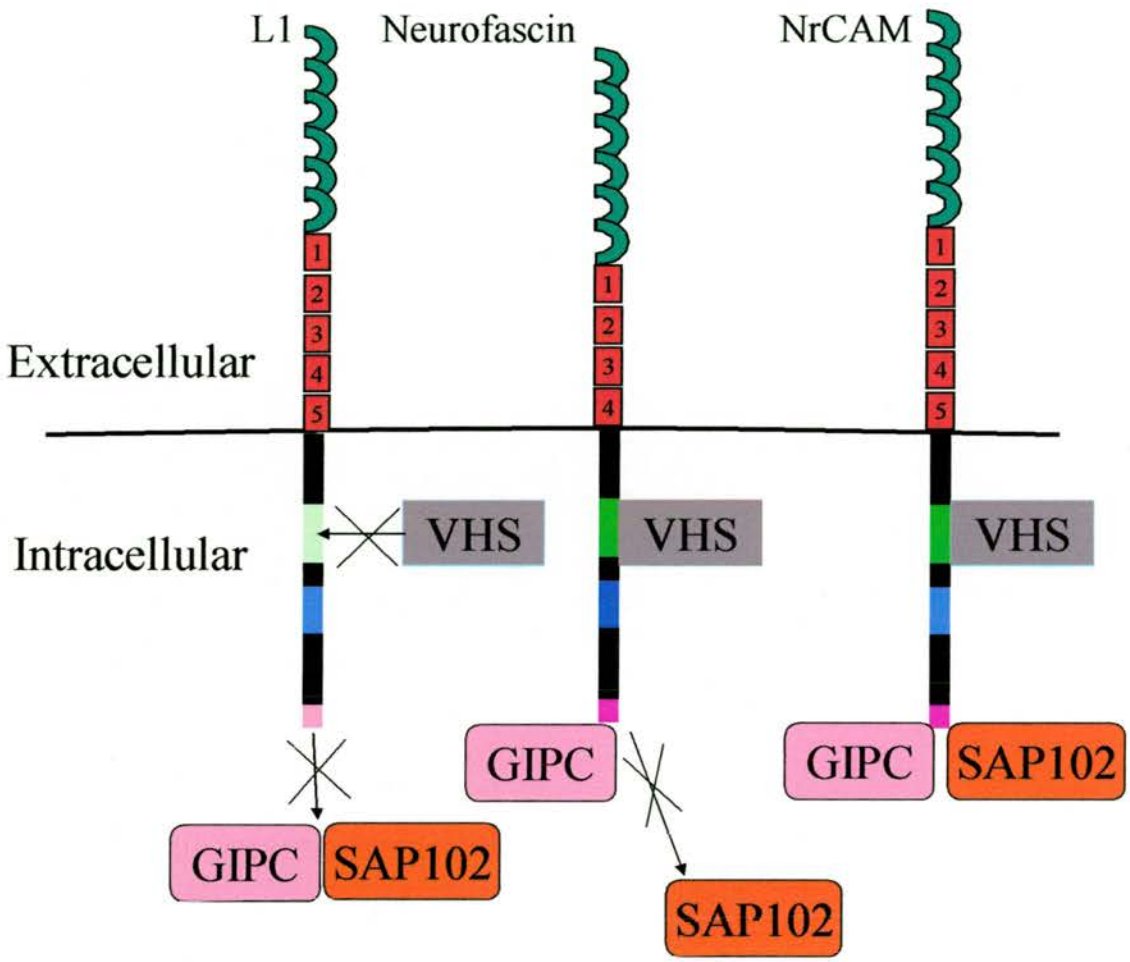

Figure 7-1. A diagrammatic representation of the results in Chapter 3 and 4. The figure demonstrates three new novel binding partners of NrCAM, namely the VHS domain of GGA1, GIPC and SAP102. L1 did not bind to any of the potential binding partners of NrCAM. Neurofascin bound to the VHS clone and to the GIPC clone but not to the SAP102 clone. The cytoplasmic termini of the L1-CAM protein have been shown diagrammatically. The green boxes represent the ankyrin-binding domain of neurofascin and NrCAM. The pale green box represents the ankyrin-binding domain L1 that was missing the LADY motif. The dark blue box is the proposed FERM binding domain of neurofascin. The pale blue box is the equivalent amino acids of the FERM domain in neurofascin present in NrCAM and L1. The dark pink boxes are the PDZ binding domains of NrCAM and neurofascin. The pale pink box is the equivalent amino acids of the PDZ domain of NrCAM present in L1.

7.2 Does NrCAM bind to proteins of the 4.1 Superfamily?

Proteins of the 4.1 superfamily that contain a FERM domain are good candidate proteins to bind to NrCAM. These proteins also link membrane receptors to the cortical cytoskeleton via their FERM domains (Bretscher *et al.*, 2002). They are also involved in inositol and kinase signaling pathways as well as growth cone formation (Bretscher *et al.*, 2000; Ramesh, 2004). Previous work done by Dr. F. Gunn-Moore had shown that FERM domain containing proteins bound to the 28 C-terminal residues of neurofascin, 14 of which contain a sequence highly homologous to a FERM domain-binding motif found in other receptors (Gunn-Moore, unpublished results). An analysis of the amino acid sequence of NrCAM showed that many of these amino acids had been conserved, suggesting it too may bind to NrCAM's cytoplasmic sequence. Therefore, FERM domain containing proteins were good candidate binding proteins for NrCAM, particularly in the growth cone. Initial studies showed that one of the 4.1 Superfamily proteins Ezrin was present at the same time and place in the cell and neuron. Yeast two hybrid studies were performed to confirm the interaction for Ezrin and two other FERM domain containing proteins radixin and willin. Unfortunately, despite the ability of neurofascin to bind to the proteins, NrCAM itself showed no measurable interaction. The L1-ezrin interaction with Ezrin was due to the presence of a RSLE motif (Dickson *et al.*, 2002). This motif is also found in certain isoforms of NrCAM. However, NrCAM containing this motif did not bind to ezrin, radixin or willin. Interestingly L1 containing the RSLE sequence, despite binding strongly to ezrin, did not show measurable binding ability to either radixin or willin. Finally, it was

tested whether NrCAM could bind to EBP50, a protein known to couple proteins with FERM domains to membrane receptors (Bretscher *et al.*, 2000). However though neurofascin did show measurable binding to EBP50 NrCAM did not. Thus, it was concluded that NrCAM, L1 and neurofascin all show different binding abilities to members of the FERM family. The results of Chapter 5 have been summarised by Figure 7-2.

7.3 How does tyrosine phosphorylation of NrCAM occur and does it affect ankyrin binding.

NrCAM's only known signalling partner was ankyrin and the NrCAM-ankyrin interaction was believed to be regulated by tyrosine phosphorylation of the tyrosine of the amino acid motif FIGQY of the NrCAM cytoplasmic terminus. Much of the previous work done on L1-CAM tyrosine phosphorylation had been completed on neurofascin and L1 and these findings were to be reconfirmed for NrCAM's interaction with ankyrin. It was further hoped that some details of the pathways upstream of FIGQY tyrosine phosphorylation could be elucidated. The two approaches used were unfortunately subject to technical difficulties.

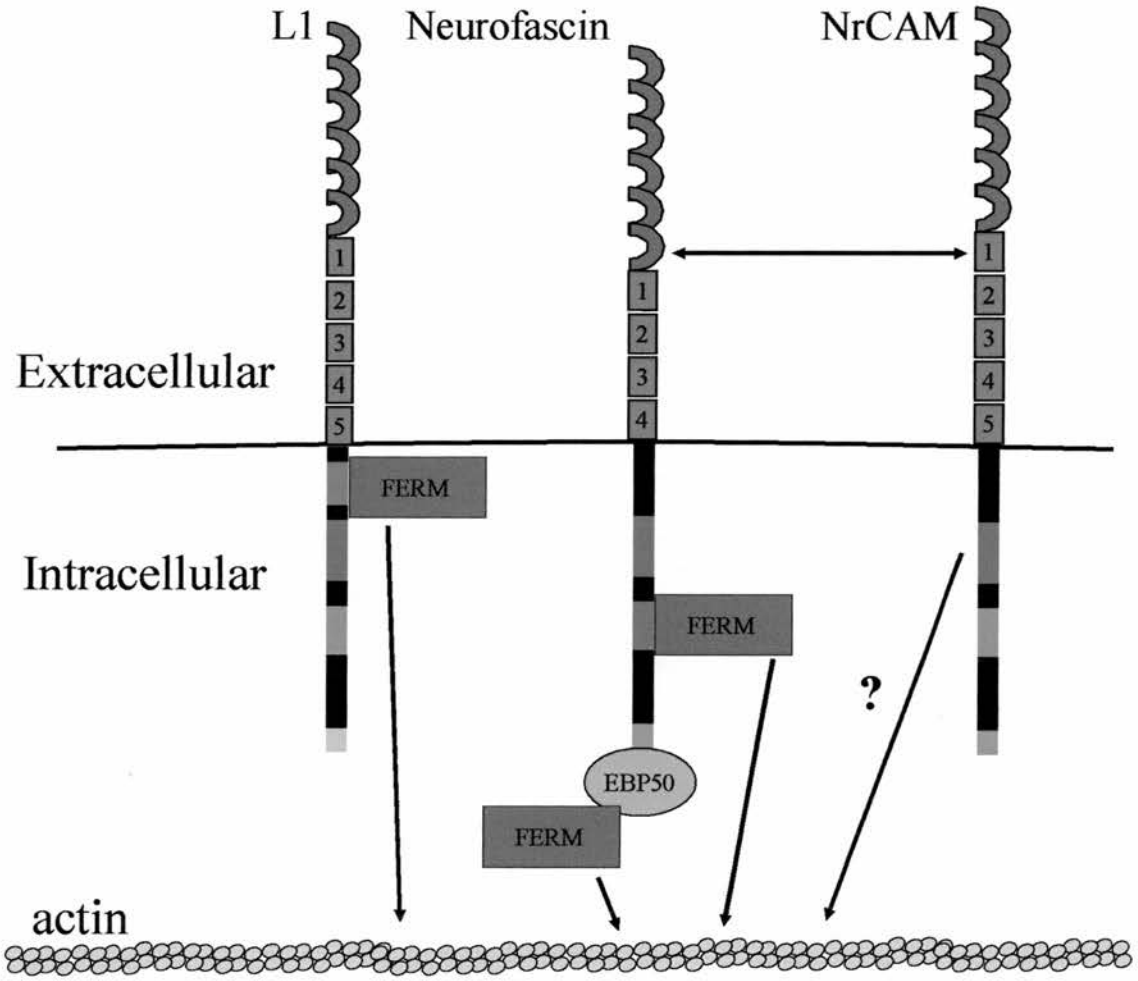

Figure 7-2. A diagrammatic representation of the results in Chapter 5, demonstrating how proteins of the 4.1 superfamily, that contain FERM domains, may link members of the L1-CAM family to the actin cytoskeleton. The cytoplasmic termini of the L1-CAM protein have been shown diagrammatically. The red box in the cytoplasmic terminus of L1 indicates the presence of an alternatively spliced RSLE motif. The green boxes represent the ankyrin-binding domain. The dark blue box is the proposed FERM binding domain of neurofascin. The pale blue box is the equivalent amino acids of the FERM domain in neurofascin present in NrCAM and L1. The dark pink boxes are the PDZ binding domains of NrCAM and neurofascin. The pale pink box is the equivalent amino acids of the PDZ domain of NrCAM present in L1.

The first approach involved the immunoprecipitation of NrCAM receptor from cells that had been stimulated by a phosphatase inhibitor. The first attempts were made to immunoprecipitate out HA-NrCAM using an antibody to the N-terminal HA epitope. However, it became clear that NrCAM immunoprecipitated out was subject to posttranslational cleavage by furin and thus may not have contained the cytoplasmic terminus of NrCAM. It was therefore necessary to find a method that was guaranteed to immunoprecipitate out NrCAM containing the cytoplasmic terminus. In order to do this it was necessary to produce an antibody to the cytoplasmic terminus of NrCAM. Unfortunately, the antibody produced could identify purified chimeric GST-NrCAM but could not identify NrCAM transfected into cell lines. It was therefore attempted to circumvent the furin cleavage problem by producing a NrCAM clone that did not have the third fibronectin type III-like (FNIII-like) repeat that is normally cleaved by furin. Unfortunately, the initial attempts at immunoprecipitation using this clone were unsuccessful.

The second approach was to use the published observation that unphosphorylated neurofascin can bind to ankyrin-GFP such that the labeled protein translocates from the cytoplasm to the plasma membrane in HEK293 cells. The initial experiments looked promising, and ankyrin-GFP was observed translocating to the plasma membrane only in cells transfected with NrCAM. However this interaction was difficult to quantify, making it unsuitable for the assays that would be necessary to establish the tyrosine phosphorylation signaling pathways. However viewing live cells did show that the NrCAM-ankyrin interaction was highly dynamic and that NrCAM in stressed cells did not appear to be binding to ankyrin. Indeed the

dynamics of this interaction were so quick that it was impossible to image them using the microscope and imaging software available.

7.4 Possible functions of the VHS-GGA/NrCAM interaction.

In Chapter 3 the VHS domain of GGA1 was also a potential binding candidate of NrCAM. Though this interaction has yet to be reconfirmed there are some possible functions of the interaction worth speculating about.

Most of the VHS-GGA/receptor interactions reported to date are believed to traffic receptors from the TGN to the early/late endosome (Bonifacino, 2004). Nothing is known about the trafficking of NrCAM to the cell surface. However NrCAM is expected to be cleaved by furin and furin is localised principally in the TGN where it cycles between the sorting compartment, the cell surface and the early endosomes (reviewed Nakayama, 1997; Thomas, 2002). Other binding partners of the GGA VHS domain such as BACE are also furin cleaved (Creemers et al., 2001). Therefore, localisation of NrCAM to the TGN and the endosome could potentially make it available to the activities of this enzyme before reaching the plasma membrane.

Furthermore the major locations of endosomes and lysosomes within developing neurons axon are around branch points and growth cones (Overly and Hollenbeck, 1996). NrCAM expression has been described as potentially being down stream of branching events in the kidney (Valerius et al., 2002) and NrCAM has an important role to play in the axonal growth cone (Faivre-Sarrailh et al., 1999). Thus, the

GGA-VHS protein could be delivering NrCAM to locations within the axon close to where it will be expressed.

Another possibility is that the GGA-VHS binding domain could target NrCAM to the lysosome (via the endosome) for destruction when the receptor is over expressed. This would require that the VHS binding motif be masked during normal protein expression and unmasked during protein over expression.

It should also be noted that GGA-VHS interaction with membrane receptors may have undefined role(s) other than its transport from the TGN to the endosome (Bonifacino, 2004) and this role could also apply to a GGA-VHS/NrCAM interaction.

However, the interaction of NrCAM and GGA still needs to be verified. A first step in considering the validity of the NrCAM-GGA interaction would be to establish does NrCAM localise to the TGN, for example does NrCAM co-localises with a marker for the TGN such as TGN38? Secondly, does NrCAM bind to full length GGA1/2/3 and can it be proven using a second biochemical technique such as the Tandem Affinity Purification procedure? Thirdly, if you interfere with the NrCAM/GGA interaction, for example by mutating the essential aspartate, will this interfere with NrCAM's trafficking to the plasma membrane surface?

7.5 Does GIPC bind to NrCAM?

In Chapter 4 it was not possible to reconfirm the NrCAM-GIPC interaction using a second biochemical technique, which suggested that NrCAM and GIPC are not

binding partners. This is a common occurrence for PDZ interactions in the yeast two-hybrid screen. For example, stargazin a protein in the post-synaptic density has a class 1 PDZ domain. PSD-95, PSD-93, SAP97 and SAP102 were found to be PDZ binding partners of stargazin, using a similar yeast two-hybrid system used in this thesis. However further testing showed that only PSD-93 and PSD-95 interacted *in vivo* (Dakoji et al., 2003). Similarly other authors believe that it is difficult to determine PDZ interactions using the yeast-two hybrid screen (where tertiary and quaternary structural information is lost) or in over-expression studies (where specificity due to binding affinities and cellular compartmentalization can be masked)" (van Zundert et al., 2004). Thus binding of NrCAM to GIPC could be a false positive of the yeast two-hybrid screen.

However proving a false positive is difficult. With the exception of TAP analysis, all of the binding assays used to test the NrCAM-GIPC interaction experienced technical difficulties and proving the binding of GIPC to any of its PDZ domain binding-partners had been reported as difficult by other groups. In general, this is believed to be due the transient nature of the GIPC-membrane receptor interaction.

It is notable for example that the potential interaction shown for the GST pull-down of GIPC in Figure 4-22 was in the strongest ionic buffer. Though the antibody to GIPC may have been unspecific, it is unlikely that this result was due to the antibody binding to GST-NrCAM breakdown products as there was no 45 kDA band (full-length GST-NrCAM) on the blot. The results have been discounted as they could not be proven using the FLAG tagged GIPC construct and because the full-

length GIPC protein did not bind using the yeast-two hybrid screen. However N-terminally tagging the full-length GIPC construct with FLAG and Gal4 could have affected its structure. Both the GH1 and GH2 domains of GIPC (Figure 3-6) are believed to interact with each other (Bunn and Jensen, 1999). It is possible that an N-terminal tag will interfere with this and cause the PDZ domain to be inaccessible to its binding partners. It may also be possible that the presence of the GH2 domain interfered with the binding of full-length GIPC to NrCAM using the yeast two-hybrid assay. The function of the GH2 domain is still unknown. However it is possible the GH2 domain may contain a competing organellular targeting sequences that interferes with the targeting of the construct to the yeast nucleus and thus prevent binding in the nucleus by (McAlister-Henn et al., 1999).

So does GIPC bind to NrCAM? GIPC is an attractive candidate to bind to NrCAM for several reasons:

GIPC binds to proteins in similar neuronal locations and with similar functions as NrCAM. For example GIPC binds to two members of the semaphorin family neuropilin-1 and Semaphorin 4C (Cai and Reed, 1999; Wang *et al.*, 1999). The semaphorin family has an important role in axon repulsion and the trans binding of L1 to neuropilin-1 converts SEM 3A induced repulsion to attraction (Castellani, 2002; Castellani et al., 2002). Importantly Semaphorin 4C also binds to SAP102 (Inagaki et al., 2001).

Furthermore GIPC seems to function in the general trafficking of newly synthesised membrane receptors from the trans Golgi network (TGN) to the plasma membrane (De Vries *et al.*, 1998; Blobe *et al.*, 2001; Liu *et al.*, 2001) and the

endocytosis/retrograde transport of receptors at the plasma membrane (De Vries *et al.*, 1998; Wang *et al.*, 1999; Lou *et al.*, 2002) and it is not unreasonable to believe that this rather general function could be its role in binding NrCAM..

Importantly one of GIPC's binding partners, myosin VI, does not bind to the PDZ domain of GIPC (Bunn and Jensen, 1999) and it is conceivable that GIPC can bind both PDZ domain containing receptors and myosin VI at the same time. Buss *et al* describe three possible functions for myosin VI in cell migration based upon the cellular locations mentioned above. 1. Myosin VI may be involved in recycling adhesion molecules from the rear end of the cell to the leading edge of the growth cone via clathrin mediated endocytosis. 2. newly synthesised adhesion molecules may be delivered from the TGN to the leading edge or 3. myosin VI binds to a stationery cell adhesion molecule complex associated with the ECM such as E-cadherin and β-catenin. This holds myosin VI stationery with regard to the substrate and as it pushes towards the minus end of the actin filament (from above actin filaments are aligned with their plus ends toward the leading surface of the growth cones) it generates the force necessary for membrane protrusion at the leading edge. It is interesting that NrCAM in cerebellar granule cells shows retrograde actin dependent movement from the leading edge to the base of the growth cone when presented with F3 conjugated microspheres (Faivre-Sarrailh et al., 1999). One speculation would be that bound GIPC and myosin VI allow this retrograde flow.

However, without a second biochemical assay that confirms the NrCAM-GIPC interaction it would be unwise to conclude that the two proteins are binding.

7.6 What is the function of NrCAM binding to SAP102?

The NrCAM-SAP102 interaction has been satisfactorily shown using yeast-two hybrid, TAP analysis and GST-pulldowns (Davey *et al.*, 2005). Further studies have confirmed that the interaction of NrCAM and SAP102 occurs at the second PDZ domain of NrCAM (communication Dr Davey, University of St Andrews). So what is the function of this interaction?

NrCAM is involved in synaptogenesis (Backer *et al.*, 2002). However until recently it has been believed to be presynaptic only. Recently however a paper has been published showing both NrCAM and SAP102 at the post-synaptic density of P2 CA1 hippocampal synapses (Petralia *et al.*, 2005). This is the first report of NrCAM at this location. Importantly NrCAM was at both the pre-synaptic density and post-synaptic density and was seen as clusters of gold particles across the synaptic cleft suggesting that pre-synaptic and post-synaptic NrCAM may be binding homophillically (Petralia *et al.*, 2005). This may suggest a role for NrCAM in the adhesiveness of the synapse. SAP102 could be trafficking NrCAM to this post-synaptic location via the secretory pathway or it could be organizing NrCAM at the post-synaptic density.

The secretory pathway describes a pathway where membrane and secretory proteins are synthesised in the endoplasmic reticulum and sent to the Golgi apparatus and subsequently to the trans Golgi network, where they are organised into secretory vesicles and targeted to the plasma membrane (Burgess and Kelly, 1987; Guo et al., 2000). The exocyst complex (Sec6/8 complex) may aid targeting of these secretory vesicles to the plasma membrane and consists of eight proteins

Sec3, Sec5, Sec6, Sec10, Sec15, Exo70 and Exo84 (Hsu *et al.*, 1996; Hsu *et al.*, 1999). This complex of proteins has been found in the growth cone of cultured differentiated pheochromocytoma cells (PC12) and hippocampal neurons (Hazuka et al., 1999; Vega and Hsu, 2001). The exocyst complex is believed to be a downstream effector of the NGF induced MAP kinase pathway and is essential for neurite outgrowth (Vega and Hsu, 2001). The first two PDZ domain of SAP102 bind to sec8, a member of the exocyst complex (Sans et al., 2003). SAP102 co-localises with Sec6-Sec8 at the rough endoplasmic reticulum, organelles and vesicles of hippocampal neuronal soma, neurites, growth cones, early synaptic contacts and post-synaptic densities (Sans et al., 2003). As discussed in Chapter 3 SAP102 binds to NR2B subunits of the NMDA receptor via its PDZ domains (Muller et al., 1996). Disruption of the exocyst-SAP102 PDZ domain interaction blocks delivery of NMDARS to the post synaptic density of neurons (Sans et al., 2003). Thus, the exocyst-SAP102 interaction is currently believed to be necessary for the correct targeting of at least one binding partner of SAP102 to the plasma membrane of the post-synaptic density. The question remains could it also be targeting NrCAM?

SAP102 may also be acting as a scaffolding molecule that clusters membrane receptors and cytoplasmic proteins to NrCAM. Details of SAP102's other binding partners have been given in Table 3-5. Notably it binds to SynGAP, a synaptic RasGAP that may regulate signal transduction via the Ras signalling pathway (Kim et al 1998) and Pyk2, a tyrosine receptor kinase important in the calcium signalling cascade (Seabold 2003).

NrCAM has a class 1 PDZ domain and therefore, it may bind to other members of the MAGUK family. Notably part length PSD-95 cDNA had been isolated by the Yeast two-Hybrid screen in Chapter 3, although this interaction was not reconfirmed by further screening. Co-localisation of full length PSD-95 and NrCAM was attempted in COS-7 cells (Davey *et al.*, 2005). The two proteins did not co-localise with each other however. This shows that NrCAM can distinguish between both proteins despite having the published binding motif for both (a situation similar to that found for stargazin). This could be due to residues other than the P0 valine and P-2 serine of NrCAMs PDZ binding domain. For example the P-1 and P-6 residues allow SAP102 to bind to $5HT_C$ and not $5HT_{2A}$ receptors (Becamel et al., 2004).

NrCAM's binding to the other MAGUKS PSD-93 and SAP97 has not been tested yet. SAP97 is a particularly intriguing possibility as it is presynaptic (Muller et al., 1995) and NrCAM staining has recently been shown to more dense at presynapses than post synapses (Petralia *et al.*, 2005).

7.7 Does NrCAM bind to members of the 4.1 superfamily?

The sequences within the cytoplasmic terminus of neurofascin and L1 that bind to FERM domain containing proteins may reflect the different functions of 4.1 superfamily binding to both proteins. Neurofascin binds to FERM domain containing proteins at a sequence C-terminal to its ankyrin-binding site that is present in all reported isoforms of neurofascin. L1 however will only bind to ezrin if the RSLE motif is present. The RSLE motif is only present in neuronal isoforms of

L1 and is responsible for sorting the receptor to the growth cone and its AP-2 mediated endocytosis within the growth cone (Kamiguchi and Lemmon, 1998; Kamiguchi et al., 1998). Therefore this suggests that L1 binding to ezrin may be specific to neuronal growth cones and have a role in growth cone advance. As NrCAM does not appear to interact directly with members of the 4.1 superfamily the question remains how does it couple to retrograde flow in a growth cone? There are several possibilities:

1. For example α-actinin has been suggested as a potential candidate to bind to NrCAM (Falk et al., 2004). TAG-1 beads bind in trans to the extracellular part of NrCAM in the plasma membrane of neuroblastoma cells and subsequently α-actinin and F-actin are recruited to the site of cell contact with TAG-1 beads but ezrin is not (Falk et al., 2004). 2. It is also possible that NrCAM is linked to the retrogradly moving cytoskeleton solely via ankyrin. Ankyrin binding to L1 has been shown to induce stationary behaviour by L1 in neuroblastomas (Gil *et al.*, 2003b). However ankyrin binding has also been shown to mediate rear-ward movement of L1 in neurite initiation (Nishimura et al., 2003). Therefore, there is potential for ankyrin to play at least a small role in NrCAM retrograde movement. Furthermore, there is potentially an as yet unidentified PDZ domain containing protein that could link NrCAM to the retrogradly moving cytoskeleton.

3. EBP50 is not the only known protein that links membrane receptors to ezrin and other FERMs. E3KARP is a protein that is closely related to EBP50 and which also links membrane receptors to FERM proteins (Bretscher et al., 2000). If an, as yet,

unidentified linker protein is binding to NrCAM and ezrin this could explain their co-localisation?

4. NrCAM could be binding to a FERM domain containing protein other than ezrin, radixin and willin. For example moesin has been shown to be important in growth cone morphology (Paglini et al., 1998).

5. NrCAM may be binding in cis to another membrane receptor that in turn binds to that actin cytoskeleton via an FERM domain containing protein. For example the extracellular region of NrCAM binds to neurofascin and neurofascin binds to ezrin (Grumet, 1997). Indeed deletion of NrCAM's cytoplasmic terminus does not reduce its ability to move retrogradly in neuroblastoma cells (Falk et al., 2004). Furthermore, deletion of the extracellular fibronectin type III-like (FNIII-like) repeats of NrCAM did not interfere with its retrograde movement. However, deletion of both the FNIII-like domain and the cytoplasmic terminus together eliminates NrCAM retrograde movement (Falk et al., 2004). This implies that NrCAM must bind to both an extracellular molecule and intracellular molecule to couple to the retrogradly moving cytoskeleton.

7.8 The tyrosine phosphorylation of NrCAM and its binding to ankyrin.

Despite the technical problems in developing an assay to identify the signalling pathways involved in the tyrosine phosphorylation of NrCAM in Chapter 6, the search for cytoplasmic binding partners of NrCAM in chapter 3 and 4 have identified two intriguing possibilities. One potential binding partner was the VHS

domain of GGA1, which bound to the ankyrin binding site of the L1-CAMs. As speculated above GGA1 may be trafficking NrCAM to locations in the neuron. However, it did not bind to NrCAM when the tyrosine of the FIGQY motif was mutated to a glutamate. This is thought to mimic phosphorylation of the NrCAM receptor, thus raising the possibility that tyrosine phosphorylation not only regulates ankyrin binding but GGA1 binding and subsequently NrCAM's trafficking. The other binding partner GIPC can also bind to TrkA, which is the neurotrophic receptor for nerve growth factor. It is believed that GIPC simultaneously binds to TrkA and a PDZ binding receptor (Lou *et al.*, 2001). Thus, GIPC could be linking TrkA to NrCAM. Hence, the phosphorylation of NrCAM may be a direct event between the tyrosine kinase domain and of the Trk receptor and NrCAM. Before either of these possibilities can be investigated further, the GGA1 and GIPC interactions will have to be reconfirmed.

References:

Agatep, R., Kirkpatrick, R. D., Parchaliuk, D. L., Woods, R. A. and Gietz, R. D. (1998). Transformation of Saccharomyces cerevisiae by the lithium acetate/single-stranded carrier DNA/polyethylene glycol (LiAc/ss-DNA/PEG) protocol.: Technical Tips Online.

Aitkenhead, M., Wang, S. J., Nakatsu, M. N., Mestas, J., Heard, C. and Hughes, C. C. (2002). Identification of endothelial cell genes expressed in an in vitro model of angiogenesis: induction of ESM-1, (beta)ig-h3, and NrCAM. *Microvasc. Res.* **63**, 159-171.

Arroyo, E. J. and Scherer, S. S. (2000). On the molecular architecture of myelinated fibres. *Histochem. Cell Biol.* **113**, 1-18.

Atkins, A. R., Chung, J., Deechongkit, S., Little, E. B., Edelman, G. M., Wright, P. E., Cunningham, B. A. and Dyson, H. J. (2001). Solution structure of the third immunoglobulin domain of the neural cell adhesion molecule N-CAM: can solution studies define the mechanism of homophilic binding? *J. Mol. Biol.* **311**, 161-172.

Awan, A., Lucic, M. R., Shaw, D. M., Sheppard, F., Westwater, C., Lyons, S. A. and Stern, P. L. (2002). 5T4 interacts with TIP-2/GIPC, a PDZ protein, with implications for metastasis. *Biochem. Biophys. Res. Commun.* **290**, 1030-1036.

Backer, S., Sakurai, T., Grumet, M., Sotelo, C. and Bloch-Gallego, E. (2002). Nr-CAM and TAG-1 are expressed in distinct populations of developing precerebellar and cerebellar neurons. *Neuroscience* **113**, 743-748.

Bamburg, J. R. (2003). Introduction to cytoskeletal dynamics and pathfinding in neuronal growth cones. *J. Histochem. Cytochem.* **51**, 407-409.

Bartel, P. L. and Field, S. (1997). The yeast two-hybrid system. Oxford: Oxford University Press.

Bartsch, U. (2003). Neural CAMs and their role in the development and organization of myelin sheaths. *Front. Biosci.*, d477-490.

Becamel, C., Gavarini, S., Chanrion, B., Alonso, G., Galeotti, N., Dumuis, A., Bockaert, J. and Marin, P. (2004). The Serotonin 5-HT2A and 5-HT2C Receptors Interact with Specific Sets of PDZ Proteins. *J. Biol. Chem.* **279**, 20257-20266.

Bennett, V. and Chen, L. (2001). Ankyrins and cellular targeting of diverse membrane proteins to physiological sites. *Curr. Opin. Cell Biol.* **13**, 61-67.

Bennett, V. and Lambert, S. (1999). Physiological roles of axonal ankyrins in survival of premyelinated axons and localization of voltage-gated sodium channels. *J. Neurocytol.* **28**, 303-18.

Berghs, S., Aggujaro, D., Dirkx, R. J., Maksimova, E., Stabach, P., Hermel, J.-M., Zhang, J.-P., Philbrick, W., Slepnev, V., Ort, T. et al. (2000). βIV Spectrin, a new spectrin localised at axon initial segments and nodes of Ranvier in the central and peripheral nervous system. *J. Cell Biol.* **151**, 985-1001.

Bezprozvanny, I. and Maximov, A. (2001). Classification of PDZ domains. *FEBS Lett.* **509**, 457-462.

Bhat, M. A. (2003). Molecular organization of axo-glial junctions. *Curr. Opin. Biol.* **13**, 552-559.

Blobe, G. C., Liu, X., Fang, S. J., How, T. and Lodish, H. F. (2001). A novel mechanism for regulating transforming growth factor beta (TGF-beta) signaling. Functional modulation of type III TGF-beta receptor expression through interaction with the PDZ domain protein, GIPC. *J Biol. Chem.* **276**, 39608-39617.

Bohlson, S. S., Zhang, M., Ortiz, C. E. and Tenner, A. J. (2004). CD93 interacts with the PDZ domain-containing adaptor protein GIPC: implications in the modulation of phagocytosis. *J. Leukocyte Biol.* **77**, 1-10.

Boman, A. L. (2001). GGA proteins: new players in the sorting game. *J. Cell Sci.* **114**, 3413-3418.

Boman, A. L., Zhang, C., Zhu, X. and Kahn, R. A. (2000). A family of ADP-ribosylation factor effectors that can alter membrane transport through the trans-Golgi. *Mol. Biol. Cell* **11**, 1241-1255.

Bonifacino, J. S. (2004). The GGA proteins: adaptors on the move. *Nature Reviews: Molecular Cell Biology* **5**, 23-32.

Bonifacino, J. S. and Traub, L. M. (2003). Signals for sorting of transmembrane proteins to endosomes and lysosomes. *Ann. Rev. Biochem.* **72**, 395-447.

Breen, K. C., Coughlan, C. M. and Hayes, F. D. (1998). The role of glycoproteins in neural development function, and disease. *Mol Neurobiol* **16**, 163-220.

Bretscher, A., Chambers, D., Nguyen, R. and Reczek, D. (2000). ERM-Merlin and EBP50 protein families in plasma membrane organization and function. *Ann. Rev. Cell Dev. Biol.* **16**, 113-143.

Bretscher, A., Edwards, K. and Fenon, G. (2002). ERM proteins and merlin: integrators at the cell cortex. *Nat. Rev. Mol. Cell Biol.* **3**, 589-599.

Brophy, P. J. (2001). Axoglial junctions: Separate the channels or scramble the message. *Curr. Biol.* **11**, R555-557.

Brower, D. L., Brower, S. M., Hayward, D. C. and Ball, E. E. (1997). Molecular evolution of integrins: genes encoding integrin β subunits from a coral and a sponge. *Proc. Natl. Acad. Sci.* **94**, 9182-9187.

Brummendorf, T., Kenwrick, S. and Rathjen, F. G. (1998). Neural cell recognition molecule L1: from cell biology to human hereditary brain malformations. *Curr. Opin. Neurobiol.* **8**, 87-97.

Brummendorf, T. and Rathjen, F. G. (1996). Structure/function relationships of axon-associated adhesion receptors of the immunoglobulin superfamily. *Curr. Opin. Neurobiol.* **6**, 584-593.

Buhusi, M., Midkiff, B. R., Gates, A. M., Richter, M., Schachner, M. and Maness, P. F. (2003). Close homolog of L1 (CHL1) is an enhancer of integrin-mediated cell migration. *J. Biol. Chem.* **278**, 25024-25031.

Bunn, R. C. and Jensen, M. A. (1999). Protein interactions with the Glucose Transporter Binding Protein GLUT1CBP That provide a link between GLUT1 and the Cytoskeleton. *Mol. Biol. Cell* **10**, 819-832.

Burgess, T. L. and Kelly, R. B. (1987). Constitutive and regulated secretion of proteins. *Annu. Rev. Cell Biol.* **3**, 243-294.

Cai, H. and Reed, R. R. (1999). Cloning and characterization of neuropilin-1-interacting protein: a PSD-95/Dlg/ZO-1 domain-containing protein that interacts with the cytoplasmic domain of neuropilin-1. *J. Neurosci.* **19**, 6519-6527.

Calderwood, D. A., Shattil, S. J. and Ginsberg, M. H. (2000). Integrins and actin filaments: reciprocal regulation of cell adhesion and signaling. *J. Biol. Chem.* **275**, 22607-22610.

Castellani, V. (2002). The function of neuropilin/L1 complex. *Adv. Exp. Med. Biol.* **515**, 91-102.

Castellani, V., De Angelis, E., Kenwrick, S. and Rougon, G. (2002). Cis and trans interactions of L1 with neuropilin-1 control axonal responses to semaphorin 3A. *EMBO J.* **21**, 6348-6357.

Castelo, L. and Jay, D. G. (1999). Radixin is involved in lamellipodial stability during nerve growth cone motility. *Mol. Biol. Cell* **10**, 1511-1520.

Chaisuksunt, V., Campbell, G., Zhang, Y., Schachner, M., Lieberman, A. R. and Anderson, P. N. (2000a). The cell recognition molecule CHL1 is strongly upregulated by injured and regenerating thalamic neurons. *J. Comp. Neurol.* **425**, 382-392.

Chaisuksunt, V., Zhang, Y., Anderson, P. N., Campbell, G., Vaudano, E., Schachner, M. and Lieberman, A. R. (2000b). Axonal regeneration from CNS neurons in the cerebellum and brainstem of adult rats: correlation with the patterns of expression and distribution of messenger RNAs for L1, CHL1, c-jun and growth-associated protein-43. *Neuroscience* **100**, 87-108.

Chen, D., Xu, W., Bales, E., Colmenares, C., Conacci-Sorrell, M., Ishii, S., Stavnezer, E., Campisi, J., Fisher, D. E., Ben-Ze'ev, A. et al. (2003). SKI activates WNT/-B-Catenin signaling in human melanoma. *Cancer Res.* **63**, 6626-6634.

Chen, S., Mantei, N., Dong, L. and Schachner, M. (1999). Prevention of neuronal cell death by neural adhesion molecules L1 and CHL1. *J. Neurobiol.* **38**, 428-439.

Chishti, A. H., Kim, A. C., Marfatia, S. M., Lutchmeman, M., Hanspal, M., Junidal, H., Liu, S., Low, P. S., Rouleau, G. A., Mohandas, N. et al. (1998). The FERM domain: a unique module involved in the linkage of the cytoplasmic proteins to membrane. *Trends Biochem. Sci.* **23**, 281-282.

Chung, H. J., Huang, Y. H., Lau, L.-F. and Huganir, R. L. (2004). Regulation of the NMDA receptor complex and trafficking by activity-dependent phosphorylation of the NR2B subunit PDZ ligand. *J. Neurosci.* **24**, 10248-10259.

Collinson, J. M., Marshall, D., Gillespie, C. S. and Brophy, P. J. (1998). Transient expression of neurofascin by oligodendrocytes at the onset of myelinogenesis: implications for mechanisms of axon-glial interaction. *Glia* **23**, 11-23.

Conacci-Sorrell, M. E., Ben-Yedidia, T., Shtutman, M., Feinstein, E., Einat, P. and Ben-Ze'ev, A. (2002). Nr-CAM is a target gene of the beta-catenin/LEF-1 pathway in melanoma and colon cancer and its expression enhances motility and confers tumorigenesis. *Genes Dev.* **16**, 2058-2072.

Cramer, L. P. (1997). Molecular mechanism of actin-dependent retrograde flow in lamellipodia of motile cells. *Front. Biosci.* **2**, d260-270.

Creemers, J. W., Ines Dominguez, D., Plets, E., Serneels, L., Taylor, n. A., Multhaup, G., Craessaerts, K., Annaert, W. and De Strooper, B. (2001). Processing of the beta-secretase by furin and other members of the proprotein convertase family. *J. Biol. Chem.* **276**, 4211-4217.

Crossin, K. L. and Krushel, L. A. (2000). Cellular signaling by neural cell adhesion molecules of the Immunoglobulin superfamily. *Dev. Dyn.* **218**, 260-279.

Custer, A. W., Kazarinova-Noyes, K., Sakurai, T., Xu, X., Simon, W., Grumet, M. and Shrager, P. (2003). The role of ankyrin binding NrCAM in node of Ranvier formation. *J. Neurosci.* **23**, 10032-10039.

Dahlin-Huppe, K., Berglund, E. O., Ranscht, B. and Stallcup, W. B. (1997). Mutational analysis of the L1 neuronal cell adhesion molecule identifies membrane-proximal amino acids of the cytoplasmic domain that are required for cytoskeletal anchorage. *Mol. Cell. Neurosci.* **9**, 144-156.

Dakoji, S., Tomita, S., Karimzadegan, S., Nicoll, R. A. and Bredt, D. S. (2003). Interaction of transmembrane AMPA receptor regulatory proteins with multiple membrane associated guanylate kinases. *Neuropharmacology* **45**, 849-856.

Dance, A. L., Miller, M., Seragaki, S., Aryal, P., White, B., Aschenbrenner, L. and Hasson, T. (2004). Regulation of myosin-VI targeting to endocytic compartments. *Traffic* **5**, 798-813.

Davey, F., Hill, M., Falk, J., Sans, N. and Gunn-Moore, F. J. (2005). Synapse associated protein 102 is a novel binding partner to the cytoplasmic terminus of neurone-glial related cell adhesion molecule. *J. Neurochem.* **94**, 1243-1253.

Davis, J. Q. and Bennett, V. (1993). Ankyrin-binding activity of nervous system cell adhesion molecules expressed in adult brain. *J. Cell Sci. Suppl.* **17**, 109-117.

Davis, J. Q. and Bennett, V. (1994). Ankyrin binding activity shared by the neurofascin/L1/NrCAM family of nervous system cell adhesion molecules. *J. Biol. Chem.* **269**, 27163-27166.

Davis, J. Q., Lambert, S. and Bennett, V. (1996). Molecular composition of the node of Ranvier: identification of ankyrin-binding cell adhesion molecules neurofascin (mucin+/third FNIII domain-) and NrCAM at nodal axon segments. *J. Cell Biol.* **135**, 1355-1367.

Davis, J. Q., McLaughlin, T. and Bennett, V. (1993). Ankyrin-binding proteins related to nervous system cell adhesion molecules: candidates to provide transmembrane and intercellular connections in adult brain. *J. Cell Biol.* **121**, 121-133.

De Vries, L., Lou, X., Zhao, G., Zheng, B. and Farquhar, M. G. (1998). GIPC, a PDZ domain containing protein, interacts specifically with the C terminus of RGS-GAIP. *Proc. Natl. Acad. Sci. U S A* **95**, 12340-12345.

Dell'Angelica, E. C., Puertollano, R., Mullins, C., Aguilliar, R. C., Vargas, J. D., Hartnell, L. M. and Bonifacino, J. S. (2000). GGAs: A family of ADP Ribosylation Factor-binding Proteins Related to Adaptors and Associated with the Golgi Complex. *J. Cell Biol.* **149**, 81-93.

DeMali, K. A., Wennerberg, K. and Burridge, K. (2003). Integrin signaling to the actin cytoskeleton. *Curr. Opin. Cell Biol.* **15**, 572-582.

DeMarco, S. J. and Strehler, E. E. (2001). Plasma membrane Ca2+-atpase isoforms 2b and 4b interact promiscuously and selectively with members of the membrane-associated guanylate kinase family of PDZ (PSD95/Dlg/ZO-1) domain-containing proteins. *J. Biol. Chem.* **276**, 21594-21600.

Demyanenko, G. P., Shibata, Y. and Maness, P. F. (2001). Altered distribution of dopaminergic neurons in the brain of L1 null mice. *Brain Res. Dev. Brain Res.* **126**, 21-30.

Demyanenko, G. P., Tsai, A. Y. and Maness, P. F. (1999). Abnormalities in neuronal process extension, hippocampal development, and ventricular system of L1 knockout mice. *J. Neurosci.* **19**, 4907-4920.

Dent, E. W. and Gertler, F. B. (2003). Cytoskeletal dynamics and transport in growth cone motility and axon guidance. *Neuron* **40**, 209-227.

Dhodapkar, K. M., Friedlander, D., Scholes, J. and Grumet, M. (2001). Differential expression of the cell-adhesion molecule Nr-CAM in hyperplastic and neoplastic human pancreatic tissue. *Hum. Pathol.* **32**, 396-400.

Dickson, B. J. (2001). Rho GTPases in growth cone guidance. *Curr. Opin. Neurobiol.* **11**, 103-110.

Dickson, B. J. and Senti, K.-A. (2002). Axon guidance: growth cones make an unexpected turn. *Curr. Biol.* **12**, R218-R220.

Dickson, T. C., Mintz, C. D., Benson, D. L. and Salton, S. R. J. (2002). Functional binding interaction identified between the axonal CAM L1 and members of the ERM family. *J. Cell Biol.* **157**, 1105-1112.

Doherty, P., Williams, G. and Williams, E. J. (2000). CAMs and axonal growth: a critical evaluation of the role of calcium and the MAPK cascade. *Mol. Cell Neurosci.* **16**, 283-295.

Doray, B., Bruns, K., Ghosh, P. and Kornfeld, S. A. (2002). Autoinhibition of the ligand-binding site of GGA1/3 VHS domains by an internal acidic cluster-dileucine motif. *Proc. Natl. Acad. Sci. U S A* **99**, 8072-8077.

Dry, K., Kenwrick, S., Rosenthal, A. and Platzer, M. (2001). The complete sequence of the human locus for NgCAM-related cell adhesion molecule reveals a novel alternative exon in chick and man and conserved genomic organization for the L1 subfamily. *Gene* **273**, 115-122.

Dunican, D. J. and Doherty, P. (2000). The generation of localised calcium rises mediated by cell adhesion molecules and their role in neuronal growth cone motility. *Mol. Cell Biol. Res. Comm.* **3**, 255-263.

Durfee, T. and et, a. (1993). *Genes Dev* **7**, 555-569.

Dzamba, B. J., Bolton, M. A. and Desimone, D. W. (2001). The integrin family of cell adhesion molecules. In *Cell Adhesion*, (eds B. D. Hames and D. M. Glover), pp. 100-154. Oxford: Oxford university press.

El Mourabit, H., Poinat, P., Koster, J., Sondermann, H., Wixler, V., Wegener, E., Laplantine, E., Geerts, D., Georges-Labouesse, E., Sonnenberg, A. et al. (2002). The PDZ domain of TIP-2/GIPC interacts with the C-terminus of the integrin alpha5 and alpha6 subunits. *Matrix Biol* **21**, 207-214.

Faivre-Sarrailh, C., Falk, J., Pollerberg, E., Schachner, M. and Rougon, G. (1999). NrCAM, cerebellar granule cell receptor for the neuronal adhesion molecule F3, displays an actin-dependent mobility in growth cones. *J. Cell Sci.* **112**, 3015-3027.

Falk, J., Bonnon, C., Girault, J. A. and Faivre-Sarrailh, C. (2002). F3/contactin, a neuronal cell adhesion molecule implicated in axogenesis and myelination. *Biol. Cell* **94**, 327-334.

Falk, J., Thoumine, O., Dequidt, C., Choquet, D. and Faivre-Sarrailh, C. (2004). NrCAM coupling to the Cytoskeleton Depends on Multiple Protein Domains and Partitioning into Lipid Rafts. *Mol. Biol. Cell* **15**, 4695-4709.

Fanning, A. S. and Anderson, J. M. (1999). PDZ domains: functional building blocks in the organization of protein complexes at the plasma membrane. *J. Clinical Invest.* **103**, 767-772.

Fields, S. and Song, O. (1989). A novel genetic system to detect protein-protein interactions. *Nature* **340**, 245-246.

Firestein, B. L., Brenman, J. E., Aoki, C., Sanchez-Perez, A. M., El-Husseini, A. E. and Bredt, D. S. (1999). Cypin: a cytosolic regulator of PSD-95 postsynaptic targeting. *Neuron* **24**, 659-672.

Fitzli, D., Stoeckli, E. T., Kunz, S., Siribour, K., Rader, C., Kunz, B., Kozlov, S. V., Buchstaller, A., Lane, R. P., Suter, D. M. et al. (2000). A direct interaction of axonin-1 with NgCAM-related cell adhesion molecule (NrCAM) results in guidance, but not growth of commissural axons. *J. Cell Biol.* **149**, 951-968.

Fransen, E., D'Hooge, R., Van Camp, G., Verhoye, M., Sijbers, J., Reyniers, E., Soriano, P., Kamiguchi, H., Willemsen, R., Koekkoek, S. K. et al. (1998). L1 knockout mice show dilated ventricles, vermis hypoplasia and impaired exploration patterns. *Hum. Mol. Genet.* 7, 999-1009.

Fransen, E., Van Camp, G., Vits, L. and Willems, P. J. (1997). L1-associated diseases: clinical geneticists divide, molecular geneticists unite. *Hum. Mol. Genet.* **6**, 1625-1632.

Fujita, A. and Yoshihisa, K. (2000). SAP family proteins. *Biochem. Biophys. Res. Commun.* **269**, 1-6.

Furuyama, K. and Sassa, S. (2000). Interaction between succinyl CoA synthetase and the heme-biosynthetic enzyme ALAS-E is disrupted in sideroblastic anemia. *J. Clin. Invest.* **105**, 757-764.

Gao, Y., Li, M., Chen, W. and Simons, M. (2000). Synectin, syndecan-4 cytoplasmic domain binding PDZ protein, inhibits cell migration. *J. Cell Physiol.* **184**, 373-379.

Garcia, E. P., Mehta, S., Blair, L. A., Wells, D. G., Shang, J., Fukushima, T., Fallon, J. R., Garner, C. C. and Marshall, J. (1998). SAP90 binds and clusters kainate receptors causing incomplete desensitization. *Neuron* **21**, 727-739.

Garver, T. D., Ren, Q., Tuvia, S. and Bennett, V. (1997). Tyrosine phosphorylation at a site highly conserved in the L1 family of cell adhesion molecules abolishes ankyrin binding and increases lateral mobility of neurofascin. *J. Cell Biol.* **137**, 703-714.

Gietz, R. D., Triggs-Raine, B., Robbins, A., Graham, K. C. and Woods, R. A. (1997). Identification of proteins that interact with a protein of interest: Applications of the yeast two-hybrid system. *Mol. Cell. Biochem.* **172**, 67-79.

Gietz, R. D. and Woods, R. A. (2002a). Screening for protein-protein interactions in the yeast two-hybrid system. *Methods Mol. Biol.* **185**, 471-486.

Gietz, R. D. and Woods, R. A. (2002b). Transformation of yeast by the Liac/SS carrier DNA/PEG method. *Methods in Enzymology* **350**, 87-96.

Gil, O. D., Sakuai, T., Bradley, A. E., Fink, M. Y., Cassella, M. R., Kuo, J. A. and Felsenfeld, D. P. (2003). Ankyrin binding mediates L1CAM interactions with static components of the cytoskeleton and inhibtis retrograde movement of L1 on the cell surface. *J. Cell Biol.* **162**, 719-730.

Girault, J. A., Oguievetskaia, K., Carnaud, M., Denisenko-Nehrbass, N. and Goutebroze, L. (2003). Transmembrane scaffolding proteins in the formation and stability of nodes of Ranvier. *Biol. Cell* **95**, 447-452.

Girault, J. A. and Peles, E. (2002). Development of nodes of Ranvier. *Curr. Opin. Neurobiol.* **12**, 476-485.

Glienke, J., Schmitt, A. O., Pilarsky, C., Hinzmann, B., Weiss, B., Rosenthal, A. and Thierauch, K. H. (2000). Differential gene expression by endothelial cells in distinct angiogenic states. *Eur. J. Biochem.* **267**, 2820-2830.

GonzalezAgosti, C. and Solomon, F. (1996). Response of radixin to peturbance of growth cone morphology and motility in chick sympathetic neurons *in vitro*. *Cell Motility Cytoskel.* **34**, 122-136.

Gottardi, C. J., Niessen, C. M. and Gumbiner, B. M. (2001). The adherens junction. In *Cell Adhesion*, (ed. M. C. Beckerle), pp. 259-287. Oxford: Oxford University Press.

Grumet, M. (1997). Nr-CAM: a cell adhesion molecule with ligand and receptor functions. *Cell Tissue Res.* **290**, 423-428.

Grumet, M., Mauro, V., Burgoon, M. P., Edelman, G. M. and Cunningham, B. A. (1991). Structure of a new nervous system glycoprotein, Nr-CAM, and its relationship to subgroups of neural cell adhesion molecules. *J. Cell Biol.* **113**, 1399-1412.

Guo, W., Sacher, M., Barrowman, J., Ferro-Novick, S. and Novick, P. (2000). Protein complexes in transport vesicles targeting. *Trends Cell Biol.* **10**, 251-255.

Harper, J. W., Adami, G. R., Wei, N., K., K. and S.J., E. (1993). The p21 cdk-interacting protein Cip1 is a potent inhibitor of [G.sub.1] cyclin-dependent kinases. *Cell* **75**, 805-816.

Harris, B. Z. and Wendell, A. L. (2001). Mechanism and role of PDZ domains in signalling complex assembly. *J. Cell Sci.* **114**, 3219-3231.

Hassel, B., Rathjen, F. G. and Volkmer, H. (1997). Organization of the neurofascin gene and analysis of developmentally regulated alternative splicing. *J. Biol. Chem.* **272**, 28742-28749.

Hazuka, C. D., Foletti, D. L., Hsu, S. C., Kee, Y., Hopf, W. and Scheller, R. H. (1999). The sec6/8 complex is located at neurite outgrowth and axonal synapse-assembly domains. *J. Neurosci.* **19**, 1324-1334.

He, X., Zhu, G., Koelsch, G., rodgers, K. K., Zhang, X. C. and Tang, J. (2003). Biochemical and Structural Characterization of the Interaction of Memapsin 2 (β-Secretase) Cystolic Domain with the VHS Domain of GGA Proteins. *Biochemistry* **42**, 12174-12180.

Hengen, P. H. (1997). False positives from the yeast two-hybrid screen. *Tends in Biocchem. Sci.* **22**, 33-34.

Hillenbrand, R., Molthagen, M., Montag, D. and Schachner, M. (1999). The close homologue of the neural adhesion molecule L1 (CHL1): patterns of expression and promotion of neurite outgrowth by heterophilic interactions. *Eur. J. Neurosci.* **11**, 813-826.

Hillier, B. J., Christopherson, K. S., Prehoda, K. E., Bredt, D. S. and Lim, W. A. (1999). Unexpected modes of PDZ domain scaffolding of nNOS-syntrophin complex. *Science* **284**, 812-815.

Hirakawa, T., Galet, C., Kishi, M. and Acoli, M. (2003). GIPC binds to the human lutropin receptor (LHR) through an unusual PDZ domain binding motif and it regulates the sorting of the internalised human choriogonadotropin (hCG) and teh density of cell surface LHR. *J. Biol. Chem.* **278**, 49348-49357.

Hirst, J., Lindsay, M. R. and Robinson, M. S. (2001). GGAs: Roles of different domains and comparison with AP-1 and clathrin. *Mol. Biol. Cell* **12**.

Hirst, J., Lui, W. W. Y., Bright, N. A., Totty, N., Seaman, M. N. J. and Robinson, M. S. (2000). A family of proteins with γ-Adaptin and VHS Domains that facilitate trafficking between the Trans-Golgi Network and the Vacuole/Lysosome. *J. Cell Biol.* **149**, 67-79.

Hortsch, M. (1996). The L1 family of neural cell adhesion molecules: old proteins performing new tricks. *Neuron* **17**, 587-93.

Hortsch, M. (2000). Structural and functional evolution of the L1 family: are four adhesion molecules better than one? *Mol. Cell Neurosci.* **15**, 1-10.

Hortsch, M. (2003). Drosophila Echinoid is an antagonist of Egfr signalling, but is not a member of the L1-type family of cell adhesion molecules. *Development* **130**, 3725-3733.

Hrniewicz-Janowska, A., Czogalla, A., Bok, E. and Sikorsk, A. F. (2002). Ankyrins, multifunctional proteins involved in many cellular pathways. *Folia. Histochem. Cytobiol.* **40**, 239-249.

Hsu, S. C., Hazuka, C. D., Foletti, D. L. and Schneller, R. H. (1999). Targeting vesicles to specific sites on the plasma membrane: the role of teh Sec6/8 complex. *Trends Cell Biol.* **8**, 150-153.

Hsu, S. C., Ting, A. E., Hazuka, C. D., Davanger, S., Kenny, J. W., Kee, Y. and Scheller, R. H. (1996). The mammalian brain rsec6/8 complex. *Neuron* **17**, 1209-1219.

Hu, L. A., Chen, W., Martin, N. P., Whalen, E. J., Premont, R. and Lefkowitz, R. J. (2003). GIPC interacts with the beta 1-adrenergic receptor and regulates beta 1-adrenergic receptor mediated ERK activation. *J. Biol. Chem.* **278**, 26295-26301.

Huang, Y., Jellies, J., Johansen, K. M. and Johansen, J. (1997). Differential glycosylation of tractin and LeechCAM, two novel Ig superfamily members, regulates neurite extension and fascicle formation. *J. Cell Biol.* **138**, 143-157.

Huang, Y. Z., Wang, Q., Won, S., Luo, Z. G., Xiong, W. C. and Mei, L. (2002). Compartmentalized NRG signaling and PDZ domain-containing proteins in synapse structure and function. *Int. J. Dev. Neurosci.* **20**, 173-185.

Huntley, G. W., Gil, O. and Bozdagi, O. (2002). The Cadherin Family of Cell Adhesion Molecules: Multiple roles in synaptic plasticity. *Neuroscientist* **8**, 221-233.

Hynes, R. O. (2002). Integrins: bidirectional, allosteric signalling machines. *Cell* **110**, 673-687.

Inagaki, S., Ohoka, Y., Sugimoto, H., Fujioka, S., Amazaki, M., Kurinami, H., Miyazaki, N., Tohyama, M. and Furuyama, T. (2001). Sema4c, a transmembrane semaphorin, interacts with a post-synaptic density protein, PSD-95. *J. Biol. Chem.* **276**, 9174-9181.

Ives, J. H., Fung, S., Tiwari, P., Payne, H. L. and Thompson, C. L. (2004). Microtubule-associated protein light chain 2 is a stargazin-AMPA receptor complex interacting protein, in vivo. *J. Biol. Chem.*

Jacobsen, L., Madsen, P., Nielsen, M. S., Wijnand, P. M. G., Gliemann, J., Smit, A. B. and Petersen, C. M. (2002). The sorLA cytoplasmic domain interacts with GGA1 and -2 and defines minimum requirements for GGA binding. *FEBS Lett.* **511**, 155-158.

Jay, D. G. (1996). Molecular mechanisms of directed growth cone motility. *Perpect. Dev. Neurobiol.* **4**, 137-145.

Jay, D. G. (2001). A Src-astic response to mounting tension. *J. Cell Biol.* **155**, 327-330.

Jeanneteau, F., Diaz, J., Sokoloff, P. and Griffon, N. (2004). Interactions of GIPC with Dopamine D_2, D_3, but not D_4 Receptors Define a Novel Mode of Regulation of G-Protein -coupled Receptors. *Mol. Biol. Cell* **15**, 696-705.

Jenkins, S. M. and Bennett, V. (2001). Ankyrin-G coordinates assembly of the spectrin-based membrane skeleton, voltage-gated sodium channels, and L1 CAMs at Purkinje neuron initial segments. *J. Cell Biol.* **155**, 739-746.

Jenkins, S. M., Kizhatil, K., Kramarcy, N. R., Sen, A., Sealock, R. and Bennett, V. (2001). FIGQY phosphorylation defines discrete populations of L1 cell adhesion molecules at sites of cell-cell contact and in migrating neurons. *J. Cell Sci.* **114**, 3823-3835.

Jie, C., Xu, Y., Wang, D., Lukin, D., Zipser, B., Jellies, J., Johansen, K. M. and Johansen, J. (2000). Posttranslational processing and differential glycosylation of Tractin, an Ig-superfamily member involved in regulation of axonal outgrowth. *Biochim. Biophys. Acta.* **1479**, 1-14.

Jie, C., Zipser, B., Jellies, J., Johansen, K. M. and Johansen, J. (1999). Differential glycosylation and proteolytical processing of LeechCAM in central and peripheral leech neurons. *Biochim. Biophys. Acta.* **1452**, 161-71.

Kamiguchi, H., Hlavin, M. L., Yamasaki, H. and Lemmon, V. (1998a). Adhesion molecules and inherited disease of the human nervous system. *Annu. Rev. Neurosci.* **21**, 97-125.

Kamiguchi, H. and Lemmon, K. (1998). A neuronal form of the cell adhesion molecule L1 contains a tyrosine-based signal required for axonal sorting to the growth cone. *J. Neurosci.* **18**, 3749-3756.

Kamiguchi, H. and Lemmon, V. (2000a). IgCAMs: bidirectional signals underlying neurite growth. *Current Opin. Cell Biol.* **12**, 598-605.

Kamiguchi, H. and Lemmon, V. (2000b). Recycling of the cell adhesion molecule L1 in axonal growth cones. *J. Neurosci.* **20**, 3676-3686.

Kamiguchi, H., Long, K. E., Pendergast, M., Schaefer, A. W., Rapoport, I., Kirschhausen, T. and Lemmon, V. (1998b). The neural cell adhesion molecule L1 interacts with the AP-2 adaptor and is endocytosed via the Clathrin-mediated pathway. *J. Neurosci.* **18**, 5311-5321.

Kamiguchi, H. and Yoshihara, F. (2001). The role of endocytic L1 trafficking in polarized adhesion and migration of nerve growth cones. *J. Neurosci.* **21**, 9194-9203.

Kaplan, M. R., Cho, M.-H., Ullian, E. M., Isom, L. L., Levinson, S. R. and Barres, B. A. (2001). Differential control of clustering of the sodium channels $Na_v1.2$ and $Na_v1.6$ at developing CNS node of Ranvier. *Neuron* **30**, 105-119.

Katoh, M. (2002). GIPC gene family (Review). *Int J Mol Med* **9**, 585-589.

Kayyem, J. F., Roman, J. M., de la Rosa, E. J., Schwarz, U. and Dreyer, W. J. (1992). Bravo/Nr-CAM is closely related to the cell adhesion molecules L1 and Ng-CAM and has a similar heterodimer structure. *J. Cell Biol.* **118**, 1259-1270.

Kenwrick, S., Watkins, A. and De Angelis, E. (2000). Neural cell recognition molecule L1: relating biological complexity to human disease mutations. *Hum Mol Genet* **9**, 879-886.

Kim, E., Naisbitt, S., Hsueh, Y. P., Rao, A., Rothschild, A., Craig, A. M. and Sheng, M. (1997). GKAP, a novel synaptic protein that interacts with the guanylate kinase-like domain of the PSD-95/SAP90 family of channel clustering molecules. *J. Cell Biol.* **136**, 669-678.

Kim, J. H., Liao, D., Lau, L. F. and Huganir, R. L. (1998). SynGAP: a synaptic RasGAP that associates with the PSD-95/SAP90 protein family. *Neuron* **20**, 683-691.

Kim, S. H., Palukaitis, P. and Park, Y. I. (2002). Phosphorylation of cucumber mosaic virus RNA polymerase 2a protein inhibits formation of replicase complex. *EMBO J.* **21**, 2292-2300.

Kizhatil, K., Wu, Y. X., Sen, A. and Bennett, V. (2002). A new activity of doublecortin in recognition of the phospho-FIGQY tyrosine in the cytoplasmic domain of neurofascin. *J. Neurosci.* **22**, 7948-7958.

Kordeli, E., Lambert, S. and Bennett, V. (1995). AnkyrinG. A new ankyrin gene with neural-specific isoforms localized at the axonal initial segment and node of Ranvier. *J. Biol. Chem.* **270**, 2352-2359.

Koroll, M., Rathjen, F. G. and Volkmer, H. (2001). The neural cell recognition molecule neurofascin interacts with syntenin-1 but not with syntenin-2, both of which reveal self-associating activity. *J. Cell Biol.* **276**, 10646-54.

Krushel, L. A., Prieto, B. A., Cunningham, B. A. and Edelman, G. M. (1993). Expression patterns of the cell adhesion molecule Nr-CAM during histogenesis of the chick nervous system. *Neuroscience* **53**, 797-812.

Kuwahara, H., Araki, N., Makino, K., Masuko, N., Honda, S., Kaibuchi, K., Fukunaga, K., Miyamoto, E., Ogawa, M. and Saya, H. (1999). A novel NE-dlg/SAP102-associated protein, p51-nedasin, related to the amidohydrolase superfamily, interferes with the association between NE-dlg/SAP102 and N-methyl-D-aspartate receptor. *J. Biol. Chem.* **274**, 32204-32214.

Lambert, S., Davis, J. Q. and Bennett, V. (1997). Morphogenesis of the node of Ranvier: co-clusters of ankyrin and ankyrin-binding integral proteins define early developmental intermediates. *J. Neurosci.* **17**, 7025-7036.

Lane, R. P., Chen, X. N., Yamakawa, K., Vielmetter, J., Korenberg, J. R. and Dreyer, W. J. (1996). Characterization of a highly conserved human homolog to the chicken neural cell surface protein Bravo/Nr-CAM that maps to chromosome band 7q31. *Genomics* **35**, 456-465.

Larsson, M., Hjalm, G., Sakwe, A. M., Engstrom, A., Hoglund, A. S., Larsson, E., Robinson, R. C., Sundberg, C. and Rask, L. (2003). Selective interaction of megalin with postsynaptic density-95 (PSD-95)-like membrane-associated guanylate kinase (MAGUK) proteins. *Biochem. J.* **373**, 381-91.

Lau, L. F., Mammen, A., Ehlers, M. D., Kindler, S., Chung, W. J., Garner, C. C. and Huganir, R. L. (1996). Interaction of the N-methyl-D-aspartate receptor complex with a novel synapse-associated protein, SAP102. *J. Biol. Chem.* **271**, 21622-21628.

Lehmann, M., Rigot, V., Seidah, N. G., Marvaldi, J. and Lissitzky, J.-C. (1996). Lack of integrin alpha-chain endoproteolytic cleavage in furin-deficient human colon adenocarcinoma cells LoVo. *Biochem. J.* **317**, 803-809.

Lemaillet, G., Walker, B. and Lambert, S. (2003). Identification of a conserved ankyrin-binding motif in the family of sodium channel alpha subunits. *J. Biol. Chem.* **278**, 27333-27339.

Lennon, G., Auffray, C., Polymeropoulos, M. and Soares, M. B. (1996). The I.M.A.G.E. Consortium: an integrated molecular analysis of genomes and their expression. *Genomics* **33**, 151-152.

Leonoudakis, D., Conti, L. R., Anderson, S., Radeke, C. M., McGuire, L. M., Adams, M. E., Froehner, S. C., Yates, J. R., 3rd and Vandenberg, C. A. (2004). Protein trafficking and anchoring complexes revealed by proteomic analysis of inward rectifier potassium channel (Kir2.x)-associated proteins. *J. Biol. Chem.* **279**, 22331-22346.

Lim, I. A., Hall, D. D. and Hell, J. W. (2002). Selectivity and promiscuity of the first and second PDZ domains of PSD-95 and synapse-associated protein 102. *J. Biol. Chem.* **277**, 21697-21711.

Lin, C. H., Espreafico, E. M., Mooseker, M. S. and Forscher, P. (1996). Myosin drives retrograde F-actin flow in neuronal growth cones. *Biol. Bull.* **192**, 183-185.

Lin, C. H. and Forscher, P. (1995). Growth cone advance is inversely proportional to retrograde F-actin flow. *Neuron* **14**, 763-771.

Liu, T. F., Kandala, G. and Setaluri, V. (2001). PDZ domain protein GIPC interacts with the cytoplasmic tail of melanosomal membrane protein gp75 (tyrosinase-related protein-1). *J. Biol. Chem.* **276**, 35768-35777.

Logeat, F., Bessia, C., Brou, C., LeBail, O., Jarriault, S., Seidah, N. G. and Israel, A. (1998). The Notch1 receptor is cleaved constitutively by a furin-like convertase. *Proc. Natl. Acad. Sci.* **95**, 8108-8112.

Lohi, O., Poussu, A., Mao, Y., Quicho, F. and Lehto, V.-P. (2002). VHS domain - a longshoreman of vesicle lines. *FEBS Lett* **513**, 19-23.

Lou, X., McQuistan, T., Orlando, R. A. and Farquhar, M. G. (2002). GAIP, GIPC and Galphai3 are concentrated in endocytic compartments of proximal tubule cells: putative role in regulating megalin's function. *J. Am. Soc. Nephrol.* **13**, 918-927.

Lou, X., Yano, H., Lee, F., Chao, M. V. and Farquhar, M. G. (2001). GIPC and GAIP form a complex with TrkA: a putative link between G protein and receptor tyrosine kinase pathways. *Mol. Biol. Cell* **12**, 615-627.

Lustig, M., Sakurai, T. and Grumet, M. (1999). Nr-CAM promotes neurite outgrowth from peripheral ganglia by a mechanism involving axonin-1 as a neuronal receptor. *Dev. Biol.* **209**, 340-351.

Lustig, M., Zanazzi, G., Sakurai, T., Blanco, C., Levinson, S. R., Lambert, S., Grumet, M. and Salzer, J. L. (2001). Nr-CAM and neurofascin interactions regulate ankyrin G and sodium channel clustering at the node of Ranvier. *Curr. Biol.* **11**, 1864-1869.

Luthl, A., Laurent, J. P., Figurov, A., Muller, D. and Schachner, M. (1994). Hippocampal long-term potentiation and neural cell adhesion molecules L1 and NCAM. *Nature* **372**, 777-779.

Makino, K., Kuwahara, H., Masuko, N., Nishiyama, Y., Morisaki, T., Sasaki, J., Nakao, M., Kuwano, A., Nakata, M., Ushio, Y. et al. (1997). Cloning and characterization of NE-dlg: a novel human homolog of the Drosophila discs large (dlg) tumor suppressor protein interacts with the APC protein. *Oncogene* **14**, 2425-2433.

Maley, F., Trimble, R. B., Tarentino, A. L. and Plummer, T. H. J. (1989). Characterization of glycoproteins and their associated oligosaccharides through the use of endoglycosidases. *Anal. Biochem* **180**, 195-204.

Masuko, N., Makino, K., Kuwahara, H., Fukunaga, K., Sudo, T., Araki, N., Yamamoto, H., Yamada, Y., Miyamoto, E. and Saya, H. (1999). Interaction of NE-dlg/SAP102, a neuronal and endocrine tissue-specific membrane-associated guanylate kinase protein, with calmodulin and PSD-95/SAP90. A possible regulatory role in molecular clustering at synaptic sites. *J. Biol. Chem.* **274**, 5782-90.

Matise, M. P., Lustig, M., Sakurai, T., Grumet, M. and Joyner, A. L. (1999). Ventral midline cell are required for local control of commissural axon guidance in the mouse spinal cord. *Development* **126**, 3649-3659.

Mauro, V. P., Krushel, L. A., Cunningham, B. A. and Edelman, G. M. (1992). Homophilic and heterophilic binding activities of Nr-CAM, a nervous system cell adhesion molecule. *J. Cell Biol.* **119**, 191-202.

McAlister-Henn, L., Gibson, N. and Panisko, E. (1999). Applications of the Yeast Two-Hybrid System. *Methods* **19**, 330-337.

Mechtersheimer, S., Gutwein, P., Agmon-Levin, N., Stoeck, A., Oleszewski, M., Riedle, S., Postina, R., Fahrenholz, F., Fogel, M., Lemmon, V. et al. (2001). Ectomain shedding of L1 adhesion molecule promotes cell migration by autocrine binding to integrins. *J. Cell Biol.* **155**, 661-673.

Melendez-Vasquez, C. V., Rios, J. C., Zanazzi, G., Lambert, S., Bretsher, A. and Salzer, J. L. (2001). Nodes of Ranvier form in association with ezrin-radixin-moesin (ERM)-positive Schwann cell processes. *Proc. Natl. Acad. Sci.* **98**, 1235-1240.

Michaely, P. and Bennett, V. (1995). Mechanism for binding site diversity on ankyrin. Comparison of binding sites on ankyrin for neurofascin and the Cl-/HCO3- anion exchanger. *J. Biol. Chem.* **270**, 31298-31302.

Mintz, C. D., Dickson, T. C., Gripp, M. L., Salton, S. R. J. and Benson, D. L. (2003). ERMs colocalise transiently with L1 during neocortical growth. *J. Comp. Neurol.* **464**, 438-448.

Mitchison, T. and Kirscher, M. (1988). Cytoskeletal dynamics and nerve growth. *Neuron* **1**, 761-772.

Mohler, P. J., Gramolini, A. O. and Bennett, V. (2002). Ankyrins. *J. Cell Sci.* **115**, 1565-1566.

Molloy, S. S., Anderson, E. D., Jean, F. and Thomas, G. (1999). Bi-cycling the furin pathway: from TGN localization to pathogen activation and embryogenesis. *Trends Cell Biol.* **9**, 28-35.

Montag-Sallaz, M., Schachner, M. and Montag, D. (2002). Misguided axonal projections, neural cell adhesion molecule 180 mRNA upregulation, and altered behavior in mice deficient for the close homolog of L1. *Mol. Cell Biol.* **22**, 7967-7981.

Morales, G., Hubert, M., Brummendorf, T., Treubert, U., Tarnok, A., Schwarz, U. and Rathjen, F. G. (1993). Induction of axonal growth by heterophilic

interactions between the cell surface recognition proteins F11 and Nr-CAM/Bravo. *Neuron* **11**, 1113-1122.

More, M. I., Kirsch, F. P. and Rathjen, F. G. (2001). Targeted ablation of NrCAM or ankyrin-B results in disorganized lens fibers leading to cataract formation. *J. Cell Biol.* **154**, 187-196.

Muller, B. M., Kistner, U., Kindler, S., Chung, W. J., Kuhlendahl, S., Fenster, S. D., Lau, L. F., Veh, R. W., Huganir, R. L., Gundelfinger, E. D. et al. (1996). SAP102, a novel postsynaptic protein that interacts with NMDA receptor complexes in vivo. *Neuron* **17**, 255-265.

Muller, B. M., Kistner, U., Veh, R. W., Cases-Langhoff, C., Becker, B., Gundelfinger, E. D. and Garner, C. C. (1995). Molecular characterization and spatial distribution of SAP97, a novel presynaptic protein homologous to SAP90 and the Drosophila discs-large tumor suppressor protein. *J. Neurosci.* **15**, 2354-2366.

Nagar, B., Overduin, M., Ikura, M. and Rini, J. M. (1996). Structural basis of calcium-induced E-cadherin rigidification and dimerization. *Nature* **380**, 360-364.

Nakayama, K. (1997). Furin: a mammalian substilisin/Kex2p-like endoprotease involved in processing of a wide variety of precursor proteins. *Biochem. J.* **327**, 625-635.

Nayeem, N., Silletti, S., Yang, X.-M., Lemmon, V. P., Reisfeld, R. A., Stallcup, W. B. and Montgomery, A. M. P. (1999). A potential role for the plasmin(ogen) system in the posttranslational cleavage of the neural cell adhesion molecule L1. *J. Cell Sci.* **112**, 4739-4749.

Needham, L. K., Thelen, K. and Maness, P. F. (2001). Cytoplasmic domain mutations of L1 Cell Adhesion Molecule reduce L1-ankyrin interactions. *J. Neurosci.* **21**, 1490-1500.

Nielsen, M. S., Madsen, P., Christensen, E. I., Nykjar, A., Gliemann, J., Kasper, D., Pohlmann, R. and Petersen, C. M. (2001). The sortilin cytoplasmic tail conveys Golgi-endosome transport and binds the VHS domain of the GGA2 sorting protein. *EMBO J.* **20**, 2180-2190.

Nishimura, K., Yoshihara, F., Tojima, T., Ooashi, N., Yoon, W., Mikoshiba, K., Bennett, V. and Kamiguchi, H. (2003). L1-dependent neuritogenesis involves ankyrinB that mediates L1-CAM coupling with retrograde actin flow. *J. Cell Biol.* **163**, 1077-1088.

Overly, C. C. and Hollenbeck, P. J. (1996). Dynamic organization of endocytic pathways in axons of cultured sympathetic neurons. *J. Neurosci.* **16**, 6056-6064.

Paglini, G., Kunda, P., Quiroga, S., Kosik, K. and Caceres, A. (1998). Suppression of radixin moesin alters growth cone morphology, motility and process formation in primary cultured neurons. *J. Cell Biol.* **143**, 443-455.

Parchaliuk, D. L., Kirkpatrick, R. D., Agatep, R., Simon, S. L. and Gietz, R. D. (1999a). Yeast two-hybrid system screening. Part A-screen preparation., pp. 1:66:P01616: Technical tips Online.

Parchaliuk, D. L., Kirkpatrick, R. D., Agatep, R., Simon, S. L. and Gietz, R. D. (1999b). Yeast two-hybrid system screening. Part B-screening procedures., pp. 1:66:P01713: Technical Tips Online.

Pavlou, O., Theodorakis, K., Falk, J., Kutsche, M., Schachner, M., Faivre-Sarrailh, C. and Karagogeos, D. (2002). Analysis of interactions of the adhesion

molecule TAG-1 and its domains with other immunoglobulin superfamily members. *Mol. Cell Neurosci.* **20**, 367-381.

Petralia, R. S., Sans, N., Wang, Y.-X. and Wenhold, R. J. (2005). Ontogeny of postsynaptic density proteins at glutamergic synapses. *Mol. Cell. Neurosci.* **29**, 436-452.

Posthaus, H., C.M., D. and Muller, E. (2003). Novel insights into cadherin processing by subtilisin-like convertases. *FEBS Lett.* **536**, 203-208.

Posthaus, H., Dobois, C. M., Laprise, M.-H., Grondin, F., Suter, M. M. and Muller, E. (1998). Proprotein cleavage of E-cadherin by furin in baculovirus over-expression system: potential role of other convertases in mammalian cells. *FEBS Lett.* **438**, 306-310.

Ptashne, M. and Ma, J. (1988). Converting a eukaryotic transcriptional inhibitor into an activator. *Cell* **55**, 443-446.

Puertollano, R., Aguilar, R. C., Gorshkova, I., Crouch, R. J. and Bonifacino, J. S. (2001). Sorting of Mannose 6-Phospatase Receptors Mediated by GGAs. *Science* **292**, 1712-1716.

Radice, G. L. and Takeichi, M. (2001). Cadherins. In *Cell Adhesion*, (ed. B. M.), pp. 62-99. Oxford: Oxford University Press.

Ramesh, V. (2004). Merlin and the ERM proteins in Schwann cells, neurons and growth cones. *Nat. Rev. Neur.* **5**, 462-470.

Raper, J. A. and Tessier-Lavigne, M. (1999). Growth cones and axon pathfinding, pp. 519-541: Academic Press.

Ratcliffe, C. F., Westenbroek, R. E., Curtis, R. and Catterall, W. A. (2001). Sodium channel beta1 and beta3 subunits associate with neurofascin through their extracellular immunoglobulin-like domain. *J. Cell Biol.* **154**, 427-434.

Rongo, C. (2001). Disparate cell types use a shared complex of PDZ proteins for polarized protein localisation. *Cytokine Growth Factors Reviews* **12**, 349-359.

Rosa, E. J. d. l., Kayyem, J. F., Roman, J. M., Stierhof, Y.-D., Dreyer, W. J. and Schwartz, U. (1990). Topologically restricted appearance in the developing chick retinotectal system of Bravo, a neural surface protein: experimental modulation of environmental cues. *J. Cell Biol.* **111**, 3087-3096.

Rosenbluth, J. (1999). A brief history of myelinated nerve fibres: one hundred and fifty years of controversy. *J. Neurocytol.* **28**, 251-252.

Rousset, R., Fabre, S., Desbois, C., Bantignies, F. and Jalinot, P. (1998). The C-terminus of the HTLV-1 Tax oncoprotein mediates interaction with the PDZ domain of cellular proteins. *Oncogene* **16**, 643-654.

Rutishauser, U. (2000). Defining a role and mechanism for IgCAM function in vertebrate axon guidance. *J. Cell Biol.* **149**, 757-759.

Sakurai, K., Migita, O., Toru, M. and Arinami, T. (2002). An association between a missense polymorphism in the close homologue of L1 (CHL1, CALL) gene and schizophrenia. *Mol. Psychiatry* **7**, 412-415.

Sakurai, T., Friedlander, D. R. and Grumet, M. (1996). Expression of polypeptide variants of receptor-type protein tyrosine phosphatase β: the secreted form, phosphacan, increases dramatically during embryonic development and modulates glial behaviour in vitro. *J. Neurosci. Res.* **43**, 694-706.

Sakurai, T., Lustig, M., Babiarz, J., Furley, A. J., Tait, S., Brophy, P. J., Brown, S. A., Brown, L. Y., Mason, C. A. and Grumet, M. (2001). Overlapping

functions of the cell adhesion molecules Nr-CAM and L1 in cerebellar granule cell development. *J. Cell Biol.* **154**, 1259-1273.

Sakurai, T., Lustig, M., Nativ, M., Hemperly, J. J., Schlessinger, J., Peles, E. and Grumet, M. (1997). Induction of neurite outgrowth through contactin and NrCAM by extracellular regions of glial receptor tyrosine phosphatase β. *J. Cell Biol.* **136**, 907-918.

Salzer, J. L. (1997). Clustering sodium channels at the node of Ranvier: close encounters of the axon glia kind. *Neuron* **18**, 843-846.

Salzer, J. L. (2003). Polarized domains of myelinated axons. *Neuron* **40**, 297-318.

Sans, N., Petralia, R. S., Wang, Y. X., Blahos, J., 2nd, Hell, J. W. and Wenthold, R. J. (2000). A developmental change in NMDA receptor-associated proteins at hippocampal synapses. *J. Neurosci.* **20**, 1260-1271.

Sans, N., Prybylowski, K., Petralia, R. S., Chang, K., Wang, Y. X., Racca, C., Vicini, S. and Wenthold, R. J. (2003). NMDA receptor trafficking through an interaction between PDZ proteins and the exocyst complex. *Nat Cell Biol* **5**, 520-530.

Saugier-Veber, P., Martin, C., Le Meur, N., Lyonnet, S., Munnich, A., David, A., Henocq, A., Heron, D., Jonveaux, P., Odent, S. et al. (1998). Identification of novel L1CAM mutations using fluorescence-assisted mismatch analysis. *Hum. Mutat.* **12**, 259-266.

Scherer, S. S. and Arroyo, E. J. (2002). Recent progress on the molecular organization of myelinated axons. *J. Peripher. Nerv. Syst.* **7**, 1-12.

Schmid, R. S., Pruitt, W. M. and Maness, P. F. (2000). A MAP kinase-signaling pathway mediates neurite outgrowth on L1 and requires Src-dependent endocytosis. *J. Neurosci.* **20**, 4177-4188.

Schurmann, G., Haspel, J., Grumet, M. and Erikson, H. P. (2001). Cell adhesion molecule L1 in folded (horseshoe) and extended conformations. *Mol. Biol. Cell* **12**, 1765-1773.

Seabold, G. K., Burette, A., Lim, I. A., Weinberg, R. J. and Hell, J. W. (2003). Interaction of the tyrosine kinase Pyk2 with the N-methyl-D-aspartate receptor complex via the Src homology 3 domains of PSD-95 and SAP102. *J. Biol. Chem.* **278**, 15040-8.

Seeds, N. W., Siconolfi, L. B. and Haffke, S. P. (1997). Neuronal extracellular proteases facilitate cell migration, axonal growth, and pathfinding. *Cell Tissue Res.* **290**, 367-370.

Sehgal, A., Boynton, A. L., Young, R. F., Vermeulen, S. S., Yonemura, K. S., Kohler, E. P., Aldape, H. C., Simrell, C. R. and Murphy, G. P. (1998). Cell adhesion molecule Nr-CAM is over-expressed in human brain tumors. *Int. J. Cancer* **76**, 451-458.

Sheng, M. and Sala, C. (2001). PDZ domains and the organization of supramolecular complexes. *Annu. Rev. Neurosci.* **24**, 1-29.

Shiba, T., Kametaka, S., Kawasaki, M., Shibata, M., Waguri, S., Uchiyama, Y. and Wakatsuki, S. (2004). Insight into the Phosphoregulation of β-Secretase Sorting Signal by the VHS Domain of GGA1. *Traffic* **5**, 437-448.

Shin, H., Hsueh, Y. P., Yang, F. C., Kim, E. and Sheng, M. (2000). An intramolecular interaction between Src homology 3 domain and guanylate kinase-like

domain required for channel clustering by postsynaptic density-95/SAP90. *J. Neurosci.* **20**, 3580-3587.

Silletti, S., Mei, F., Sheppard, D. and Montgomery, A. M. (2000). Plasmin-sensitive dibasic sequences in the third fibronectin-like domain of L1-cell adhesion molecule (CAM) facilitate homomulterization and concomitant integrin recruitment. *J. Cell Biol.* **149**, 1485-1501.

Sonderegger, P. (1997). Axonin-1 and NgCAM as "recognition" components of the pathway sensor apparatus of growth cones: a synopsis. *Cell Tissue Res.* **290**, 429-439.

Sotelo, C. (2002). The chemotactic hypothesis of Cajal: a century behind. *Prog. Brain Res.* **136**, 11-20.

Stoeckli, E. T. (1998). Molecular mechanisms of commissural axon pathfinding. *Prog. Brain Res.* **117**, 105-114.

Stoeckli, E. T. and Landmesser, L. T. (1998). Axon guidance at choice points. *Curr. Opin. Neurobiol.* **8**, 73-79.

Suter, D. M. and Forscher, P. (1998). An emerging link between cytoskeletal dynamics and cell adhesion molecules in growth cone guidance. *Curr. Opin. Neurobiol.* **8**, 432-436.

Suter, D. M. and Forscher, P. (2001). Transmission of growth cone traction force through apCAM-cytoskeletal linkages is regulated by Src family tyrosine kinase activity. *J. Cell Biol.* **155**, 427-438.

Suter, D. M., Pollerberg, G. E., Buchstaller, A., Giger, R. J., Dreyer, W. J. and Sonderegger, P. (1995). Binding between the neural cell adhesion molecules axonin-1 and Nr-CAM/Bravo is involved in neuron-glia interaction. *J. Cell Biol.* **131**, 1067-1081.

Tacke, R., Moos, M., Teplow, D. B., Fruh, K., Scherer, H., Bach, A. and Schachner, M. (1987). Identification of cDNA clones of the mouse neural cell adhesion molecule L1. *Neurosci. Lett.* **82**, 89-94.

Takeuchi, M., Hata, Y., Hirao, K., Toyoda, A., Irie, M. and Takai, Y. (1997). SAPAPs. A family of PSD-95/SAP90-associated proteins localized at postsynaptic density. *J. Biol. Chem.* **272**, 11943-11951.

Tan, C., Deardorff, D. A., Saint-Jeannet, J. P., Yang, J. and Arzomanian, A. (2001). Kermit, a frizzled interacting protein, regulates frizzled 3 signaling in neural crest development. *Development* **128**, 3665-3674.

Tani, T. T. and Mercurio, A. M. (2001). PDZ interaction sites in integrin alpha subunits. T14853, TIP/GIPC binds to a type I recognition sequence in alpha 6A/alpha 5 and a novel sequence in alpha 6B. *J. Biol. Chem.* **276**, 36535-36542.

Tessier-Lavigne, M. and Goodman, C. S. (1996). The molecular biology of axon guidance. *Science* **274**, 1123-1133.

Thelen, K., Kedar, V., Panicker, A. K., Schmid, R. S., Midkiff, B. R. and Maness, P. F. (2002). The neural cell adhesion molecule L1 potentiates integrin-dependent cell migration to extracellular matrix proteins. *J. Neurosci.* **22**, 4918-4981.

Thomas, G. (2002). Furin at the cutting edge: from protein trafffic to embryogenesis and disease. *Nature Rev: Mol. Cell Biol.* **3**, 753-766.

Treubert, U. and Brummendorf, T. (1998). Functional cooperation of beta1-integrins and members of the Ig superfamily in neurite outgrowth induction. *J. Neurosci.* **18**, 1795-1805.

Tuvia, S., Garver, T. D. and Bennett, V. (1997). The phosphorylation state of the FIGQY tyrosine of neurofascin determines ankyrin-binding activity and patterns of cell segregation. *Proc. Natl. Acad. Sci.* **94**, 12957-12962.

Valerius, M. T., Patterson, L. T., Feng, Y. and Potter, S. S. (2002). Hoxa 11 is upstream of Integrin alpha8 expression in the developing kidney. *Proc. Natl. Acad. Sci.* **99**, 8090-8095.

van Zundert, B., Yoshii, A. and Constantine-Paton, M. (2004). Receptor compartmentalisation and trafficking at glutamtate synpases: a developmental proposal. *Trends in Neurosciences.* **27**, 428-437.

Vega, I. E. and Hsu, S. C. (2001). The exocyst complex associated with microtubles to mediate vesicle targeting and neurite outgrowth. *J. Neurosci.* **21**, 3839-3848.

Voet, D. and Voet, J. G. (1995). Biochemistry, pp. 58-60.

Volkmer, H. (2001). The immunoglobulin superfamily of cell adhesion molecules. In *Cell Adhesion*, (ed. M. C. Beckerle), pp. 1-24. Oxford: Oxford University Press.

Volkmer, H., Hassel, B., Wolff, J. M., Frank, R. and Rathjen, F. G. (1992). Structure of the axonal surface recognition molecule neurofascin and its relationship to a neural subgroup of the immunoglobulin superfamily. *J. Cell Biol.* **118**, 149-161.

Volkmer, H., Leuschner, R., Zacharias, U. and Rathjen, F. G. (1996). Neurofascin induces neurites by heterophilic interactions with axonal NrCAM while NrCAM requires F11 on the axonal surface to extend neurites. *J. Cell Biol.* **135**, 1059-1069.

von Arnim, C. A. F., Tangredi, M. M., Peltan, I. D., Lee, B. M., Irizarry, M. C., Kinoshita, A. and Hyman, T. (2004). Demonstration of BACE (β-secretase) phosphorylation and its interaction with GGA1 in cells by fluorescence-lifetime imaging microscopy. *J. Cell Sci.* **117**, 5437-5445.

Walsh, F. S. and Doherty, P. (1997). Neural cell adhesion molecules of the immunoglobulin superfamily: role in axon growth and guidance. *Ann. Rev. Cell Dev. Biol.* **13**, 425-456.

Wang, B., Williams, H., Du, J. S., Terrett, J. and Kenwrick, S. (1998). Alternative Splicing of Human NrCAM in Neural and Nonneural Tissues. *Mol. Cell Neurosci.* **10**, 287-295.

Wang, L. H., Kalb, R. G. and Strittmatter, S. M. (1999). A PDZ protein regulates the distribution of the transmembrane semaphorin, M-SemF. *J. Biol. Chem.* **274**, 14137-46.

Welch, M. D., Mallavarpu, A., Rosenblatt, J. and Mitchison, T. J. (1997). Actin dynamics *in vivo*. *Curr. Opin. Biol.* **9**, 54-61.

Welzl, H. and Stork, O. (2003). Cell adhesion molecules: key players in memory consolidation? *News Physiol. Sci.* **18**, 147-150.

Wiencken-Barger, A. E., Mavity-Hudson, J., Batsch, U., Schacher, M. and Casagrande, V. A. (2004). The role of L1 in axon pathfinding and fasciculation. *Cerebral cortex* **14**, 121-131.

Wood, W. and Martin, P. (2002). Molecules in focus: Structures in focus-filopodia. *Int. J. Biochem. Cell Biol.* **34**, 726-730.

Xu, Y. Z., Ji, Y., Zipser, B., Jellies, J., Johansen, K. M. and Johansen, J. (2003). Proteolytic cleavage of the ectodomain of the L1 CAM family member Tractin. *J. Cell Biol.* **278**, 4322-4330.

Zacharias, U., Norenberg, U. and Rathjen, F. G. (1999). Functional interactions of the immunoglobulin superfamily member F11 are differentially regulated by the extracellular matrix proteins tenascin-R and tenascin-C. *J. Biol. Chem.* **274**, 24357-24365.

Zhang, X., Davis, J. Q., Carpenter, S. and Bennett, V. (1998a). Structural requirements for association of neurofascin with ankyrin. *J. Biol. Chem.* **273**, 30785-30794.

Zhang, Y., Roslan, R., Lang, D., Schachner, M., Lieberman, A. R. and Anderson, P. N. (2000). Expression of CHL1 and L1 by neurons and glia following sciatic nerve and dorsal root injury. *Mol. Cell Neurosci.* **16**, 71-86.

Zhang, Z., Devarajan, P., Dorfman, A. L. and Morrow, J. S. (1998b). Structure of the ankyrin-binding domain of alpha-Na,K-ATPase. *J. Biol. Chem.* **273**, 18681-18684.

Zhao, G. and Hortsch, M. (1998). The analysis of genomic structures in the L1 family of cell adhesion molecules provides no evidence for exon shuffling events after the separation of arthropod and chordate lineages. *Gene* **215**, 47-55.

Appendix 1: Suppliers.

Supplier	Address
Amaxa biosystems	Koeln, Germany
Applied Precision	Distributed by: Ian Corless, Preston UK
BD Clontech	Oxford, U.K
European Collection of Cell Culture (ECACC)	Distributed by Sigma, Dorset.
Globepharm,	Essex, U.K
Invitrogen	Paisley, UK
Melford laboratories	Suffolk. UK
New England Biolabs	Hertfordshire, Uk
Pierce	Tattenhall, U.K
Promega	Southampton, UK
Qiagen	Crawley, U.K
Roche	East Sussex, UK
Santa Cruz	Calne, U.K
Sigma	Dorset, U.K
Stratagene	Cambridge, U.K
Thistle Scientific	Glasgow, UK
Ultratec Ltd	Hertfordshire, Uk
VWR	Leicestershire, UK

Appendix 2: Lysis buffers

RIPA buffer:
tris-HCl 50 mM, pH 7.4, NP-40 1 %, Na-deoxycholate 0.25 %.

GIPC Buffer 1 (GB1):
10mM Tris-HCl pH7.5, 150mM NaCl, 1% NP40.

GIPC HEK Buffer 1 (GBH1):
Dubleccos Phosphate buffered saline (DPBS) (SIGMA give code), 1% v/v triton x-100, 0.2% SDS, 0.5% deoxycholate and 1mM PMSF.

GIPC HEK Buffer 2 (GHB2):
PBS (Sigma give code), 5mM EDTA, 5mM EGTA, 0.1mM PMSF, 10u/ml aprotinin.

GIPC HEK Buffer 3 (GHB3):
100mM Tris pH8.0, 150mM NaCl, ImM EDTA, 1% NP-40. 0.12mg/ml PMSF, 2mg/ml leupeptin, 1mg/ml aprotinin, 10mM NAF and 1mM sodium orthovanadate.

Appendix 3

Epitope	Extracellular NrCAM	Extracellular NrCAM	Cytoplasmic NrCAM	SAP102
First Block	TBS-T(0.5%) 5% milk 2 hours room temperature	TBS-T(0.5%) 5% milk overnight 4°C	TBS-T(0.5%) 5% milk overnight 4°C	TBS-T(0.5%) 5% milk 2 hours room temperature
Washes	three five minute TBS-T	three five minute TBS-T	three five minute TBS-T	three five minute TBS-T
Primary Ab	NrCAM (N-18) and NrCAM (C-16) Santa Cruz sc-18958 and sc-18960 1/1,000 TBS-T 3% milk Overnight 4°C	Anti 1-4IgG C.Favire Sarrailh, 1/1,000 TBS-T 3% milk room temperature one hour	A2541 and A2542 Invitrogen 1/1,000 (or 1/100 AP) TBS-T 3% milk room temperature one hour	anti-SAP102 Affinity Bioreagents 1/300 TBS-T 3% milk Overnight 4°C
Washes	three ten minute TBS-T	three ten minute TBS-T	three ten minute TBS-T	three ten minute TBS-T
Secondary Ab	donkey anti goat IgG HRP conjugate Santa Cruz sc-sc-2020 1/20,000 TBS-T 5% milk room temperature one hour	goat anti-rabbit IgG HRP conjugate Santa Cruz sc-2004 1/10,000 TBS-T 5% milk room temperature one hour	goat anti-rabbit IgG HRP conjugate Santa Cruz sc-2004 1/10,000 TBS-T 5% milk room temperature one hour	goat anti-rabbit IgG HRP conjugate Santa Cruz sc-2004 1/10,000 TBS-T 3% milk room temperature one hour
Washes	two ten minute TBS-T one ten minute TBS	two ten minute TBS-T one ten minute TBS	two ten minute TBS-T one ten minute TBS	two ten minute TBS-T one ten minute TBS

Appendix 3

Epitope	FLAG-constructs FLAG GIPC, FLAG SAP102, FLAG Ezrin	GIPC	HA-NrCAM, HA-NrCAMDPDZ HA-NrCAMDFN2&3, HA-Neurofascin	Phosphorylated Tyrosines
First Block	TBS 3% milk	TBS-T(0.5%) 5% milk	TBS-T(0.5%) 5% milk	PBS 3% milk
	room temperature 30 minutes (or O/N 4°C)	2 hours RT or O/N 4°C	2 hours RT or O/N 4°C	45 minutes room temperature
Washes	one five minute TBS	three five minute TBS-T	three five minute TBS-T	no washes
Primary Ab	anti-FLAG m2, mouse monoclonal	GIPC (N-19), goat polyclonal	Anti-HA High Affinity, rat monoclonal	anti-phosphotyrosine, clone 4G10
	SIGMA F3165	Santa Cruz sc-9648	Roche 1 867 423	Upstate, 05-321
	10mg/ml or 1/500	1/2,000	1/1,000	1/500
	TBS 3% milk	TBS-T 3% milk	TBS-T 3% milk	PBS 3% milk
	room temperature 30 minutes	room temperature one hour	room temperature one hour	Overnight 4°C
Washes	one five minute TBS	three ten minute TBS-T	three ten minute TBS-T	two times with water
Secondary Ab	goat anti-mouse IgG HRP conjugate	donkey anti goat IgG HRP conjugate	goat anti-mouse IgG HRP conjugate	goat anti-mouse IgG HRP conjugate
	Santa Cruz sc-2005	Santa Cruz sc-sc-2020	Santa Cruz sc-2005	Santa Cruz sc-2005
	1/20,000	1/20,000	1/20,000	1/20,000
	TBS 3% milk	TBS-T 5% milk	TBS-T 3% milk	PBS 3% milk
	room temperature one hour	room temperature one hour	room temperature one hour	room temperature one hour
Washes	eight 2.5 minute washes TBS-T	two ten minute TBS-T	two ten minute TBS-T	two times with water
	final TBS wash 5 minutes	one ten minute TBS	one ten minute TBS	5 minutes in PBS-T(0.05%)
				five times with water

Appendix 4. List of PCR primers.

CN1	GGAATTCAGGAGGAATAAAGGTGGC
CN4	CGGGATCCTCATTTTTTGCCGCTGTATTGTC
GIPC 1	GGAATTCACCATGGCACTGGGACTGGGGCG
GIPC 3	GTGGATCCGAGGTTCGGTGAGTTTGAG
GIPC 6A	GATCCGTAGCGGCCAACCTTGGCATC
GIPC 7	CGGGATCCGAATGCCACTGGGACTGGGGCG
GIPC 70F	CGGGATCCCCACTGGGACTGGGGCGAAGG
GIPC 71R	CCCAAGCTTTTAGTAGCGGCCAACCTTGGC
GIPC 8	GGAATTCTTAGTAGCGGCCAACCTTGGAT
NrCAM 1	GGAATTCAGAAGAAACAAACAAGGGTGGT
NrCAM 2	CGGGATCCTTAAACAAAGGAGTTCATTGC
NrCAM 21	GGAATTCAGTGGTAAGAAAGAGAAAG
NrCAM 32	CGGGATCCTTAGTTCATTGCGTTGACAGGA
NrCAM 33	CGGGATCCGAAGAAGAAACAAGGGTGGT
NrCAM 34	GGAATTCTTAAACAAAGGAGTTCATTGCG
NrCAM F1	TCCGGGCCCGCCAGCGCCGACAGAGGCTTC
NrCAM F2	GGAATTCTTAAACAAAGGAGTCATTGCG
SAP102H	GGAATTCGAATGCACAAGCACCAGCACTGC
SAP102I	GGAATTCTCAGAGTTTTTCAGGGGATGGG